ANALYSIS OF MEMBRANE EXCHANGE BETWEEN LYMPHOCYTES

Sarah Yvonne de Guzman

A THESIS SUBMITTED FOR THE DEGREE OF DOCTOR OF PHILOSOPHY
AT THE AUSTRALIAN NATIONAL UNIVERSITY

JULY 2016

© Copyright by Sarah Yvonne de Guzman 2016
All Rights Reserved

To Michael,
for always making me laugh.

Declaration

The experimental work presented in this thesis constitutes original work by myself unless otherwise stated in the text. Mr Cameron Jack, from the Genome Discovery Unit (GDU), assisted with the bioinformatics screening for cell penetrating peptide motifs. Jason Price, from Lipotek Pty Ltd., prepared and donated the liposomes used in this work. Dr. Benjamin Quah and Dr. Jasmine Li prepared the samples for gene expression analysis.

This thesis conforms to The Australian National University guidelines and regulations. The work contained within has not been submitted for the purpose of obtaining any other degree at this or other universities.

Sarah Yvonne de Guzman
(Author, PhD Candidate)

Christopher R. Parish
(Supervisor)

Benjamin J.C. Quah
(Co-supervisor)

Cancer and Vascular Biology Group
Department of Cancer Biology and Therapeutics
The John Curtin School of Medical Research
The Australian National University

Acknowledgements

A thesis is not a solitary piece of work; it involves a team of dedicated people to whom I am indebted.

First and foremost, I would like to thank my supervisors, Chris Parish and Ben Quah for their guidance, encouragement and extreme patience over the years. Chris, thank you for taking me under your wing and not giving up on me. Your seemingly endless knowledge, amazing ability to retain information and meticulous attention to detail was essential in this project’s success. Ben, thank you for your constant encouragement and for always keeping a cool head, even when mine was red-hot. I am tremendously grateful for all you have done and thankful to have you as supervisors.

I would also like to thank my advisory panel, Carola Vinuesa and Sudha Rao, for advice on various aspects of this project. A special thanks to Harpreet, Mick, Anne and Cathy in the Imaging and Cytometry Facility for their hours of invaluable assistance with flow cytometry, histology and microscopy.

A huge thank you to Lipotek Pty Ltd., in particular Jason Price, for not only providing liposomes but also for important advice regarding liposomes and kayak fishing.

Thank you also goes to the animal husbandry staff of the Australian Phenomics Facility for taking exceptional care of my mice.

Thank you to the Australian Cancer Research Foundation (ACRF) Biomolecular Resource Facility (BRF) and the Genome Discovery Unit (GDU) for their help with all things molecular.

The assistance provided by Terry Neeman from the Statistical Consulting Unit was instrumental in both experimental design and analysis, and for this I am extremely appreciative.

Thank you to Anna, Wendy and Charani for managing all the paperwork and ensuring that I am enrolled each year.

I am eternally grateful to everyone in the Parish Laboratory who provided not only assistance and support in the lab but also for providing a fantastic place to work each and every day. You became my Canberra family, and for this I am so thankful. I will miss the witty banter.

I feel so lucky to have such an amazing family and the most fabulous friends who supported me throughout this rollercoaster ride. Not only have I achieved such a large piece of work, but I have also met my incredibly handsome husband, raised a fur-baby, brought into this world a beautiful little princess and learnt to bake amazing cakes. It truly has been a tremendously busy few years and this work would not have been possible without the unwavering support and encouragement from my family and friends.

Lastly, thank you to Michael. Thank you for dealing with my erratic emotional way of life. Thank you for pretending to listen to my babble. Thank you for pretending to understand what a B cell is. Thank you for cooking me dinner whilst I sat at the computer. Thank you for loving boxer dogs. Thank you for our princess. Thank you for putting a smile on my face when I wanted to cry. Most of all, thank you for loving me regardless. This Thesis would not have been possible without you.

Abstract

Membrane transfer is the cell-to-cell contact dependent exchange of plasma membrane and surface molecules between cells. It has been described for a wide range of immune cells, nevertheless the molecular mechanisms mediating this exchange remain unclear. The studies outlined in this Thesis provide new insights and a better understanding of the transfer process.

Previous studies in my supervisor’s laboratory showed that activated antigen-specific B cells and T cells readily donate their antigen-specific receptors to neighbouring lymphocytes of an unrelated specificity via plasma membrane exchange. Results obtained in this Thesis confirmed and further characterised several properties of antigen receptor transfer as well as suggesting new potential mediators of membrane exchange.

The results in Chapter 3 detail important properties of membrane exchange between B cells, and based on these unique features propose a molecular mechanism for this process. It was confirmed that B cells require appropriate activation conditions in order to donate membranes and cell surface proteins, with naïve B cells being much less capable of transfer. Additionally, it was confirmed that activated B cells are capable of transferring membranes and surface proteins at 4°C, thus excluding many of the currently proposed energy dependent mechanisms. Chapter 3 describes the investigation of an energy independent mechanism of exchange involving cell penetrating peptide (CPP) motifs. The results obtained demonstrate that analogous to transfer between B cells, CPPs are up to 40-fold more efficiently taken up by activated, rather than naïve, B cells and that this uptake occurs at both 37°C and 4°C. These data suggest that receptors involved in the initiation of membrane transfer may contain CPP motifs important in facilitating this process.

Chapter 4 describes attempts to identify the molecular basis of membrane transfer via a comparative gene expression analysis. This study took advantage of the finding that B cells require appropriate activation conditions to achieve efficient levels of membrane transfer. In an effort to unravel the proteins involved in this process, transcriptomes of LPS stimulated B cells, which are known to efficiently transfer membranes, were compared with the transcriptomes of CpG stimulated and unstimulated B cells which are less efficient at transferring membranes. Bioinformatics analysis identified five proteins containing CPP motifs that may play a role in B cell membrane transfer, namely ALCAM, AMIGO2, CTLA-4, Slp3 and TIGIT. Monoclonal antibodies (mAbs) specific for ALCAM, CTLA-4, TIGIT and the TIGIT ligand, PVR, demonstrated increased expression of all these proteins on the cell surface of LPS activated B cells. Furthermore, incubation of B cells with ALCAM, TIGIT and TIGIT + PVR mAbs resulted in significantly enhanced membrane transfer, whereas the CTLA-4 mAb, known to block CTLA-4 binding, had no effect. Based on these data and other published findings it is hypothesised that mAbs specific for ALCAM and TIGIT/PVR may crosslink these receptors, creating a patching effect, similar to a lipid raft, in which there are areas of localised membrane destabilisation and, consequently, more accessible areas for CPP-mediated membrane fusion.

Based on the current understanding of membrane transfer it should be possible to harness this phenomenon to enhance antigen specific CTL responses in the adoptive immunotherapy of established tumours. Thus, experiments described in Chapter 5 used an adoptive T cell immunotherapy model to investigate whether TCR sharing can be harnessed to control tumour growth. The model utilised the ovalbumin (OVA)-expressing EG7 (EG7-OVA) thymoma cell line to establish tumours in mice. These tumours are susceptible to killing by OVA-specific TCR transgenic (OT-I) CTL, thus resulting in a reduction in EG7-OVA tumour volume. To establish the influence of antigen receptor transfer in the control of tumour growth, perforin deficient OT-I CTLs, which have been shown previously to be less effective at bringing about tumour rejection due to their lack of perforin, and CTLs of an unrelated specificity (B6.SJL.TCRP14 CTLs) were used. Transferred alone each of these CTL populations should be incapable of inducing tumour regression. However, when adoptively transferred together if TCR transfer occurs the B6.SJL.TCRP14 CTL should acquire OVA-specific TCR from the perforin deficient OT-I CTLs and gain the capacity to recognise and eliminate the EG7-OVA tumour cells and thereby mediate tumour regression. The results obtained, however, demonstrated that perforin deficient OT-I CTLs, but not B6.SJL.TCRP14 CTLs, were as efficient as wild type OT-I CTLs at eliminating established EG7-OVA tumours *in vivo*. This finding indicated that the CTLs used in this model do not require perforin to control tumour growth, with subsequent *in vitro* studies suggesting involvement of the Fas/FasL pathway. Furthermore, results described in this Chapter demonstrate that extrodinarily small numbers of CTLs within tumours can induce tumour regression, suggesting that *in vivo* many other mechanisms work in concert to control EG7-OVA tumour growth, NK cells being the most obvious. In addition, variations in the results obtained with the EG7-OVA cell line in different laboratories may be due to genetic drift of the cell line, thus highlighting the importance of stringent cell line authentication.

In conclusion, this Thesis identified several candidate proteins required for efficient membrane transfer between B cells as well as providing evidence for a potential membrane exchange mechanism involving proteins that contain CPP motifs that facilitate membrane fusion and thus the transfer of membranes and associated cell surface proteins.

Table of contents

Declaration.....5

Acknowledgements.....7

Abstract.....9

Abbreviations.....18

Chapter 1: Literature Review.....25

- 1.1 Introduction.....26
- 1.2 The Adaptive Immune System.....28
  - 1.2.1 B cell activation.....29
  - 1.2.2 T cell activation.....32
  - 1.2.3 The Immunological Synapse.....33
- 1.3 Membrane Transfer in the Immune System.....37
- 1.4 Mechanisms of intercellular transfer.....39
  - 1.4.1 Direct membrane transfer via cell contact.....39
  - 1.4.2 Nanotube-mediated membrane transfer.....42
  - 1.4.3 Exosomes and membrane transfer.....43
- 1.5 Functional consequences of membrane transfer.....48
- 1.6 Concluding remarks.....53
- 1.7 Thesis Experimental Aims.....54

Chapter 2: Materials and Methods.....57

- 2.1 Materials.....58
  - 2.1.1 General reagents and equipment.....58
  - 2.1.2 Media, buffers and solutions.....58
  - 2.1.3 Animals.....58
  - 2.1.4 Mammalian cell lines.....58
  - 2.1.5 Antibodies.....60
  - 2.1.6 Kits.....60
  - 2.1.7 Oligonucleotides.....60
  - 2.1.8 Cell Penetrating Peptides.....60
  - 2.1.9 Liposomes.....61
  - 2.1.10 Flow cytometry equipment and software.....61
- 2.2 Methods.....67
  - 2.2.1 Cell biology.....67

2.2.1.1 In vitro 67
2.2.1.1.1 Primary mouse splenocyte preparation 67
2.2.1.1.2 Activation of B cells 67
2.2.1.1.3 Activation of CD8$^+$ T cells 68
2.2.1.1.4 Activation of CD4$^+$ T cells 68
2.2.1.1.5 Cell Staining 69
2.2.1.1.5.1 Cell surface labelling 69
2.2.1.1.5.2 Dead cell labelling 70
2.2.1.1.5.3 Intracellular labeling with 5-(and 6)-carboxyfluorescein diacetate succinimidyl ester (CFSE) 70
2.2.1.1.5.4 Membrane staining using Vybrant® DiI cell labelling solution 71
2.2.1.1.5.5 Cytotoxicity assay 71
2.2.1.2 In vivo 72
2.2.1.2.1 Subcutaneous tumour establishment 72
2.2.1.2.2 Tumour measurement 72
2.2.1.2.3 Adoptive immunotherapy of tumours..............................72
2.2.1.2.4 Tumour-infiltrate profiles 73
2.2.1.2.5 Depletion of NK cells in mice 73
2.2.1.2.6 Depletion of macrophages in mice 74
2.2.1.2.7 Depletion of neutrophils in mice 74
2.2.2 Molecular Biology 74
2.2.2.1 DNA isolation 74
2.2.2.2 Total RNA isolation 75
2.2.2.3 RNA purity and quality assessment 76
2.2.2.4 First strand cDNA synthesis 76
2.2.2.5 Quantitative Real-time PCR analysis 77
2.2.2.6 Comparative gene expression analysis 77
2.2.3 Statistical significance 79
Chapter 3: Cell penetrating peptides as mediators of membrane exchange between B cells 81
3.1 Abstract 82
3.2 Introduction 83
3.3 Results 87

3.3.1 B cell membrane transfer: the methodology..................................87

3.3.1.1 Transfer of cell surface proteins between B cells 87

3.3.1.2 Transfer of plasma membranes between B cells...................88

3.3.2 B cell membrane transfer: the conditions 94

3.3.2.1 Transfer between B cells is enhanced after LPS activation...94

3.3.2.2 Transfer of B cell membranes occurs at both 4ºC and 37ºC .95

3.3.3 Cell penetrating peptides (CPPs) as a mechanism of transfer between B cells...101

3.3.3.1 Classification of CPPs 102

3.3.3.2 Interaction of CPPs with activated B cells and their effect on B cell viability...105

3.3.3.3 The influence of B cell activation on CPP uptake by B cells 110

3.3.3.4 The influence of temperature on CPP uptake by B cells 111

3.3.3.5 Kinetics of CPP uptake by LPS activated B cells................116

3.4 Discussion 120

Chapter 4: Identifying molecular mechanisms of membrane exchange between B cells

Chapter 4: Identifying molecular mechanisms of membrane exchange between B cells.....127

4.1 Abstract 128

4.2 Introduction...130

4.3 Results...133

4.3.1 Membrane transfer between unstimulated, LPS stimulated and CpG stimulated B cells 133

4.3.2 Quality assessment of RNA preparations isolated from different B cell populations...135

4.3.3 Global effects of B cell stimulation on the B cell transcriptome 140

4.3.4 Downstream effect analysis of genes up or down regulated following B cell stimulation...146

4.3.5 Identification of candidate genes involved in membrane transfer between B cells...150

4.3.5.1 LPS inducibility and plasma membrane association............150

4.3.5.2 Involvement in cell communication and cell adhesion functions 158

4.3.5.3 The presence of a cell penetrating peptide (CPP) motif 160

4.3.6 Validation by real-time PCR of genes of interest identified by microarray analysis..164

4.3.7 Involvement of the genes of interest in membrane transfer between B cells....168
4.3.7.1 Activated leucocyte adhesion molecule, ALCAM....168
4.3.7.2 CTLA-4....172
4.3.7.3 T cell immunoreceptor with Ig and ITIM domains, TIGIT....176
4.3.8 B Cell Receptor (BCR) specific antigen enhances membrane transfer between B cells....181
4.4 Discussion....184
4.4.1 Activated leukocyte cell adhesion molecule, ALCAM....187
4.4.2 Amphoterin-induced gene and ORF (open reading frame) 2, AMIGO2....191
4.4.3 Cytotoxic T lymphocyte associated protein 4 (CTLA-4)....194
4.4.4 Synaptotagmin-like protein 3 (Slp3)....196
4.4.5 T cell immunoreceptor with Ig and ITIM domains (TIGIT)....198
4.4.6 Conclusions....202
Chapter 5: Investigation into whether TCR sharing between CTLs can be harnessed for adoptive immunotherapy of tumours....205
5.1 Abstract....206
5.2 Introduction....208
5.3 Results....211
5.3.1 Establishing the optimum adoptive immunotherapy model for analysis of tumour regression.....211
5.3.2 Effect of antigen-specific TCR transfer between CD8+ T cells on tumour growth....216
5.3.3 Leukocyte infiltrates in EG7-OVA tumours in untreated and OVA-specific OT-I CTL treated mice....219
5.3.4 Effect of OVA-specific OT-II CD4+ T cells and OT-I CTL-derived IFNγ on EG7-OVA tumour growth....225
5.3.5 The efficiency of OVA-specific OT-I CTLs in achieving regression of EG7-OVA tumours in *Rag1-/-* mice in the absence of NK cells....228
5.3.6 The efficiency of OVA-specific OT-I CTLs in achieving regression of EG7-OVA tumours in *Rag1-/-* mice in the absence of neutrophils....233
5.3.7 The efficiency of OVA-specific OT-I CTLs in achieving regression of EG7-OVA tumours in *Rag1-/-* mice in the absence of macrophages....237
5.3.8 Cytolytic activity of OVA-specific wild type and perforin deficient OT-I CTLs in vitro....241

5.3.9 Role of Fas/FasL pathway in the cytolytic activities of OVA-specific wild type and perforin deficient OT-I CTLs in vitro 248

5.4 Discussion 251

Chapter 6: Final discussion 260

6.1 Introduction 261

6.2 Mechanisms of membrane transfer between B cells 263

6.2.1 Cell Penetrating Peptides (CPPs) as potential mediators of membrane transfer 263

6.2.2 Cell surface protein involvement in transfer 266

6.2.3 Proposed mechanism of membrane transfer between B cells 269

6.3 Physiological relevance of membrane exchange 272

6.4 Clinical implications: the adoptive immunotherapy of tumours 275

6.5 Future research 278

6.6 Conclusions 282

References....284

Abbreviations

1A8	Anti-Ly6G antibody
Ab	Antibody
ADCC	Antibody dependent cell mediated cytotoxicity
AE	Qiagen elution Buffer
Ag	Antigen
ANOVA	Analysis of variance
ANU	Australian National University
APC	Antigen presenting cell
APC	Allophycocyanin
ATP	Adenosine triphosphate
AW1	Qiagen wash buffer
AW2	Qiagen wash buffer
B6	C57BL/6 mouse strain
BCR	B cell receptor
BSA	Bovine serum albumin
Ca^{2+}	Calcium
CD	Cluster of differentiation
CD40L	CD40 ligand
cDNA	Copy-deoxyribonucleic acid
CFSE	Carboxyfluorescein succinimidyl ester
ClodLip	Clodronate liposome
cm	Centimetre

CMA	Concanamycin A
CO_2	Carbon dioxide
CpG	5-C-phosphate-G-3
CPP	Cell penetrating peptide
CTL	Cytotoxic T lymphocyte
DC	Dendritic cell
ddH_2O	Double distilled water
DEPC	Diethylpyrocarbonate
DiI	1,1'-Dioctadecyl-3,3,3',3'-Tetramethylindocarbocyanine Perchlorate
DNA	Deoxyribonucleic acid
dNTP	Deoxy-nucleotidetriphosphate
ds	Double stranded
DTT	Dithiothreitol
ECTV	Ectromelia virus
EG7	EL4 transduced to express OVA
EG7-OVA	EL4 transduced to express OVA
EL4	Mouse lymphoma cell line
FACS	Flourescence activated cell sorting
Fc	Fragment crystallisable region
FCS	Foetal calf serum
FITC	Fluorescein isothiocyanate
FSC	Forward scatter
g/L	Gram/litre
GAGs	Glycosaminoglycan
GDU	Genome Discovery Unit

GFP	Green fluorescent protein
GM-CSF	Granulocyte-macrophage colony-stimulating factor
gp33	Lymphocytic choriomeningitis virus (LMCV) peptide
GTP	Guanosine’5’triphosphate
H&E	Hematoxylin and eosin stain
HEPES	[4-(2-hydroxyethyl)-piperazino]-ethanesulfonic acid
HIV-1	Human immunodeficiency virus type 1
Hr	Hour
i.p.	Intraperitoneal injection
i.v.	Intravenous injection
IAV	Influenza A virus
ICAM	Intercellular adhesion molecule
IFN	Interferon
Ig	Immunoglobulin
IL	Interleukin
IS	Immunological synapse
JCSMR	John Curtin School Medical Research
kDa	Kilodalton
KEGG	Kyoto Encyclopedia of Genes and Genomes
L	Litre
Lck	Lymphocyte-specific protein tyrosine kinase
LCMV	Lymphocytic choriomeningitis virus
LPS	Lipopolysaccharide

LRR	Leucine-rich repeat
M	Molar
M	Metre
mAb	Monoclonal antibody
MACS	Magnetic activated cell sorting
MFI	Mean fluorescence intensity
mg/L	Miligrams/Litre
$MgCl^2$	Magnesium chloride
MHC	Major histocompatibility complex
Min	Minute
mL	Millilitre
mM	Milimolar
NCBI	National Centre fro Biotechnology Information
NK	Natural Killer cell
nM	Nanomolar
NO	Nitric oxide
^{o}C	Degree Celsius
ODN	Oligodeoxynucleotides
ORF	Open reading frame
OVA	Ovalbumin
P14	B6.SJL.TCRP14
pAb	Polyclonal Antibody
PANTHER	Protein Analysis Through Evolutionary Relationships
PBS	Phosphate buffered saline
PCR	Polymerase chain reaction

PE	Phycoerythrin
PerCP	Peridinin chlorophyll
POPC	1-palmitoyl-2-oleoyl-sn-glycero-3-phosphocholine
Prf	Perforin
qPCR	Quantitative real-time polymerase chain reaction
Rag	Recombination-activating gene
RNA	Ribonucleic acid
RNase	RNA-cleaving enzyme
RPMI	Rosewell Park Memorial Institute medium
RT-PCR	Reverse transcription polymerase chain reaction
RTX	Rituximab
SEM	Standard error of the mean
SIINFEKL	Ovalbumin peptide
SSC	Side scatter
TAM	Tumour associated macrophage
TAT	Transcription transactivating
TCR	T cell receptor
TF	Transcription factor
Tg	Transgenic
Th	Helper T lymphocyte
TLR	Toll-like receptor
TNF	Tumour necrosis factor
TP10	Transportan10
Treg	Regulatory T lymphocyte

UV	Ultra violet
V(D)J	Variable-Diversifying and Joining
WEHI	Walter and Eliza Hall Institute of Medical Research
WT	Wild type
ZAP-70	Zeta-chain (TCR) associated protein kinase 70 kDa
µg	Microgram
µl	Microlitre
µm	Micromolar

Chapter 1

Literature Review

1.1 Introduction

Immune cells circulate throughout the body, transiently interacting with a variety of neighbouring cells and forming cell-cell contacts necessary for a functioning immune system. In a linear model of immune function, these immune cells are characterized by the molecules they express on their cell surface and by the functions they perform on the basis of these phenotypic characteristics (Ahmed and Xiang, 2011). However, it has become increasingly clear that some of these cell surface molecules are capable of being transferred, such that proteins usually considered specific for one leukocyte subset are found expressed on the surface of other subsets, suggesting that the immune system is much more fluid than originally thought.

The first evidence of intercellular transfer of cell surface proteins was the T cell acquisition of major histocompatibility complex (MHC) molecules from B cells (Cone et al., 1972, Hudson et al., 1974, Hudson and Sprent, 1976) and foreign antigens from the surface of macrophages (Bona et al., 1973). However, only much more recently with the advancement of scientific techniques have the extensive networks of intercellular transfer of cell surface molecules between leukocytes been experimentally verified. Since then, numerous studies have demonstrated that many cell surface molecules are capable of being transferred by many different leukocyte subsets, including B cells (Quah et al., 2008), T cells (Chaudhri et al., 2009), natural killer (NK) cells (Nakamura et al., 2013), macrophages (Pham et al., 2011) and dendritic cells (Harshyne et al., 2001), as well as non-immune cells, such as endothelial cells and tumour cells (Rafii et al., 2008), with transfer usually being associated with plasma membrane exchange. Different laboratories refer to this process of membrane transfer by different names such as snatching, stripping, shaving, trapping or most commonly, trogocytosis. Additionally, different laboratories describe different characteristics associated with this process, such as uni- versus bi-directionality, dependence on cell-cell contact, whether it can occur between T cells and B cells in the absence or presence of specific antigen or if co-stimulatory molecules can trigger it, and whether transfer is dependent on the activation state of the donor and/or the recipient cells. However, although many aspects of this phenomenon are well documented, both *in vitro* and *in vivo,* the molecular mechanisms that underpin this process remain elusive. Furthermore, whether the examples of intercellular membrane transfer described in the literature all share the same molecular mechanisms or different molecular processes are involved depending on the cell type being studied is also yet to be elucidated. In this introductory Chapter, the important concepts and characteristics of membrane transfer between cells of the immune system are reviewed, including potential molecular mechanisms and the functional relevance of this process, with a particular emphasis on adaptive immunity. Before embarking on such a review of membrane transfer, however, some salient features of the adaptive immune system that are relevant to membrane transfer will be briefly reviewed.

1.2 The Adaptive Immune System

The body's immune system is a complex system of leukocytes, tissues and molecules that all play an important role in protecting the body against the numerous potentially pathogenic micro-organisms in the surrounding environment. It is composed of innate and adaptive immune systems. Innate immunity is the body's first line of defence and consists of a range of non-specific mechanisms that protect the body during the first critical hours and days following exposure to harmful pathogens. These defence strategies include:

- protective barriers, such as surface epithelium,
- phagocytic cells, such as macrophages, dendritic cells and neutrophils which ingest and destroy invading micro-organisms and parasites,
- and the complement system which can enhance the phagocytosis of these micro-organisms via opsonisation.

These responses depend on pattern recognition receptors that recognise pathogen-associated molecular patterns including nucleic acids, lipids and polysaccharides (Medzhitov, 2007). Additionally, the innate immune response is critical for the activation of adaptive immunity.

In contrast to innate immunity, adaptive immunity is highly specific, highly flexible and adapts to the nuances of the invading pathogen. Our current understanding of the adaptive immune system is critically dependent upon Burnet's Clonal Selection Theory of antibody diversity. This theory was proposed in 1957 by Sir Frank Macfarlane Burnet and has become the most widely accepted model of how the adaptive immune system defends the body in response to potentially a plethora of foreign antigens. It expresses the idea that the specificity for the diverse range of foreign antigens that the body can encounter is encoded in lymphocytes prior to antigen exposure. It further proposes that each lymphocyte expresses receptors specific for one particular antigen and clonally expands upon encounter with that antigen (Burnet, 1957). Lymphocytes are the principal participants mediating adaptive immune responses and originate from hematopoietic stem cells in the bone marrow (Yuseff et al., 2013, Bertrand et al., 2000). A subset of these migrate to the thymus to develop into mature T cells, whilst others remain in the bone marrow and complete their development into mature B cells before migrating around the body to secondary lymphoid organs and peripheral tissues where they can be activated in response to antigen (Halin et al., 2005).

T cells are responsible for cell-mediated immunity and are typically classified into CD4$^+$ helper and CD8$^+$ cytotoxic cells depending on their expression of surface receptors. Cell mediated immunity is initiated when foreign antigen is processed and presented on dendritic cells via MHC class I and class II molecules to T cells (den Haan et al., 2014). B cells mediate humoral immunity through the secretion of antibodies following antigenic stimulation and usually interaction with CD4$^+$ helper T cells. These antibodies circulate through the bloodstream and support the removal of pathogens via opsonisation and complement-mediated lysis (den Haan et al., 2014).

1.2.1 B cell activation

For successful activation B cells must first encounter specific antigen recognised by the B cell receptor (BCR) and receive a co-stimulatory signal. Activated helper T cells can provide the co-stimulatory signal in the form of CD40 ligand (CD40L) or cytokines including interleukin (IL)-4 (Frauwirth and Thompson, 2002). Alternatively, the co-stimulatory signal can be provided by motifs on the surface of pathogens binding to Toll-Like Receptors (TLR) expressed by B cells (Vos et al., 2000). This binding event initiates intracellular signalling leading to altered gene expression, reorganisation of the cytoskeleton and antigen internalisation (Harwood and Batista, 2011). The absence of the secondary signal, namely engagement of the BCR alone, results in B cell apoptosis or anergy, and thus the requirement of these two signals is an inherent protective mechanism to avoid the activation of an immune response in an otherwise healthy individual.

The BCR is composed of a membrane-associated immunoglobulin (Ig) heavy chain of one isotype (i.e., (IgD, IgM, IgA, IgG, or IgE), one light chain (κ or λ) and Ig-α/Ig-β chains, termed CD79a and CD79b, that contain immunoreceptor tyrosine activation motifs (ITAMs) in their intracellular domains. The process by which the BCR encounters and respond to antigen and how this translates to receptor activation remains a topic of debate. It appears to be dependent on both the nature and size of the antigen and the cellular context and location in which the antigen presentation occurs.

The classical view, commonly referred to as the cross-linking model, is that in a resting state BCRs exist as monomers on the cell surface and are unable to freely diffuse in the plane of the B cell membrane. The binding of antigen by the BCR results in receptor clustering which subsequently allows associated Src kinases to phosphorylate tyrosine residues on the now adjacent ITAM motifs of nearby BCR molecules (Liu et al., 2010, Tolar and Pierce, 2010). This triggers the formation of branched signalling cascades necessary for the formation of the immunological synapse (see Figure 1.1).

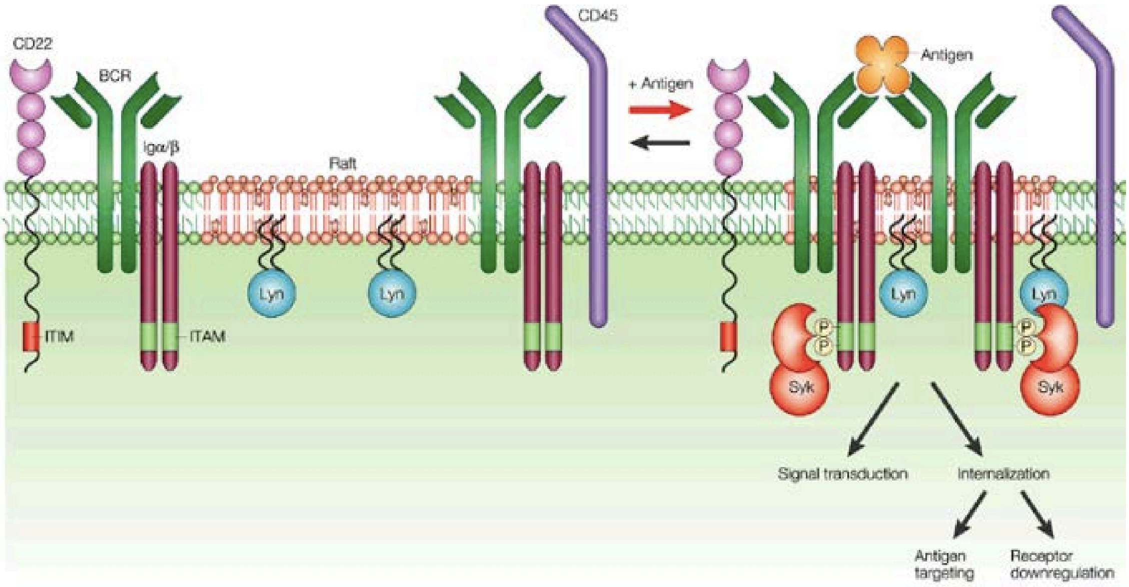
CD22
BCR
Igα/β
Raft
CD45
+ Antigen
Antigen
Lyn
Lyn
Lyn
Lyn
ITIM
ITAM
P
P
P
P
Syk
Syk
Signal transduction
Internalization
Antigen targeting
Receptor downregulation

Figure 1.1 The classic model of B cell activation. BCR engagement by antigen triggers the formation of BCR oligomers which converge to form signalling platforms called microclusters. Various signalling molecules are also recruited to these microclusters, such as Syk and Lyn, resulting in the phosphorylation of the ITAMs and initiation of downstream signalling cascades (Pierce, 2002)**.**

However, it is thought that the cross-linking model of receptor dimerization cannot provide an explanation for B cell activation when consideration is given to the diverse library of BCR ligands and the likelihood that two BCR-complexes are available on the cell surface at the right distance preferred for signalling. Furthermore, this model is in conflict with the finding that many monovalent antigens can engage the BCR and elicit B cell activation (Kim et al., 2006, Avalos et al., 2014, Mukherjee et al., 2013).

Many studies have demonstrated that BCRs exist as pre-clustered oligomeric complexes on the surface of resting B cells (Schamel and Reth, 2000, Fiala et al., 2013, Yang and Reth, 2010, Depoil et al., 2009). A model proposed by Reth and Yang (2010) suggest the ITAM motifs of the BCR oligomer are not accessible for phosphorylation prior to binding of antigen, but upon binding of antigen there is a conformational change in the BCR whereby the oligomer dissociates leaving the ITAM motifs available to Src kinases, and thus leading to B cell activation (Figure 1.2) (Yang and Reth, 2010). A major advantage of this conformational change is that it can explain how monovalent antigens can activate B cells, it being difficult to envisage how monovalent antigen binding can induce BCR clustering in the crosslinking model, However, further experimental evidence to support this model is still required.

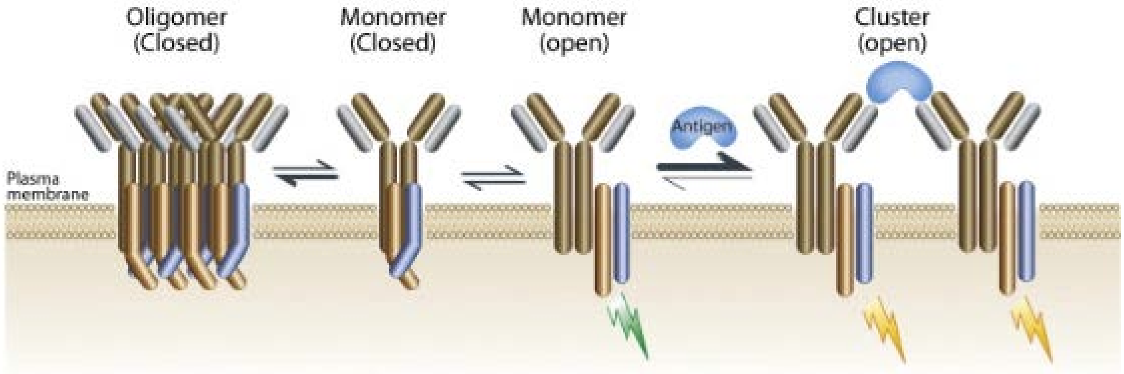

Figure 1.2 The model of B cell activation as proposed by Reth and Yang. Schematic of the model proposed by Reth and Yang. According to this model the BCR exists in an oligomeric structure on resting B cells. In this state the ITAM motifs are not accessible to kinase (closed). In the presence of antigen the equilibrium between closed BCR oligomers and monomers is shifted toward the open clustered monomers. It is the dissociation that makes the Ig tails more accessible for phosphorylation and this drives activation (Adapted from Yang and Reth, 2010).

1.2.2 T cell activation

The primary signal for T cell activation occurs through the binding of the T cell receptor (TCR) to antigenic peptides bound to MHC molecules displayed on the surface of antigen presenting cells (APCs) (Malissen et al., 2014). The TCR is a complex consisting of an αβ-heterodimer that recognizes peptide-MHC, and

CD3 proteins which contain one or several ITAMs in their cytoplasmic tails. The co-receptors CD8 and CD4 assist the TCR in the recognition of peptide presented on MHC class I and MHC class II molecules, respectively (Malissen et al., 2014). Binding of the TCR to peptide-MHC complexes on the cell surface leads to phosphorylation of the ITAMs on associated CD3 proteins and subsequently the recruitment and activation of zeta associated protein 70kDa (ZAP-70). The activation of ZAP-70 initiates several downstream signalling pathways through the Linker of Activated T cells (LAT) molecule (Dustin and Depoil, 2011).

Similar to B cells, T cells require co-ligation of other cell surface receptors which provide additional signals required for productive T cell activation, proliferation and effector differentiation (Smith-Garvin et al., 2009). There are numerous surface receptors that have been described as having co-stimulatory functions, however, the most well described and physiologically relevant co-stimulatory receptor on T cells is CD28. Binding of CD28 to its ligands CD80 or CD86 on the surface of APCs results in the activation of PI3K that ultimately leads to increased production of the transcription factor NF-κB, which acts to sustain antigen-induced proliferation of T cells. In response to signalling via the TCR and CD28, T cells quickly become responsive to cytokines such as IL-12 and IL-4 which are produced and delivered by the APC to the T cells and result in the activation of lineage-specific transcription factors that control the differentiation of T cells into various effector types (Malissen et al., 2014).

1.2.3 The Immunological Synapse

Antigen recognition by B cells and MHC-peptide recognition by T cells triggers an intercellular signalling cascade that directs the formation of an immunological synapse (IS) between the two interacting cells (Kuokkanen et al., 2015). In the case of T cells, formation of the IS is an important event in initial T cell activation following MHC-peptide recognition. In contrast, B cells can respond to soluble antigen but IS formation becomes particularly important in germinal centres when somatically mutated B cells are being selected for BCRs with higher affinity for antigen, the antigen being displayed on the surface of follicular dendritic cells as Fc receptor bound immune complexes. The IS structure is characterized by a dynamic spatial reorganisation of antigen receptors, co-stimulatory molecules and adhesion proteins to specific membrane domains that are connected to the underlying cytoskeleton at the cell-cell interface (Rocha-Perugini et al., 2015). This compartmentalisation exists as a two-phase process that first involves spreading of the cell membrane to maximize contacts with the adjacent cell followed by a contraction phase (Figure 1.3) (Kuokkanen et al., 2015, Kumari et al., 2014). It is thought that the spreading phase is to significantly increase the surface area of the cell-cell contact, thereby enabling the sampling of maximal amounts of antigen (Ueda et al., 2011). During the spreading phase, antigen-receptor complexes, costimulatory proteins and signalling molecules coalesce into micro-clusters. These micro-clusters form in the periphery of the IS prior to converging towards the centre of the IS known as the central supra-molecular activation cluster (cSMAC) (Smith-Garvin et al., 2009). The cSMAC is surrounded by a peripheral SMAC (pSMAC) where integrins and adhesion receptors are localized (Figure 1.3) (Rocha-Perugini et al., 2015, Kuokkanen et al., 2015, Carrasco et al., 2004). Once the defined pSMAC and cSMAC are spatially segregated the synapse is termed a mature immunological synapse (Batista and Harwood, 2009).

Although the formation and organization of immune synapses is well defined, less well known is how they function, which remains a topic of controversy.

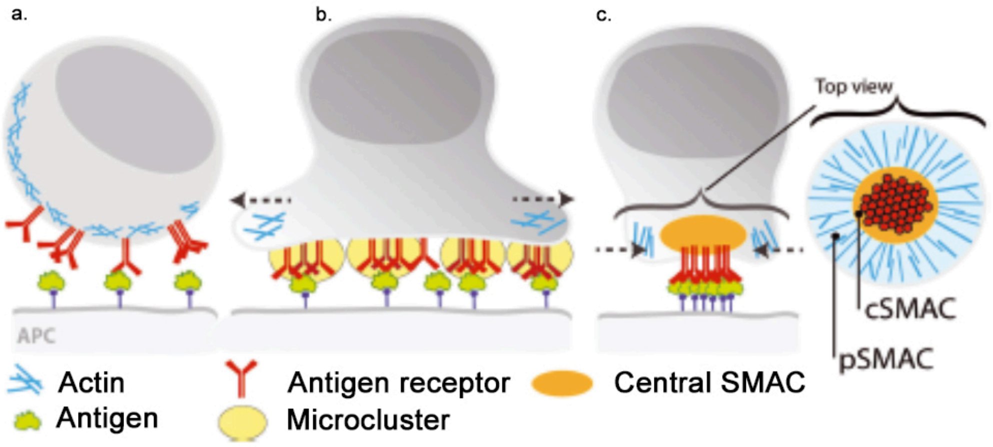

Figure 1.3 Formation of an immunological synapse (IS). (a) The formation of the IS is triggered by the binding of the antigen receptor to its specific antigen on the APC, antigen being peptide-MHC in the case of T cells or antigen containing immune complexes, typically bound to Fc receptors, in the case of B cells. (b) Next, the lymphocyte spreads over the APC and forms signalling micro-clusters. (c) During the maturation of the synapse, the cell contracts and gathers the antigen in the central cluster, cSMAC. (d) A top-view of the concentric structure of the IS, showing antigen-receptor rich cSMAC and actin-rich pSMAC (adapted from Kuokkanen et al., 2015).

However, it is evident that the IS has unique functions in different cell types. In B cells the IS serves as a platform for antigen internalization (Kuokkanen et al., 2015). Internalisation most likely occurs at the cSMAC where antigen is gathered into micro-clusters, endocytosed, processed into peptides and subsequently loaded onto MHC class II molecules and relocated back to the cell surface for presentation to CD4$^+$ T cells (Kuokkanen et al., 2015, Harwood and Batista, 2011). Although T cells and B cells have considerable similarities in synapse formation, T cells do not process antigen further and thus the increased TCR internalization at the IS is suggested to be a mechanism to down regulate TCR at high MHC-peptide concentrations (Martinez-Martin et al., 2011, Cemerski et al., 2008). In contrast, the T cell IS also serves to boost TCR triggering in the presence of low MHC-peptide concentrations by enhancing the stimulatory potency of weak agonists (Cemerski et al., 2008).

Relevant here is the possibility that the IS can facilitate intercellular communication, with several findings suggesting that another function of IS formation is the transfer of cell surface proteins and associated membranes between cells (Stinchcombe et al., 2001, Batista et al., 2001). Thus, Wetzel *et al.* (2005) demonstrated that as T cells spontaneously disassociate from APCs they often capture MHC-peptide complexes directly from the immunological synapse. B cells can also acquire membrane bound antigen from target cells following formation of an IS between the two cells (Batista et al., 2001). NK cells also transfer molecules through synapses (Tabiasco et al., 2002), as do tumour cells (Poupot and Fournie, 2003). Typically acquisition occurs within minutes of synapse formation and although the acquired molecule is often internalized, in some circumstances it remains or is returned to the surface of the recipient cell in a functional form (Rechavi et al., 2007, McCann et al., 2007).

1.3 Membrane Transfer in the Immune System

While Burnets Clonal Selection Theory has been invaluable in expanding our knowledge of how the immune system responds to infections, studies have indicated that the single specificity model proposed by Burnet may not be absolute. In fact, it has been shown that lymphocytes can actively transfer their antigen receptors to non-specific neighbouring lymphocytes via membrane transfer (Quah et al., 2008, Chaudhri et al., 2009), resulting in recipient lymphocytes expressing antigen receptors of different specificities. This phenomenon provides a mechanism for rapidly amplifying the immune response to a foreign antigen that is independent of cell division. Thus, for B cells antigen receptor transfer would greatly increase the number of antigen-specific B cells that can capture and present antigen to CD4$^+$ T cells,, thus potentially enhancing the speed at which the adaptive immune response can respond to an infection. For T cells, antigen receptor transfer via membrane exchange would rapidly increase the number of antigen specific CD4$^+$ and CD8$^+$ T cells at sites of infection and thus help contain the pathogen.

Membrane transfer itself is not a new phenomenon, it being first described over 30 years ago when T cells were shown to acquire surface immunoglobulin molecules from B cells (Hudson and Sprent, 1976, Hudson et al., 1974, Cone et al., 1972) and foreign antigens from macrophages (Bona et al., 1973). However, only more recently with advances in scientific techniques such as flow cytometry, has this process been studied more broadly and shown to be widespread. The majority of such studies in the early 2000’s focused on protein and membrane acquisition by T cells (Arnold and Mannie, 1999, Huang et al., 1999, Hwang et al., 2000, Hudrisier et al., 2001), with fewer reports of membrane transfer by B cells (Batista et al., 2001) and NK cells (Carlin et al., 2001). In 2002, Hudrisier and Joly termed this process ‘trogocytosis’, with ‘trogo’ meaning ‘to gnaw’ or ‘to nibble’ in ancient Greek. They described trogocytosis as the unidirectional passage of plasma membrane components from a presenting cell to a lymphocyte (Hudrisier and Joly, 2002), as the T cell acquisition of ligands from the APCs was largely unidirectional.

However, there are many occurrences of bidirectional membrane transfer between cells. For instance, membrane transfer between NK cells and their targets has been shown to be bidirectional. Cell to cell interactions between NK cells and target cells expressing MHC class I resulted in NK cells expressing MHC class I and target cells expressing the inhibitory NK receptors Ly49a, in experiments with mouse target cells, and killer immunoglobulin-like receptors or KIRs, in experiments with human target cells (Vanherberghen et al., 2004). Moreover, bidirectional membrane transfer has been demonstrated between dendritic cells and T cells (He et al., 2007), macrophages/monocytes and monoclonal Ab-opsonised target cells (Daubeuf et al., 2010b), and between B cells (Quah et al., 2008). As such, the term ‘trogocytosis’ is used less rigorously and commonly refers to the cell-to-cell contact dependent exchange of plasma membrane and surface molecules between cells, regardless of directionality. However, these diverse characteristics described by different groups have meant that the intercellular transfer of cell surface proteins and membranes is referred to by different names including absorption, acquisition, internalization, snatching, stripping and shaving (Rechavi et al., 2009). However, whether these are unique phenomena with distinctive mechanisms or whether they all refer to an identical process is still to be elucidated.

1.4 Mechanisms of intercellular transfer

Despite numerous investigations, the molecular mechanisms that control membrane transfer remain unclear. However, at the cellular level there are a number of mechanisms generally thought to be responsible for facilitating transfer of proteins and membranes between cells, each with its own unique characteristics. Features include transfer via direct cell-cell contact, exosome uptake and membrane nanotube formation and are described below.

1.4.1 Direct membrane transfer via cell contact

Membrane transfer is often strictly dependent on cell-to-cell contact and is completely inhibited when a semi-permeable transwell membrane separates the donor and recipient cells (Rechavi et al., 2009, Herrera et al., 2004, Game et al., 2005). Transfer via direct cell-cell contact can be distinguished from other mechanisms of transfer as being a process that allows the rapid transfer of intact cell-surface proteins between cells in contact with one another (Davis, 2007). There is evidence to suggest that the avidity of interaction between cells, particularly during IS formations, is sufficient for the transfer of molecules in the form of membrane fragments. When a lymphocyte forms an IS with its target the association is stabilised by the cytoskeleton and can lead to local membrane fusion (Sprent, 2005, Huang et al., 1999, Stinchcombe et al., 2001). Dissociation of the cells may cause portions of the membrane to be pinched off one cell and transferred to another (Sprent, 2005). Using live cell imaging Wetzel *et al* (2005) were able to demonstrate that T cells, whilst spontaneously dissociating from APC’s, commonly acquire MHC-peptide complexes directly from the IS (Figure 1.4a) (Wetzel et al., 2005). In fact, many cell types transfer molecules through synapses, for example, B cells take up antigen from T cells following synapse formation (Batista et al., 2001), NK cells capture membrane fragments during engagement with target cells (Tabiasco et al., 2002, Carlin et al., 2001), and even some tumour cell lines can take up patches of autologous membranes through IS-like structures (Poupot and Fournie, 2003). Transfer of bystander molecules and membranes commonly accompanies this process (Cox et al., 2007, Xiang et al., 2005), suggesting that a portion of the membrane is transferred as a whole membrane fragment, including its cell surface proteins. Transfer occurs within minutes of IS formation (Huang et al., 1999, Tabiasco et al., 2002) and the transferred molecules commonly appear at the cell surface and are fully functional.

In the case of T cells, Martinez-Martin *et al* (2011) recently examined the mechanism of TCR internalization at the IS and demonstrated that it was coupled to TCR-triggered acquisition of membranes and cell-surface proteins from the APC. They further showed that this transfer is dependent on the small GTPases TC21 and RhoG which co-localise with the TCR at the IS (Delgado et al., 2009). Martinez-Martin *et al* (2011) found that TC21 is necessary for TCR internalization from the IS by a clathrin-independent mechanism and that this is dependent on RhoG. T cells derived from TC21- or RhoG-deficient mice exhibited only slightly reduced TCR down regulation, suggesting that clathrin-mediated internalization of TCRs was occurring. In contrast, the transfer of membrane patches and associated MHC molecules was substantially decreased in both CD4$^+$ and CD8$^+$ T cells from these deficient mice. Due to RhoG having previously been associated with phagocytosis, the authors suggest that the process is a consequence of an incomplete phagocytosis of the entire APC by the T cells, subsequently resulting in the removal of APC membranes and associated molecules. The destiny of the internalized TCR and accompanying APC membrane fragments remains unclear, although preliminary data indicate that they may be recycled to the plasma membrane (Martinez-Martin et al., 2011).

The activation state of T and B lymphocytes plays an important role in membrane transfer. There is a multitude of literature demonstrating that activated lymphocytes perform membrane transfer to a far greater extent than their naïve counterparts (Poupot and Fournie, 2003, Hudrisier et al., 2005, Quah et al., 2008). It has been suggested that the increased expression of particular molecules by activated lymphocytes leads to increased adhesion that could facilitate this difference (Hwang et al., 2000). Consistent with this is the increased expression and conformational changes of adhesion molecules in both activated B and T cells (Hivroz and Saitakis, 2016, Nishida et al., 2006, den Haan et al., 2014).

Also, there is experimental evidence to suggest that the mechanism of direct membrane transfer of membrane fragments varies between different immune cells. For example, the requirements for membrane transfer by B cells appear to be less stringent than those for T cells. Membrane transfer is an energy-dependent process in T and NK cells, requiring both receptor signalling and actin cytoskeletal remodelling (Aucher et al., 2008), whereas this appears to be not the case with B cells (Aucher et al., 2008, Quah et al., 2008). Thus, B cells but not T cells, remain capable of membrane transfer in the presence of inhibitors of the Src- Syk- and phosphatidylinositol-3-kinase pathways, which target important enzymes in antigen receptor signalling pathways in both B and T cells.

B cells are also capable of membrane transfer in the presence of the actin polymerization inhibiting drugs latrunculin B and cytochalasin D (Aucher et al., 2008). These inhibitors have limited effects on membrane transfer experiments with B cells, however, they markedly inhibit membrane transfer by both CD4$^+$ and CD8$^+$ T cells. Similarly, B cells remain capable of membrane transfer at temperatures as low as 4°C whereas this is less evident with T cells (Quah et al., 2008), providing further evidence that T cells require the actin cytoskeleton and certain enzymatic activities to perform membrane transfer whereas these processes are dispensable for membrane transfer by B cells.

In summary, it appears that tight junctions formed between two cells, such as with the IS, play an important role in the transfer of membranes and associated proteins, with the strength of the interaction often determining the amount of membrane transferred (Hwang et al., 2000, Sabzevari et al., 2001). However, the contrasting features required for membrane transfer by different cell types suggests that the exact mechanism may vary. Thus, it appears that membrane transfer is influenced by the nature of the cells involved, their state of activation and the surrounding environment.

1.4.2 Nanotube-mediated membrane transfer

Another cell-contact dependent method of membrane transfer between immune cells is through membrane nanotubular networks. Nanotubes are long membranous tethers formed between cells either at the termination of the IS as the cells dissociate, or through an extension of membrane from one cell fusing to another (Onfelt et al., 2004), although it is likely that these two processes are not mutually exclusive events. Nanotube formation has been observed in a range of cell types, including T cells, B cells, NK cells, neutrophils and monocytes (Ahmed and Xiang, 2011). Although the functional role for nanotubes is still under debate, studies have shown that nanotubes between myeloid cells can mediate intercellular calcium fluxes and thus induce phenotypic changes including lamellipodial spreading (Watkins and Salter, 2005). They can also provide for the exchange of cell-surface proteins and membranes as well as cytoplasmic content (Gerdes and Carvalho, 2008). Studies using time-lapse imaging have shown membrane nanotube formation between B cells (B721.221) and T cells (Jurkat) following prolonged cell-cell contact (Rainy et al., 2013). Rainy *et al* (2013) demonstrated that following separation of the IS between B and T cells, the cells maintain contact through fine plasma membrane derived extensions, otherwise known as nanotubes and that these nanotube facilitate the lateral diffusion of GFP-H-Ras-enriched plasma membrane patches to the T cell surface (Figure 1.4b). Additionally, during the formation of an IS between B and T cells the same study demonstrated that H-Ras is also directly transferred to the T cell in a process that resembles membrane transfer (Rainy et al., 2013), indicating that these processes are not necessarily mutually exclusive events.

Studies have shown that nanotube formation requires that cells be in contact for a considerable length of time - if cells dissociate too quickly nanotube formation does not occur (Sowinski et al., 2008). This may reflect the amount of time required to create intercellular contacts of strong avidity which can withstand the forces required to draw out surface membranes as cells dissociate (Davis and Sowinski, 2008). Additionally, this property potentially eliminates the involvement of nanotubes as a mechanism for the ‘rapid’ transfer of membranes and cell surface proteins between cells.

1.4.3 Exosomes and membrane transfer

In addition to cell contact dependent mechanisms of membrane transfer many cells utilise a cell contact independent method to transfer molecules via the secretion of exosomes (Figure 1.4c). Exosomes are small membrane vesicles (50-100 nm in diameter) secreted by a wide range of different cell types and represent another mechanism of intercellular membrane transfer between cells (Ahmed et al., 2008, Ahmed and Xiang, 2011). They are formed by inward budding of endosomal membranes or multi-vesicular bodies (MVB) within the cell and are secreted when the MVB fuses with the outer cellular membrane (van Niel et al., 2006).

Exosomes can transfer membranes and molecules that can be degraded and reprocessed for presentation on endogenous MHC molecules by recipient APCs (Morelli et al., 2004). Alternatively, they can donate preformed MHC-peptide complexes that have demonstrated functional capacity (Thery et al., 2002, Thery et al., 2009, Wolfers et al., 2001). For example, MHC-deficient dendritic cells can acquire MHC class II molecules from dendritic cell-derived exosomes, integrate these molecules into their membranes and subsequently stimulate antigen-specific CD4$^+$ T cell proliferation *in vitro* (Thery et al., 2002). Similarly, studies by Nolte't Hoen et al (2009) demonstrated that mature dendritic cells pulsed with exosomes stimulate enhanced cytotoxic T lymphocyte (CTL) responses and anti-tumour immunity and that, in this instance, the uptake of exosomes by mature dendritic cells is mediated through the LFA-1/ICAM-1 receptor ligand interaction and is dependent upon T cell activation via TCR/CD28-mediated signalling (Nolte-'t Hoen et al., 2009).

Although some features of exosome-mediated membrane transfer and membrane transfer between B cells is similar, they are considered to be distinct mechanisms due to a few unique features. As described above, membrane transfer between B cells is rapid, with substantial BCR transfer evident within 10-20 min (Quah et al., 2008). Transfer between NK and target cells is similarly rapid, with 3% of total NK cell KIRs (~3000 molecules per cell) being transferring after an hour of co-incubation. Such transfer is significantly faster

Figure 1.4 Intercellular exchange of membranes and cell surface proteins via direct membrane transfer, exosomes and nanotubes. (a) Tight contacts between lymphocytes and their targets allows for the exchange of membranes and cell-surface-bound molecules. Some ligands are acquired following interaction with specific receptors and other non-specific bystander ligands, and membrane patches may also be transferred simultaneously. (b) Long membrane nanotubes that extend between neighbouring cells also promote contact-dependent transfer of membranes and cell-surface molecules. Nanotubes are also formed following cell-cell contact. (c) Exosomes are membrane vesicles formed from multivesicular bodies (MVBs). They are secreted by a variety of cell types and can transfer proteins and signals from one cell type to another. Adapted from Rechavi et al., (2009).

a. Membrane Transfer

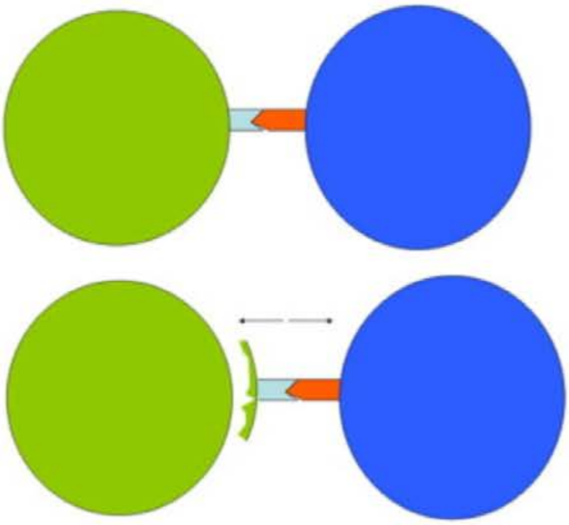

b. Nanotubes

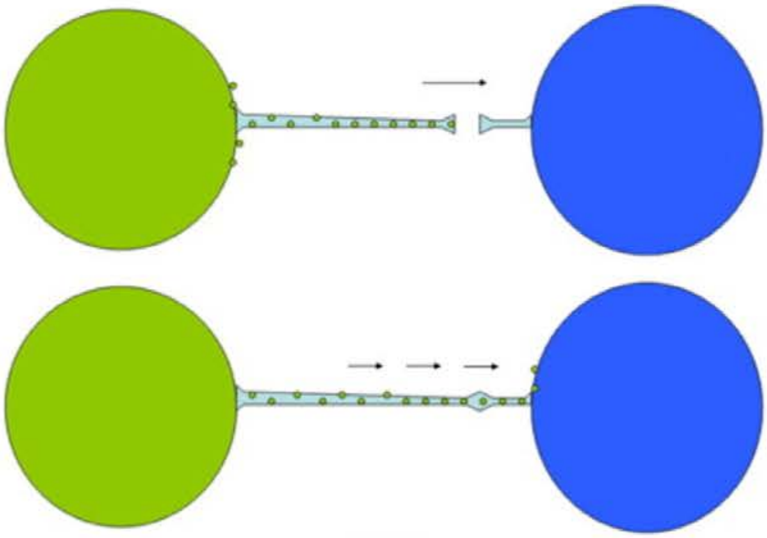

c. Exosomes

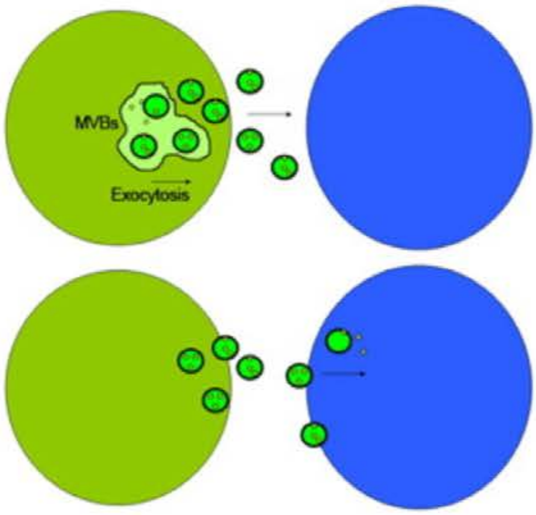
MVBs
Exocytosis

than could possibly occur through constitutive transfer via exosomes, which typically takes several hours (Davis, 2007, Wakim and Bevan, 2011, Smyth et al., 2008). Exosome-mediated transfer is not only a relatively slow process, but rather than requiring direct cell contact, can occur over substantial distances, being not inhibited by a semi-permeable transwell system (Rechavi et al., 2009, Davis, 2007, Zomer et al., 2010). However, recently it was demonstrated that T cells can secrete exosomes upon formation of a functional IS at the APC contact site (Mittelbrunn et al., 2011). Thus, under these circumstances, the separation of T cells and APCs via a semipermeable membrane, as in the transwell culture system, would not only prevent membrane exchange by direct cell contact but also inhibit exosomal-mediated transfer, demonstrating the difficulty in experimentally discriminating between different mechanisms of intercellular membrane transfer.

1.5 Functional consequences of membrane transfer

Transfer of membranes and cell surface proteins has also been shown to result in altered cell functions. For instance, CD4$^+$ T cells can acquire MHC class I and class II molecules and costimulatory molecules from APCs following formation of an IS and subsequently act as APCs (Xiang et al., 2005, Wetzel et al., 2005). The acquired molecules were demonstrated to be functional, with the ovalbumin (OVA)-MHC-I specific antigen-presenting CD4$^+$ T cells capable of inducing OVA-specific OT-I CD8$^+$ T cells to proliferate and differentiate into CTL effectors both *in vitro* and *in vivo* (Xiang et al., 2005). Moreover, the antigen-presenting CD4$^+$ T cells were able to induce OVA-specific anti-tumour immunity in C57BL/6 mice growing OVA-expressing B16 melanoma (Umeshappa et al., 2009, Xiang et al., 2005), with this anti-tumour effect being mediated by endogenous CD40L, acquired CD80 co-stimulator molecules and endogenous IL-2 secretion (Umeshappa et al., 2009).

MHC-peptide complex acquisition by T cells has also been reported to contribute to sustained T cell signalling (Osborne and Wetzel, 2012, Zhou et al., 2005). Acquired MHC-peptide complexes in concert with other APC membrane molecules co-localise with TCR and the TCR signalling molecules, pZAP-70 and Lck on CD4+ T cells following dissociation from APCs (Osborne and Wetzel, 2012, Wetzel et al., 2005). This accumulation of signalling molecules coincides with an increase in total tyrosine phosphorylation and activation of TCR signalling molecules. Osborne and Wetzel (2012) also demonstrated, using a Src inhibitor, that the acquired molecules continued to engage their receptors following transfer and resulted in sustained TCR signalling. Furthermore, the recipient T cells preferentially survived in cell culture when compared to T cells that had not acquired membrane patches, suggesting that sustained signalling may provide a selective advantage (Osborne and Wetzel, 2012). This could play an important role in immune modulation, the sustained signalling due to membrane transfer leading to increased T cell effector function or, alternatively, resulting in cellular exhaustion and activation induced cell death.

Dendritic cells (DCs) also acquire MHC class I from neighbouring cells through membrane transfer (Harshyne et al., 2001, Russo et al., 2000). Usually, APCs such as DCs acquire antigen, process it intracellularly, and present it in the context of their own MHC molecules thereby activating T cells that are restricted to the MHC genotype and peptide specificity generated by the DC (Bevan, 2006). In contrast, membrane transfer of intact MHC–peptide complexes requires no further processing, thus representing an alternative mechanism of indirect antigen presentation. DCs presenting antigen to T cells without the need of further processing has been demonstrated both *in vitro* and *in vivo* in the context of boosting both anti-viral and anti-tumour responses (Chaudhri et al., 2009, Wakim and Bevan, 2011, Dolan et al., 2006a, Dolan et al., 2006b, Bonaccorsi et al., 2014).

Wakim and Bevan (2011) showed that DCs from B6.GFP mice, following co-culture with DCs from SIINFEKL pulsed B6.SJL mice, were capable of driving T cell expansion of OT-I transgenic T cells which express a TCR that recognizes SIINFEKL, and that this was a result of the B6.GFP DCs acquiring MHC-SIINFEKL peptide complexes. Fixation of the recipient DCs prior to co-culture with donor DC’s abolished their ability to stimulate OT-I T cell proliferation, however, MHC-peptide transfer occurred when recipient DCs were deficient in transporter associated with antigen processing (TAP) molecules thus indicating that the MHC-peptide acquisition is not a consequence of conventional cross presentation. It was further shown that acquisition of peptide-MHC complexes by the recipient DCs was not via exosomes released by donor DCs, nor was it due to free peptide in the culture medium. Rather, the DCs acquired MHC-peptide complexes capable of driving CD8+ T cell activation via a mechanism that requires cell contact as physical separation of donor and recipient DCs using a transwell system prevented MHC-peptide transfer. Wakim and Bevan were also able to demonstrate that recipient DCs are able to present antigen *in vivo* and that such presentation can promote the expansion of resting memory T cells (Wakim and Bevan, 2011). Similarly, in a collaborative study undertaken by the laboratory of my supervisor, Professor Christopher Parish, and the laboratory of Dr Guna Karupiah, it was demonstrated that virus-specific CD8$^+$ CTL could transfer their TCR to nearby CTL of an irrelevant specificity resulting in the rapid expansion of virus-specific T cell clones (Chaudhri et al., 2009). The study involved ectromelia virus (ECTV)-specific CTL whose effector function depends upon perforin (Prf)-mediated cytotoxicity. The investigation made use of the knowledge that adoptive transfer of WT ECTV-specific CTL, but not perforin deficient (Prf-/-) CTL, results in the control of ECTV in infected recipients. However, it was demonstrated that when Prf-/- ECTV-specific CTL were transferred in combination with CTL of an irrelevant specificity the ECTV infection was cleared, suggesting that the non-cytolytic Prf-/- CTL were capable of transferring their TCR to bystander CTL of an irrelevant specificity. This interpretation was confirmed by the demonstration *in vitro* that the bystander CTL had gained cytolytic activity against ECTV. Similar results were obtained with the co-transfer of Prf-/- OVA-specific TCR-transgenic OT-I CTL and influenza A virus (IAV)-specific transgenic CTL into ECTV-OVA infected mice. The IAV-specific CTL were able to act as recipients of the OVA-specific TCR and gained the ability to clear the OVA-expressing ECTV. This illustrates that TCR sharing allows rapid expansion of virus specific CTL resulting in the protection of the host from an otherwise lethal viral infection.

Membrane transfer has been previously implicated in tumour immunology, both in the control of tumour growth and as a mechanism of tumour escape. NK cells that acquire NKG2D ligands from tumour cells not only stimulate activation of autologous NK cells, but also become targets for NK cell fratricide (Nakamura et al., 2013, Lopez-Cobo et al., 2015). The expression of NKG2D ligands is induced during times of cellular stress such as infection or malignant transformation (Nakamura et al., 2013). Thus, the activating receptor NKG2D on NK cells can recognise potentially dangerous cells such as tumour cells and eliminate them via NK-cell mediated lysis. Interestingly, along with cytolytic activity NK cells can rapidly acquire NKG2D ligands from tumour cells, thus rendering the recipient NK cell susceptible to fratricide. Studies have also shown that NKG2D expressing malignant cells are capable of down regulating NKG2D expression by NK cells (Ogasawara et al., 2003), so together with NK cell fratricide, this represents a new mechanism for tumour escape from NK cell lysis (Nakamura et al., 2013, Ogasawara et al., 2003).

This is not the only example where membrane transfer has been implicated in tumour immune escape. Indeed, acquisition of human leukocyte antigen (HLA)-G by T cells from HLA-G expressing tumour cells can result in the recipient T cells becoming temporarily suppressive towards other T cells (LeMaoult et al., 2007). HLA-G can be expressed by many types of malignancies and is associated with a strong immunosuppressive function. Examples of immune regulatory effects following HLA-G acquisition from tumour cells include inhibition of NK cell and CTL lytic activities and their ongoing cellular proliferation (LeMaoult et al., 2007, Maki et al., 2008, Caumartin et al., 2007), and the generation of regulatory T cells (Brown et al., 2012). Furthermore, LeMaoult *et al* (2015) have recently demonstrated that tumour-tumour transfer of HLA-G is prominent, indicating that tumour cells may be capable of sharing immune escape strategies via membrane exchange.

1.6 Concluding remarks

Collectively, the data presented in this review show that cells of the immune system can acquire from other leukocytes membranes and cell surface proteins that are functional and potentially allow the recipient cells to utilise proteins that they do not endogenously express. This means that the functions that an immune cell actually performs may differ from the functions that they originally set out to perform and it is evident that the environment in which a cell resides can dictate these functions. Thus, membrane transfer could be contributing to an enhanced immune response by multiplying the number of cells recognising or presenting antigen, expanding the repertoire of cells that can function as APCs, and sustaining signalling in the absence of APC-T cell interactions. Alternatively, membrane transfer could also be contributing to the down regulation of immune responses by aiding the induction of peripheral tolerance and the loss of effector function. Based on the above, membrane transfer may have profound consequences for the immunological responses against tumours and infectious diseases and may also modulate autoimmune diseases. For all these reasons, future work to determine the mechanisms that mediate membrane transfer, including the roles of the donor and recipient cells during transfer and the particular physical properties that influence the efficiency of transfer, is considered of upmost importance.

1.7 Thesis Experimental Aims

Previous studies in my supervisor's laboratory have shown that B cells, when activated by either LPS or T helper cell signals (e.g., CD40L), can donate their BCR by membrane transfer to both naïve and activated neighbouring B cells both *in vivo* and *in vitro* (Quah et al., 2008). The BCR transfer between activated B cells was found to be extremely rapid, with substantial transfer being observed within 10-20 minutes, and by 60 minutes the recipient B cells gaining ~60% the BCR level that the recipient B cells expressed after 3 days of continuous co-culture. Furthermore, activated B cells from µM2-/- mice, which do not have the ability to secrete IgM, were also capable of BCR transfer, indicating that BCR transfer is independent of Ig secretion. In addition, the level of BCR transfer increased in the presence of BCR-specific antigen. Possibly the most important feature of this transfer was that the transferred BCR on recipient B cells was functionally active, capable of capturing and presenting antigen to CD4$^+$ T cells.

Although the process of membrane transfer has becoming increasingly recognized, particularly between cells of the immune system, the molecular mechanisms involved remain a topic of debate. Thus, the first two aims of this thesis involve different techniques that attempt to define the molecular basis of membrane transfer between B cells, specifically:

1. To determine the similarities and potential involvement of positively charged residues in the process of membrane transfer between B cells
2. To identify potential cell surface proteins that may be involved in membrane transfer between B cells by using comparative microarray technologies with the knowledge that B cells require specific activation conditions for membrane transfer to occur.

As discussed in Section 1.6, in another membrane transfer study in my supervisor's laboratory, it was demonstrated that virus-specific CD8$^+$ cytotoxic T lymphocytes (CTL) can transfer their TCR to bystander CTL of an irrelevant specificity, thus rapidly expanding the number of virus-specific CTL and resulting in the protection of the host from an otherwise lethal viral infection. Based on these observations it was anticipated that membrane transfer can enhance antigen specific immune responses in a variety of settings with adoptive CTL immunotherapy against tumours being an obvious clinical application. With this in mind the final aim of this thesis was:

To investigate whether TCR sharing between CTL can be harnessed for adoptive immunotherapy of tumours. In order to achieve this aim an adoptive T cell immunotherapy model involving OVA expressing EG7 tumour cells and OVA-specific OT-I CTL was used, advantage being taken of previous reports that OT-I mediated lysis of the EG7 tumour cells is perforin dependent. Thus, perforin deficient OT-I CTL and bystander P14 CTLs with an irrelevant antigen specificity could be used to detect TCR sharing in the adoptive immunotherapy of EG7 tumours, this approach being very similar to that used to measure TCR exchange between viral-specific CTLs (Chaudhri et al., 2009).

Collectively, it was hoped that the studies undertaken for this PhD thesis would shed some light on the molecular basis of membrane exchange and provide a clinically relevant example of the harnessing of membrane exchange, namely the enhancing of CTL-mediated cancer immunotherapy.

Chapter 2

Materials and Methods

This Chapter details the materials and methods used for the experiments documented in this thesis.

2.1 Materials

2.1.1 General reagents and equipment

All reagents used were of analytical grade, or the highest grade obtainable.

2.1.2 Media, buffers and solutions

Media was prepared by the Media Facility within The John Curtin School of Medical Research (JCSMR), Australian National University (ANU), Canberra, Australia or commercially purchased as noted in Table 2.1. Media was prepared using double distilled Milli-Q water (ddH2O) and filtered through a 0.22 μm Millipore (Billerica, MA) filters.

2.1.3 Animals

The strain, phenotype, background and source of mice used are detailed in Table 2.2. Experimental procedures were performed in accordance with the animal handling protocol (No. A2011/35) approved by the Animal Experimentation Ethics Committee of the Australian National University. The mice were maintained in PC2 facilities. Daily care and breeding was conducted by the staff of the Animal Services Division, Australian National University.

2.1.4 Mammalian cell lines

EL4 and EL4 transduced to express OVA (EG7-OVA) mouse lymphoma cell lines were purchased from the American Type Culture Collection (Manassas, VA). A frozen aliquot was thawed and grown in complete RPMI-1640 medium (Table 2.1) at 37°C and 5% CO_2 for each experiment. EG7-OVA cells were grown in the presence of 200 μg/mL G418 (Invivogen, San Diego, CA) to maintain the expression of the transfected OVA gene.

Table 2.1

Buffer/solution	**Components**	**Supplier**
1 X Lysis Buffer	10% (v/v) 10 x BD PharmLyse™ Lysis buffer	BD Pharmingen
Hank's Balanced Salt Solution (Prepared by Media Facility, JCSMR)	$NaCl$ 8 g/L KCl 400 mg/L $MgSO_4.7H_2O$ 100 mg/L $MgCl_2.6H_2O$ 100 mg/L $CaCl_2$ 112 mg/L Glucose 1 g/L Phenol Red 20 mg/L $NaH_2PO_4.2H_2O$ 78 mg/L KH_2PO4 60 mg/L	Merck, BDH Fronine, AR Ajax Chemicals Ajax Chemicals Merck, BDH Merck, BDH Sigma Merck, BDH Ajax Chemicals
Penicillin Streptomycin Neomycin (PSN) Antibiotics (Prepared by Media Facility, JCSMR)	Penicillin G 30.072 g/L Streptomycin sulphate 50 g/L Neomycin sulphate 50 g/L	ICN Sigma Sigma
Complete RPMI-1640	RPMI-1640 10% (v/v) foetal calf serum (FCS) 2 mM L-glutamine 0.1% PSN antibiotic 100 mM HEPES 1 mM sodium pyruvate 0.05 mM 2-mercaptoethanol	Sigma Fisher Biotec Media Facility, JCSMR Media Facility, JCSMR Gibco-Invitrogen Sigma Sigma
0.1% bovine serum albumin (BSA)/ phosphate buffered saline (PBS)	PBS 0.1% (w/v) BSA	Sigma Sigma

2.1.5 Antibodies

Table 2.3 details the antibodies used. All antibodies were purchased from commercial sources. Cells stained with biotin-conjugated primary antibodies were subsequently stained with 0.4 µg/mL of allophycocyanin-conjugated streptavidin (streptavidin-APC; BD Pharmingen). Isotype matched controls were used to ensure the specificity of antibody binding.

2.1.6 Kits

QIAamp® DNA Blood Mini Kit	QIAGEN
SuperScript™III	Invitrogen
2X SYBR Green PCR Master Mix	Applied Biosystems
2X Taqman® Universal PCR Master Mix	Applied Biosystems

2.1.7 Oligonucleotides

Oligonucleotides used in the experiments in this thesis are listed in Table 2.4

Primers used for quantitative cDNA real-time PCR for the validation of Affymetrix microarray analysis were purchased online from Taqman® Gene Expression Assays (Applied Biosystems, Forster City, CA).

Oligonucleotide CpG ODN 1668 was used for B cell stimulation and purchased from GeneWorks Pty Ltd, Adelaide, SA, Australia.

2.1.8 Cell Penetrating Peptides

Cell penetrating peptides (listed below) used for cell association studies were synthesised by GL biochem, (Shanghai) Ltd. Shanghai, China, with a biotin or fluorescein isothiocyanate (FITC) molecule added at the N-terminal amino group of the peptide sequence using 6-aminohexanioc acid as a spacer between the peptide and the conjugate.

Transcription transactivating (TAT) – GRKKRRQRRRPPQ

Penetratin – RQIKIWFQNRRMKWKK

Transportan10 (TP10) – AGYLLGKINLKALAALAKKIL

2.1.9 Liposomes

Liposomes suspensions were provided courtesy of Lipotek Pty Ltd., Canberra, ACT, Australia. Liposomes were prepared by mixing lipid stock solutions prepared in chloroform or ethanol, transferring to 10 mL round-bottomed flasks, and drying to a thin film using a rotary evaporator with a water bath set to 42°C. Non-PEGylated liposomes were comprised of POPC, cholesterol and□□-BODIPY 500-512 C12-HPC (see Table 2.5 for details) at the molar ratio of 155:44:1, and were prepared at a total lipid concentration of 8 mM. PEGylated liposomes were comprised of POPC, cholesterol, DSPE-PEG750 and□□-BODIPY 500-512 C12-HPC at the molar ratio of 150:44:5:1, and were prepared at a total lipid concentration of either 8 mM or 16 mM. After drying, thin lipid films were rehydrated in saline by gentle hand-shaking for 20 min, then manually extruded 15 times through either a 0.1 µm or 1 µm polycarbonate membrane using an Avanti Mini-extruder (Avanti Polar Lipids Inc, Alabaster, AL).

2.1.10 Flow cytometry equipment and software

Samples were analysed on a Becton, Dickinson and Company (BD) LSR Fortessa or a BD LSRII machine using BD CellQuest™ software (Franklin Lakes, NJ) or BD FACSDiva™ software (Franklin Lakes, NJ). Analysis of flow cytometry data was performed using FlowJo software (Tree Star Inc., Ashland OR).

Table 2.2 Animals used in Experimental Procedures

Mouse Strain Short Name	Mouse Strain	Background	Phenotype	Source	Reference
C57BL/6	C57BL/6	C57BL/6	WT	ANU Bioscience Research Facility (ABRF)	NA
OTI Prf-/-	C57BL/6.Prf^{1tm1Sdz} Tg(TcraTcrb)1100Mjb	C57BL/6	Transgenic TCR to recognize ovalbumin residues 257-264 in the context of H2K^{b}. Absence of perforin.	Guna Karupiah, JCSMR, ANU, Canberra, Australia	(Hogquist et al., 1994)
BALB/c	BALB/c	BALB/c	WT	ABRF	NA
B6.SJL.TCRP14	C57BL/6.Tg(TCRLCMVP14)-Tcra^{tm1Msm}.SJL-Ptprc^{a}Pep^{3b}/BoyJ	C57BL/6	Transgenic TCR specific for the lymphocytic choriomeningitis virus (LCMV) peptide gp33 in the context of H2K^{b} and CD45.1 congenic.	Guna Karupiah, JCSMR, ANU, Canberra, Australia	(Pircher et al., 1989)
OT-I	C57BL/6.Tg(TcraTcrb)1100Mjb	C57BL/6	Transgenic TCR to recognize ovalbumin residues 257-264 in the context of H2K^{b}	Chris Parish, JCSMR, ANU, Canberra, Australia	(Hogquist et al., 1994)
OT-I IFNγ-/-	C57BL/6-Infngtm1TsTg(Tcr	C57BL/6	Transgenic TCR to	Guna Karupiah, JCSMR,	(Hogquist et al., 1994)

Mouse Strain Short Name	Mouse Strain	Background	Phenotype	Source	Reference
	aTcrb)1100Mjb		recognize ovalbumin residues 257-264 in the context of H2K^{b}. Absence of interferon-gamma.	ANU, Canberra, Australia	
B6.SJL	C57BL/6.SJL-Ptprc^{a}Pep^{3b}/BoyJ	C57BL/6	CD45.1 congenic strain	ABRF	(Shen et al., 1985)
OT-II	C57BL/6 C-H-2bm1	C57BL/6	Transgenic TCR to recognize ovalbumin residues 323-339 in the context of I-A^{b}.	ABRF	(Barnden et al., 1998)
Rag1-/-	C57BL/6.129S7-Rag1tm1Mom/J	C57BL/6	Absence of functional B and T cells	ABRF	(Mombaerts et al., 1992)
HamLet:B6	HamLet:B6	C57BL/6	Transgenic Ig to recognize hen egg lysozyme (HEL)	Keisuke Horikawa, JCSMR, ANU, Canberra, Australia	(Mason et al., 1992)

Table 2.3 Antibodies used in Experimental Procedures

Antigen	Alternative names	Species	Raised in	IgG isotype	Clone	Source	Catalogue Number
Purified monoclonal antibodies							
CD32/CD16	Fcγ III/II Receptor	Mouse	Rat	IgG2b, k	2.4G2	BD Pharmingen	553142
Ly6G	Gr-1	Mouse	Rat	IgG2a	1A8-4-10-9	WEHI antibody facility	
CD152	CTLA-4	Mouse	Syrian Hamster	IgG	9H10	Biolegend	106202
	Isotype control		Rat	IgG2a		WEHI antibody facility	
	Isotype control		Syrian Hamster	IgG	SHG-1	Biolegend	402002
PE conjugated monoclonal antibodies							
IgM^{a}	Igh-6a	Mouse	Mouse (C57BL/6)	IgG1, k	DS-1	BD Pharmingen	553517
IgM^{b}	Igh-6b	Mouse	Mouse (BALB/c)	IgG1, k	AF6-78	BD Pharmingen	553521
Ly-6B.2		Mouse	Rat	IgG2a	7/4	Serotec	MCA771PE
NK1.1	NKR-P1B, NKR-P1C	Mouse	Mouse (C3H x	IgG2a, k	PK136	BD Pharmingen	553165
Vα2 TCR		Mouse	Rat	IgG2a, λ	B20.1	Biolegend	127808
TIGIT	VSTM3, WUCAM	Mouse	Rat	IgG2a, k	GIGD7	eBioscience	12-9501
CD166	ALCAM	Mouse	Rat	IgG2a, k	ebioALC48	eBioscience	12-1661
	Isotype control		Rat	IgG2a, k	R35-95	BD Pharmingen	553930
APC-eFluor® 780 conjugated monoclonal antibodies							
CD8a	Ly-2	Mouse	Rat	IgG2a, k	53-6.7	eBioscience	47-0081-82
APC conjugated monoclonal antibodies							
CD8a	Ly-2	Mouse	Rat	IgG2a, k	53-6.7	BD Pharmingen	553035
CD155	Polio Virus Receptor,	Mouse	Rat	IgG2a	TX56	eBioscience	17-1551
CD130	gp130, IL-6RB	Mouse	Rat	IgG2a, k	KGP130	eBioscience	17-1302

Antigen	Alternative names	Species	Raised in	IgG isotype	Clone	Source	Catalogue Number
CD223	LAG-3	Mouse	Rat	IgG1, k	C9B7W	Biolegend	125210
Vα2 TCR		Mouse	Rat	IgG2a, λ	B20.1	Biolegend	127810
	Isotype Control		Rat	IgG1, k	RTK2071	Biolegend	400412
	Isotype Control		Rat	IgG2a, k	R35-95	BD Pharmingen	553932
PerCP-Cy5.5 conjugated monoclonal antibodies							
CD45R	B220, Ly-5	Human/Mouse	Rat	IgG2a, k	RA3-6B2	eBioscience	45-0452
CD45.1	Ly-5.1	Mouse	Mouse (A.SW)	IgG2a, k	A20	Biolegend	110728
CD45.2	Ly-5.2	Mouse	Mouse (SJL)	IgG2a, k	104	BD Pharmingen	552950
CD11b	Integrin α_M chain	Human/Mouse	Rat	IgG2b, k	M1/70	BD Pharmingen	550993
Biotin conjugated monoclonal antibodies							
Vβ5.1/5.2	Vb5.1, Vb5.2	Mouse	Mouse	IgG1, k	MR9-4	BD Pharmingen	553188
CD45	LCA, T200, Ly-5	Mouse	Rat	IgG2b, k	30-F11	Biolegend	103104
PE/Cy7 conjugated monoclonal antibodies							
CD45.1	Ly-5.1	Mouse	Mouse (A.SW)	IgG2a, k	A20	Biolegend	110730
F4/80	EMR1, Ly71	Mouse	Rat	IgG2a, k	BM8	Biolegend	123114
Alexa Fluor® 700 conjugated monoclonal antibodies							
CD4	L3T4	Mouse	Rat	IgG2a, k	RM4-5	BD Pharmingen	557956
CD45R	B220, Ly-5	Human/Mouse	Rat	IgG2a, k	RA3-6B2	eBioscience	56-0452
FITC conjugated monoclonal antibodies							
IgM^a	Igh-6a	Mouse	Mouse (C57BL/6)	IgG1, k	DS-1	BD Pharmingen	553516
Pacific Blue monoclonal antibodies							
CD45R	B220, Ly-5	Human/Mouse	Rat	IgG2a, k	RA3-6B2	BD Pharmingen	558108

Table 2.4 Oligonucleotides used in Experimental Procedures

Primers used in the validation of Affymetrix microarray data (Applied Biosystems)

Gene	Catalog #	Assay Id
Alcam	4448892	Mm00711623_m1
Amigo2	4448892	Mm00662105_s1
CD80	4453320	Mm00711660_m1
Ctla4	4453320	Mm00486849_m1
Il6st	4453320	Mm00439665_m1
Lag3	4448892	Mm00493071_m1
Plxd1	4448892	Mm01184367_m1
Sema7a	4448892	Mm00441361_m1
Sytl3	4448892	Mm00473333_m1
Tigit	4448892	Mm03807522_m1
Gapdh	4453320	Mm99999915_g1
Rpl32	4453320	Mm02528467_g1

Oligonucleotide used in the activation of B cells (GeneWorks)

Name	Sequence
CpG ODN1668	TCCATGAC*GTTCCTGAC*GTT

- denotes phosphorothioate linkage

Table 2.5 Liposome reagents

Reagent	Supplier	Cat#
POPC	Avanti Polar Lipids	850475P
Cholesterol	Avanti Polar Lipids	700000P
DSPE-PEG750	Avanti Polar Lipids	880620P
b-BODIPY 500-512 C12-HPC	Molecular Probes (Life Technologies)	D3793
Normal saline	Baxter	AHF7124
0.1 µm PC membrane 19 mm	Whatman	800309
1 µm PC membrane 19 mm	Whatman	800319
Avanti mini-extruder	Avanti Polar Lipids	610000

2.2 Methods

2.2.1 Cell biology

2.2.1.1 In vitro

2.2.1.1.1 Primary mouse splenocyte preparation

Mice were sacrificed by cervical dislocation, their spleens excised under sterile conditions and placed into 5 mL of Hanks balanced salt solution. Spleens were processed into a single cell suspension by pushing them through a 70 μm nylon cell strainer with a plunger from a 3 mL syringe. Cells were pelleted by centrifugation (300xg for 5 min at 4°C) and the supernatant discarded. Red blood cells were lysed by resuspending the pellet in 2 mL of 1xBD PharmLyse™ Lysis buffer (BD Pharmingen) per spleen and incubating for 7 min at room temperature. The splenocytes were washed 3 times in RPMI-1640 supplemented with 5% FCS, before resuspending in complete RPMI-1640 (See Table 2.1) in preparation for cell culture. Cell counts were determined using a Vi-CELL XR counter (Beckman-Coulter, Miami, FL)

2.2.1.1.2 Activation of B cells

Splenocytes were purified as previously described (see Section 2.2.1.1.1). Purified splenocytes were resuspended at a concentration of $2x10^{6}$ cells per mL in complete RPMI-1640 medium. Cells were seeded into 24 well flat bottomed plates in a final volume of 2 mL of complete RPMI-1640 alone or with combinations of the following stimulants; 10 μg/mL of LPS (Sigma), 2 μg/mL of recombinant mouse CD40L (R&D Systems, Inc., Minneapolis, MN), 50 ng/mL of murine IL-4 (Peprotech Inc., Rocky Hill, CT), 100 ng/mL of hen egg lysozyme (HEL) (EC3.2.1.17, Sigma Chemical Co., St. Louis, MO) and 25 μM CpG ODN

1668 (Geneworks Pty Ltd, Adelaide, SA, Australia). Cultures were incubated for 3 days at 37°C in 5% CO_2.

2.2.1.1.3 Activation of CD8$^+$ T cells

Splenocytes were purified as previously described (see Section 2.2.1.1.1). Purified total splenocytes from one spleen (~50-80 x 10^6 cells) of either OT-I, OT-I *Prf1-/-* or B6.SJL.TCRP14 mice were cultured in complete RPMI-1640 medium with 5 µg/mL of LPS and 10 ng/mL of IL-2. Purified total splenocytes from one spleen (~60-90 x 10^6 cells) from C57BL/6 mice were used as antigen presenting cells and were loaded with 1 µg/mL of either the $OVA_{257-264}$ (SIINFEKL) peptide for OT-I and OT-I *Prf1-/-* CTLs or the LCMV gp33-41 (KAVYNFATM) peptide for B6.SJL.TCRP14 CTLs for 1 hr at 37°C and then washed 3 times (300xg for 5 min at 4°C) with complete RPMI-1640 medium before adding to splenocyte (OT-I, OT-I *Prf1-/-* or B6.SJL.TCRP14) cultures (1:1). Splenocyte cultures were divided equally between five 75 cm^2 flasks (Nunc, Sigma-Aldrich). Total culture volume was 30 mL per 75cm^2 flask (Nunc) and was incubated for 4 days at 37°C in 5% CO_2. Culture flasks were incubated upright for 48 hr, before being cultured lying down. After 3 days cultures were split 1:1 and on day 4 the percentage of CD8$^+$ effector T cells in cultures was determined via flow cytometry, with purity being routinely >90%.

2.2.1.1.4 Activation of CD4$^+$ T cells

Splenocytes were purified as previously described (see Section 2.2.1.1.1). Purified total splenocytes from one spleen (~50-80 x 10^6 cells) from OT-II mice were cultured in complete RPMI-1640 medium with 5 µg/mL of LPS, 10 ng/mL of IL-2 and 0.5 µg/mL of the $OVA_{323-339}$ peptide. Purified total splenocytes from one spleen (~60-90 x 10^6 cells) from C57BL/6 mice were used as antigen presenting cells and were loaded with the $OVA_{323-339}$ peptide (1µg/mL) for 1 hr at 37°C and then washed 3 times (300xg for 5 min at 4°C) with complete RPMI-1640 medium before adding to total OT-II splenocyte culture. Splenocyte cultures were divided equally between five 75 cm^{2} flasks. Total culture volume was 30 mL per 75 cm^{2} flask and was incubated for 4 days at 37°C in 5% CO_2 as described above for CD8^{+} T cells, with resultant CD4^{+} T cell effectors routinely being >90% pure.

2.2.1.1.5 Cell Staining

2.2.1.1.5.1 Cell surface labelling

Cell surface marker expression on mouse leukocytes was determined using immunofluorescence flow cytometry. Table 2.4 lists the antibodies used.

Cells were resuspended in PBS supplemented with 0.1% BSA (w/v) at 2-4x10^{6} cells/mL and transferred into 96-well U-bottomed plates. Where stated, Fc receptors were blocked with an anti-CD32/CD16 mAb (10 µg/mL) on ice for 15 min prior to addition of other mAbs. Cells were incubated with fluorochrome or biotin conjugated mAbs for 20 min on ice in the dark. Following incubation the cells were pelleted by centrifugation (300xg for 5 min at 4°C) and the supernatant removed. Cells were washed two times by resuspending cell pellets in 200 µL/well of PBS/0.1% BSA followed by centrifugation (300xg for 5 min at 4°C) and removal of supernatants. Cells stained with biotin-conjugated primary antibodies were subsequently stained with 0.4 µg/mL of allophycocyanin-conjugated streptavidin (streptavidin-APC; BD Pharmingen) and incubated for 20 min on ice in the dark. Following incubation, cells were pelleted by centrifugation (300xg for 5 min at 4°C) and washed two times by resuspending cell pellets in in 200 µL/well of PBS/ 0.1% BSA followed by centrifugation and removal of supernatants. Following the final wash, cells were resuspended in 50 µL/well of PBS/0.1%BSA and transferred to FACS tubes (Costar Corning Inc., Lowell, MA) for analysis via flow cytometry.

2.2.1.1.5.2 Dead cell labelling

Dead cell labelling was always done in conjunction with cell surface labelling (Section 2.2.1.1.5.1). The UV excitable dye Hoechst 33258 (Calbiochem, La Jolla, CA) was used to distinguish viable cells from dead and apoptotic cells. Cells were stained with 1 µg/mL of Hoechst 33258 and incubated for 20 min on ice. Following incubation the cells were pelleted by centrifugation (300xg for 5 min at 4°C) and the supernatant removed. Cells were washed two times by resuspending pellets in 200 µL/well of PBS/0.1% BSA followed by centrifugation (300xg for 5 min at 4°C) and removal of supernatants. Following the final wash, cells were resuspended in 50 µL/well of PBS/0.1%BSA and transferred to FACS tubes for analysis via flow cytometry.

2.2.1.1.5.3 Intracellular labelling with 5-(and 6)-carboxyfluorescein diacetate succinimidyl ester (CFSE)

The tumour cell lines EL4, peptide-pulsed EL4 and EG7-OVA were labelled with 5-(and 6)-carboxyfluorescein diacetate succinimidyl ester (CFSE) in order to act as targets to assess CD8$^+$ T cell effector cytolytic activity. Cell populations were labelled with different concentrations (either 250 nM or 5000 nM) of CFSE in 10%FCS RPMI-1640 medium in order to be able to distinguish between different target cells. Cells were incubated with CFSE for 5 min at room temperature. Following incubation the cells were pelleted by centrifugation (300xg for 5 min at 4°C) and the supernatants removed. Cells were washed twice by resuspending cell pellets in RPMI-1640 medium supplemented with 5% FCS, followed by centrifugation (300xg for 5 min at 4°C) and removal of supernatants.

2.2.1.1.5.4 Membrane staining using Vybrant® DiI cell labelling solution

In order to assess the exchange of plasma membranes between cells a lipophilic membrane stain, DiI (Molecular Probes, Eugene, OR) was used. Cells were resuspended at 2x10^6 cells/mL in RPMI-1640. DiI (5 µL/mL 0.1% BSA PBS) was added to cell suspensions mixed well, and incubated for 25 min at 37°C. Cells were washed through a FCS cushion at 300xg for 5 min at 4°C. The supernatant was aspirated, the cells were transferred to a new tube and washed twice more by resuspending the cell pellet in complete RPMI-1640 medium followed by centrifugation (300xg for 5 min at 4°C), carefully aspirating off supernatants and using a new tube at each wash.

2.2.1.1.5.5 Cytotoxicity assay

CD8$^+$ T cell cytolytic activity was determined in an overnight assay using three targets; EL4, peptide pulsed EL4 and EG7-OVA tumour cell lines. Antigen loading of EL4 tumour cells was performed using the OVA $_{257\text{-}264}$ peptide (SIINFEKL), EL4 cells being incubated for 1 hr at 37°C in 5% CO_2 with 10 µg/mL of SIINFEKL. After pulsing, the peptide loaded cells were washed three times by centrifugation with complete RPMI-1640 medium (300xg for 5 min at 4°C). SIINFEKL pulsed EL4 and unpulsed EL4 were then labelled with 5000 nM and 250 nM CFSE, respectively, for 5 min at room temperature. Labelling was stopped by adding complete medium and washing 3 times each by resuspending cell pellets in RPMI-1640 supplemented with 5% FCS, followed by centrifugation (300xg for 5 min at 4°C) and removal of supernatants. For experiments with all three targets, the CFSE^{hi} peptide pulsed EL4, CFSE^{low} un-pulsed EL4, and CFSE$^-$ EG7-OVA were then combined in equal cell numbers and labelled with DiI (as described in section 2.2.1.1.5.4). CD8$^+$ T cells (effectors) were prepared as described in section 2.2.1.1.3 from wild type and perforin-deficient OT-I transgenic mice and incubated overnight at various effector: target ratios, including samples with no effectors added to be used as controls. The number of CFSE and DiI labelled cells was determined using flow cytometry, and the percentage of specific target cell lysis was calculated using the following formula;

$$\%\ \text{specific killing} = \left(1 - \frac{\text{(targets peptide-pulsed/targets peptide-pulsed control)}}{\text{(targets unpulsed/ targets unpulsed control)}}\right) \text{x100}$$

2.2.1.2 In vivo

2.2.1.2.1 Subcutaneous tumour establishment

The EG7-OVA cell line was harvested at mid-log phase and washed 3 times (300xg, 5 min) with PBS. Cells were resuspended at $1\text{x}10^6$cells/mL in PBS and 200 μl ($2\text{x}10^5$ cells in total) injected subcutaneously into the right flank of mice to establish tumours.

2.2.1.2.2 Tumour measurement

Subcutaneous tumours were measured every 1-2 days on two perpendicular axes using a ruler. A measure of tumour size was calculated by multiplying the measured lengths. Mice with tumours reaching 15 mm^2 in size were considered moribund and sacrificed.

2.2.1.2.3 Adoptive immunotherapy of tumours

Effector T cells were generated as described in section 2.2.1.1.3. At day-10 post injection of EG7-OVA cells, when tumours were approximately 7 mm in diameter, $5\text{x}10^6$ effector T cells were injected i.v. via the tail vein in 200µL of PBS. Control groups received PBS alone. Tumour growth or regression was measured as described above.

2.2.1.2.4 Tumour-infiltrate profiles

At day-15 post injection of EG7-OVA cells, mice were sacrificed and the spleens and tumours were excised. Tissues were processed into a single cell suspension by pushing them through a 70 μm nylon cell strainer with a plunger from a 3 mL syringe and labelled with antibodies for analysis of infiltrating leukocytes using flow cytometry (section 2.2.1.1.5.1). Non-specific staining via Fc receptors was blocked by incubation with an anti-CD16/CD32 antibody as described in section 2.2.1.1.5.1. Cell populations were stained with mAbs specific for mouse CD8, CD4, NK1.1, CD11b, F4/80, Ly6G and Ly6B.2. Absolute numbers of cells was calculated using Flow-Count™ Fluorospheres (Beckman Coulter Inc. Brea, CA). When known numbers of Flow-Count™ Fluorospheres were added per sample the absolute count of the cells can be calculated using the following formula;

$$\text{Absolute cell count} = \frac{\text{Total number of Fluorospheres added per sample}}{\text{Total number of Fluorospheres counted via FACs}} \times \text{total number of cells counted}$$

Sample staining profiles and cell numbers were obtained using flow cytometry.

2.2.1.2.5 Depletion of NK cells in mice

To deplete mice of NK cells, 50 µL of a rabbit polyclonal anti-asialo GM1 antiserum (#986-10001, Wako Pure Chemical Industries, Osaka, Japan) was mixed with 100 µL of 0.9% saline and injected i.v. via the tail vein 24 hr prior to injection of effector T cells. Control groups received the 0.9% saline solution alone. NK cell depletion was confirmed by flow cytometric analysis of spleen cell suspensions of treated mice using a mAb specific for mouse NK1.1.

2.2.1.2.6 Depletion of macrophages in mice

Injection of liposomes encapsulating clodronate is a well established method for the depletion of macrophages *in vivo* (Rooijen and Sanders, 1994*)*. Clodronate and control (PBS) liposomes were made and purchased from Dr Nico van Rooijen of ClodronateLiposomes.org (Netherlands)(Rooijen and Sanders, 1994). The suspension of liposomes with encapsulated clodronate contained 5 mg of clodronate/mL of suspension. To deplete mice of macrophages, 200 μL of Clodronate or control (PBS) liposome suspensions were injected i.v. via the tail vein 24 hr prior to injection of effector T cells. Depletion of macrophages was confirmed by flow cytometric analysis of splenocytes isolated from treated mice using mAbs specific for mouse F4/80 and CD11b.

2.2.1.2.7 Depletion of neutrophils in mice

To deplete mice of neutrophils, 0.5 mg/mouse of the 1A8-4-10-9 mAb specific for Ly-6G (supplied by WEHI Antibody Facility) was injected i.p. 3 hr prior to injection of effector T cells. Control groups received 0.5 mg/mouse of a rat IgG2a isotype control. Depletion of neutrophils was confirmed by flow cytometric analysis of splenocytes from treated mice using mAbs specific for mouse CD11b and Ly6B.2.

2.2.2 Molecular Biology

2.2.2.1 DNA isolation

DNA was extracted from cells for analysis by real-time PCR using the QIAamp® DNA mini kit (QIAGEN, Valencia, CA) according to the manufacturer’s guidelines. Briefly, to 200 μL of cell suspension 200 μL of Lysis Buffer AL (QIAGEN) was added, the sample vortexed and incubated for 10 min at 56°C. Following incubation, 200 μL of 100% ethanol was added to the sample and it again vortexed. The lysed cell suspension was then carefully dispensed into a QIAamp Spin Column, placed in a 2 mL collection tube, and centrifuged at 16,100xg for 1 min. The QIAamp Spin Column was then placed in a clean collection tube, the filtrate discarded, 500 μL of Wash buffer AW1 (QIAGEN) added and the column centrifuged at 6000xg for 1 min. Again, the QIAamp Spin Column was placed in a clean collection tube, the filtrate discarded, 500 μL of Wash buffer AW2 (QIAGEN) added to the column and the column centrifuged at 16,100xg for 3 min. To ensure no residual wash buffer AW2 was in the eluate the QIAamp Spin Column was placed in another clean collection tube and further centrifuged for another 1 min at 16,100xg. The QIAamp Spin Column was then placed in a clean 1.5 mL eppendorf tube, 50 μL of Elution buffer AE carefully added to the column and the column incubated at room temperature for 5 min before centrifugation at 6000xg for 1 min. The quantity and quality of the DNA in the column eluate was then estimated using the NanoDrop® spectrophotometre ND-1000 (NanoDrop Technologies, Inc., Wilmington, DE) using ND-1000 V3.30 software.

2.2.2.2 Total RNA isolation

Total RNA was extracted from pelleted cell samples using TRIzol® Reagent (Invitrogen, Carlsbad, CA) to inactivate the endogenous RNases. In order to dissociate RNA from protein, cells were homogenized in 1 mL of TRIzol® Reagent by pipetting up and down for 5 min at room temperature. To extract RNA, samples were diluted with 200 μL of chloroform and vortexed vigorously for 10 sec. Following a 15 min incubation on ice, samples were centrifuged at 10,000xg for 20 min at 4ºC, and the upper aqueous layer carefully collected and transferred to a clean 1.5 mL eppendorf tube. An equal volume of isopropanol was added to the aqueous phase to precipitate the RNA, and incubated for 1 hr on dry ice. Following incubation, the samples were again centrifuged at 10,000xg for 20 min at 4°C and the supernatant discarded. Next, RNA pellets were washed with 200 µL of 75% ethanol and vortexed for a few seconds before incubating the samples for 10 min at room temperature to dissolve possible residual traces of guanidinium. The suspension was then centrifuged at 10,000xg for 5 minutes at 4°C, the supernatant removed, and the pellet allowed to air dry for 10 min at room temperature. Samples were resuspended in 20 µL of nuclease free DEPC-treated water (Ambion, Sydney, NSW, Australia).

2.2.2.3 RNA purity and quality assessment

For real-time PCR analysis RNA quantity and assessment of purity was conducted using the NanoDrop® spectrophotometre ND-1000 (NanoDrop Technologies, Inc., Wilmington DE) and using ND-1000 V3.30 software.

A further analysis of RNA purity was used prior to microarray analysis. A 2100 Bioanalyser (Agilent Technologies, Santa Clara, CA) was used to determine the quality and quantity of RNA samples. The RNA integrity number estimated by the Bioanalyser provides a more robust measure of the integrity of RNA samples.

2.2.2.4 First strand cDNA synthesis

Total RNA was reverse transcribed using the SuperScript® III First-Strand synthesis system for RT-qPCR (Invitrogen, Carlsbad, CA) as detailed in the manufacturer’s guidelines. Briefly, total RNA was incubated with a 0.5 mM dNTP mix and 5 µM OligodT at 65°C for 5 min, before placing on ice for 1 min. Next, 10 µL of SuperScript® III First-Strand cDNA Synthesis Mix (10X RT Buffer, $MgCl_2$, 10 mM DTT, RNase OUT™ and 50U of SuperScript® III RT enzyme) was added to the dNTP RNA mixture to give a final reaction volume of 20 µL, and incubated at 50°C for 50 min to allow synthesis of first strand cDNA. Samples were then heated to 85°C for 5 min to terminate the reaction.

2.2.2.5 Quantitative real-time PCR analysis

All RT-qPCR analyses were performed on the ABI-7900 instrument (Applied Biosystems, Foster City, CA) using the FAM or SYBR green probe channels. For microarray validation assays TaqMan® Gene Expression Assays were performed. Primers are outlined in Table 2.4. Single reaction mixtures contained 1:100 dilution of cDNA in a total volume of 10 µL (0.5 µL of 20X TaqMan® Gene Expression Assay, 5 µL of 2X TaqMan® Gene Expression Master Mix and nuclease free water to 10 µL). This is a slight deviation from the manufacturer's guidelines (TaqMan® Gene Expression Assays protocol).

2.2.2.6 Comparative gene expression analysis

Splenic C57BL/6 B cells were purified for microarray analysis. Spleens were isolated and processed as outlined in section 2.2.1.1.1. Red blood cell depleted splenocytes were labelled with anti-Thy1.2-biotin, anti-CD11c-biotin, anti-CD11b-biotin, anti-CD4-biotin, anti-CD8-biotin, anti-CD43-biotin and anti-TER119-biotin mAbs for 12 min at room temperature. Labelled splenocytes were then resuspended in MACs buffer (Miltenyi Biotec, Macquarie Park, NSW, Australia) and incubated with streptavidin-microbeads for 15 min at room temperature. Using negative depletion on an AutoMACS magnetic separator (Miltenyi Biotec) B cells were isolated from labelled splenocytes, resuspended to 2×10^6 cells/mL in complete RPMI-1640 medium with either 10 µg/mL of LPS or 25 µM CpG ODN 1668. Cells were cultured in 24 well flat-bottomed plates for 3 days at 37°C and in 5% CO_2. B cell purity, as determined by flow cytometry using an anti-B220 mAb, was routinely >96%. RNA was isolated from activated and freshly isolated purified B cell samples as outlined in section 2.2.2.2. Quality and quantity of total RNA isolated was determined as outlined in section 2.2.2.3. RNA samples were then submitted to the Ramaciotti Centre (UNSW, Randwick, NSW, Australia) for labelling with the Ambion WT Assay and Affymetrix WT labelling kit (Affymetrix), hybridization to mouse GeneChip® Gene 1.0 ST Array (Affymetrix) and scanning. Analysis of expression data was performed using the Affy package of R statistical software. Data were normalised using the robust multi-array averaging (RMA) method using the 26890 main probes. Genes considered upregulated by LPS stimulation were designated our genes of interest. Requirements for gene upregulation were gene expression to be a minimum of 2-fold greater in LPS stimulated B cells in comparison to unstimulated cells (LPS 2-fold > Naïve), and gene expression to be a minimum of 1.4-fold greater in LPS stimulated B cells in comparison to CpG stimulated cells (LPS 1.4-fold > CpG). Raw signals of the samples had to be greater than 100. Gene ontology screening was based on ontology data from the National Centre for Biotechnology Information (NCBI). Functional analysis of genes was performed using Kyoto Encyclopaedia of Genes and Genomes (KEGG) pathway database, Protein Analysis Through Evolutionary Relationships (PANTHER) Classification System and by eye based on its known or predicted cellular function reported in the literature. Cell penetrating peptide motifs were defined as being regions of 20 amino acids with a minimum of 4 positively charged amino acids with no negatively charged amino acids, resulting in a minimum total charge of 4+. Genes were screened for the presence of cell penetrating peptide motifs courtesy of the Genome Discovery Unit (GDU) at the Australian National University.

2.2.3 Statistical significance

Statistical analyses were performed using Prism version 5 software (GraphPad, La Jolla, CA) and Genstat (VSN international Ltd.). Data are presented as means and standard error of the means (SEM). For statistical significance, the unpaired two-tailed Students *t*-test or general analysis of variance (ANOVA) was used. Unpaired two-tailed Students *t*-tests were performed using Prism software. ANOVA was performed using GenStat. For ANOVA analysis, mean fluorescence intensity values less background were converted to Log10 values to satisfy variance assumptions. The Y-variate was Log10 of mean fluorescence intensity, the blocking factor was experiments and treatments were cell state (stimulated versus naïve), temperature (4^oC versus 37^oC), cargo (FITC versus APC-streptavidin-biotin) and in some analyses, peptide (TAT, Penetratin, TP10). All interactions were analysed. Data were considered statistically significant with a p value of 0.05 or less (see Table 2.6 for p value symbols and meanings). Dr Terry Neeman from the Statistical Consulting Unit, Australian National University, provided invaluable assistance with statistical analyses.

Table 2.6 p value symbols and meanings

p value	**Significance Level**	**Designation**
> 0.05	Not significant	Ns
0.01 to 0.05	Significant	*
0.001 to 0.01	Quite significant	**
0.0001 to 0.001	Very significant	***
> 0.0001	Extremely significant	****

Chapter 3

Cell penetrating peptides as mediators of membrane exchange between B cells

3.1 Abstract

Studies from my supervisor’s laboratory demonstrated that activated B cells donate cell surface proteins and membranes to both naïve and activated bystander B cells through a process of membrane exchange. However, the molecular mechanisms involved in this exchange remain unknown. An important feature of membrane exchange which was confirmed by experiments described in this Chapter, is that the B cells need to be appropriately activated in order to donate cell surface proteins and membranes to bystanders, with naïve B cells being less capable of membrane exchange. Another unique feature of membrane exchange between B cells, also confirmed in this Chapter, is that it occurs at 4°C, excluding many proposed molecular pathways involved in membrane exchange that require the B cells to be metabolically active. Earlier studies in my supervisor’s laboratory have used over 60 different agents to block currently proposed membrane exchange mechanisms, without any effect. This indicates involvement of a unique membrane transfer mechanism. Cell penetrating peptides (CPP) are short hydrophilic molecules capable of translocating across plasma membranes, independently of receptors or specific transport mechanisms. This study demonstrates that CPPs are capable of rapidly translocating into LPS activated B cells, whereas uptake of CPPs into naïve B cells is up to 40-fold less efficient. Most importantly, translocation occurs efficiently at both 4°C and 37°C. Based on these findings we postulate that B cell membrane exchange involves expression of cell surface protein(s) containing CPP motifs that bind to the plasma membrane of bystander cells and facilitate membrane exchange.

3.2 Introduction

For several decades studies have documented the exchange of membranes and proteins between cells of the immune system. For example, immune cells have been shown to acquire MHC class I and II proteins (Cone et al., 1972), co-stimulatory proteins (Quandt et al., 2007) and membrane fragments (Hudrisier et al., 2001) through membrane exchange. In addition, cells not involved in the immune system, notably endothelial cells, can also transfer membrane proteins to immune cells (Brezinschek et al., 1999, Merkenschlager, 1996).

In several circumstances the transfer mechanism has been shown to involve exosomes, nanotubes or endocytosis (Davis and Sowinski, 2008, Morelli et al., 2004). However, more often the molecular mechanisms underlying the intercellular transfer of membranes and cell-surface proteins remain substantially unknown (Quah et al., 2008, Ahmed and Xiang, 2011, Ahmed et al., 2008). Furthermore, it appears that the molecular mechanisms utilised by cells may vary between the different cell types involved and/or different conditions that the cells are subjected to whilst participating in membrane transfer (Ahmed and Xiang, 2011).

My supervisor’s laboratory has extensively studied the transfer of membranes between B cells in an effort to delineate the molecular basis of this exchange. More than 60 agents have been used in an attempt to impede the transfer of membranes with the vast majority displaying no significant effect (Quah et al., 2008). These agents include, but are not limited to, blocking monoclonal antibodies (mAb) against cell adhesion molecules, cytoskeleton disrupters, ion channel blockers and metabolic inhibitors. The only agents capable of inhibiting transfer were the biological fixatives glutaraldehyde and paraformaldehyde. In contrast, there were a number of agents that enhanced transfer, including L-lysine, anti-CD44, anti-CD48, anti-CD19 and anti-CD62L mAbs, and BCR specific antigen (Quah et al., 2008). However, how they achieve this and their role in membrane transfer between B cells remains unclear.

A unique feature of membrane transfer between B cells is its ability to occur at low temperatures (4ºC)(Quah et al., 2008). This eliminates the majority of currently proposed mechanisms for membrane transfer, as they require cells to be metabolically active. Cell penetrating peptides (CPPs) are short, positively charged, hydrophilic, peptides that are capable of penetrating and translocating across the plasma membrane of cells, independent of receptors or specific transport mechanisms. Interestingly, translocation of CPPs occurs at 4ºC, thus they represent good candidates for mediating membrane transfer between B cells.

Countless CPPs, both natural and synthetic, have been described and are commonly classified according to the physico-chemical properties of their sequences (Ziegler and Seelig, 2011). There are three main classes: primary amphipathic, secondary amphipathic and nonamphipathic CPPs.

Primary amphipathic CPPs (such as MPG, transportan, TP10 and Pep-1) typically contain more than 20 amino acids, and often contain only a few basic residues. Their primary structure is composed of sequential hydrophobic and cationic residues and they bind with strong affinity to neutral and anionic lipid membranes (Deshayes et al., 2008, Ziegler and Seelig, 2011). Primary amphipathic CPPs insert themselves into the cell membrane, usually deeper into the hydrophobic core than other CPPs, and create a reduction in the surface tension of the membrane. They do not span the bilayer, but rather self associate in the head group region, relevant for many proposed models of direct translocation (Ziegler, 2008). It is known that some primary amphipathic

CPPs, such as TP10, can induce membrane leakiness (probably as a consequence of their mechanism of cellular entry), and are therefore often toxic to cells (Saar et al., 2005).

Secondary amphipathic CPPs (such as penetratin and pVEC) are generally shorter than primary amphipathic CPPs, and contain a higher proportion of basic residues. Their amphipathic properties are demonstrated when they interact with phospholipid membranes, upon which they form alpha helices or beta sheet structures thus separating their charged and non-charged residues. Their membrane affinity increases conjointly with the anionic lipid content of the membrane, which appears to impact on their secondary structure (Ziegler, 2008). Secondary amphipathic CPPs, in comparison to primary amphipathic CPPs, only insert into the membrane minimally (Persson et al., 2002). This is a possible reason for the lack of membrane perturbations observed with secondary amphipathic CPPs.

Non-amphipathic CPPs (such as R9 and TAT) are generally the shortest CPPs comprised often exclusively of cationic residues. They rely heavily on the presence of a high fraction of anionic lipids for membrane binding, do not experience structural changes upon binding, do not appear to insert into the lipid bilayer, and do not evoke membrane leakiness at low concentrations (Kramer and Wunderli-Allenspach, 2003, Ziegler and Seelig, 2004). Non-amphipathic CPPs appear to be only superficially adsorbed to cell membranes, relying heavily on electrostatic contributions, rather than hydrophobic interactions that appear to play a major role with the other two classes of CPPs, particularly with the primary amphipathic CPPs. It is highly likely that these key features play an important role in the CPPs mechanism of uptake. Due to this, it is generally thought that the translocation mechanism is not the same for the different families of CPPs.

The studies described in this Chapter are based on the proposal that CPPs are responsible for mediating membrane exchange between B cells. It is postulated that upon B cell activation certain proteins with regions containing a high proportion of basic residues (arginines and lysines) and CPP features are upregulated and expressed at the cell surface. Through electrostatic forces and/or hydrophobic interactions the proteins bind to the phospholipid containing membranes of adjoining cells. This interaction is likely to lead to a distortion of the phospholipid bilayer, produce an area of membrane thinning or weakened membrane that could favour the process of membrane fusion, and thus lead to the exchange of membranes between B cells. Experiments that support this concept are presented in this Chapter.

3.3 Results

3.3.1 B cell membrane transfer: the methodology

There are two different methods that have been used in this thesis to detect membrane transfer between B cells. The first method described involves detecting the transfer of particular molecules expressed on the cell surface of B cells. The second method involves detecting the global transfer of plasma membranes between B cells using fluorescent, membrane intercalating, lipids.

3.3.1.1 Transfer of cell surface proteins between B cells

To demonstrate that cell surface proteins could be transferred between B cells, B cell populations from two different mouse strains were used, MD4 and B6.CD45.1. These mice express different allotypes for the B cell surface molecules IgM and CD45. The MD4 mouse is a BCR transgenic strain on a C57BL/6 (B6) background. The transgene encodes a B cell IgM heavy chain constant region of allotype ‘a’ (IgM^a) with heavy and light chain variable regions forming an antibody molecule specific for hen egg lysozyme (HEL)(Goodnow et al., 1988). The MD4 mouse B cells also express the CD45.2 allele of the leukocyte common antigen, CD45. In comparison, B6.CD45.1 mice are B6 mice congenic for the CD45.1 allotype and although the two CD45 allotypes are functionally identical CD45.1 is easily distinguishable from CD45.2 by specific antibody labelling. Furthermore, B6.CD45.1 mice express the ‘b’ allotype of Ig (IgM^b), which is polyclonal (not transgenic) and so specific for a wide variety of antigens. These allotypic IgM differences can be detected with fluorescently labelled allotype-specific antibodies, and consequently transfer of IgM^a molecules between MD4 and B6.CD45.1 B cells can be readily analysed using flow cytometry. Thus, IgM transfer from MD4 B cells to B6.CD45.1 B cells would be indicated by expression of IgM^a on the B6.CD45.1 B cell surface.

An example of the gating strategy used to determine the amount of cell surface transfer of IgM^a between LPS activated MD4 and CD45.1 B cells is shown in Figure 3.1. Initially LPS activated lymphocyte populations were identified using forward scatter versus side scatter parameters (Figure 3.1a). Doublets were excluded using forward scatter height versus forward scatter width, and side scatter height versus side scatter width (Figures not shown). Next, viable B cells were identified as having high B220 levels (B220$^+$) and low Hoechst 33258 fluorescence (Figure 3.1b). The two different B cell populations were distinguishable by expression of IgM^a and CD45.1, with the IgM^{a+}CD45.1$^-$ subset corresponding to MD4 B cells (Figure 3.1c and e), and the IgM^{a-}CD45.1$^+$ subset corresponding to B6.CD45.1 B cells (Figure 3.1d and e). The cultured alone populations (Figure 3.1c and d) were used as a reference control to calculate the percentage of B6.CD45.1 B cells in the 2-hour co-culture that had acquired IgM^a from the MD4 B cells (Figure 3.1e and f). Overton’s subtraction calculates the difference between the histograms of two samples and was used to determine the percentage of recipient CD45.1 B cells acquiring IgM^a from the donor MD4 B cells (Overton, 1988). Using Overton subtraction, in the example shown, 37% of the co-cultured B6.CD45.1 B cell population had acquired IgM^a molecules on their surface following 2 hours of co-culture (Figure 3.1f). These data are similar to those previously published by my supervisor’s laboratory (Quah et al., 2008).

3.3.1.2 Transfer of plasma membranes between B cells

My supervisor’s laboratory has previously demonstrated that IgM^a transfer occurs concomitantly with CD45.2 transfer from MD4 B cells to B6.CD45.1 B cells (Quah et al., 2008). This co-transfer of IgM^a and CD45.2 indicated that the transfer of cell surface molecules could be a product of membrane sharing between B cells, and this was demonstrated by the use of the lipophilic dye, PKH-26 (Quah et al., 2008). To show that plasma membrane transfer occurs between B cells a similar method was used here, however, instead of PKH-26 another lipophilic dye, DiI was used. DiI is a lipophilic cationic indocarbocyanine membrane dye, which diffuses laterally in cell membranes to stain the whole cell. It is superior to PKH-26 as it is weakly fluorescent until incorporated into lipid membranes and has no effect on cell viability (Li et al., 2008).

Day-3 LPS-activated MD4 splenocytes were labelled with DiI, then mixed with LPS activated B6.CD45.1 splenocytes and incubated for 2 hours to allow for membrane transfer. Separate cultures of MD4 or B6.CD45.1 splenocytes were also maintained as controls. Figure 3.2 shows the gating strategy used to determine the transfer of plasma membranes between B cells, which is similar to that described in section 3.3.1.1 for IgM^a transfer. Viable LPS activated MD4 B cells were assessed for membrane transfer using DiI and transfer was calculated as the percentage of recipient ‘unlabelled’ B6.CD45.1 B cells that had acquired DiI labelled plasma membranes from donor MD4 cells. Using Overton subtraction, in the example shown, 47% of recipient B cells had acquired plasma membranes from the DiI labelled donor cells during the 2-hour co-incubation period (Figure 3.2e and f).

Figure 3.1 Gating strategies for BCR transfer. Day-3 LPS-activated MD4 (IgM^a) and B6.CD45.1 splenocytes were harvested and mixed 1:1 or left alone in culture for 2 hours to allow for BCR transfer. Transfer was detected through mAb labelling and analysed using flow cytometry; (a) Blasting splenocytes were identified based on forward versus side scatter; (b) Live B cells were identified by low Hoechst 33258 fluorescence and high B220 expression; (c) MD4 B cells cultured alone were identified as IgM^{a+}CD45.1$^-$; (d) B6.CD45.1 B cells cultured alone were identified as IgM^{a-}CD45.1$^+$; (e) Co-cultured MD4 and CD45.1 B cells; (f) The percentage of B6.CD45.1 B cells acquiring IgM^a in the co-culture is shown (green line) compared with the B6.CD45.1 B cells (blue line) and MD4 B cells (red line) cultured alone. Percentage acquisition was calculated using Overton subtraction (Overton, 1988).

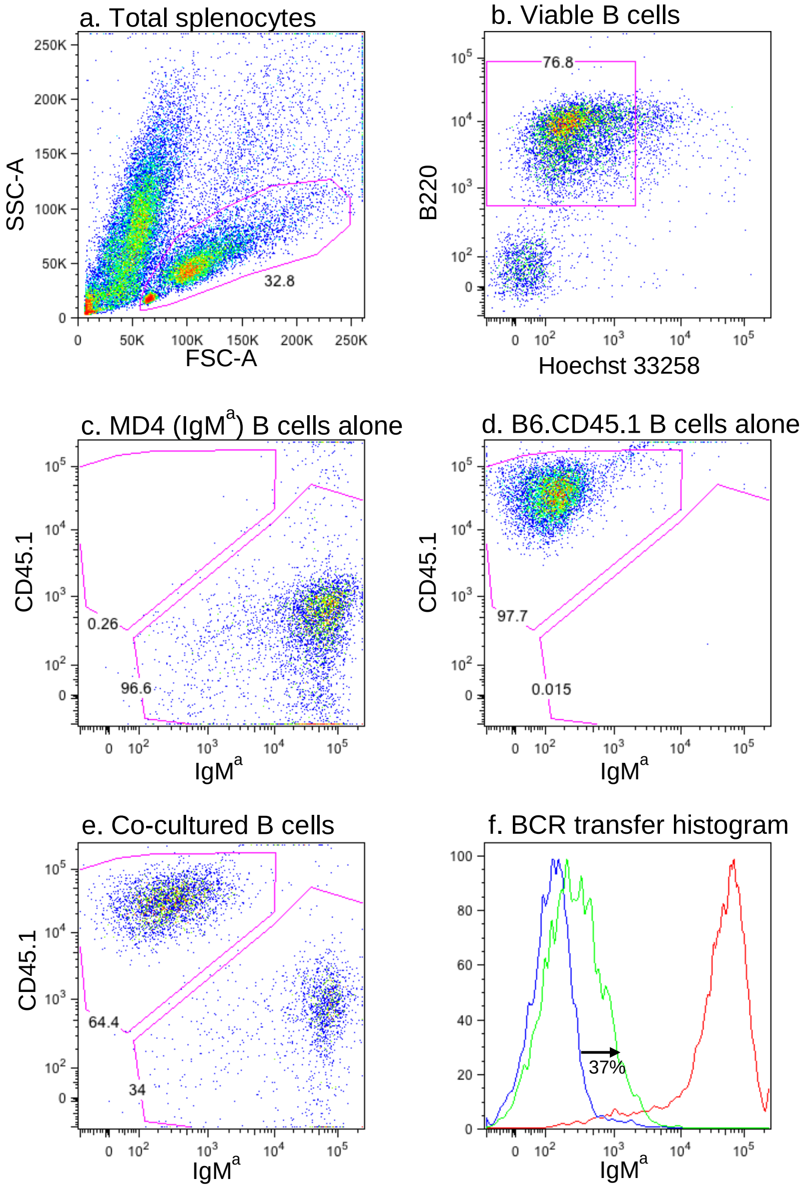
a. Total splenocytes
SSC-A
FSC-A
250K
200K
150K
100K
50K
0
32.8
b. Viable B cells
B220
Hoechst 33258
76.8
c. MD4 (IgM^a) B cells alone
CD45.1
IgM^a
0.26
96.6
d. B6.CD45.1 B cells alone
97.7
0.015
e. Co-cultured B cells
64.4
34
f. BCR transfer histogram
100
80
60
40
20
37%
10^2
10^3
10^4
10^5

Figure 3.2 Gating strategies for membrane transfer. Day-3 LPS-activated MD4 (CD45.2) and B6.CD45.1 splenocytes were harvested and mixed 1:1 or left alone in culture for 2 hours to allow for membrane transfer. Transfer was detected through labelling MD4 cell membranes with DiI and flow cytometry; (a) Blasting splenocytes were identified based on forward versus side scatter; (b) Live B cells were identified by low Hoechst 33258 fluorescence and high B220 expression; (c) MD4 B cells cultured alone were identified as DiI^{+}; (d) B6.CD45.1 B cells cultured alone were identified as DiI^{-} (e) co-cultured MD4 and CD45.1 B cells; (f) The percentage of B6.CD45.1 B cells acquiring DiI in the co-culture is shown (green line) compared with the B6.CD45.1 B cells (blue line) and MD4 B cells (red line) cultured alone. Percentage acquisition was calculated using Overton subtraction (Overton, 1988).

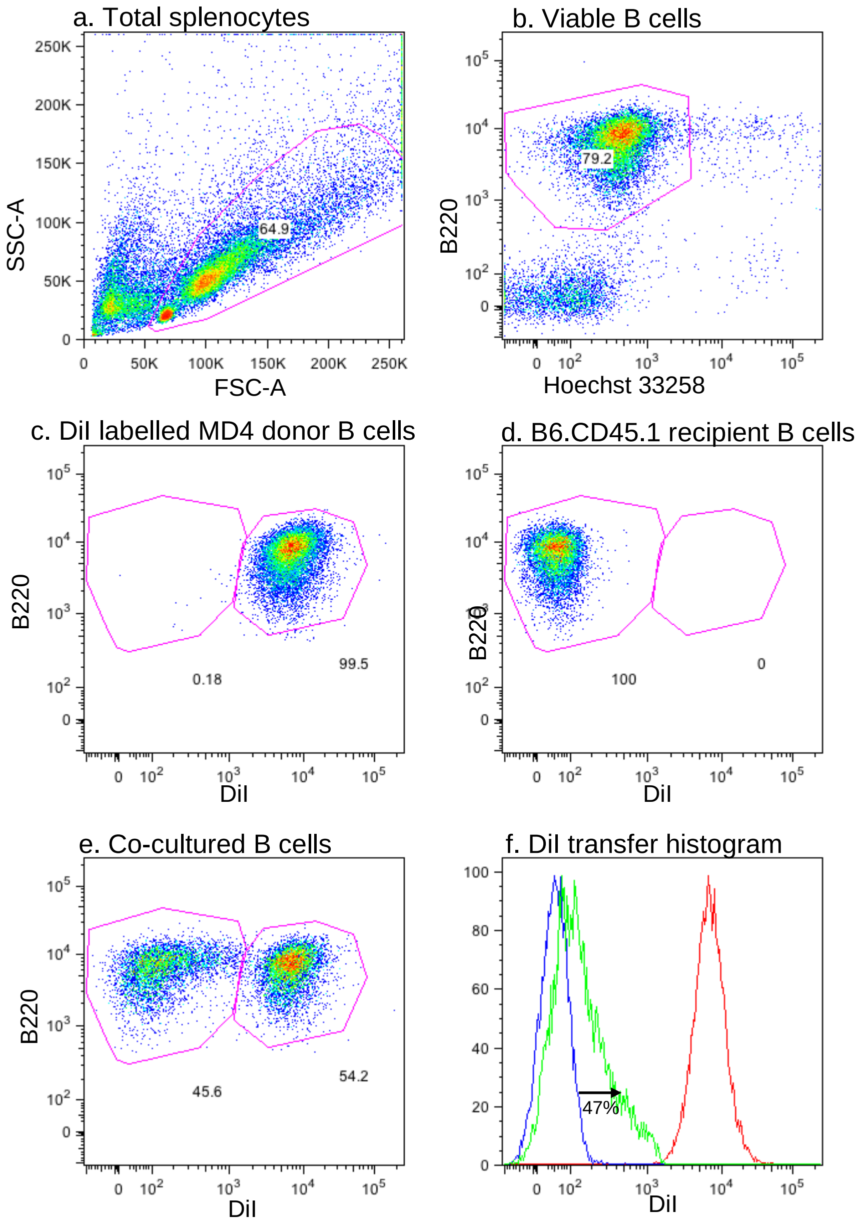
a. Total splenocytes
SSC-A
FSC-A
250K
200K
150K
100K
50K
0
50K
100K
150K
200K
250K
64.9
b. Viable B cells
B220
Hoechst 33258
10^5
10^4
10^3
10^2
0
79.2
c. DiI labelled MD4 donor B cells
B220
DiI
0.18
99.5
d. B6.CD45.1 recipient B cells
B220
DiI
100
0
e. Co-cultured B cells
B220
DiI
45.6
54.2
f. DiI transfer histogram
100
80
60
40
20
0
47%
DiI

3.3.2 B cell membrane transfer: the conditions

In order to elucidate the molecular mechanisms involved in BCR and membrane transfer it is important to confirm the known characteristics of this transfer. Previous studies have described specific conditions that are required for transfer to occur between B cells (Quah et al., 2008). The current section consolidates these findings.

3.3.2.1 Transfer between B cells is enhanced after LPS activation

Quah *et al* (2008) described previously that BCR transfer was restricted to activated B cells, with freshly isolated B cells being much less able to transfer their BCR to bystander B cells.

To assess BCR transfer in activated versus non-activated B cells, splenocytes from MD4 and B6.CD45.1 mice were cultured in the presence or absence of the B cell polyclonal activator lipopolysaccharide (LPS) (10 μg/ml). Either day-3 LPS activated MD4 or freshly isolated MD4 splenocytes were labelled with the membrane dye DiI prior to mixing with day-3 LPS activated B6.CD45.1 splenocytes or freshly isolated B6.CD45.1 splenocytes, respectively. Mixed populations were incubated for a further 2 hours at 37^oC to allow for transfer of DiI labelled membranes and cell surface proteins. Populations of both day-3 LPS activated and freshly isolated B6.CD45.1 splenocytes were cultured alone as a control. Membrane transfer between B cells was determined via percentage acquisition of donor MD4 B cell IgM^a molecules (as described in section 3.3.1.1) and donor DiI labelled MD4 B cell membrane (as described in section 3.3.1.2) by recipient B6.CD45.1 B cells. The results demonstrate that membrane transfer is low when freshly isolated MD4 splenocytes were used, with an average 11% acquisition of DiI labelled MD4 membranes by the unlabelled recipient B6.CD45.1 B cells (Figure 3.3a). In comparison, LPS activation of MD4 B cells resulted in an almost 4-fold increase in membrane transfer, with approximately 44% of B6.CD45.1 recipient B cells acquiring DiI labelled MD4 membranes (Figure 3.3a). Correspondingly, the transfer of donor IgM^a molecules from LPS activated MD4 B cells to recipient B6.CD45.1 B cells was enhanced by ~3.7-fold compared to IgM^a transfer between naïve B cells (Figure 3.3b). These data are consistent with previous findings suggesting that B cell activation is important for membrane transfer between B cells (Hudrisier et al., 2005, Quah et al., 2008). Consequently, day-3 LPS activated B cells were used as membrane donors in subsequent experiments.

3.3.2.2 Transfer of B cell membranes occurs at both 4°C and 37°C

Commonly described mechanisms by which proteins traffic between cells include endocytosis and exosomal uptake, both of which require energy generated by metabolic activity (van Niel et al., 2006, Gillette et al., 2009). Quah *et al* (2008) have indicated that transfer of membranes or cell surface proteins can occur at 4°C, indicating an energy independent mechanism.

To confirm previous reports of membrane transfer at 4°C, day-3 LPS activated DiI labelled MD4 splenocytes were mixed with day-3 LPS activated unlabelled B6.CD45.1 splenocytes and incubated for 2 hours at 37°C or 4°C. Day-3 LPS activated B6.CD45.1 splenocytes were also cultured alone as a control. Membrane transfer between B cells was determined via percentage acquisition of donor DiI labelled membranes and IgM^a by recipient B6.CD45.1 B cells, as described in sections 3.3.1.1 and 3.3.1.2. At 37°C, substantial transfer of DiI labelled MD4 membranes to unlabelled B6.CD45.1 B cells was evident, with an average of ~ 56% of B6.CD45.1 B cells acquiring DiI (Figure 3.4a). At 4°C, an average of 46% of B6.CD45.1 B cells had acquired DiI labelled MD4 membrane

Figure 3.3 B cells require activation to optimally transfer membrane components. Freshly isolated (naïve) MD4 splenocytes were labelled with DiI and added to unlabelled freshly isolated B6.CD45.1 splenocytes. Similarly, day-3 LPS activated MD4 splenocytes, labelled with DiI, were added to day-3 LPS activated B6.CD45.1 splenocytes. Co-cultures were incubated at 37°C for 2 hours. Different B cell populations were identified as in Figures 3.1 and 3.2. The percentage of B6.CD45.1 B cells acquiring (a) DiI and (b) IgM^{a} is shown. Data represents mean ± SEM (a. n=6, b. n=3) representative of at least ten independent experiments. **** $p < 0.0001$, unpaired Students *t*-test.

a. Transfer of DiI labelled membranes

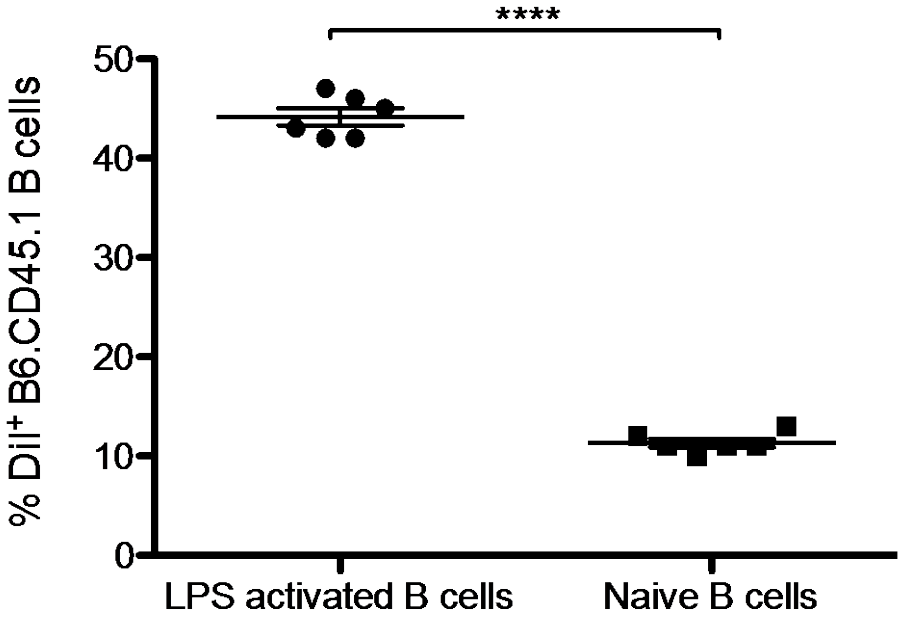

b. Transfer of IgM^a

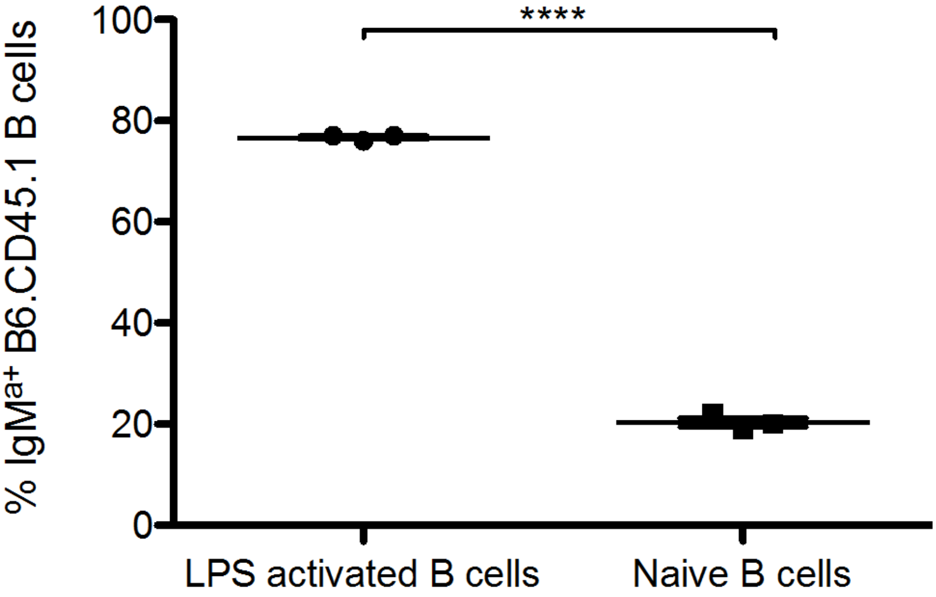

Figure 3.4 Activated B cells transfer membrane components at both 37°C and 4°C. Day-3 LPS activated MD4 splenocytes, labelled with DiI, were added to unlabelled day-3 LPS activated B6.CD45.1 splenocytes. Co-cultures were incubated at 37°C or 4°C for 2 hours. Different B cell populations were identified as in Figures 3.1 and 3.2. The percentage of B6.CD45.1 B cells acquiring (a) DiI and (b) IgM^{a} is shown. Data represents mean ± SEM (a. n=12, b. n=6) representative of at least ten independent experiments. *** $p < 0.001$, **** $p < 0.0001$, unpaired Students *t*-test.

a. Transfer of DiI labelled membranes

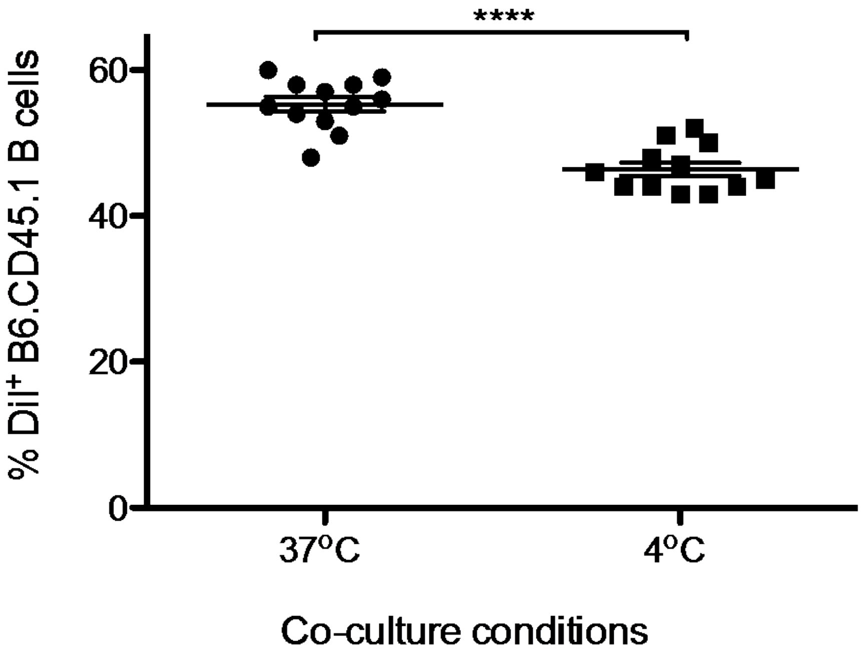

b. Transfer of IgM^a

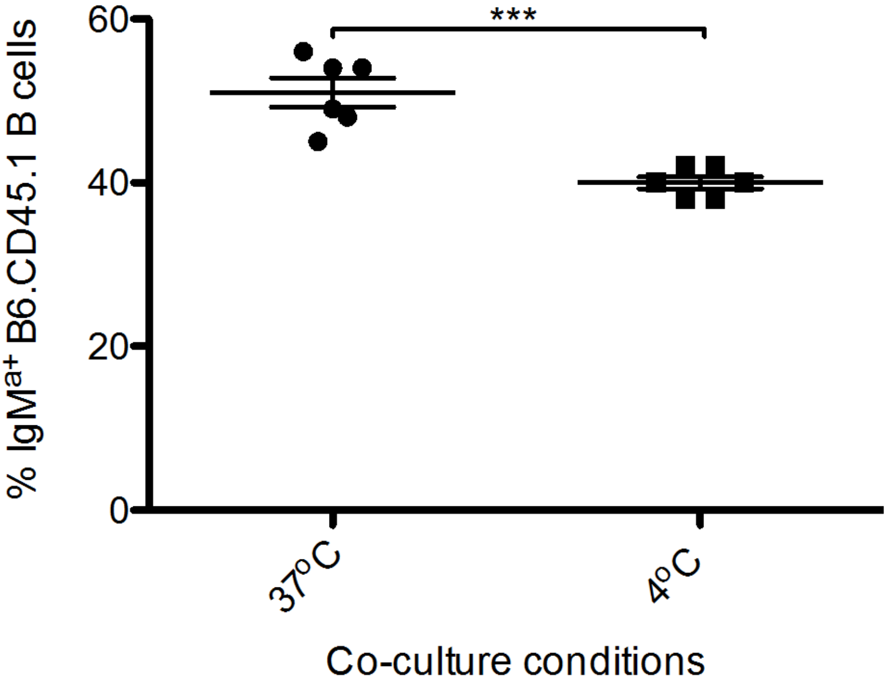

(Figure 3.4a). Similarly, there was only a modest increase in donor MD4 IgM^a transfer to B6.CD45.1 B cells at 37^oC (1.3-fold) compared to the transfer observed at 4^oC (Figure 3.4b). Although the amount of membrane and IgM^a transfer between B cells at 4^oC is significantly less than that seen at 37^oC, it is still substantial in comparison to the considerably lower transfer seen with unstimulated donor B cells.

3.3.3 Cell penetrating peptides (CPPs) as a mechanism of transfer between B cells

In the previous section it was demonstrated that activation of B cells enhances transfer of their membrane components to bystander B cells and this transfer by activated B cells occurs at both 37ºC and 4ºC. However, the molecular mechanisms underlying this transfer remain largely unknown. The fact that transfer occurs at 4ºC excludes many molecular pathways that can mediate membrane exchange. This indicates involvement of a unique membrane transfer mechanism. Cell penetrating peptides (CPP) are short hydrophilic molecules capable of translocating across plasma membranes, independently of receptors or specific transport mechanisms (Bechara and Sagan, 2013). They are typically 5 – 30 amino acids in length, commonly with a large proportion of arginine and lysine residues, and are very rarely negatively charged. Despite CPPs sharing these characteristics, they have great sequence and structural diversity, which may relate to different modes of uptake into cells. There is evidence to support both energy-dependent and energy-independent mechanisms of uptake, with major mechanisms used by CPPs being endocytosis (energy-dependent) and direct translocation (energy-independent). Important for the current study is the energy-independent mechanism of CPP uptake. Several studies have demonstrated CPP translocation can occur at 4ºC (Jiao et al., 2009, Ter-Avetisyan et al., 2009, Derossi et al., 1994), thus cell membrane proteins containing CPP motifs represent potential mediators of BCR and membrane sharing.

3.3.3.1 Classification of CPPs

To assess the involvement of CPPs in the transfer of membranes between B cells, experiments were designed to analyse the characteristics of some common CPPs. Assays were also planned such that the results obtained would indicate whether or not this mechanistic theory of CPPs being mediators of membrane exchange is a possibility. It is important to note that the physiochemical properties underlying the CPPs, described in section 3.2, may affect their uptake into cells. Likewise, it is plausible that these properties could have an impact on transfer of membranes between B cells. Thus not all mechanisms of CPP uptake may be conducive to membrane exchange between B cells. To avoid potentially limiting the study to one particular model or mechanism of CPP uptake, for the current study a commonly used (based on literature) CPP from each CPP class was chosen.

Table 3.1 shows the sequences of the 3 CPPs used in this study. Non-amphipathic TAT peptide was the first peptide capable of penetrating cell membranes to be discovered (Frankel and Pabo, 1988). It is a peptide derived from the HIV-1 transactivator of transcription (TAT) protein, the sequence responsible for cell penetration being 13 amino acid residues long (Vives et al., 1997), with 8 residues being positively charged (Table 3.1). Penetratin, a secondary amphipathic CPP, is also a protein derived CPP with its origins being from the *Drosophila* Antennapedia homeodomain. The 16 amino acid domain responsible for cellular internalisation of the protein is known as penetratin, and contains 7 basic residues (Derossi et al., 1994). In contrast to the protein-derived CPPs TAT and penetratin, TP10 is a chimeric peptide, formed by the fusion of two naturally occurring sequences. TP10 contains motifs from mastoparan and galanin, and is a shorter analogue of its predecessor, transportan (Soomets et al., 2000). It is a primary amphipathic CPP that consists of 21 amino acid residues, with only 4 residues being positively charged (Soomets et al., 2000) (Table 3.1).

Table 3.1 The cell penetrating peptides (CPP) used in this study and their physicochemical properties.

Peptide	Origin	Class	No. of Arginines	No. of Lysines	No. of Residues	Sequence[a]	Total Charge	Reference
Transcription transactivating (TAT)	HIV-1 transactivator of transcription (48-60)[b]	Non-amphipathic	6	2	13	GRKKRRQRRRPPQ	+8	(Vives et al., 1997)
Penetratin	Antennapedia homeodomain (43-58)[b]	Secondary amphipathic	3	4	16	RQIKIWFQNRRMKWKK	+7	(Derossi et al., 1994)
Transportan10 (TP10)	Mastoparan and galanin	Primary amphipathic	-	4	21	AGYLLGKINLKALAALAKKIL	+4	(Soomets et al., 2000)

[a] Red letters indicate positively charged amino acids.

[b] Location of CPP within parent protein.

3.3.3.2 Interaction of CPPs with activated B cells and their effect on B cell viability

Previous studies have shown that CPPs commonly utilise more than one mechanism of cellular entry. Conditions such as the type of cargo, the link between the CPP and the cargo, the lipid composition of the target cell, the extracellular CPP concentration and incubation time can all affect the uptake of the CPP (Fischer et al., 2002, Verdurmen et al., 2013, Yandek et al., 2007, Ziegler and Seelig, 2011, Fretz et al., 2007, Säälik et al., 2011). It is likely that the down regulation of one entry pathway may result in the upregulation of another pathway. Also, at certain concentrations CPPs can be toxic for cells. This is thought to be a result of the direct translocation route of entry into cells and is manifested as a general increase in plasma membrane permeability. Currently, no CPP studies have been conducted using resting or activated B cells. Thus, it was important to assess the toxicity of CPPs for activated B cells, as well as the level of interaction with these B cells.

The most common method of detecting the interaction between CPPs and cells is to couple the peptide to a fluorophore and measure the fluorescence of the treated cells by flow cytometry. In this study fluorescein isothiocyanate (FITC) and biotin labels were used to monitor CPP interactions with B cells. Prior to incubation with cells, the biotinylated CPPs were coupled with streptavidin-allophycocyanin (APC) to form multimeric complexes. The biotin-CPP-streptavidin-APC complex is approximately 60 kDa and due to there being four biotin-binding sites on each streptavidin molecule, there is the potential for four CPPs to bind, forming multimeric biotin-CPP-streptavidin-APC complexes. These complexes resemble a protein containing multiple CPP motifs and provide a better representation of cell surface proteins containing CPP motifs potentially involved in membrane sharing between B cells.

The interaction of FITC conjugated CPPs with day-3 LPS activated B cells was assessed by measuring the FITC fluorescence of CPP treated B cells. Uptake of TAT, penetratin and TP10 by the B cells was found to be proportional to the concentration of FITC-CPP added to the B cell suspension (Figure 3.5a, b and c). The toxicity of the 3 FITC-CPPs for the B cells was evaluated based on the percentage of cells not labelled with the dead cell marker, Hoechst 33258. For concentrations in the range 1 to 12.5 μM B cells viability was not affected by any of the FITC-CPP constructs (Figure 3.5a, b and c). FITC-Penetratin at concentrations of 25 and 50 μM produced a modest decrease in B cell viability but there was no affect on cell viability when cells were incubated with increasing concentrations of FITC-TAT and FITC-TP10. Although there was a 10% decrease in cell viability at the highest concentration of FITC-penetratin used, the fluorescence signal continued to increase in the presence of 25 and 50 μM of the peptide, indicating increased FITC-penetratin uptake by the remaining viable B cells (Figure 3.5a, b and c).

The interaction of biotin-CPP-streptavidin-APC multimeric complexes with day-3 LPS activated B cells was also assessed and measured as described above. Fluorescence intensity was proportional to the concentration of biotin-TAT-streptavidin-APC incubated with the B cells (Figure 3.5d). In contrast to the biotin-TAT multimeric complexes, there was a much lower B cell uptake of the biotin-penetratin multimeric complexes (Figure 3.5e) and negligible uptake of the biotin-TP10- multimeric complexes (Figure 3.5f), despite the FITC versions of these CPPs interacting strongly with B cells. Cell viability was not affected when B cells were incubated with either biotin-TAT or biotin-penetratin multimeric complexes at the concentrations tested (Figure 3.5d and e). However, although there was no evidence of uptake of the biotin-TP10-streptavidin-APC multimeric complexes by the B cells, B cell viability was dramatically reduced by this conjugated CPP at concentrations of 25 and 50 μM, there being few viable B cells remaining in the presence of 50 μM of the biotin-TP10 multimeric complex. Western blot analysis confirmed that the TP10 and penetratin peptides were biotinylated and complexed with streptavidin-APC (data not shown). Thus, it appears that biotin-TP10 multimeric complexes are highly toxic for B cells despite only weakly interacting with B cells and consequently were omitted from further experiments.

Figure 3.5 Uptake of different monomeric and multimeric CPPs by LPS activated B cells and effects on B cell viability. C57BL/6 splenocytes were cultured for 3 days with 10 μg/ml of LPS and then incubated with either FITC labelled or biotinylated versions of TAT (a and d), penetratin (b and e) and TP10 (c and f) for 1 hour. Viable B cells were identified by Hoechst 33258 uptake and B220 staining as in Figure 3.1. Biotinylated peptides were incubated with streptavidin–APC prior to addition to cells to form multimeric biotin-CPP complexes. Viability (% viable B cells) and mean fluorescence intensity (MFI) of CPP uptake was determined by flow cytometry and measured as a function of peptide concentration. Each graph represents an individual experiment. Mean ± SEM is shown (n=3).

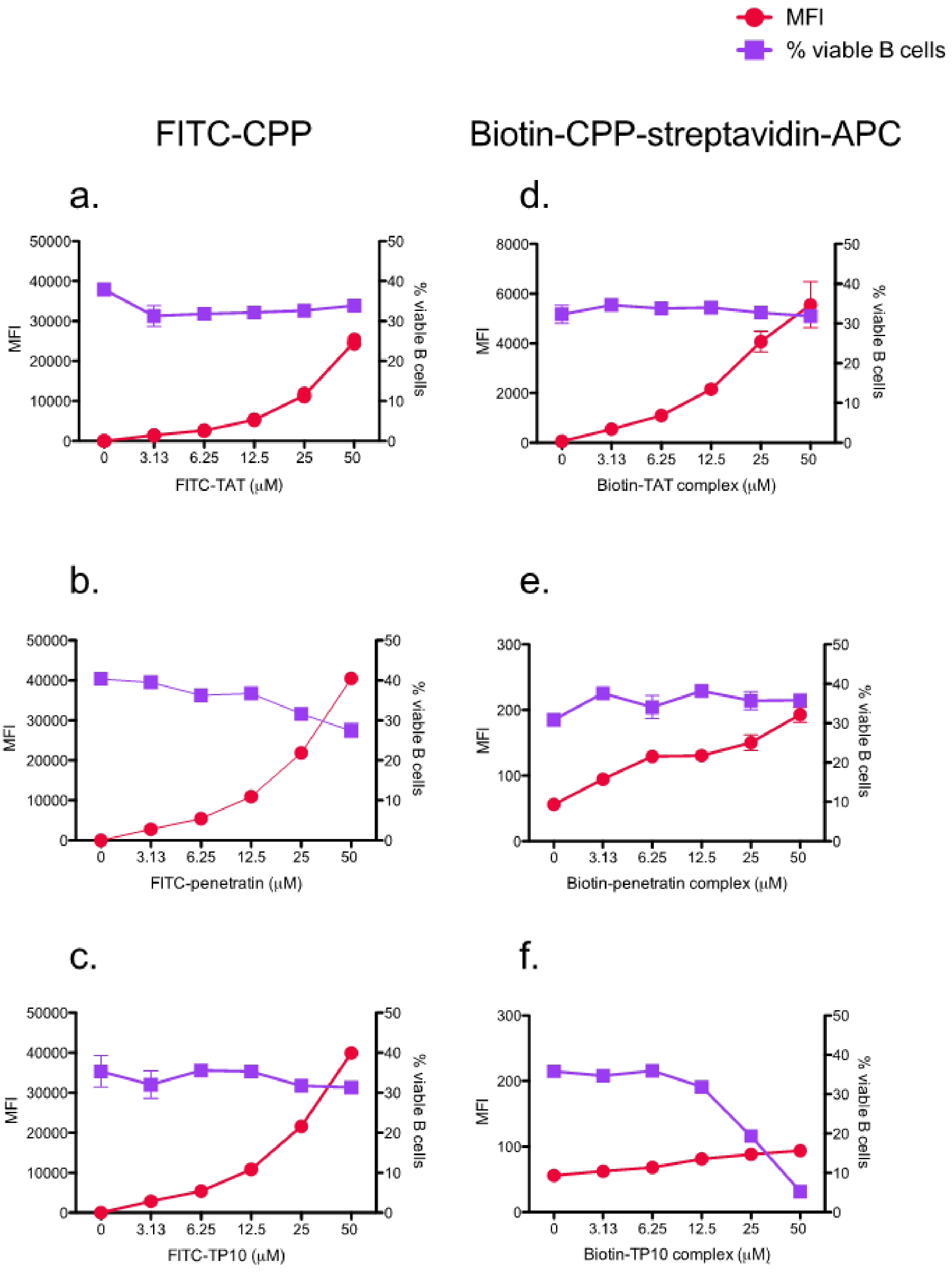
MFI
% viable B cells
FITC-CPP
Biotin-CPP-streptavidin-APC
a.
MFI
% viable B cells
FITC-TAT (μM)
0
3.13
6.25
12.5
25
50
0
10000
20000
30000
40000
50000
d.
Biotin-TAT complex (μM)
0
2000
4000
6000
8000
b.
FITC-penetratin (μM)
e.
Biotin-penetratin complex (μM)
0
100
200
300
c.
FITC-TP10 (μM)
f.
Biotin-TP10 complex (μM)
0
10
20
30
40
50

3.3.3.3 The influence of B cell activation on CPP uptake by B cells

An important feature of B cell membrane sharing is that it is enhanced significantly upon activation of B cells. Day-3 LPS activated B cells are capable of efficiently transferring membranes to neighbouring B cells, whereas freshly isolated B cells are only able to transfer much smaller amounts of membranes (Figure 3.3)(Quah et al., 2008). If CPPs were mediating this transfer it is expected that they would more favourably interact with activated B cells in comparison to freshly isolated B cells. Using the three different CPPs selected, either biotinylated or FITC coupled, it was possible to assess (a) whether there is a particular class of CPP that interacts with either freshly isolated or activated B cells, and (b) whether the FITC-CPPs and multivalent biotin-CPPs differ in their uptake by LPS activated versus freshly isolated B cells.

Day-3 LPS activated B cells or freshly isolated B cells were incubated with each of the CPPs at a non-toxic concentration (10 μM) for 1 hour. The interaction of the B cells with the CPPs was assessed by flow cytometry and displayed as mean fluorescence intensity (MFI) minus the auto-fluorescence of the B cells (less background). All FITC coupled CPPs were taken up by the LPS activated B cells to a much greater extent than by the naïve B cells (Figure 3.6a), although the differences were much more marked for FITC-TP10 (9-fold) than FITC-TP10 (3-fold) and FITC-penetratin (3-fold). Similarly, the biotin-CPP multimeric complexes also associated with LPS activated B cells to a much greater extent than naïve B cells (Figure 3.6b), this difference being most evident with the TAT complex (40-fold) than the penetratin complex (6-fold). Nevertheless, although the uptake of all CPPs by naïve B cells is significantly lower than that by LPS activated B cells, the MFI values are greater than background clearly indicating that CPPs are also taken up by naïve B cells (Figure 3.6).

3.3.3.4 The influence of temperature on CPP uptake by B cells

Membrane sharing between B cells occurs at 4°C eliminating energy-dependent processes such as endocytosis. In order for CPPs to mediate membrane exchange they must be capable of interacting with B cells at 4°C. To evaluate this day-3 LPS activated B cells were incubated with CPPs for 1 hour at 4°C and 37°C. Again, the interaction of the B cells with the CPPs was assessed by flow cytometry and displayed as mean fluorescence intensity (MFI) minus the auto-fluorescence of the B cells (less background). The uptake of each CPP preparation by LPS activated B cells at 4°C and 37°C is shown in Figure 3.7a and b.

The differences between uptake of CPPs by LPS activated B cells at 4°C and 37°C, when they occurred, were modest. Penetratin uptake, whether mono- or multivalent, was unaffected by temperature with uptake by LPS activated B cells being approximately equivalent at both 4°C and 37°C. The uptake of TAT by LPS activated B cells, whether mono- or multivalent, was only slightly but significantly enhanced at 37°C (1.4-fold). FITC-TP10 uptake by LPS activated B cells was the most affected by temperature being 2-fold higher at 37°C than 4°C. This indicates that endocytosis or other energy-dependent mechanisms may participate in the uptake of TAT and TP10, however, in circumstances where these processes are unable to be utilised then energy-independent mechanisms such as direct translocation are employed. Collectively these results indicate that, in general, CPPs are capable of being taken up by LPS activated B cells at 4°C. Furthermore, it appears that different CPPs may use different methods of interacting with and translocating into B cells.

Figure 3.6 CPPs interact with LPS activated B cells much more effectively than with freshly isolated B cells. Freshly isolated (naïve) or day-3 LPS activated splenocytes were incubated with either FITC (a) or biotin (b) conjugated TAT, penetratin and TP10 CPPs (10 μM) for 1 hour at 37°C. Biotinylated peptides were incubated with streptavidin – APC prior to addition to cells to form multimeric complexes. Viable B cells were identified by Hoechst 33258 uptake and B220 staining as in Figure 3.1 and mean fluorescence intensity (MFI) was determined via flow cytometry with plotted values background subtracted. Data presented are representative of three independent experiments and is given as mean ± SEM (n=3). ***p < 0.001, based on general analysis of variance.

a. FITC-CPP

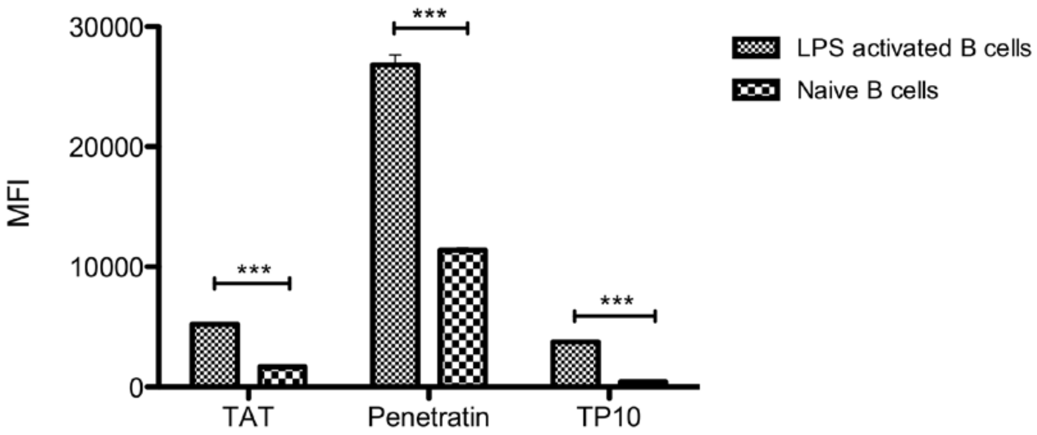

b. Biotin-CPP-streptavidin-APC

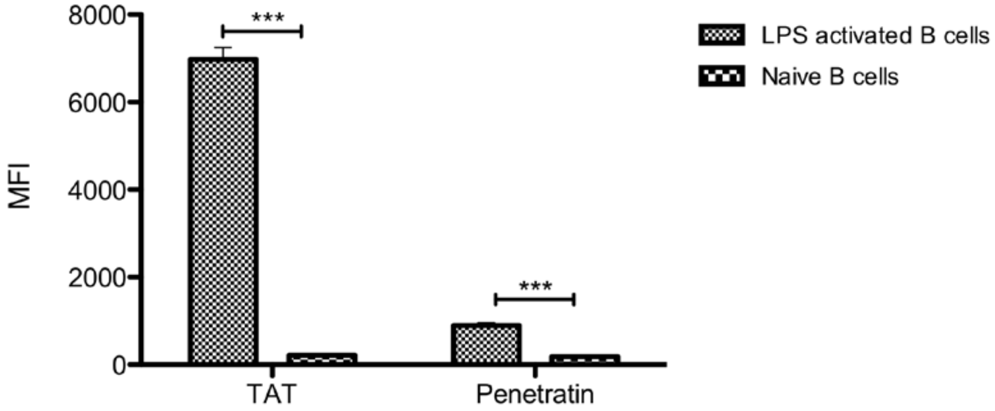

Figure 3.7 CPPs interact with LPS activated B cells at both 4°C and 37°C. Day-3 LPS activated splenocytes were incubated with either FITC (a) or biotin (b) conjugated TAT, penetratin and TP10 CPPs (10 μM) for 1 hour at 4°C or 37°C. Biotinylated peptides were incubated with streptavidin – APC prior to addition to cells to form multimeric complexes. Viable B cells were identified by Hoechst 33258 uptake and B220 staining as in Figure 3.1 and mean fluorescence intensity (MFI) of CPP uptake was determined by flow cytometry, with plotted values in (a) and (b) background subtracted. Data presented are representative of three independent experiments and is given as mean ± SEM (n=3). ns: not significant, ***p < 0.001, based on general analysis of variance.

a. FITC-CPP

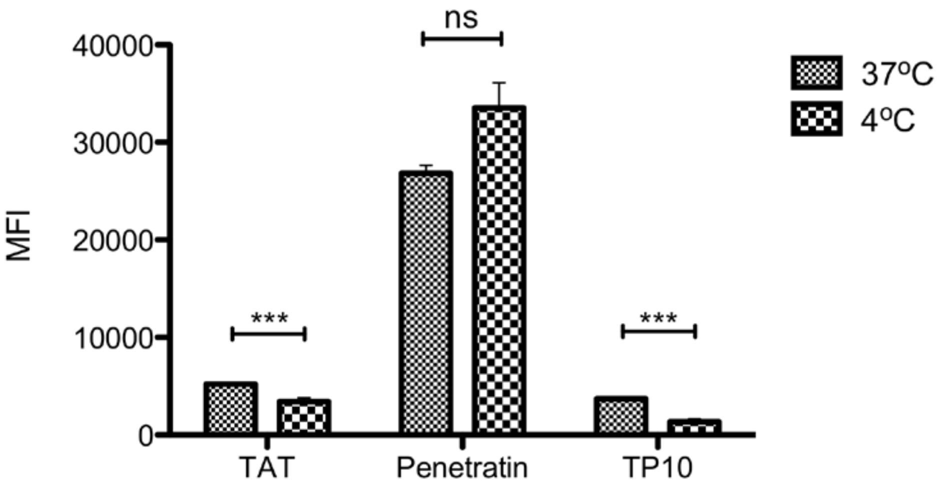

b. Biotin-CPP-streptavidin-APC

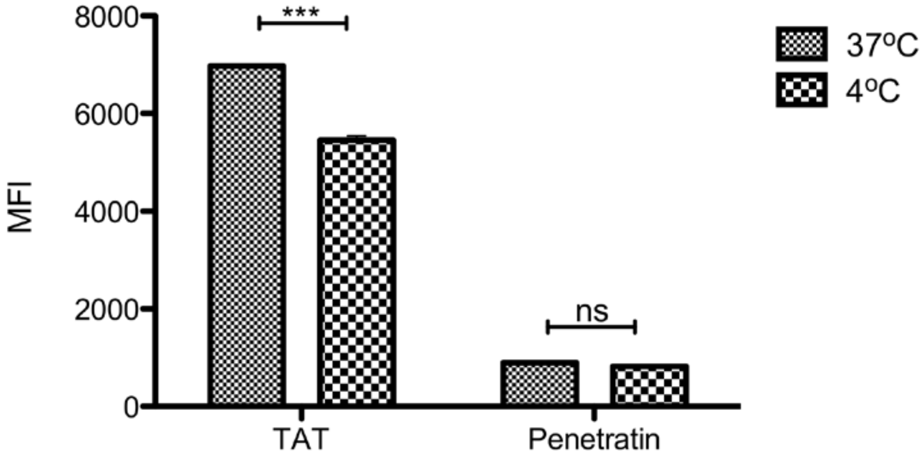

3.3.3.5 Kinetics of CPP uptake by LPS activated B cells

Studies described earlier in this thesis have shown that membrane and cell surface protein exchange can occur more efficiently between B cells following activation by LPS (section 3.3.2.1) and that LPS activated B cells take up CPPs to a greater extent than naïve B cells (section 3.3.3.3). Studies performed previously by my supervisor's laboratory (Quah et al., 2008) demonstrated that acquisition of donor B cell surface proteins was clearly evident after 1-3 days of co-culture of B cells in the presence of LPS. Thus, it was of interest to extend these findings and examine the kinetics of CPP uptake by B cells activated by LPS for different periods of time.

To compare the kinetics of membrane exchange between B cells and the uptake of CPP by B cells these processes were assessed after 0, 2, 8, 24, 48, and 72 hours LPS stimulation (Figure 3.8). The results show the level of membrane exchange between B cells and are measured as the percentage of unlabelled recipient B cells acquiring DiI labelled membranes from donor B cells. Incubation with the B cell mitogen, LPS, for 0-8 hours resulted in a level of B cell activation that was not conducive for membrane transfer, as is evident from the low number of DiI positive recipient B cells (Figure 3.8a). However, after 24 hours of LPS activation substantial membrane transfer occurred, with over 60% of unlabelled recipient B cells acquiring donor-derived DiI labelled membranes (Figure 3.8a), this level of membrane transfer plateauing after 24, 48 and 72 hours of LPS stimulation (Figure 3.8a).

Figures 3.8b and 3.8c display the interaction of B cells with FITC-CPPs and multimeric biotin-CPPs, respectively, at 0, 2, 8, 24, 48 and 72 hours post LPS stimulation. Similar to membrane exchange between B cells, there was minimal uptake of FITC-CPPs by B cells prior to 24 hours of LPS stimulation, with after

24-72 hours stimulation the B cell uptake of each FITC-CPP increasing steadily (Figure 3.8b). For CPPs labelled with biotin and assembled into multimeric complexes, the interaction with B cells was evident after 8 hours of LPS stimulation. However, for biotin-TAT complexes the uptake by B cells increased significantly from 8-24 hours, as the B cells became more activated, with uptake declining after 48 hours, possibly due to a decrease in B cell viability. For biotin-TP10 complexes, as was shown previously in this thesis, there was negligible uptake by 3 day LPS activated B cells (Figure 3.5f), the kinetic study confirming this finding, and further showing that at no stage of B cell activation does there appear to be uptake of biotin-TP10 multimeric complexes by B cells (Figure 3.8c). Thus, these results indicate that a level of B cells activation, reached after 8-24 hours of stimulation with the B cell mitogen LPS, is required for both membrane exchange and uptake of CPPs by B cells (Figure 3.8a, b, c). Thus, these data lend support to the notion that CPPs may be mediators of membrane sharing between B cells.

Figure 3.8 B cell membrane transfer and CPP uptake by B cells follows similar B cell activation kinetics. B6.CD45.1 and MD4 splenocytes were cultured with 10 µg/ml of LPS and harvested after allocated activation times (0-72 hours). (a) At the allocated harvest times B6.CD45.1 splenocytes were mixed with DiI labelled MD4 splenocytes for 2 hours. Membrane exchange was assessed by flow cytometry as outlined in Figure 3.2, and presented as percentage of B6.CD45.1 B cells acquiring DiI. (b) FITC conjugated CPPs and (c) biotin conjugated CPPs were incubated for 1 hour with C57BL/6 splenocytes that had been activated with LPS for 0-72 hours. Conjugated peptides were used at a concentration of 10 μM. Biotinylated CPPs were incubated with streptavidin-APC prior to addition to cells. Viable B cells were identified by Hoechst 33258 uptake and B220 staining as in Figure 3.1. CPP uptake by B cells was measured by flow cytometry. All experiments were performed at 4°C. Data expressed as mean ± SEM (n=3) and is representative of at least 2 - 4 independent experiments.

a. Membrane transfer

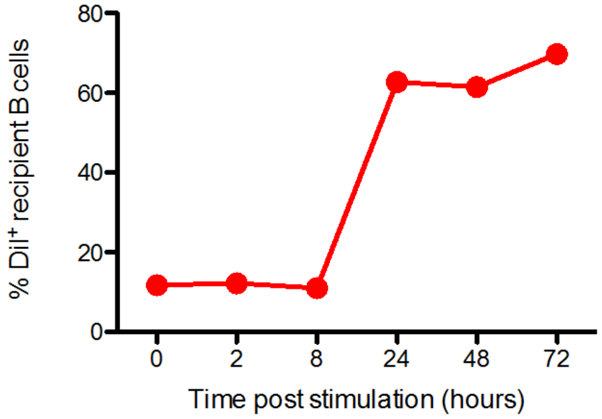

b. FITC-CPP uptake

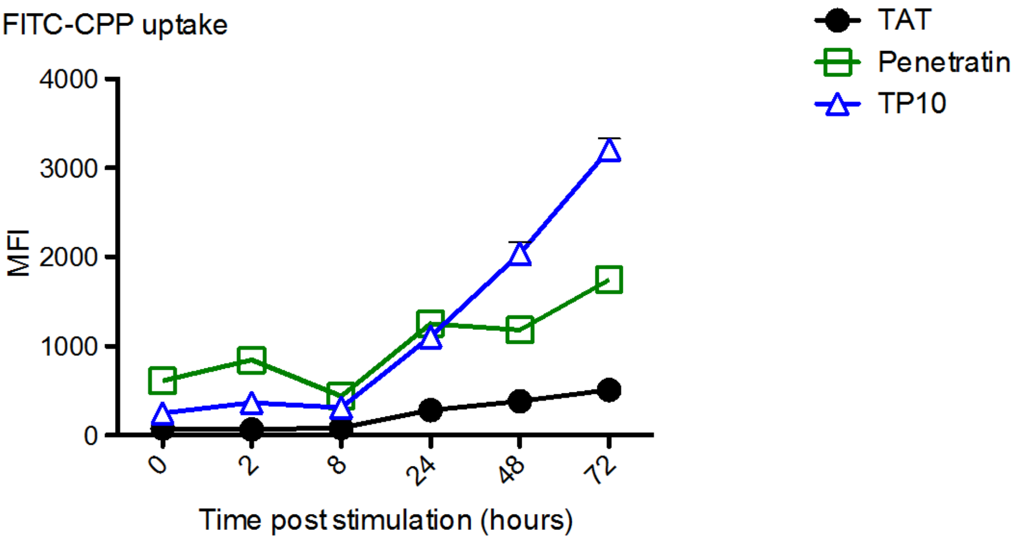

c. Biotin-CPP-streptavidin-APC uptake

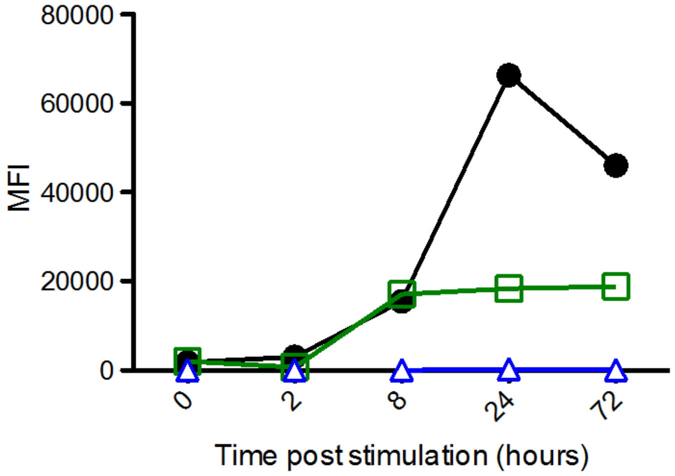

3.4 Discussion

Over the past decade there has been an increasing number of reports documenting the transfer of membranes and associated cell surface proteins between cells of the immune system (Quah et al., 2008, Chaudhri et al., 2009, Aucher et al., 2008, Hudrisier et al., 2005, Daubeuf et al., 2010a), however, the molecular mechanisms involved in these processes remain unclear. The data presented in this Chapter provide three key findings supporting a role for CPPs in B cell membrane exchange, namely; (i) Membrane exchange occurs predominantly between activated B cells, with lower exchange being observed between freshly isolated B cells (Figure 3.3). Similarly, CPPs are taken up by LPS activated B cells to a greater extent than by freshly isolated B cells (Figure 3.6). (ii) It is also evident that approximately the same kinetics of B cell activation (~ 8-24 hours) is required for both membrane exchange and CPP uptake by B cells (Figure 3.8). (iii) Lastly, membrane transfer between activated B cells occurs efficiently at both 4°C and 37°C (Figure 3.4), as does the uptake of most CPPs by B cells (Figure 3.7).

In the present study we characterised the interaction of three major CPPs with B cells. Two of the CPPs chosen, penetratin and TAT, are highly cationic and show little to no amphipathic capabilities. The third CPP, TP10, is more amphipathic, less cationic and longer chain than the other two CPPs studied (Table 3.1). Common between all these CPPs is their ability in a monomeric state to efficiently interact with and cross the plasma membrane of cells.

There are few published papers documenting the interactions between CPPs and primary lymphocytes (Rodrigues et al., 2013, Muller et al., 2013), particularly with activated primary lymphocytes. Usually, CPP studies employ immortalised cell lines (Sasaki et al., 2008, Deshayes et al., 2008, Letoha et al., 2003), and when studies using primary cells are undertaken the cells are naïve (Rodrigues et al., 2013, Muller et al., 2013). The current work utilises both day-3 LPS activated and freshly isolated B cells, and looks at their interaction with CPPs coupled with either FITC or biotin, the latter conjugates being made multimeric and fluorescent by the addition of streptavidin-APC.

CPPs differ in their cytotoxicity depending on their sequence and the cargo attached, such as FITC and the biotin-streptavidin-APC moiety, the latter mimicking a protein containing multiple CPP motifs. This study assessed the cytotoxic properties of the conjugated CPPs on B cells, and whether the different conjugates influenced the uptake of CPPs by B cells. The toxicity of TAT was minimal on activated B cells, regardless of the concentration used, and did not differ between FITC and biotin-labelled CPPs. Penetratin, when coupled to FITC, showed a slight increase in the level of toxicity as the concentration of the peptide increased. In contrast, when penetratin was biotinylated and assembled in a multimeric complex there appeared to be no toxic effect on B cells, however the uptake by B cells was substantially reduced. These differences demonstrate the importance of the cargo attached to CPPs, and that the level of interaction with B cells does not necessarily translate into toxicity. The third peptide, TP10, when FITC conjugated had no effect on B cell viability and is readily taken up by LPS activated B cells. In contrast, the uptake of multimeric biotin-TP10 by B cells was negligible, although above a concentration of 12.5μM the conjugate was highly toxic for activated B cells. Previous studies have shown that TP10 is toxic for malignant cell lines through inducing severe membrane leakage, and is significantly more toxic in comparison to penetratin and TAT (Saar et al., 2005, Magzoub et al., 2003). The structure of TP10 is one with high hydrophobicity and the potential to form amphipathic α-helices in membranes. It has been suggested that this is important for its ability to interact with and cross plasma membranes (Yandek et al., 2007). The addition of a biotin-streptavidin-APC complex to TP10 may sterically hinder the formation of the secondary structure that TP10 requires to interact with phospholipid membranes, although how this translates into cytotoxicity is unknown.

It is also evident that biotin-penetratin multimeric complexes interact less effectively with B cells. Penetratin is a secondary amphipathic molecule, which has 7 basic residues that are crucial for its uptake into cells. Substitution of the basic residues for alanine results in a significant decrease in penetratin uptake (Fischer et al., 2000). However, penetratin has also been shown to adopt α-helical and β-strand structures upon interaction with lipids (Magzoub et al., 2002, Letoha et al., 2003, Christiaens et al., 2004). Whether there is a direct correlation between CPP secondary structure and its translocation ability is yet to be deciphered, however, the importance of the structural polymorphism and malleability of CPPs has been shown to be important for membrane interaction and internalisation (Deshayes et al., 2008). Thus, we suggest the addition of the biotin-streptavidin-APC complex interferes with the structural flexibility of primary and secondary amphipathic CPPs thereby hindering their interaction with B cells. In contrast, non-amphipathic CPPs, such as TAT, remain unstructured upon interaction with plasma membrane and appear to rely exclusively on electrostatic interactions with the phospholipids on the cell surface (Lattig-Tunnemann et al., 2011). This may indicate that the protein(s) involved in membrane transfer between B cells has a highly cationic non-amphipathic region that relies on electrostatic interactions with the phospholipid membrane to initiate membrane transfer between B cells, rather than interactions that depend upon formation of a secondary structure.

It has been previously shown that lymphocyte activation is important for the process of transfer of cell surface proteins and membranes from one cell to another (Hudrisier et al., 2005, Quah et al., 2008). In agreement with this, we demonstrated that activation of B cells led to a ~4-fold increase in acquisition of DiI labelled donor membranes by the unlabelled recipient B cells, when compared with freshly isolated B cells. Likewise, all three CPPs, irrespective of their label, interacted with activated B cells to a far greater extent (up to 40-fold) than was evident with freshly isolated B cells (Figure 3.6). Cellular activation is likely to be important due to several contributing factors. Firstly, activation increases the expression of many B cell surface molecules, many being involved in adhesion and cellular communication. It is likely that one or several of these cell surface proteins that are upregulated, contain CPP motifs that could increase membrane transfer between B cells. Secondly, upon B cell activation there is a significant amount of membrane re-organisation, including plasma membrane depolarisation, redistribution of cell surface proteins and a reduction in the fluidity of the membrane (Printen et al., 1993). These structural changes in B cell composition are likely to dictate the efficiency with which B cells are able to transfer membrane components, or interact with CPPs. It could be suggested that these membrane changes are a result of the formation of large signalling lipid rafts. Lipid rafts are plasma membrane micro-domains that are partially ordered resulting from the close packing together of glycosphingolipids and cholesterol (Brown and London, 1998). The activation of immune cells results in the coalescence of lipid micro-domains into much larger, and more stable, entities. This is accompanied by the rapid recruitment and concentration of key signalling molecules, such as the kinases Lyn and Syk, thereby ensuring efficient and sustained signal transduction (Gaus et al., 2005, Dykstra et al., 2003, Gupta and DeFranco, 2007). One can speculate that these accumulations of cell surface proteins include proteins containing CPP motifs important for the transfer of membrane components. Interestingly, CPPs bind to and can induce glycosaminoglycan (GAG) clusters on the cell surface (Ziegler and Seelig, 2011), and GAGs have been shown to induce the coalescence of lipid rafts (Hogue et al., 2011). Moreover, it has been demonstrated that the secondary amphipathic CPP, penetratin, is capable of inducing phospholipid domain separation and membrane undulations, which could also contribute to membrane reorganisation and transfer (Lamaziere et al., 2010).

Interestingly, both membrane transfer between B cells and CPP uptake by B cells occurs at temperatures as low as 4ºC, indicating energy independent mechanisms exist for these processes. It should be noted that lipid raft coalescence in B cells has been demonstrated to occur efficiently at 4ºC (Cheng et al., 1999, Cheng et al., 2001). B cell uptake of TAT and TP10 at 4ºC was somewhat reduced in comparison to their uptake by B cells at 37ºC. However, we commonly see a similar effect in the transfer of cell surface protein and membranes between B cells, with slightly less transfer evident at 4ºC, than at 37ºC (Figure 3.4). Thus, although TAT and TP10 uptake was reduced at 4ºC, cell surface proteins containing similar motifs could still potentially mediate membrane exchange.

CPPs are well known to be capable of translocating across cell membranes at 4ºC (Jiao et al., 2009, Ter-Avetisyan et al., 2009, Derossi et al., 1994), however, the molecular basis of translocation has been the subject of controversies, reviewed in (Bechara and Sagan, 2013, Madani et al., 2011). A multitude of mechanisms have been suggested, including inverted micelle formation (Kawamoto et al., 2011), adaptive translocation (Rothbard et al., 2005) and the pore formation model (Herce et al., 2009). The precise mechanism of internalisation differs for each model, and is thought to be highly dependent upon peptide concentration, peptide sequence and lipid composition. Common to all, however, is the interaction of the negatively charged cellular membrane components with the positively charged amino acid residues of the CPP. This is deemed as the first step that leads to cellular uptake, and we propose, the transfer of membrane components between B cells. The plasma membrane is composed of anionic phospholipids, sialylated proteins and glycosaminoglycans (e.g., heparan sulfate), all of which contribute to the overall net negative charge of the membrane (Derossi et al., 1998). The electrostatic interaction, subsequent folding and insertion of CPPs into the phospholipid bilayer can lead to local destabilisation of the cellular membrane. This perturbance of the lipid bilayer has been proposed as a mechanism that leads to peptide internalisation (Yandek et al., 2007, Schmidt et al., 2010). Thus, one can speculate that this process is also involved in membrane transfer between B cells.

Thus, from the data presented in this chapter and the literature available, a mechanism can be proposed in which B cells transfer cell surface proteins and membranes. This model suggests that, when appropriately activated, a B cell upregulates the expression of cell surface protein(s), that contain CPP motifs with a significant proportion of positively charged residues. These positively charged residues will be attracted to, and subsequently interact with, the negatively charged membrane components of a recipient B cell. This electrostatic interaction could be with GAGs already associated with a lipid raft structure, or could lead to the coalescence of micro-domains into a lipid raft.

Both the rearrangement that occurs with the formation of lipid raft structures and the interaction of the CPP with the lipid membrane could lead to a localised area of membrane destabilisation. This weakened membrane on the recipient B cell makes the plasma membrane surface more accessible for fusion and is likely to be favourable for the transfer of cell surface proteins and membranes between B cells.

Chapter 4

Identifying molecular mechanisms of membrane exchange between B cells

4.1 Abstract

As previously demonstrated in this thesis, both naïve and activated bystander B cells can acquire antigen-specific BCR from activated B cells through a process of membrane transfer. However, the molecular mechanisms underlying this transfer remain unknown. An important feature of membrane transfer is that B cells require appropriate activation for transfer to occur. Earlier studies from my supervisor's laboratory found that LPS but not CpG activated B cells are capable of transferring their BCR to bystander B cells. The current study takes advantage of this finding to elucidate the molecular basis of BCR transfer. Microarray technology was used to conduct a comparative analysis of the transcriptomes of LPS stimulated B cells, CpG stimulated B cells and unstimulated B cells to identify genes that may be involved in BCR transfer. Gene Ontology (GO) terms and Kyoto Encyclopaedia of Genes and Genomes (KEGG) pathway analyses were performed to identify genes involved in cell communication and cell adhesion and which possessed cell penetrating peptide sequences. From this analysis, five candidate genes were identified and confirmed by real-time PCR that may play a role in BCR transfer, namely ALCAM, AMIGO2, CTLA-4, Slp3 and TIGIT. Subsequent studies with mAbs specific for ALCAM, CTL-4, TIGIT and the TIGIT ligand, PVR, revealed that the cell surface expression of all these proteins is substantially upregulated on LPS-activated B cells. Furthermore, the ALCAM, TIGIT and TIGIT+PVR mAbs significantly enhanced membrane transfer, whereas the CTLA-4 mAb, which blocks CTLA-4 ligand binding, had no effect on membrane transfer. Based on these data and other published findings it is hypothesised that mAbs specific for ALCAM and TIGIT/PVR may crosslink these receptors, creating a patching

effect, similar to a lipid raft, in which there are areas of localised membrane destabilisation and, consequently, more accessible areas for membrane fusion.

4.2 Introduction

As previously mentioned in this thesis, the process of membrane sharing has become increasingly recognised in recent years (Chaudhri et al., 2009, Quah et al., 2008, Aucher et al., 2008, Daubeuf et al., 2010a). However, very little is known about the molecular mechanisms involved in this process. Previous studies have attempted to interfere with the process of membrane exchange between B cells, using compounds known to block cell adhesion, membrane integrity, and several other processes generally associated with membrane fusion and exchange (Quah et al., 2008). With the exception of a few monoclonal antibodies that enhanced transfer, there was little to no effect of these treatments on membrane exchange between B cells (Quah et al., 2008). The inability to inhibit membrane exchange between B cells by blocking known mediators of membrane fusion and exchange events implies a novel mechanism is involved.

The previous Chapter of this thesis focussed on taking advantage of the important finding that membrane exchange between B cells occurs at 4ºC, thereby largely eliminating the involvement of energy dependent processes. Furthermore, we devised an approach to assess the involvement of cell penetrating peptides (CPP) in membrane exchange (Chapter 3). The results demonstrated that CPP motifs might be important mediators of membrane exchange, however, the molecular mechanism and proteins involved remain unknown. The current Chapter takes advantage of another important finding, that B cells require appropriate activation conditions in order to mediate membrane exchange. More specifically, B cells can actively mediate receptor sharing when activated with lipopolysaccharide (LPS) and CD40L (Quah et al., 2008), however, it has been observed that upon stimulation with CpG-DNA (CpG) they fail to do so.

Although both LPS and CpG are potent B cell mitogens, they achieve B cell activation through different Toll-like receptors (TLR) (Takeda et al., 2003). LPS is the ligand for plasma membrane associated TLR4. Upon recognition of LPS by TLR4, intracellular signalling is initiated using one of at least two major pathways, namely the TIRAP-MyD88 or TRIF-TRAM pathways. The TRIF-TRAM pathway regulates activation of interferon regulatory factor (IRF)-3 and the subsequent induction of co-stimulatory molecules (Takeda et al., 2003, Richard et al., 2008). On the other hand, the TIRAP-MyD88 pathway regulates NF-κB activation and related inflammatory cytokine production (Peng, 2005). In contrast, CpG is recognised by nucleic acid-sensing TLR9 that is expressed in the endoplasmic reticulum. Upon recognition of its ligand, TLR9 is recruited to the endosomal compartment and initiates signalling through the MyD88 pathway, without TIRAP. Furthermore, it has been reported that primary naïve B cells, when stimulated with CpG *in vitro* move only in the plane of the culture vessel, and do not form 3D structures (Duffy and Hodgkin, 2012, Hawkins et al., 2009). Typically, activated lymphocytes cultured *in vitro* undergo homotypic adhesion, generating various sized 3D structures (Duffy and Hodgkin, 2012, Hawkins et al., 2009). These differences between TLR4 and TLR9 in intracellular location, signalling and activation induced adhesion patterns may explain the differential activation of membrane sharing between B cells by the two TLR ligands, although the functional relevance of this phenomenon is unknown.

Using this knowledge a standard mouse genome microarray analysis for mRNA expression was undertaken to compare the transcriptomes of C57BL/6 B cells, stimulated for 3 days with LPS or CpG, or unstimulated. As shown in Chapter 1, in the proposed model of membrane transfer between B cells it is hypothesised that specific stimulation of B cells will result in the up-regulation of cell surface proteins that interact with neighbouring B cells and promote the exchange of membrane and cell surface proteins. Thus, we speculated that candidate genes involved in receptor sharing will show altered gene expression in LPS stimulated B cells, compared with CpG stimulated and unstimulated B cells, a speculation that was investigated in this Chapter.

4.3 Results

4.3.1 *Membrane transfer between unstimulated, LPS stimulated and CpG stimulated B cells*

In Section 3.3.2 of this thesis it was demonstrated that day 3 LPS activated B cells were capable of membrane exchange. Furthermore, the degree of membrane exchange between unstimulated B cells was much less. In an attempt to gain a better understanding of the activation conditions required for membrane exchange between B cells to occur, advantage was taken of the previously reported finding that CpG activated B cells are much less effective at transferring membranes to bystander B cells than LPS activated B cells (Quah et al., 2008).

An experiment was initially undertaken to confirm that CpG activated B cells were defective in mediating membrane exchange. First, it was necessary to ensure that CpG stimulated B cells and LPS stimulated B cells were relatively equivalent in the level of proliferation/activation in order to compare their effect on the levels of membrane exchange. As such, splenocytes from MD4 and B6.CD45.1 mice were labelled with 5-(and 6)-carboxyfluorescein succinimidyl ester (CFSE) to assess the proliferation of B cells. CFSE-labelled MD4 and B6.CD45.1 splenocytes were then co-cultured, or cultured alone for 3 days in the presence of LPS (10 μg/ml) or CpG (25 μg/ml), or remained unstimulated.

The CFSE profile in Figure 4.1a demonstrates that ~78% of day-3 LPS stimulated MD4 B cells had proliferated, with up to 7 cell divisions observed. The majority of cells divided 3 to 6 times (Figure 4.1a). Similarly, the CFSE profile for day-3 CpG stimulated B cells shows that ~83% of cells had divided, with up to 7 divisions being observed (Figure 4.1b). However, in contrast to day-

3 LPS activated B cells, the majority of B cells were found in divisions 1 to 4, with cell numbers being roughly equivalent in each (Figure 4.1b). Although the LPS stimulated B cells appear to proliferate more than the CpG stimulated B cells, both mitogens have resulted in a high percentage (~80%) of B cells entering division. Since studies in Chapter 3 showed that LPS activation rapidly induced membrane sharing between B cells at a time (i.e., 6-24 hr) when B cell proliferation would have barely commenced (Figure 3.8a), minor differences in numbers of cell divisions should not affect membrane exchange between activated B cells.

However, although LPS stimulated B cells and CpG stimulated B cells achieved high levels of proliferation, LPS stimulated B cells are capable of sharing their BCR to a far greater extent than CpG stimulated B cells, as evident in Figure 4.1c. Thus, approximately 30% of day-3 LPS stimulated B6.CD45.1 B cells acquired IgM^a molecules from day-3 LPS stimulated MD4 B cells (Figure 4.1c). In contrast, unstimulated B6.CD45.1 B cells acquired 50% less IgM^a than that observed with the LPS stimulated B cells (Figure 4.1c), consistent with previous findings in this thesis (Figure 3.3b). Similarly, day-3 CpG stimulated B cells only achieved levels of IgM^a transfer similar to unstimulated B cells, with just over 15% of day-3 CpG stimulated B6.CD45.1 B cells acquiring IgM^a molecules from day 3 CpG stimulated MD4 B cells (Figure 4.1c). These results suggest that B cells require specific activation conditions for high rates of membrane exchange to occur, and that LPS stimulation achieves this, whereas CpG stimulation may not.

4.3.2 Quality assessment of RNA preparations isolated from different B cell populations

It has been previously established that LPS stimulated B cells are capable of sharing plasma membranes and associated cell surface proteins with bystander B cells. In contrast, CpG stimulated B cells and unstimulated B cells are less capable of transferring plasma membranes to bystander B cells (Figure 4.1c) (Quah et al., 2008). In order to gain a deeper understanding of the molecular mechanisms involved in membrane transfer, RNA was extracted from unstimulated (freshly isolated), day-3 LPS stimulated, and day-3 CpG stimulated B cells to perform a comparative transcriptome analysis using the whole transcript microarray technology. Obtaining intact RNA is a critical first step in gene expression studies. RNA preparations were analysed using the Expert Eukaryote Total RNA Nano Chip on the Agilent 2100 Bioanalyzer, which measures the quality of total RNA by capillary electrophoresis (Agilent Technologies, USA). The Agilent 2100 Bioanalyzer software automatically searches for and identifies peaks for 18S and 28S rRNAs, and peak area ratios are calculated. All RNA samples had clearly visible 18S and 28S rRNA peaks and a small amount of 5S RNA (Figure 4.2a, b and c), indicative of an intact RNA preparation. Another measurement of RNA quality is the RNA integrity number (RIN). It is an algorithm developed by Agilent technologies for assigning integrity values to RNA measurements using the shape of the curve in the electropherogram. It is based on a numbering system from 1 to 10, with 1 being the most degraded and 10 being the most intact (Schroeder et al., 2006). RNA samples all demonstrated a RIN of 8.4 or greater (Figure 4.2a, b and c), indicating that all samples contained high quality intact RNA.

Figure 4.1 LPS but not CpG stimulated B cells can exchange BCRs.

MD4 splenocytes were labelled with CFSE, incubated for 3 days with LPS (10 μg/ml) (a), or CpG (25 μM) (b) and plotted on a CFSE intensity histogram. FlowJo (Tree Star, Inc.) was used to track cell generations 0-7 (blue curves). The percentage of divided cells is shown (%Divided). (c) B6.CD45.1 (IgM^b) and MD4 (IgM^a) splenocytes were mixed in equal numbers and either unstimulated (naïve) or stimulated with LPS (10 μg/ml) or CpG (25 μM) for 3 days at 37^oC. The percentage of B6.CD45.1 B cells acquiring MD4 IgM^a is shown. Data represents mean ± SEM (n=3) and is representative of at least three independent experiments.

a. LPS stimulated

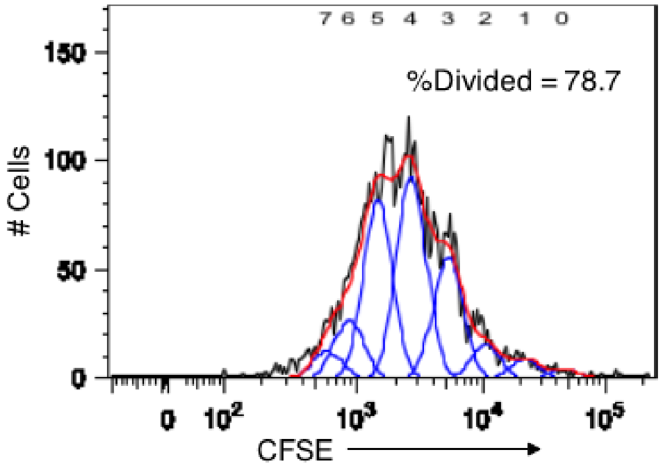

b. CpG stimulated

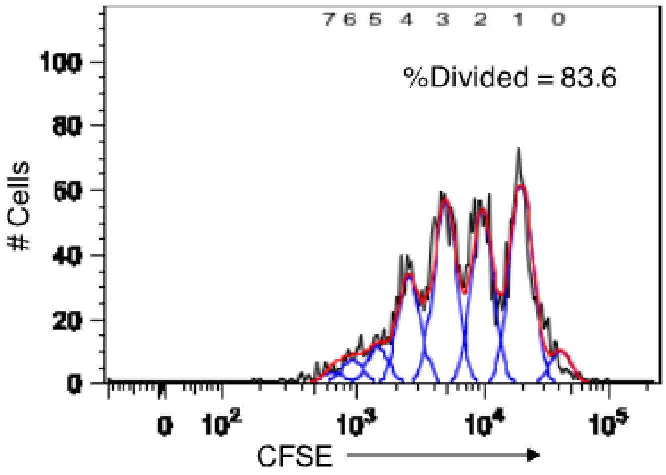

c. Transfer of BCR

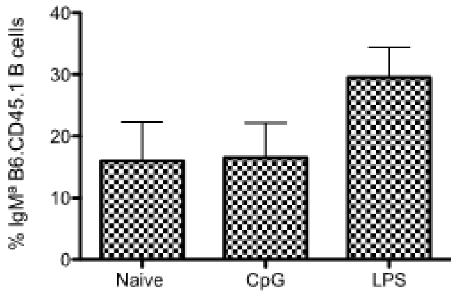

Figure 4.2 Purity assessments of RNA samples. An Agilent 2100 Bioanalyzer was used to analyse the integrity of the RNA samples from (a) unstimulated, (b) LPS stimulated and (c) CpG stimulated B cells. RNA integrity number (RIN) and a representative Bioanalyser electropherogram are shown for each sample. (FU) – arbitrary fluorescence units. (s) – time in seconds.

a. Unsitmulated

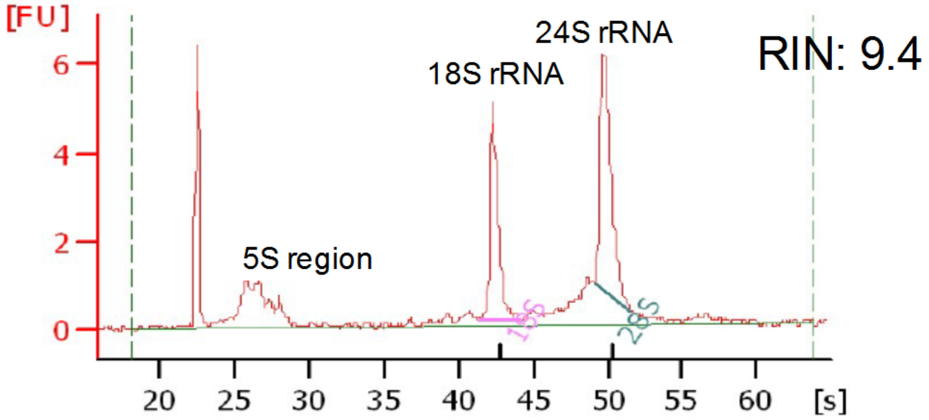

b. LPS

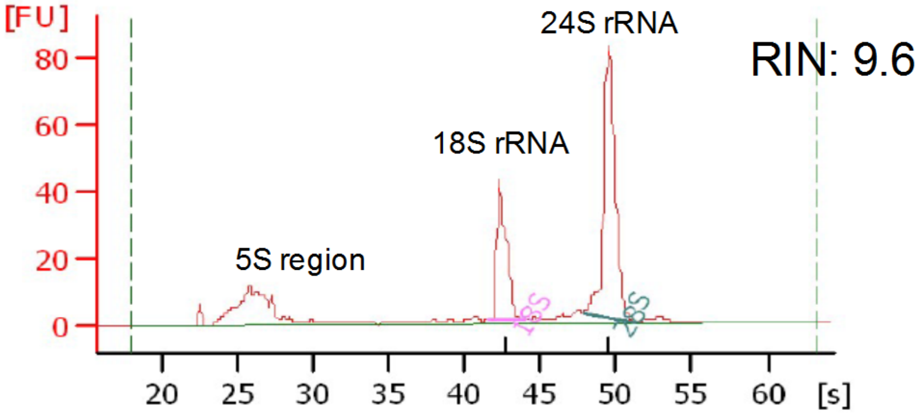

c. CpG

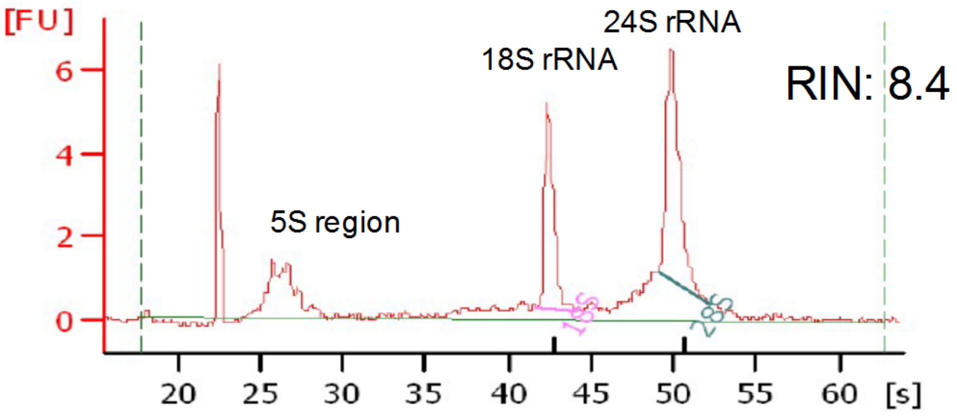

4.3.3 Global effects of B cell stimulation on the B cell transcriptome

To determine differences in gene expression between CpG stimulated B cells, LPS stimulated B cells and unstimulated B cells, the high quality intact RNA extracted from these different cell populations was subjected to gene expression profiling using mouse GeneChip® Gene 1.0ST Array (Affymetrix). The GeneChip® Gene 1.0 ST Array System for mice offers a complete and accurate view of transcriptional activity at each genomic locus, covering an estimated 28,853 well-annotated genes with 770, 317 distinct probes (Affymetrix, 2007).

A graphical depiction of the entire gene set in scatter plots is shown in Figure 4.3 comparing the different stimulation conditions. The majority of expression changes occur between the stimulated cells, CpG or LPS, and the unstimulated cells (Figure 4.3a and b). In comparison to unstimulated B cells, a total of 1017 genes were upregulated ≥2-fold in B cells stimulated with LPS and 1387 genes following CpG stimulation. Of these, 708 genes were upregulated by both LPS and CpG stimulation (Figure 4.4) with 309 and 679 genes being upregulated specifically by LPS and CpG activation, respectively. Also, there was a total of 382 genes downregulated ≥2-fold upon stimulation with LPS or CpG (Figure 4.5), with 216 of these genes being downregulated in both LPS and CpG stimulated B cells, and a further 86 genes and 80 genes, respectively, being selectively downregulated by LPS and CpG stimulation (Figure 4.5).

The comparative scatter plot between LPS stimulated and CpG stimulated B cells showed very few comparative changes in gene expression (Figure 4.3c). In fact, only 209 genes have a ≥2-fold increase in expression in CpG stimulated B cells compared with LPS stimulated cells. Similarly only 141 genes showed a selective ≥2-fold increase in expression in LPS stimulated versus CpG stimulated B cells.

Of note are the transcripts that generate high raw intensity values in the scatter plots with CpG stimulated B cells (Figure 4.3b and c). In comparison to both LPS stimulated and unstimulated B cells, transcripts with the greatest intensity seem to be more highly expressed in the CpG stimulated cells. Although this difference in expression did not result in a ≥2-fold change in expression between LPS stimulated and CpG stimulated B cells, it does appear to be slightly more evident when comparing CpG stimulated with unstimulated B cells (Figure 4.3b).

a.

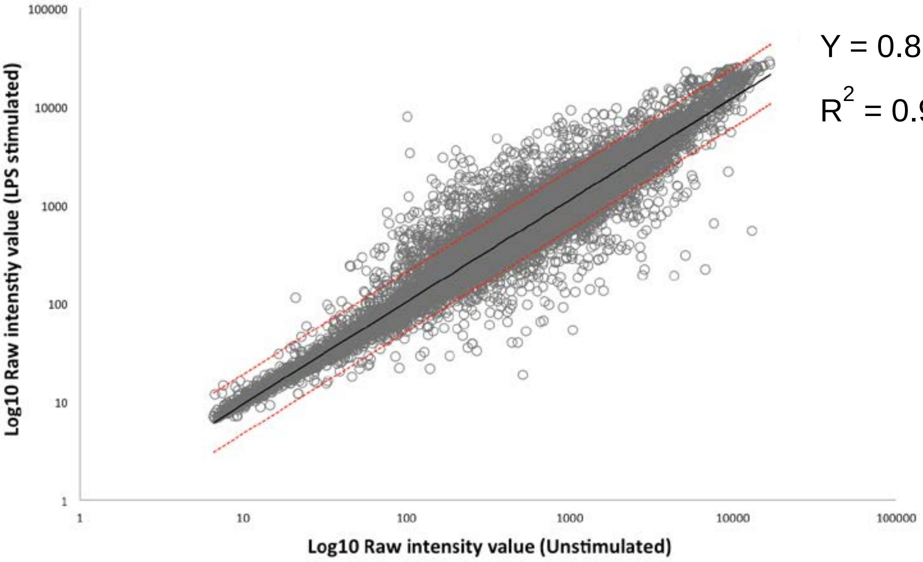

$Y = 0.8694x^{1.0367}$

$R^2 = 0.95538$

b.

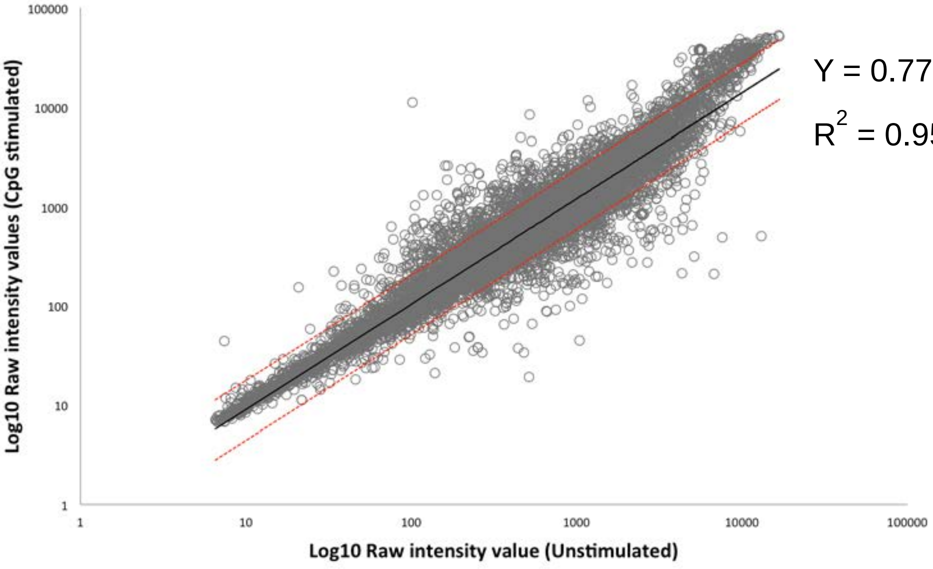

$Y = 0.7712x^{1.0637}$

$R^2 = 0.95656$

c.

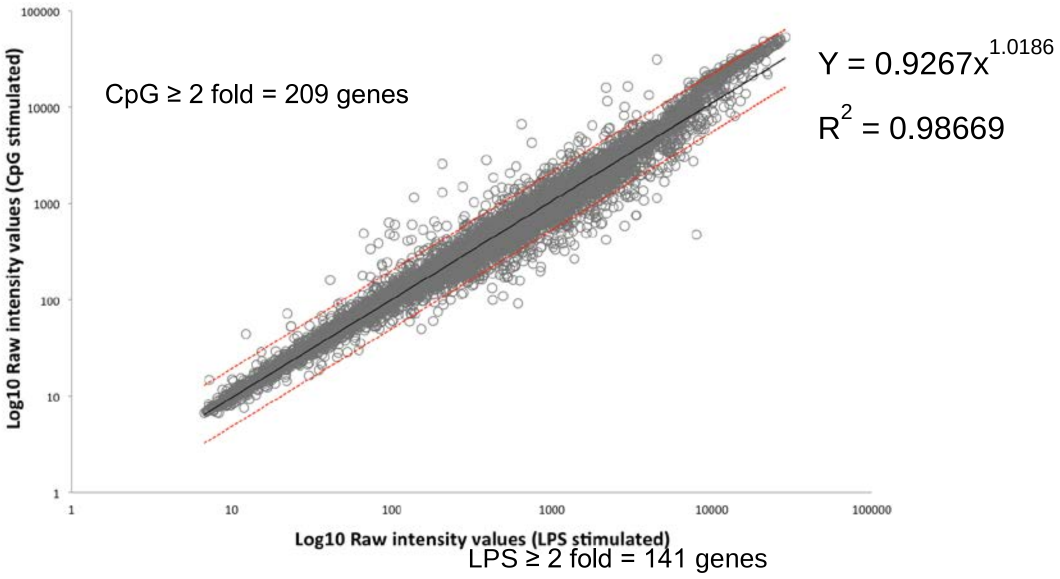

Figure 4.3 Scatter plot analysis of microarray data. Scatter plots of the mRNA expression from microarray analysis of (a) LPS stimulated versus unstimulated, (b) CpG stimulated versus unstimulated and (c) CpG stimulated versus LPS stimulated B cells. Each dot on the scatter plot corresponds to the normalised average signal intensity of a single gene. The middle line (black) indicates values that equal a ratio of 1 (equivalent levels of expression in both samples). The outer lines (red dotted) on the scatter plot indicate the 2-fold boundaries used for selecting genes with differential expression. Linear regression was performed and correlation coefficients are shown (R^2).

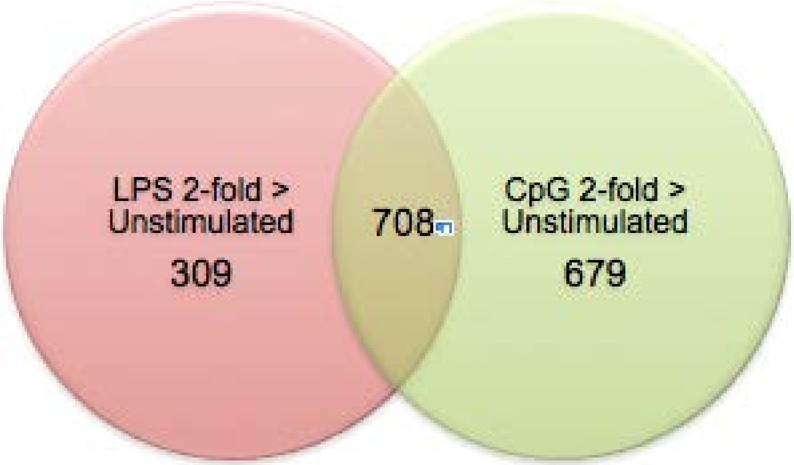

Figure 4.4 Relationship between LPS and CpG induced genes identified by cDNA microarray analysis. Venn diagram quantifying genes where expression is a minimum of 2-fold greater in LPS stimulated B cells compared to unstimulated B cells (LPS 2-fold> unstimulated) and genes where expression is a minimum of 2-fold greater in CpG stimulated B cells compared to unstimulated B cells (CpG 2-fold > unstimulated). A total of 708 genes are similarly upregulated in B cells upon LPS or CpG stimulation.

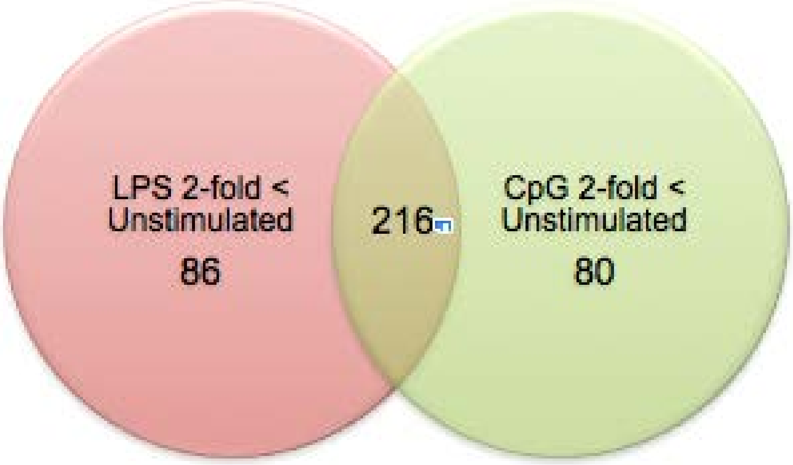
LPS 2-fold <
Unstimulated
86
216
CpG 2-fold <
Unstimulated
80

Figure 4.5 Relationship between LPS and CpG repressed genes identified by cDNA microarray analysis. Venn diagram quantifying genes where expression is a minimum of 2-fold lower in LPS stimulated B cells compared to unstimulated B cells (LPS 2-fold < unstimulated) and genes where expression is a minimum of 2-fold lower in CpG stimulated cells compared to unstimulated B cells (CpG 2-fold < unstimulated). A total of 216 genes are similarly downregulated in B cells upon both LPS and CpG stimulation.

4.3.4 Downstream effect analysis of genes up or down regulated following B cell stimulation

To explore the functionality of the genes over and under expressed following LPS or CpG stimulation we employed the simplified gene ontology function of the online bioinformatics program ‘Protein Analysis Through Evolutionary Relationships’ (PANTHER) Classification System. The PANTHER classification system is a comprehensive system that combines gene function, ontology, pathways and statistical analysis tools that enable biologists to analyse data obtained from a variety of techniques, such as gene expression experiments (Mi et al., 2013).

Functional annotation of the genes showed that a high proportion of the genes upregulated upon B cell activation with both LPS and CpG are involved in metabolic, cellular and immune processes (Table 4.1). Increased expression of genes involved in the cell cycle and cellular transport is also evident. Similarly, the highest proportion of genes that are downregulated in LPS and CpG activated B cells in comparison to unstimulated B cells also fall under the classifications of cellular processes and cell cycle (Table 4.2). There is also a large proportion of genes downregulated in response to stimulation that are involved in cellular adhesion and cellular communication (Table 4.2).

The functional classification of the changes in B cell gene expression in response to LPS stimulation closely resembles the response to CpG stimulation (Table 4.1 and 4.2). Moreover, the extent of expression also appears to be similar for both stimuli, with the number of genes whose expression is upregulated or downregulated by 2 fold being relatively constant between B cells stimulated with LPS and CpG (Table 4.1 and 4.2). Similarly, the number of genes exhibiting a 5-fold increase or decrease in level of expression for each functional category remained relatively constant when comparing LPS and CpG stimulated B cells (Table 4.1 and 4.2). The few functional differences between the LPS stimulated B cells and CpG stimulated B cells suggests that the B cells, although activated using different stimuli, are responding to each stimulus in a similar manner.

Table 4.1 Genes upregulated either 2-fold or 5-fold upon stimulation

Function	Number of genes			
	LPS		CpG	
	2-fold	5-fold	2-fold	5-fold
cell communication (GO:0007154)	102	13	97	12
cellular process (GO:0009987)	201	26	203	24
localization (GO:0051179)	3	1	2	
transport (GO:0006810)	93	11	87	7
cellular component organization (GO:0016043)	40	3	53	6
apoptosis (GO:0006915)	30	2	32	2
system process (GO:0003008)	40	6	30	5
reproduction (GO:0000003)	22	4	19	4
response to stimulus (GO:0050896)	59	10	73	13
homeostatic process (GO:0042592)	4		4	
developmental process (GO:0032502)	65	13	63	9
generation of precursor metabolites and energy (GO:0006091)	13		14	
metabolic process (GO:0008152)	340	34	365	23
cell cycle (GO:0007049)	96	15	96	11
immune system process (GO:0002376)	87	16	105	15
cell adhesion (GO:0007155)	26	3	28	5

Table 4.2 Genes downregulated either 2-fold or 5-fold upon stimulation

Function	Number of genes			
	LPS		CpG	
	2-fold	5-fold	2-fold	5-fold
cell communication (GO:0007154)	90	17	84	17
cellular process (GO:0009987)	104	18	98	20
transport (GO:0006810)	29		28	4
cellular component organization (GO:0016043)	4	3	4	1
apoptosis (GO:0006915)	19	1	19	3
system process (GO:0003008)	32	2	25	5
reproduction (GO:0000003)	9	5	10	1
response to stimulus (GO:0050896)	69	15	62	14
homeostatic process (GO:0042592)	1	1	1	
developmental process (GO:0032502)	4		4	1
generation of precursor metabolites and energy (GO:0006091)	52	12	47	13
metabolic process (GO:0008152)	2		4	
cell cycle (GO:0007049)	106	21	110	24
immune system process (GO:0002376)	20	4	25	4
cell adhesion (GO:0007155)	81	18	79	17

4.3.5 Identification of candidate genes involved in membrane transfer between B cells

4.3.5.1 LPS inducibility and plasma membrane association

In Sections 4.1 and 4.2 of this Chapter it was shown that B cell surface proteins and plasma membranes are exchanged between LPS activated B cells, but less so between CpG activated B cells. Therefore, the evidence suggests that processes induced by LPS stimulation are important for membrane transfer. However, it is evident from Table 4.1 and 4.2 that the difference between CpG and LPS stimulated B cells is minimal with regards to the functional classification of gene expression. To assist in the identification of potential genes of interest from the transcript analysis, it was proposed that the genes involved would need to meet certain criteria. Previous studies have indicated that the initiation of membrane transfer is dependent on a specific protein, or subset of proteins, expressed on the plasma membrane (Carlin et al., 2001). These findings in combination with the specific activation requirements led to a focus on genes that are upregulated under certain activation conditions, which could potentially result in the expression, or enhanced expression, of proteins at the B cell surface. Additionally, data presented earlier in Sections 4.1 and 4.2 of this Chapter led to the hypothesis that the mechanism of transfer involves a protein or proteins that are a) more LPS inducible than CpG inducible, and b) are associated with the plasma membrane.

Based on the above hypothesis, initially genes were selected on the basis of a ≥2-fold increase in expression in response to LPS stimulation, resulting in the identification of 1017 genes (Figure 4.6). Using the gene ontology (GO) term ‘plasma membrane’ genes that were associated with the plasma membrane were selected, resulting in a total of 2844 genes, 76 of which are also LPS inducible (Figure 4.6). The last criterion used was LPS inducibility in comparison to CPG inducibility. Genes selected were a minimum of 1.4-fold more highly expressed in response to LPS stimulation than CpG stimulation. It was anticipated that CpG stimulation may upregulate the expression of some genes but not to the same extent as LPS stimulation, thus, a 2-fold difference in expression was thought to be too stringent. Furthermore, studies have demonstrated that the microarray technology is able to reliably detect 1.4-fold or greater changes in gene expression (Wurmbach et al., 2003, Morey et al., 2006). The 1.4-fold cut off in increased gene expression by LPS stimulated B cells enabled the inclusion of substantially more genes satisfying the three selection criteria outlined and resulted in 38 genes being selected (Figure 4.6) that are listed in Table 4.3.

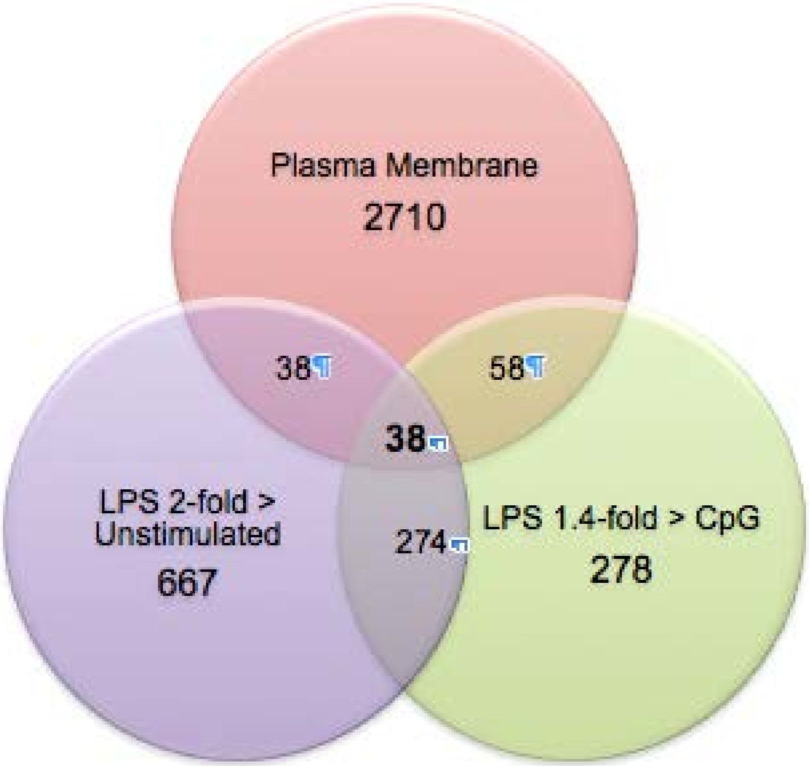
Plasma Membrane
2710
38
58
38
LPS 2-fold >
Unstimulated
667
274
LPS 1.4-fold > CpG
278

Figure 4.6 LPS inducible genes identified by cDNA microarray analysis that encode proteins associated with the plasma membrane. Venn diagram quantifying genes where expression is a minimum of 2-fold greater in LPS stimulated B cells compared to unstimulated B cells (LPS 2-fold> unstimulated), where expression is a minimum of 1.4-fold greater in LPS stimulated B cells compared to CpG stimulated B cells (LPS 1.4-fold > CpG) and contain gene ontology term ‘plasma membrane’ (Plasma Membrane). The number of genes that fit particular characteristics is shown. A total of 38 genes fit all 3 criteria.

Table 4.3 LPS inducible genes that encode proteins that are associated with the plasma membrane

Abbreviation	Gene Name	Unstimulated	LPS	CpG	LPS/ Unstim	CpG/ Unstim	LPS/ CpG	Accession number
Il2ra	interleukin 2 receptor, alpha chain	200.64	3564.41	2369.21	17.8	11.8	1.51	NM_008367
CTLA-4	cytotoxic T-lymphocyte-associated protein 4	142.50	1827.50	1301.29	12.8	9.1	1.41	NM_009843
Alpl	alkaline phosphatase, liver/bone/kidney	223.43	2687.50	1876.97	12.0	8.4	1.43	NM_007431
Flt3	FMS-like tyrosine kinase 3	179.80	1381.20	265.94	7.7	1.5	5.13	NM_010229
Slc7a3	solute carrier family 7 (cationic amino acid transporter, y+ system), member 3	111.55	852.10	220.20	7.6	2.0	3.80	NM_007515
TIGIT	T cell immunoreceptor with Ig and ITIM domains	464.85	3387.06	747.16	7.3	1.6	4.56	NM_001146325
Slp3	Synaptotagmin like 3	90.00	534.00	173.00	5.9	1.9	3.11	NM_031395
Slc7a5	solute carrier family 7 (cationic amino acid transporter, y+ system), member 5	900.76	4925.50	2368.32	5.5	2.6	2.12	NM_011404
AI324046	expressed sequence AI324046	477.36	2499.10	1569.50	5.2	3.3	1.58	D14625

Abbreviation	Gene Name	Unstimulated	LPS	CpG	LPS/ Unstim	CpG/ Unstim	LPS/ CpG	Accession number
Ppap2a	phosphatidic acid phosphatase type 2A	96.96	440.45	298.63	4.5	3.1	1.45	NM_008247
AMIGO2	Amphoterin-induced gene and ORF 2	288.82	1278.50	911.54	4.4	3.2	1.38	NM_178114
Tmem97	transmembrane protein 97	94.55	358.16	205.56	3.8	2.2	1.73	NM_133706
Pdia6	protein disulfide isomerase associated 6	513.40	1922.97	1250.48	3.7	2.4	1.54	NM_027959
Cacna1h	calcium channel, voltage-dependent, T type, alpha 1H subunit	275.83	930.54	423.85	3.4	1.5	2.27	NM_021415
Eno1	enolase 1, alpha non-neuron	1628.66	5446.40	3844.91	3.3	2.4	1.38	NM_023119
Lag3	lymphocyte-activation gene 3	175.49	578.55	247.16	3.3	1.4	2.36	NM_008479
Eno1	enolase 1, alpha non-neuron	1655.83	5211.22	3668.70	3.1	2.2	1.41	NM_023119
Pmepa1	prostate transmembrane protein, androgen induced 1	405.54	1266.45	641.16	3.1	1.6	1.94	NM_022995
Cd59a	CD59a antigen	63.83	180.58	60.48	2.8	0.9	3.11	NM_001111060
Slc44a1	solute carrier family 44,	156.25	422.50	132.98	2.7	0.9	3.00	ENSMUST00000

Abbreviation	Gene Name	Unstimulated	LPS	CpG	LPS/ Unstim	CpG/ Unstim	LPS/ CpG	Accession number
	member 1							107651
Rgs16	regulator of G-protein signalling 16	326.52	833.18	518.52	2.6	1.6	1.63	NM_011267
P4hb	prolyl 4-hydroxylase, beta polypeptide	1043.80	2741.64	1792.16	2.6	1.7	1.53	NM_011032
ALCAM	activated leukocyte cell adhesion molecule	729.41	1875.50	847.91	2.6	1.2	2.17	NM_009655
Sema7a	sema domain, immunoglobulin domain (Ig), and GPI membrane anchor, (semaphorin) 7A	905.60	2388.78	1072.26	2.6	1.2	2.17	NM_011352
Selplg	selectin, platelet (p-selectin) ligand	1084.11	2681.60	1817.74	2.5	1.7	1.47	NM_009151
Il6st	interleukin 6 signal transducer	936.99	2204.54	789.10	2.4	0.8	3.00	NM_010560
Tnf	tumor necrosis factor	571.16	1354.34	521.29	2.4	0.9	2.67	NM_013693
Abcb1b	ATP-binding cassette, sub-family B (MDR/TAP), member 1B	116.40	281.15	186.38	2.4	1.6	1.50	NM_011075
CD80	CD80 antigen	276.83	632.89	158.20	2.3	0.6	3.83	NM_009855

Abbreviation	Gene Name	Unstimulated	LPS	CpG	LPS/ Unstim	CpG/ Unstim	LPS/ CpG	Accession number
Mtdh	metadherin	1951.18	4198.93	2647.54	2.2	1.4	1.57	NM_026002
Plxnd1	plexin D1	743.83	1617.16	784.14	2.2	1.1	2.00	NM_026376
Slc39a4	solute carrier family 39 (zinc transporter), member 4	174.14	359.99	198.83	2.1	1.1	1.91	NM_028064
Fas	Fas (TNF receptor superfamily member 6)	146.78	301.16	156.24	2.1	1.1	1.91	NM_007987
Slc44a1	solute carrier family 44, member 1	464.98	963.22	639.15	2.1	1.4	1.50	NM_133891
Slc6a9	solute carrier family 6 (neurotransmitter transporter, glycine), member 9	229.64	490.34	260.83	2.1	1.1	1.91	NM_008135
Grm6	glutamate receptor, metabotropic 6	182.93	366.36	162.77	2.0	0.9	2.22	NM_173372
Ptch1	patched homolog 1	482.50	977.98	625.96	2.0	1.3	1.54	NM_008957
Lax1	lymphocyte transmembrane adaptor 1	1321.64	2679.12	1451.16	2.0	1.1	1.82	NM_001159649

Values represent relative levels of gene expression. LPS, lipopolysaccharide. Accession numbers are for the NCBI database.

Table lists genes identified by cDNA microarray analysis that have a gene ontology term ‘plasma membrane’ and demonstrate

- a minimum 2 fold higher expression in LPS stimulated versus unstimulated B cells
- a minimum 1.4 fold higher expression in LPS stimulated versus CpG stimulated B cells

4.3.5.2 Involvement in cell communication and cell adhesion functions

It is highly likely that the genes involved in the process of membrane sharing between B cells could be functionally categorised as mediators of cell communication or cell adhesion. Previous studies have demonstrated the necessity of direct cell-cell contact for the process of membrane exchange (Quah et al., 2008, Sprent, 2005, Joly and Hudrisier, 2003, Chaudhri et al., 2009). Furthermore, many instances of cellular adhesion and communication show striking similarities to membrane sharing and, in most cases, also require direct cell-cell contact (Ahmed and Xiang, 2011).

To identify genes that were involved in cell adhesion and cell communication, and thus could potentially carry out the process of membrane exchange between B cells, the bioinformatics program PANTHER and the scientific literature, where available, were used to functionally categorise the 38 genes that were differentially or uniquely expressed by LPS stimulated B cells (Figure 4.7). Thus, a complete analysis of the functional roles of the genes listed in Table 4.3 was conducted. Of the 38 genes 16 were associated with cell communication and of these 16 genes, 7 were also involved in cell adhesion (Figure 4.7). The remaining 22 genes were not considered candidates as there functions, such as transport, metabolic, cancer and apoptosis involvement, excluded them from the selection process.

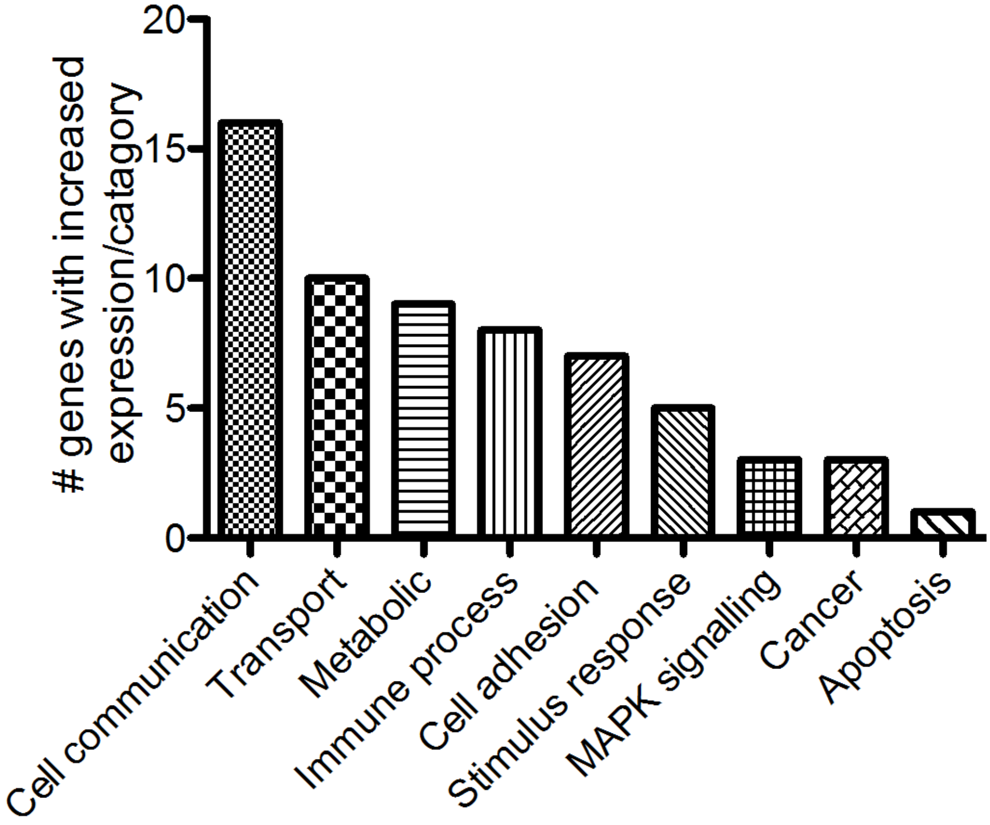

Figure 4.7 Functional clustering of LPS inducible genes that encode proteins associated with the plasma membrane. Each gene was assigned to a category using the PANTHER Pathway database and by its known or predicted cellular function. The number of genes in each functional category is shown.

4.3.5.3 The presence of a cell penetrating peptide (CPP) motif

The last criterion that was used to obtain a final set of candidate genes was the presence of cell penetrating peptide (CPP) motifs. As discussed previously (Chapter 3), it is proposed that CPPs play an important role in the mechanism of membrane exchange between B cells, with the positively charged amino acids of CPPs on a B cell surface interacting with negatively charged regions of proteins on the surface of a neighbouring B cell and bringing about conditions conducive for membrane transfer.

CPP motifs were classified as regions of 20 amino acids, of which a minimum of 4 amino acids must be positively charged (arginine or lysine), and no negatively charged amino acids are present. The Genome Discovery Unit (GDU) at the John Curtin School of Medical Research (JCSMR), Australian National University (ANU) performed this analysis on the 16 LPS-inducible genes involved in cell communication. Ten genes were identified as containing CPP motifs and are listed in Table 4.4. Charge is defined as the percentage arginine (K) and/or Lysine (R) over a 20 amino acid region. Three genes, including Lag3 (lymphocyte-activation gene 3), Plxnd1 (plexin D1) and TIGIT (T cell immunoreceptor with Ig and ITIM domains), contained 4 arginine and/or lysine residues over a 20 amino acid region, thus having a charge of 20% (Table 4.4). Five genes, including ALCAM (activated leukocyte cell adhesion molecule), AMIGO2 (amphoterin-induced gene and ORF (open reading frame) 2), CD80, CTLA-4 (cytotoxic T lymphocyte associated protein 4) and Sema7a (semaphorin 7a, sema domain, immunoglobulin domain, and GPI membrane anchor), contained 5 arginine and/or lysine residues over a 20 amino acid region, thus having a charge of 25% (Table 4.4). Interleukin 6 signal transducer (Il6st) and synaptotagmin like protein 3 (Slp3) contained 20 amino acid peptide sequences composed of 6 (30%) and 7 (35%) positively charged residues, respectively.

Also, transcript intensities for the 10 genes of interest under the different stimulation conditions are shown in Table 4.4. Eight genes, including ALCAM, CD80, Il6st, Lag3, Plxnd1, Sema7a, Slp3, and TIGIT, demonstrated significantly increased expression in B cells in response to LPS stimulation, when compared to unstimulated and CpG stimulated B cells (Table 4.4). AMIGO2 and CTLA-4 showed a significant increase in gene expression in response to CpG stimulation compared with unstimulated B cells. However, both AMIGO2 and CTLA-4 still exhibited a further 1.4-fold increase in gene expression in B cells stimulated with LPS compared with CpG stimulated cells (Table 4.4).

Table 4.4 Genes of interest

Abbreviation	Gene Name	Unstimulated	LPS	CpG	Accession Number	Charge[a]	Sequence
ALCAM	activated leukocyte cell adhesion molecule	729	1875	848	NM_009655	25%	GVVYWLYMKKSKTASKHVNK
AMIGO2	amphoterin-induced gene and ORF 2	289	1278	912	NM_178114	25%	SCTNKNLSKVPGNLFRLIKR
CD80	CD80 antigen	277	633	158	NM_009855	25%	VVVIVVIIKCFCKHRSCFRR
CTLA-4	cytotoxic T-lymphocyte-associated protein 4	143	1827	1301	NM_009843	25%	VSLSKMLKKRSPLTTGVYVK
Il6st	interleukin 6 signal transducer	937	2205	789	NM_010560	30%	LKAYLKQAAPARGPTVRTKK
Lag3	lymphocyte-activation gene 3	175	579	247	NM_008479	20%	LLVAGAFGFHWWRKQLLLRR
Plxnd1	plexin D1	744	1617	784	NM_026376	20%	RRAAGGAPPSARAAAAVPLR
Sema7a	sema domain, immunoglobulin domain (Ig), and GPI membrane anchor, (semaphorin) 7A	906	2389	1072	NM_011352	25%	APRARVLSLPARFGLPLRLR
Slp3	Synaptotagmin like protein 3	90	534	173	NM_031395	35%	RVRKLKSHLQHLRWKGAKSS
TIGIT	T cell immunoreceptor with Ig and ITIM domains	465	3387	747	NM_001146325	20%	LMVTGVTVLARKKSIRMHSI

[a]Charge refers to percentage arginine (K) and/or lysine (R) residues over a 20 amino acid region (in red), with the absence of acidic residues. LPS, lipopolysaccharide. Accession numbers are for the NCBI database.

Selected genes in B lymphocytes showing increased transcript intensities in stimulated cells (either via LPS or CpG) that are cell surface or plasma membrane associated, are involved in cell adhesion or communication and contain a cell penetrating motif. Red boxes indicate a 2-fold increase in intensity from unstimulated cells.

4.3.6 Validation by real-time PCR of genes of interest identified by microarray analysis

Real-time PCR analysis was used to confirm the findings of the microarray analysis. cDNA from LPS and CpG stimulated B cells and freshly isolated (unstimulated) B cells were used for real-time PCR assay of the ten genes of interest. For validation and normalisation of the data, reference genes Gapdh and Rpl32 were run concomitantly with the 10 genes of interest. Gene expression is indicated as arbitrary copy number. Five genes, including ALCAM, AMIGO2, CTLA-4, Slp3 and TIGIT correlated well with the corresponding microarray data, although the exact values were different (Figure 4.8a, b, d, i and j). In fact, all five genes showed a highly significant increase in expression in LPS stimulated B cells, with no evidence of CpG inducibility and, in the case of ALCAM, Slp3 and TIGIT, expression being significantly lower in CpG stimulated than unstimulated B cells (Figure 4.8a, i and j). This result deviates slightly from the increase in expression of these genes in CpG stimulated B cells observed in the microarray data set (Table 4.4). However, the real-time PCR results are more in accordance with the selection criteria of LPS inducibility. CD80 also demonstrated an increase in expression in LPS stimulated B cells, similar to the microarray data, but dissimilar to the microarray data was the increase in expression of CD80 in CpG activated B cells (Figure 4.8c and Table 4.4). This is not altogether unexpected, as CD80 is a well known marker of B cell activation. Thus, the resulting real-time PCR data is more in line with what is expected of activated B cells.

In contrast to the microarray results, the real-time PCR data showed a minimum 2-fold decrease in expression of IL6st in LPS and CpG activated B cells (Figure 4.8e). Also, contrary to the microarray data, there was no significant difference in expression of Lag3 in LPS stimulated, CpG stimulated or unstimulated B cells in the real-time PCR analysis (Figure 4.8f). Plexin D1 (PLXND1) expression also did not differ between unstimulated and LPS stimulated B cells, and there was a 6-fold reduction in expression in CpG activated B cells (Figure 4.8g). Similarly, there was little difference in sema7a expression in LPS stimulated and unstimulated B cells, however, there was a 6-fold increase in expression of sema7a in CpG activated B cells (Figure 4.8h). Thus, the real-time PCR results obtained with 5 of the 10 genes tested, namely ALCAM, AMIGO2, CTLA-4, Slp3 and TIGIT, correlate well with the corresponding microarray data, although the exact expression values differ.

a. ALCAM

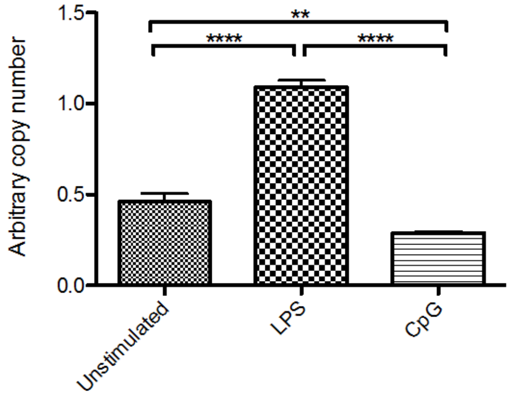

b. AMIGO2

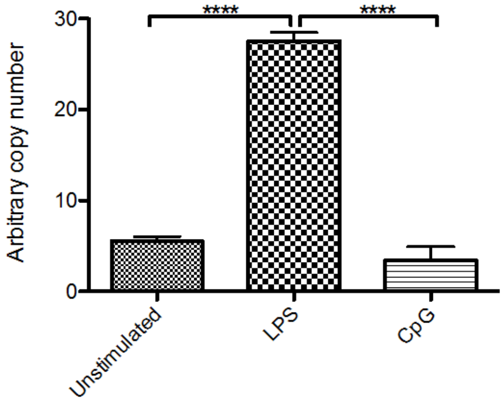

c. CD80

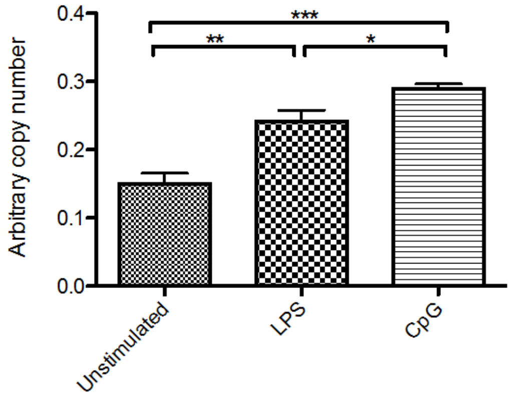

d. CTLA-4

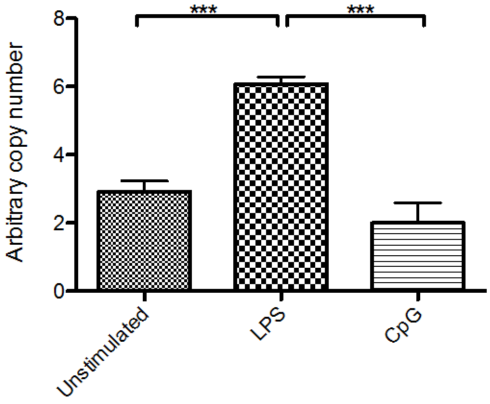

e. IL6ST

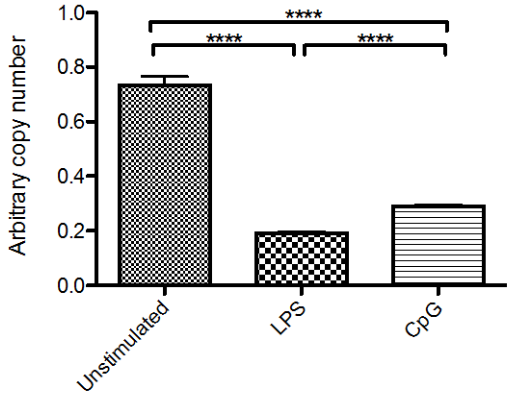

f. LAG3

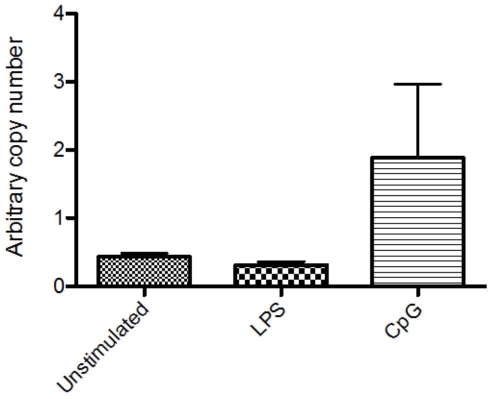

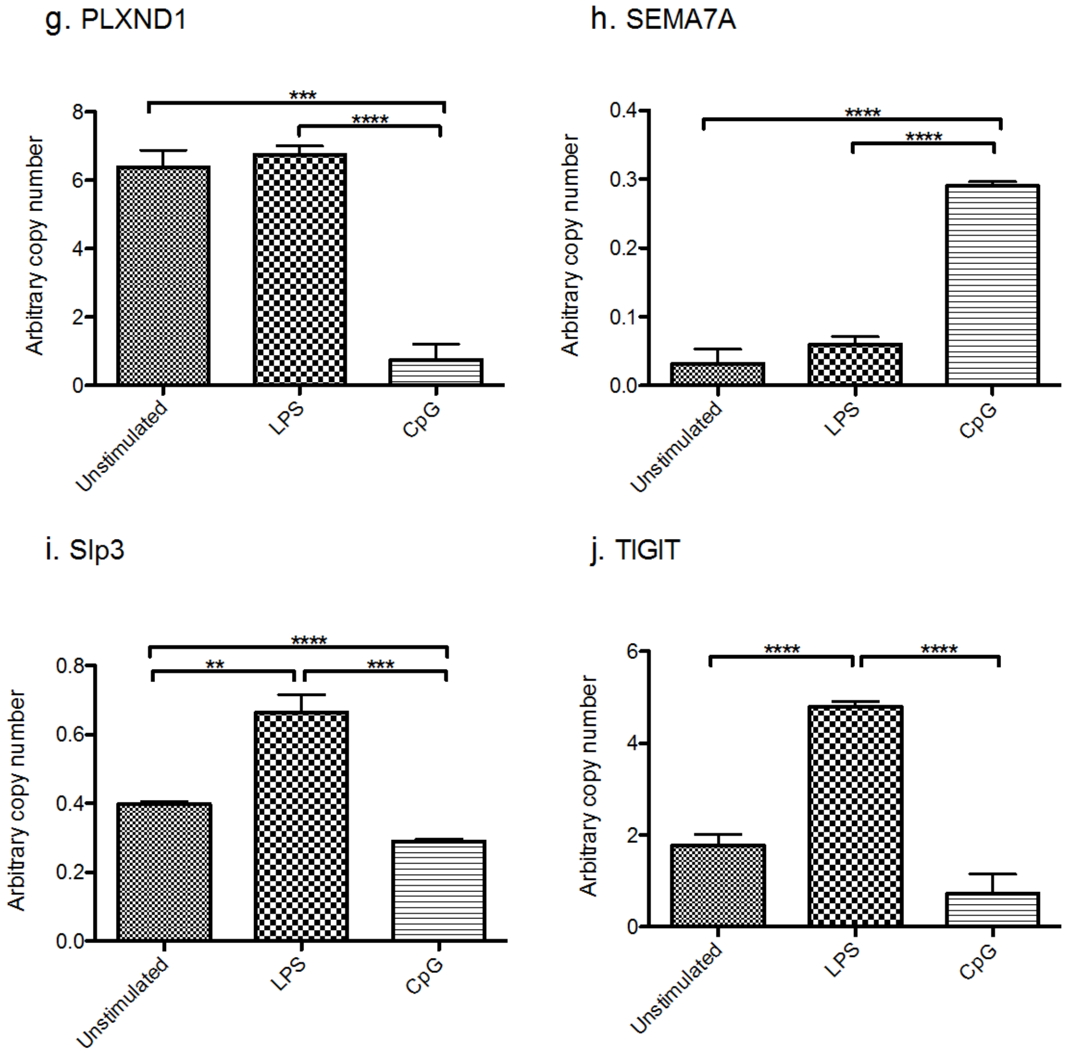

Figure 4.8 Validation of microarray data using Real-time PCR. Total RNA was isolated from LPS and CpG stimulated B cells and unstimulated B cells using the same methods as were used for the microarray experiments. Reverse transcription and *TaqMan* real-time PCR was performed on 10 genes of interest. Real-time reactions were performed using samples from an independent experiment. Data expressed as arbitrary copy number normalised to *Rpl32* expression and represent the mean ± SE (n=4). *p < 0.05, **p <0.01, ***p < 0.001, unpaired Students *t*-test.

4.3.7 Involvement of the genes of interest in membrane transfer between B cells

Real-time PCR and microarray technologies measure the transcriptional activity of genes. Real-time PCR validated the increased transcriptional activity of ALCAM, AMIGO2, CTLA-4, Slp3 and TIGIT following LPS stimulation as indicated by the microarray data. However, increased levels of transcript do not necessarily correlate with increased levels of protein (Vogel and Marcotte, 2012). As discussed previously, in the proposed model of membrane transfer between B cells it is suggested that specific B cell stimulation conditions will result in the up regulation of cell surface proteins that interact with neighbouring B cells to promote the exchange of membranes and cell surface proteins. Thus, since mAbs are available against ALCAM, CTLA-4 and TIGIT, expression of these proteins by activated B cells and their participation in B cell membrane transfer was examined using flow cytometry in the following Sections.

4.3.7.1 Activated leucocyte adhesion molecule, ALCAM

ALCAM is an immunoglobulin (Ig) like cell adhesion molecule expressed on a variety of cell types, including B cells (Swart, 2002). It mediates homo- and heterotypic cell-cell clustering through homo- (ALCAM-ALCAM) and heterotypic (ALCAM-CD6) interactions, however, splenic B cells lack CD6 on the cell surface. Studies have suggested that the cell adhesion function is controlled via its anchoring to the actin cytoskeleton, however, the components involved remain unknown (Nelissen et al., 2000).

Transcript validation by real-time PCR demonstrated an increase in expression of ALCAM in LPS stimulated B cells compared to unstimulated and CpG stimulated B cells. To determine if this high transcript level correlates with protein expression on the surface of B cells, day-3 LPS stimulated splenocytes and unstimulated splenocytes were labelled with increasing concentrations of an anti-ALCAM mAb and analysed using flow cytometry. Figure 4.9a and b reveal that ALCAM protein is present at low levels on the cell surface of unstimulated B cells. Furthermore, protein expression was markedly enhanced upon LPS-activation (Figure 4.9a and b), in agreement with the microarray and real-time PCR data.

To assess the contribution of the ALCAM protein to membrane transfer, day-3 LPS stimulated MD4 and B6.CD45.1 B cells were co-cultured in the presence or absence of an ALCAM-specific blocking mAb. Interestingly, the presence of the anti-ALCAM mAb increased the transfer of IgM^a to B6.CD45.1 B cells, and to a lesser extent CD45.1 to MD4 B cells (Figure 4.9c). Previous studies have reported that ALCAM-specific mAbs have differential effects on ALCAM-mediated cell aggregation and adhesion, with some antibodies (clone J4-81) inducing markedly increased homotypic (ALCAM-ALCAM) interactions (van Kempen et al., 2001). Potentially, in the current assay, the anti-ALCAM antibody (clone ebioALC48) could be inducing homotypic cell clustering, and thus allowing more membrane sharing between neighbouring B cells.

Figure 4.9 Membrane transfer between B cells increases in the presence of an anti-ALCAM mAb. Splenocytes were either unstimulated or stimulated with 10 μg/ml of LPS for 3 days. Day-3 splenocytes were harvested and incubated with various amounts of an ALCAM-specific mAb (up to 4 μg/ml). Expression of ALCAM on B lymphocytes was analysed by flow cytometry using a PE conjugated ALCAM mAb. (a) MFI of ALCAM mAb binding with background fluorescence subtracted. (b) Representative histograms of the expression of ALCAM on unstimulated (top panel - red) and LPS stimulated B cells (bottom panel - red). Isotype controls – blue, background – shaded grey. MFI values for each treatment are included in each panel. Data is representative of 2 independent experiments. (c) Day-3 LPS activated MD4 and B6.CD45.1 spleen cells were co-cultured at 4°C for 2 hr in the presence or absence of saturating amounts of anti-ALCAM mAb (4 μg/ml). B6.CD45.1 and MD4 B cells were then assessed for surface expression of IgM^{a} and CD45.1, respectively. Data shows percentage of B cells expressing non-endogenous IgM or CD45. Data expressed as mean ± SEM (n=3), and is representative of 3 independent experiments. **p <0.01, unpaired Students *t*-test.

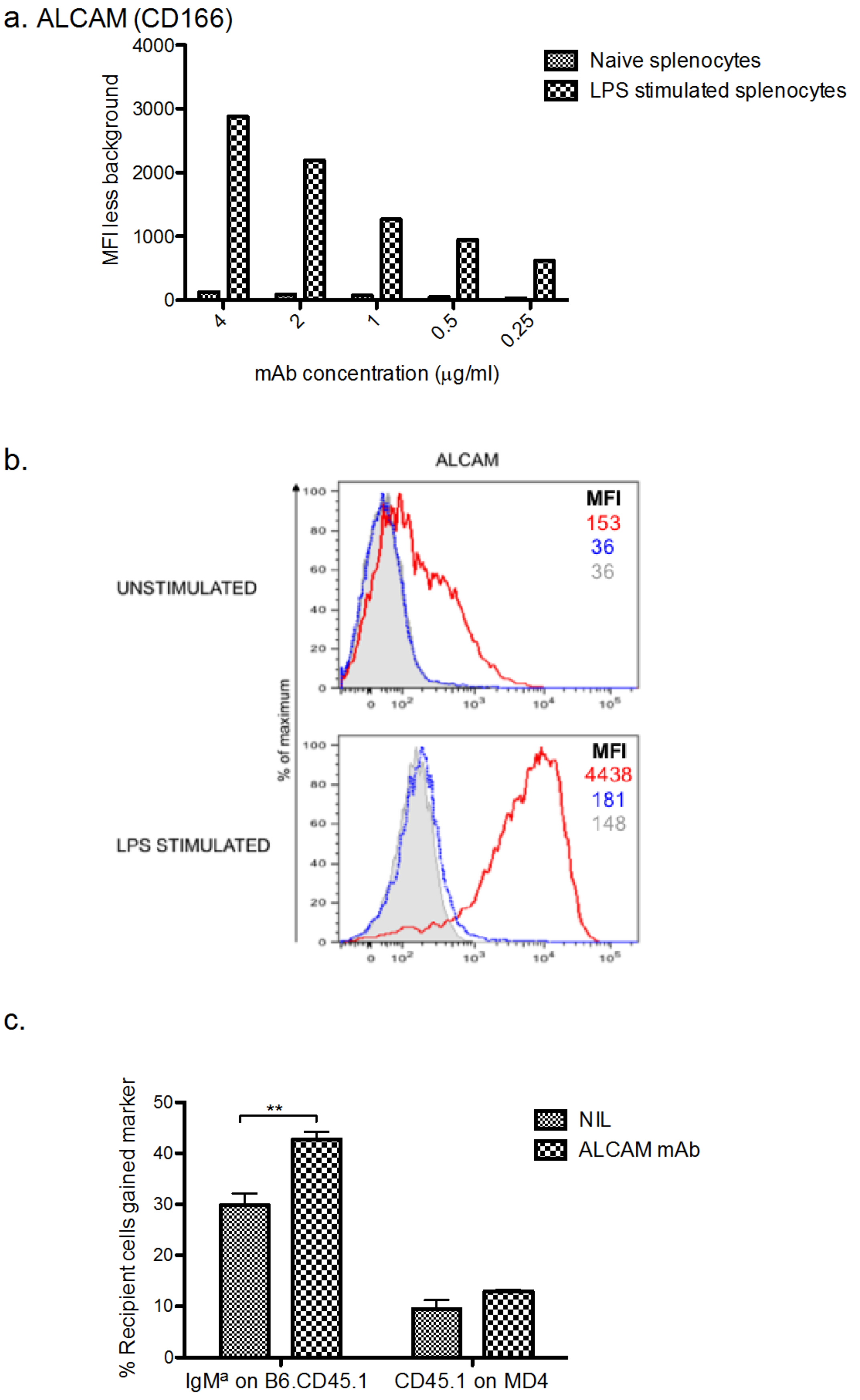
a. ALCAM (CD166)
MFI less background
4000
3000
2000
1000
0
4
2
1
0.5
0.25
mAb concentration (µg/ml)
Naive splenocytes
LPS stimulated splenocytes
b.
ALCAM
UNSTIMULATED
LPS STIMULATED
% of maximum
100
80
60
40
20
0
0
10²
10³
10⁴
10⁵
MFI
153
36
36
MFI
4438
181
148
c.
% Recipient cells gained marker
50
40
30
20
10
0
**
IgMᵃ on B6.CD45.1
CD45.1 on MD4
NIL
ALCAM mAb

4.3.7.2 CTLA-4

Previously, it has been demonstrated that CTLA-4 removes its ligands (CD80 and CD86) from neighbouring cells by a process of trans-endocytosis (Qureshi et al., 2011). Following removal, the co-stimulatory ligands are degraded in the CTLA-4 expressing cell, resulting in impaired co-stimulation via CD28 (Qureshi et al., 2011). Incubation with a blocking antibody to CTLA-4 prevented the down regulation of co-stimulatory ligands (Qureshi et al., 2011). The similarities between the mechanism that CTLA-4 utilises to achieve down regulation of T cell signalling, and the mechanism of membrane sharing between B cells present CTLA-4 as a very interesting candidate. However, there have been few reports documenting the expression of CTLA-4 on the surface of B cells (Llinas et al., 2011, Quandt et al., 2007, Pioli et al., 2000, Kuiper et al., 1995), CTLA-4 generally being regarded as a protein expressed by T cells, particularly cytotoxic and regulatory T cells (Walker and Sansom, 2011). In the current study anti-CD3ε antibody stimulated T cells were utilised as a positive control for CTLA-4 protein expression.

To assess the level of CTLA-4 protein expression on the surface of B cells, day-3 LPS stimulated splenocytes and day-2 anti-CD3ε antibody stimulated splenocytes were fixed, permeabilised, labelled with an anti-CTLA-4 mAb and analysed by flow cytometry. CTLA-4 expression at the cell surface is transient, thus in order to accurately determine its expression by B cells the cells were fixed and permeabilised. Day-3 LPS stimulated B cells, defined as B220+ cells, displayed equivalent levels of CTLA-4 protein expression as the anti-CD3ε antibody stimulated T cells (defined as CD69$^+$ cells) (Figure 4.10a).

To determine if CTLA-4 is involved in the process of membrane sharing between B cells we employed a similar method used by Qureshi et al (2011), involving the use of a CTLA-4 blocking antibody (anti-CTLA-4 antibody). Incubation with anti-CTLA-4 antibody will block the CTLA-4 molecules when expressed on the B cell surface, and thus it is postulated that its interaction with neighbouring B cells will be hindered, and the amount of membrane sharing between B cells reduced. Day-3 LPS stimulated splenocytes from MD4 and B6.CD45.1 mice were co-cultured for 2 hours at either 37°C or 4°C in the presence of the CTLA-4 blocking mAb, and membrane sharing between B cells tested as described earlier in this thesis (Figure 4.10b and c). The results showed the level of antigen receptor sharing (IgM^{a} or IgM^{b}) between B cells and is measured as the percentage of recipient B cells acquiring IgM^{a} or IgM^{b} from donor B cells. It was found that membrane transfer, as measured by IgM^{a} or IgM^{b} exchange between B cells at either 37°C (Figure 4.10b) or 4°C (Figure 4.10c), was unaffected by the presence of the CTLA-4 blocking mAb (anti-CTLA-4) (Figure 4.10b and c). This result could be an indication that CTLA-4 is not involved in membrane sharing between B cells, although further investigations are required to confirm this finding using CTLA-4 knock out mice, or through RNA interference (RNAi) knock down CTLA-4 mice.

Figure 4.10 Membrane transfer between B cells remains unaffected in the presence of antibody to CTLA-4. (a) Splenocytes were obtained from C57BL/6 mice and stimulated with either 10 μg/ml LPS or 10 μg/ml anti-CD3ε mAb. Day-3 stimulated splenocytes were fixed, permeabilised and labelled with an anti-CTLA-4 mAb. The histogram represents an overlay of intracellular CTLA-4 expression by CD69$^+$ cells (green line) from anti-CD3 Ab-stimulated splenocytes, B220$^+$ cells from LPS stimulated splenocytes (blue line) and an isotype control (grey shaded). Day 3 LPS activated MD4 and B6.CD45.1 spleen cells were co-cultured at (b) 37°C or (c) 4°C for 2 hr in the presence or absence of an anti-CTLA-4 mAb. B6.CD45.1 and MD4 B cells were then assessed for surface expression of IgM^a and IgM^b, respectively. Data shows percentage of B cells expressing the non-endogenous IgM allotype with <5% of B cells staining for the non-endogenous allotype when cultured alone (data not shown). Data expressed as mean ± SEM (n=3) and is representative of 3 independent experiments.

a.

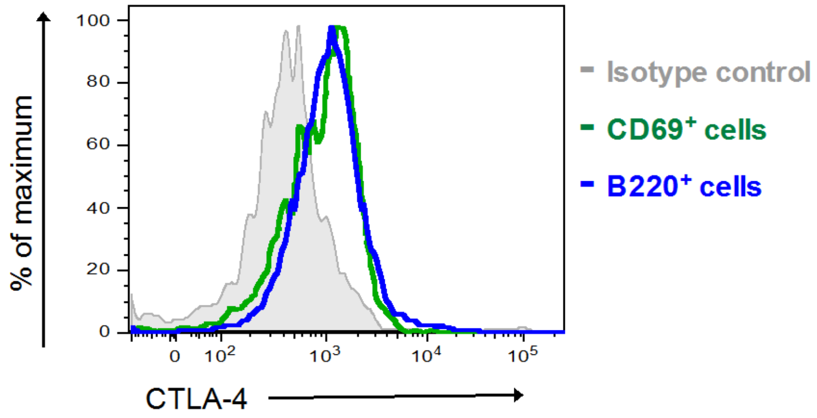
% of maximum
100
80
60
40
20
0
0
10^2
10^3
10^4
10^5
CTLA-4
Isotype control
$CD69^+$ cells
$B220^+$ cells

b. 37°C

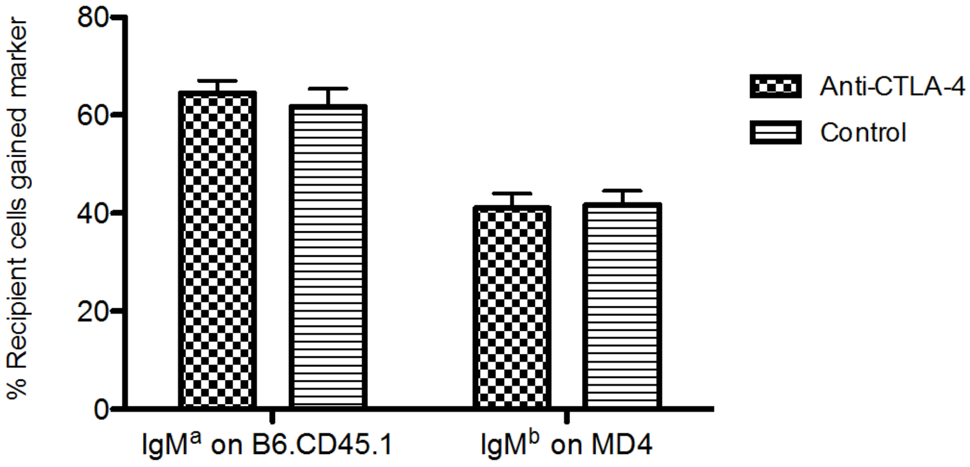
% Recipient cells gained marker
80
60
40
20
0
IgM^a on B6.CD45.1
IgM^b on MD4
Anti-CTLA-4
Control

c. 4°C

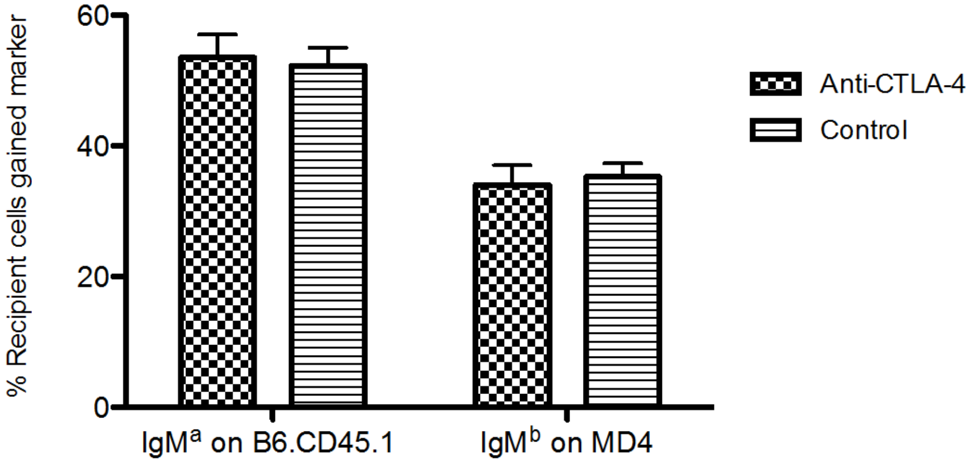
% Recipient cells gained marker
60
40
20
0
IgM^a on B6.CD45.1
IgM^b on MD4
Anti-CTLA-4
Control

4.3.7.3 T cell immunoreceptor with Ig and ITIM domains, TIGIT

TIGIT is a cell surface protein containing an immunoglobulin variable (IgV) domain, a transmembrane domain, and an immunoreceptor tyrosine-based inhibitory motif (ITIM), hence its name (Yu et al., 2009). It has been reported previously to be expressed exclusively on T cells and NK cells, but here it is shown that it is also expressed on LPS-activated B cells (see below). It binds with high affinity to its ligand, poliovirus receptor (PVR; also known as CD155 or NECL5) (Yu et al., 2009). Similar to the CTLA-4/CD28 pathway, the TIGIT-PVR interaction has been demonstrated to be important in determining the activation threshold of T cell immune responses (Joller et al., 2011). Whilst the TIGIT-PVR interaction leads to the inhibition of T cell effector functions, the interaction of PVR with its lower affinity receptor, CD226, on T and NK cells leads to the promotion of T cell responses (Joller et al., 2011, Stengel et al., 2012). Although the exact mechanism of how the TIGIT/CD226 pathway accomplishes this remains unknown, it is thought to function similarly to the CTLA-4/CD28 pathway, with TIGIT removing its ligands from the cell membrane via trans-endocytosis (Stengel et al., 2012).

In this Chapter, real-time PCR and microarray data have shown that TIGIT transcript expression in B cells is increased upon stimulation with LPS. The level of protein expressed at the B cell surface was assessed as above for ALCAM, using an anti-TIGIT mAb and flow cytometry. Results of the protein expression study correlated well with the microarray data, demonstrating a dramatically increased level of TIGIT expression on the surface of LPS stimulated B cells compared to unstimulated B cells (Figure 4.11a and b). Similarly, there was a dramatic upregulation in the cell surface expression of the

TIGIT ligand, PVR (CD155), on LPS activated B cells (Figure 4.11c). Currently, there are no readily available TIGIT blocking mAbs, however we used the available anti-TIGIT mAb at saturating amounts to observe if it had any effect on membrane transfer between B cells. Similar to the results obtained with the ALCAM blocking mAb (Figure 4.9c), the presence of the anti-TIGIT mAb resulted in enhancement of membrane transfer between B cells (Figure 4.11d). Both IgM^a transfer to B6.CD45.1 B cells and CD45.1 transfer to MD4 B cells were increased in the presence of the anti-TIGIT mAb (Figure 4.11d).

Moreover, when using the TIGIT mAb in conjunction with a mAb to the TIGIT ligand, PVR, membrane transfer was further enhanced beyond that observed in the presence of the anti-TIGIT or anti-PVR antibodies alone (Figure 4.11d). These results, in conjunction with those observed with ALCAM blocking antibody (Figure 4.9c), could suggest that cell surface proteins being cross-linked with antibody is enhancing membrane transfer between B cells.

Figure 4.11 Membrane transfer between B cells increases in the presence of anti-TIGIT and anti-PVR mAbs. Splenocytes were either unstimulated or stimulated with 10 μg/ml of LPS for 3 days. Day-3 splenocytes were harvested and incubated with various amounts of a TIGIT-specific (PE conjugated) or PVR-specific (APC conjugated) mAb (up to 4 μg/ml). Expression of TIGIT and PVR on B lymphocytes was analysed by flow cytometry. (a) MFI of TIGIT mAb binding with background fluorescence subtracted. (b) Representative histograms of the expression of TIGIT on unstimulated (top panel - red) and LPS stimulated B cells (bottom panel - red). Isotype controls – blue, background – shaded grey. MFI values for each treatment are included in each panel. (c) MFI of PVR mAb binding with background fluorescence subtracted. Data is representative of 2 independent experiments. (d) Day-3 LPS activated MD4 and B6.CD45.1 spleen cells were co-cultured at 4°C for 2 hr in the presence or absence of saturating amounts of anti-TIGIT (4 μg/ml) and/or anti-PVR mAb. B6.CD45.1 and MD4 B cells were then assessed for surface expression of IgM^{a} and CD45.1, respectively. Data shows percentage of B cells expressing non-endogenous IgM or CD45. Data expressed as mean ± SEM (n=3) and is representative of 3 independent experiments. $^{*}p < 0.05$, $^{**}p < 0.01$, $^{***}p < 0.001$, ns : not significant, unpaired Students *t*-test.

a. TIGIT

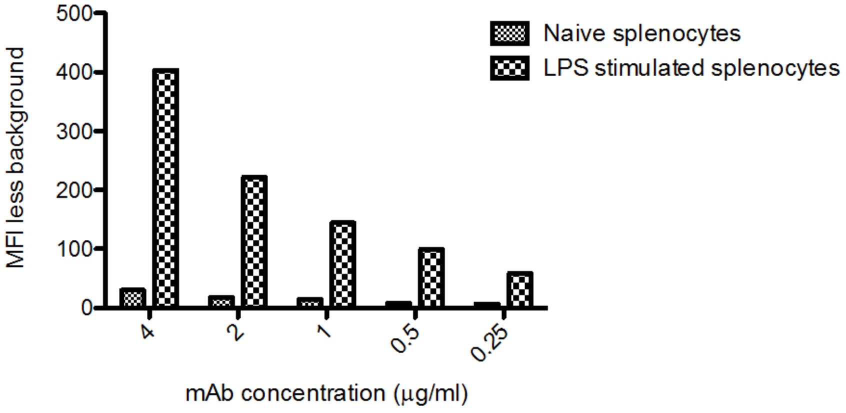
MFI less background
500
400
300
200
100
0
4
2
1
0.5
0.25
mAb concentration (µg/ml)
▨ Naive splenocytes
▨ LPS stimulated splenocytes

b.

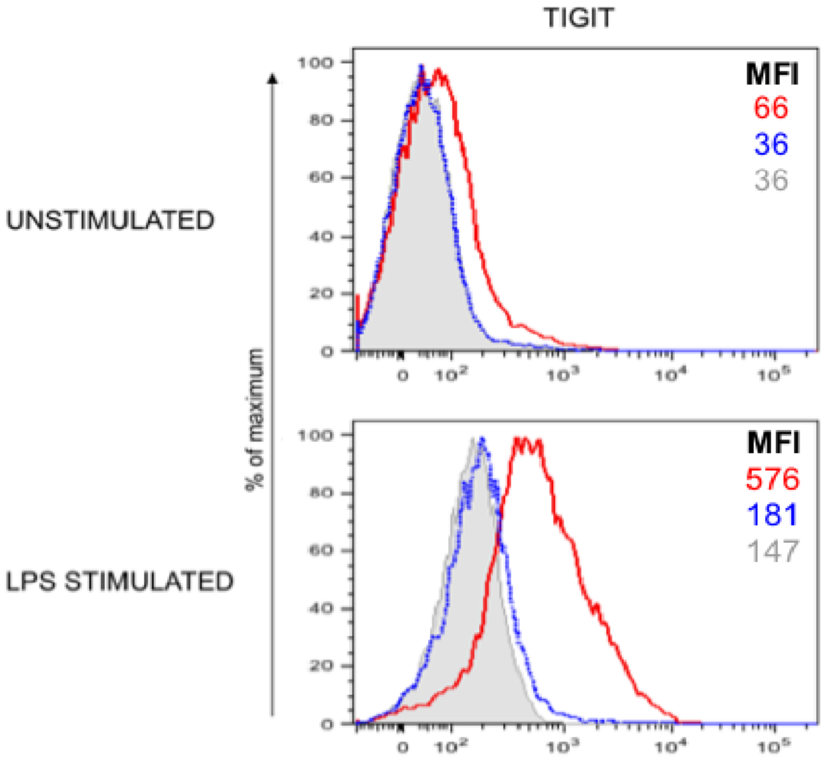
TIGIT
UNSTIMULATED
LPS STIMULATED
% of maximum
100
80
60
40
20
0
0
10²
10³
10⁴
10⁵
MFI
66
36
36
MFI
576
181
147

c. CD155 (PVR)

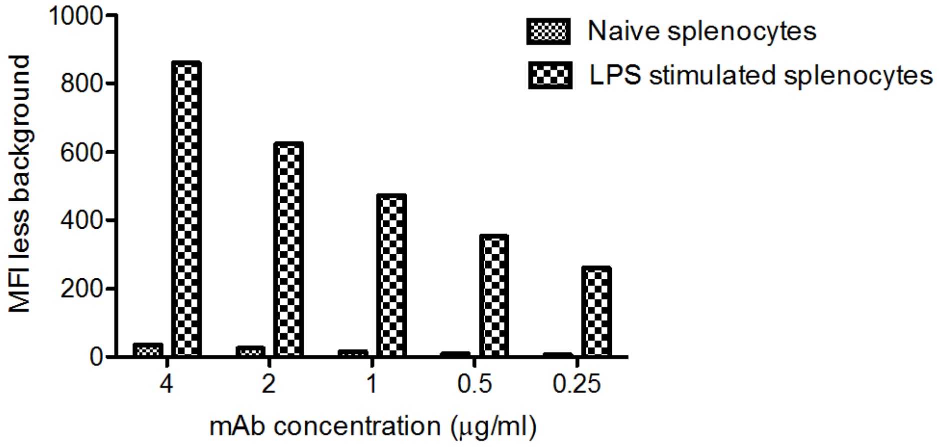
MFI less background
1000
800
600
400
200
0
4
2
1
0.5
0.25
mAb concentration (μg/ml)
Naive splenocytes
LPS stimulated splenocytes

d.

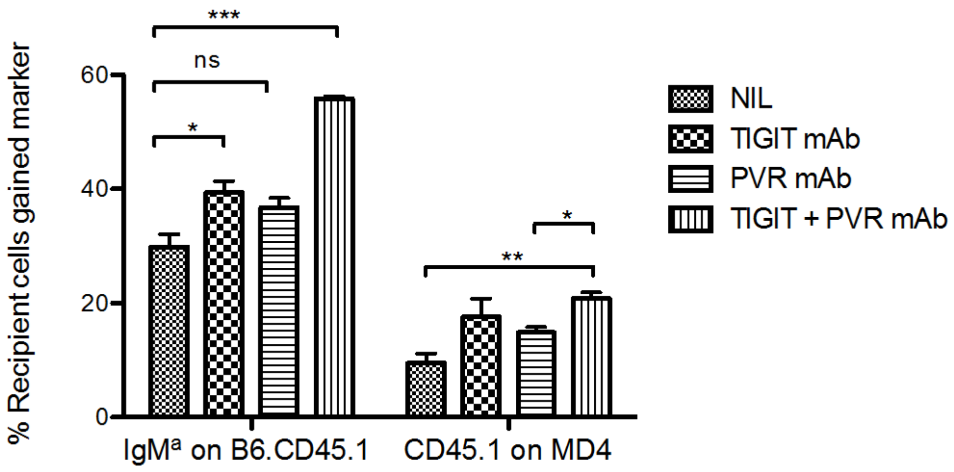
% Recipient cells gained marker
60
40
20
0
***
ns
*
**
*
IgMᵃ on B6.CD45.1
CD45.1 on MD4
NIL
TIGIT mAb
PVR mAb
TIGIT + PVR mAb

4.3.8 B Cell Receptor (BCR) specific antigen enhances membrane transfer between B cells

In line with the suggestion that antibody crosslinking of cell surface proteins enhances membrane transfer between B cells, two independent studies (Poupot and Fournie, 2003, Quah et al., 2008) have indicated that crosslinking of the B cell receptor can enhance membrane transfer between B cells. To assess this, day-3 LPS activated MD4 B cells were co-cultured with day-3 LPS activated B6.CD45.1 B cells in the presence or absence of antigen specific to MD4 B cells (HEL). In accordance with the findings of Quah *et al* (2008), the results demonstrate that in the presence of the BCR-specific antigen (HEL), membrane transfer is significantly enhanced with LPS stimulated B cells (Figure 4.12 a and b) but to a much lesser extent with unstimulated B cells (Figure 4.12 a). In these experiments, the transfer of IgM^a from MD4 B cells to B6.CD45.1 B cells at least doubled in the presence of HEL after a 2-hour co-culture (Figure 4.12a and b). It has been reported previously that the presence of BCR-specific antigen leads to crosslinking of BCRs on the surface of B cells (Batista and Harwood, 2009). Thus, the enhancement of membrane transfer in the presence of BCR-specific antigen is consistent with the hypothesis that crosslinking of BCR and other specific cell surface molecules, such as ALCAM and TIGIT, is involved in membrane transfer.

Figure 4.12 Addition of B cell specific antigen enhances the transfer of membrane IgM between neighbouring B cells. (a) Day-3 LPS-stimulated (10 μg/ml) or unstimulated HEL-specific MD4 splenocytes were incubated with day-3 LPS-stimulated or unstimulated B6.CD45.1 splenocytes, respectively, for 2 hr at 4°C in the presence of various concentrations of HEL. B cells were then assessed for expression of IgM^a via flow cytometry, with the percentage of B6.CD45.1 B cells expressing IgM^a shown. (b) Day-3 LPS-stimulated (10 μg/ml) HEL-specific MD4 splenocytes were incubated with day-3 LPS-stimulated (10 μg/ml) B6.CD45.1 splenocytes for 2 hr at 4°C in the presence or absence of 10 ng/ml of HEL. B cells were then assessed for expression of IgM^a via flow cytometry, with the percentage of B6.CD45.1 B cells expressing IgM^a shown. Data presented is representative of three individual experiments and is given as mean ± SEM (n=3). ****$p < 0.0001$, Students *t*-test.

a.

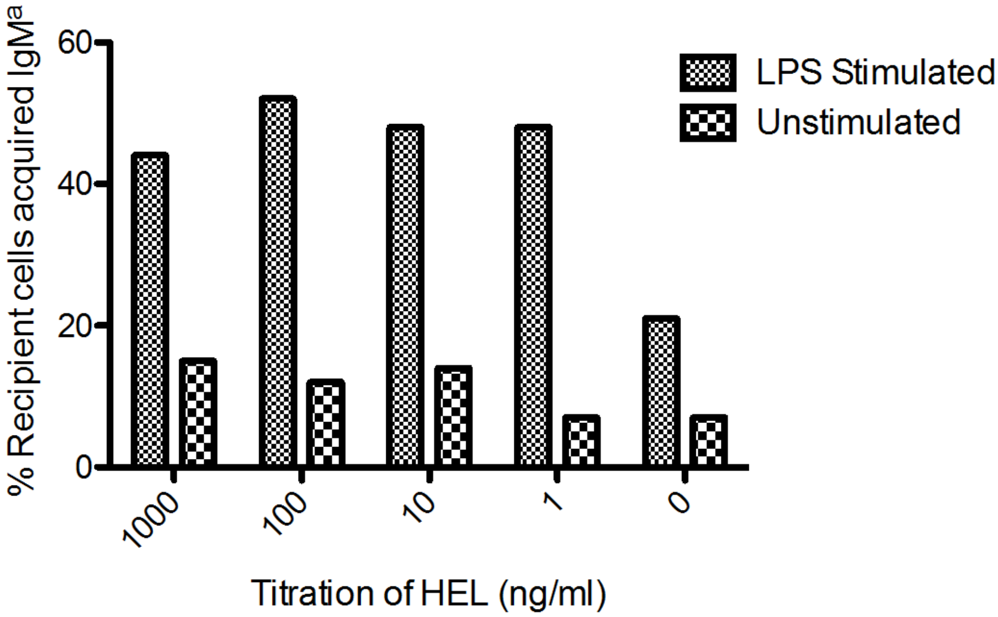
% Recipient cells acquired IgM^a
60
40
20
0
LPS Stimulated
Unstimulated
1000
100
10
1
0
Titration of HEL (ng/ml)

b.

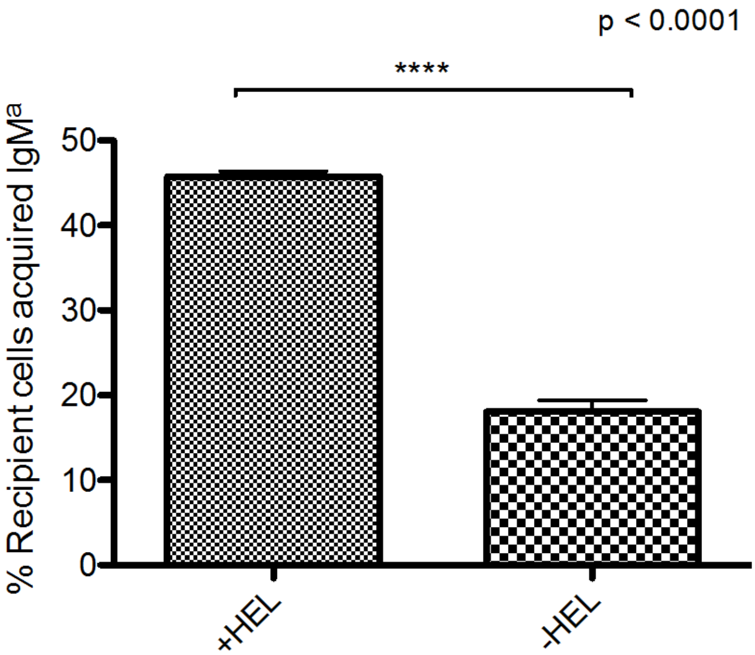
p < 0.0001
****
% Recipient cells acquired IgM^a
50
40
30
20
10
0
+HEL
-HEL

4.4 Discussion

In this Chapter a comparative transcriptome analysis by microarray was used to identify genes that are involved in the process of membrane exchange between B cells. This Chapter makes use of the knowledge that LPS activated B cells can transfer proteins and membrane to neighbouring B cells, but CpG stimulated and unstimulated B cells cannot (Figure 4.1c) (Quah et al., 2008). As such LPS-induced gene expression changes in B cells were compared, using microarray technology, to CpG-induced gene expression changes in B cells and to unstimulated B cells. The microarray analysis indicated that LPS stimulation of B cells resulted in increased expression of 1017 genes and decreased expression of 302 genes. Close to 70% of the gene expression changes observed in LPS stimulated B cells are similarly found in equivalently activated CpG stimulated cells and, as a result, there were many functional similarities observed between LPS stimulated and CpG stimulated B cells. This is consistent with the finding by Richards *et al* (Richard et al., 2008) that naïve splenic B cells respond to LPS and CpG in a similar manner in terms of proliferation and differentiation into plasma cells, although differential gene expression analysis between these two populations of activated B cells has not been previously studied.

An initial analysis of genes of interest identified 16 genes encoding plasma membrane associated proteins with known or predicted roles in cell communication and cell adhesion that were uniquely LPS inducible when compared to genes from unstimulated and CpG stimulated B cells. Further bioinformatic analysis revealed that 10 of these 16 genes encode proteins containing CPP motifs composed of from 20 - 35% positively charged amino acids. Real-time PCR was used to validate the changes in gene expression predicted by the microarray analysis for the 10 genes that were specifically LPS inducible and contained CPP motifs. It was found that 5 of the 10 genes identified in the microarray analysis were confirmed by real-time PCR to be selectively expressed by LPS-activated B cells. Although 50% seems like a relatively high false positive rate, it is not uncommon to find that not all gene expression changes identified by microarray are valid, and this false discovery rate is consistent with published data (Morey et al., 2006). For example, it has been reported (Morey et al., 2006, Wurmbach et al., 2003) that genes exhibiting <1.4-fold change commonly lack concurrence between microarray and real-time PCR, and thus were excluded in an effort to increase the reliability of the microarray data. It is also possible to increase the reliability of the microarray data by increasing the number of replicates or independent experiments that are analysed. The findings of Dow (Dow, 2003) have demonstrated that sample sizes need to be in the order of 12 or greater to improve the reliability of the microarray data, and using below 10 replicates lowers the probability of detecting genes that are differentially expressed. The presence of additional replicates would, therefore, increase the likelihood of identifying true gene targets. Furthermore, recognising that membrane exchange between B cells is an activation dependent mechanism and occurs at 24 hours post activation with LPS, an analysis of a time course of LPS activated B cells and CpG activated B cells would also increase the reliability of the microarray analysis. A time course would likely show increased and decreased expression at more than one time point. For future studies RNA-Seq analysis, rather than the microarray approach, could also be used to detect differences in the transcriptomes of LPS- and CpG-activated B cells, as RNA-Seq provides more comprehensive, reliable and accurate transcriptome information than microarrays (Kukurba and Montgomery, 2015).

For the 5 genes whose changes in gene expression were validated by real-time PCR, there was a good correlation between the magnitude of the expression changes determined by the microarray analysis and those determined by the real-time PCR analysis. Although the microarray analysis revealed some large changes in gene expression (up to 16-fold), the majority of changes were found to be ~2-fold. In the current literature, an arbitrary 2-fold cut off for microarray and real-time PCR data is commonly used, and fold changes lower than this have been suggested to be insignificant (Iyer et al., 1999, DeRisi et al., 2000). This designations is a result of the observation (Ideker et al., 2000) that the expression level of genes from identical cultures rarely vary by as much as 2-fold. However, more recently there have been several studies documenting biologically relevant changes that have occurred below the 2-fold level of detection (St. Laurent et al., 2013, Bigler et al., 2013). A recent study using microarrays to detect differentially expressed genes in psoriasis patients demonstrated accurate changes with as low as a 1.26-fold change in gene expression (Bigler et al., 2013). Another study demonstrated that half of all biologically relevant gene expression changes in an inflammation assay had fold changes of < 2 (St. Laurent et al., 2013). Morey *et al* (2006) reported that genes exhibiting at least a 1.4-fold change in expression had significantly higher correlations than those demonstrating less change by both microarray and real-time PCR analysis. In the current study we maintained a 2-fold change in gene expression between LPS stimulated and unstimulated B cells, as the number of genes observed at the lower threshold of a 1.4-fold change generated over 3000 candidates (data not shown). However, since there were far fewer changes in gene expression observed between LPS stimulated and CpG stimulated B cells, and taking into account considerations reported in the current literature, the gene change cut off was lowered to 1.4-fold in an effort to not eliminate potential candidates, and with the knowledge that this could include some gene expression changes that may eventually be found to be insignificant. Again, the real-time PCR method of validation assisted with the verification of potential candidates.

Since only 50% of the genes that were identified by microarray analysis were validated by real-time PCR analysis, care must be taken in drawing conclusions from the microarray data set as a whole. Instead, the genes that were subsequently validated using real-time PCR were focussed on as candidate genes. As a result, 5 genes, namely ALCAM, AMIGO2, CTLA-4, Slp3 and TIGIT, were identified as being possible mediators of membrane exchange between B cells. In the next Sections, the molecules encoded by these 5 genes will be discussed in detail and their possible roles in the mechanism of membrane transfer between B cells described.

4.4.1 Activated leukocyte cell adhesion molecule, ALCAM

ALCAM is a type 1 transmembrane protein and a member of the immunoglobulin superfamily (IgSF). It is composed of five extracellular immunoglobulin (Ig) domains, consisting of two amino-terminal, membrane-distal variable (V)-type and three membrane-proximal constant 2 (C2)-type Ig folds (VVC2C2C2), followed by a transmembrane region and a short cytoplasmic tail. ALCAM is detectable in a wide variety of tissues and cells including epithelia, lymphoid and myeloid cells, fibroblasts, neurons, hepatocytes, pancreas acinar and islet cells, and bone marrow. The specific tissue and cellular distribution of ALCAM suggests its involvement in dynamic growth and/or migration processes, however, exactly how ALCAM functions remains largely unresolved (Swart, 2002, Weidle et al., 2010).

In mice, ALCAM was first identified by expression cloning based on its ability to bind CD6 (Bowen et al., 1995), however, it also mediates homotypic ALCAM-ALCAM interactions (Bowen et al., 1995). Heterotypic interactions between ALCAM and CD6 are critical for optimal T cell activation, proliferation and stabilisation of the immunological synapse between T cells and APCs (Hassan et al., 2004, Zimmerman et al., 2006). CD6 is expressed on T lymphocytes and thymocytes, and a subset of B cells, namely B1 cells, which are restricted to the peritoneal and pleural cavities and are rarely found in the spleen. Marginal zone B cells and follicular B cells are the predominant B cells present in the mouse spleen, however, these B cells do not express CD6. Since the current study utilises splenic B cells for the membrane exchange experiments, this suggests that if ALCAM is involved in mediating membrane exchange between B cells, it would be through homotypic interactions.

Data presented in this Chapter demonstrates that expression of ALCAM is upregulated on day-3 LPS-activated splenic B cells *in vitro* (Figure 10a and b), consistent with previous findings (Bowen et al., 1995). The affinity of the homotypic ALCAM-ALCAM interaction is two orders of magnitude lower than that of the heterotypic ALCAM-CD6 interaction (Hassan et al., 2004). Homotypic ALCAM interactions are bimodular, depending on distinct ligand binding by the membrane distal amino terminal domain, and on avidity, controlled by actin cytoskeletal dependent clustering of ALCAM membrane proximal C2 domains at the cell surface (van Kempen et al., 2001). Studies using ALCAM deletion mutants have demonstrated that functionality of both modules is required for stable ALCAM-ALCAM interactions. Thus, it has been suggested that the oligomerisation of ALCAM at the cell surface and network formation with interacting cells may stabilise and strengthen the low affinity homophilic ALCAM-ALCAM interaction (Weidle et al., 2010). Consequently, low expression of ALCAM molecules, as observed in CpG stimulated B cells, would result in lower affinity interactions and could explain the lack of membrane exchange observed between CpG stimulated B cells. Furthermore, this mode of interaction strongly correlates with the hypothesis of a lipid raft/clustering event as proposed in Section 3.4. Thus it is postulated that appropriate stimulation will lead to increased expression of ALCAM molecules on the cell surface, which inevitably cluster and bind to apposing cells also expressing ALCAM. It is suggested that the extent of membrane exchange could coincide with the avidity of the ALCAM-ALCAM interaction, with a high avidity, strong, stabile homotypic interaction allowing for the physical uprooting of molecules from apposing cell membranes.

The importance of ALCAM molecules in the process of membrane exchange was assessed using the anti-ALCAM mAb, J4-81, previously reported to block the heterotypic interaction between ALCAM and CD6 (Bowen et al., 1996). Results showed that addition of the antibody substantially increased the amount of transfer between neighbouring B cells. In accordance with this finding, a study by van Kempen *et al* (2001) demonstrated that the addition of the J4-81 mAb markedly increased homotypic cell clustering of ALCAM positive, CD6-negative KG1 cells. Furthermore, they were able to map the epitope for the anti-ALCAM mAb J4-81 to domain V1 and suggest that addition of this antibody may induce a conformational change that promotes ligand binding (van Kempen et al., 2001).

Quah *et al* (2009) demonstrated that the process of membrane sharing was contact dependent, thus it is understood that the first step in this process involves a fusion event between two cells. There is strong evidence suggesting that extreme membrane curvature is a precursor for membrane fusion events (Martens and McMahon, 2011). Flat membranes rarely undergo spontaneous fusion. In contrast, membranes that are highly curved have a high spontaneous fusion rate, likely to be the cause of a lower energy barrier. The more unstable the highly curved membrane is, the more likely it will want to fuse with another membrane to relax into a lower energy state (Martens and McMahon, 2011). Many proteins involved in a plethora of biological contexts can contribute to membrane destabilisation induced by curvature (McMahon et al., 2010), with C2-type Ig-like domains having been implicated many times in membrane fusion processes initiated by induction of membrane curvature (Sot et al., 2013, Groffen et al., 2010, Martens et al., 2007). ALCAM contains multiple C2 domains and studies have demonstrated that these domains are important in ALCAM's cell adhesion ability (van Kempen et al., 2001, Swart, 2002).

C2 domains are lipid-binding domains around 130 residues in length and contain at their core a compact β-sandwich composed of 2 four-stranded β-sheets. They achieve lipid binding using two separate binding sites, the Ca^{2+} -binding loops and the cationic β-groove, neither of which is conserved at their primary or tertiary structure (Rizo and Sudhof, 1998). The majority of the Ca^{2+} -binding loops contain cationic residues that non-selectively bind anionic phospholipid membranes through non-specific electrostatic interactions. Some Ca^{2+} -binding loops contain a conserved set of acidic residues that are capable of co-ordinating Ca^{2+} ions, thus reversing the negative charge and enabling electrostatic interaction with phosphatidylserine in lipid membranes (Rizo and

Sudhof, 1998, McMahon et al., 2010). However, C2 domains have also been shown to bind phospholipids in a calcium-independent manner. Beyond the calcium-binding motif is a cationic β-groove that can bind, and penetrate lipids in the absence of Ca^{2+}.

The insertion of C2 domains penetrates only one leaflet of the target membrane to approximately the depth of lipid glycerol backbones, the region of maximum rigidity (Chapman, 2008, Herrick et al., 2006). Each C2 domain causes a localised curvature, but the effects of these insertions is additive. A sufficiently high density of C2 domains on the cell membrane can create large-scale deformations of the lipid membrane. The close positioning of ALCAM's multiple C2 domains appears to be perfectly adapted to cause maximal possible local curvature. In addition, the tendency for ALCAM molecules to cluster on the cell surface indicates a high density of localised C2 domains, thus increasing the likelihood of high membrane curvature and instability in the membrane, conducive for cellular fusion and membrane exchange events.

4.4.2 Amphoterin-induced gene and ORF (open reading frame) 2, AMIGO2

In 2003 Kuja-Panula and colleagues identified a gene induced in neurons by the heparin-binding protein amphoterin, aptly naming it amphoterin-inducing gene and ORF (AMIGO) (Kuja-Panula et al., 2003). Two homologues were also identified, AMIGO2 and AMIGO3. Together, these three AMIGO's form a family of type I transmembrane proteins with six extracellular leucine-rich repeats (LRRs) and a single immunoglobulin (Ig) C2-like domain located adjacent to the transmembrane region (Kuja-Panula et al., 2003). All members of the AMIGO family were shown to display homotypic binding and also to bind to each other in a heterotypic fashion, suggesting the three AMIGOs are a novel family of cell adhesion molecules (Kuja-Panula et al., 2003).

In addition, two other research groups independently identified AMIGO2. Ono *et al* (2003) discovered a gene that inhibits apoptosis and promoted depolarisation dependent survival of cerebellar granule neurons, and named it alivin1 (Ono et al., 2003). Similarly, two homologues were discovered, alivin2 and alivin3. Rabenau and colleagues (2004) identified a gene that was differentially expressed in approximately 45% of human gastric adenocarcinomas from gastric cancer patients. It was named differentially expressed in gastric carcinomas, or DEGA. Shortly thereafter AMIGO2, Alivin1 and DEGA were discovered to represent the same gene.

AMIGO2 is expressed predominantly in the cerebellum, retina, liver and lung, with lower expression evident in the cerebrum, kidney, small intestine, spleen and testis (Kuja-Panula et al., 2003). AMIGO2 has been suggested to act as a signalling cell adhesion molecule (Kuja-Panula et al., 2003), however, besides its expression in the spleen, it has not been previously implicated in the immune system. In this study, expression of AMIGO2 was detected in splenic B cells. Microarray analysis revealed that expression of AMIGO2 was upregulated upon B cell stimulation, with expression in LPS stimulated B cells being 4.4 fold greater in comparison to unstimulated B cells. Day-3 LPS stimulated B cells also appeared to upregulate expression of AMIGO2 to a greater extent (1.4 fold) than day-3 CpG stimulated B cells.

Leucine-rich repeats (LRR) are a widespread structural motif that has been identified in thousands of proteins with diverse functions. The primary function of LRRs is to mediate protein-protein interactions and their presence in AMIGO2 in combination with an extracellular C2 Ig-like domain adds further evidence to support a role in cell adhesion and/or ligand binding (Kobe and Kajava, 2001).The LRRs are typically 20 – 30 amino acids long and rich in the hydrophobic amino acid leucine (Bella et al., 2008). Protein domains composed of LRR form curved solenoid structures with each turn of the solenoid representing one repeat. Typically each repeat unit has a β-strand-turn-α-helix structure, resulting in the concave feature of the solenoid being defined by a β-sheet lining the circumference, with the outer surface being composed of α-helices. The region between the β-sheet and α-helices forms a highly hydrophobic core, sterically packed with leucine residues. The curved architecture provides a framework for protein-protein interactions with the concave β-sheet surface providing effective ligand-binding sites (Bella et al., 2008). Since the LRR is an efficient structure for protein-protein interactions, proteins that contain LRR domains, such as the three AMIGOs, are well suited to regulate intercellular communication and cell-cell adhesion (Ko, 2012)

The study by Kuja-Panula *et* al (2003) showed that beads coated with AMIGO1 aggregated strongly, implying that it had an adhesive function, or the capability to make homo-oligomers across the cell surface (Kuja-Panula et al., 2003, Kajander et al., 2011). A recent study demonstrated how AMIGO molecules may function in cellular adhesion. AMIGO1 exists as a dimer, with the LRR regions forming the dimer interface. The residues involved in forming the dimer interface are conserved in the entire AMIGO family, thus suggesting that AMIGO2 and AMIGO3 also form dimers. Small-angle X-ray scattering (SAXS) gave further evidence for the existence of AMIGO2 as a dimer, and indicated that the LRR:Ig domain interface is quite flexible. From these results and previously published results using the bead aggregation assay, Kajander *et al* (2011) suggested that the same interface can be used for trans-homodimerisation, and that it is possible that the formation of trans-dimers across cell-cell contacts could be responsible for the adhesive functions of the

AMIGO molecules. They also note, however, that it is also likely that the same interface can be involved in multiple interactions (dimerization and ligand binding) such as is seen in the decorin family of proteins (Kajander et al., 2011, Islam et al., 2013). Further biochemical analysis of AMIGO2, and its LRRs, is necessary to reveal how it mediates cell – cell adhesion and potentially B cell membrane exchange. Furthermore, the lack of AMIGO2-specific mAbs hampers studies of the role of this protein in membrane exchange.

4.4.3 Cytotoxic T lymphocyte associated protein 4 (CTLA-4)

Cytotoxic T lymphocyte associated protein 4 (CTLA-4) is one of the most studied members of the immunoglobulin super family. It is a transmembrane glycoprotein widely described as the major inhibitory molecule for T cell immune responses (Walker and Sansom, 2011). In T cells, CTLA-4 molecules are predominantly stored in intracellular vesicles and are rapidly recruited to the T cell surface upon antigen receptor engagement (Greenwald et al., 2005, Chambers et al., 2001). The current study has demonstrated the expression of CTLA-4 by activated B cells, where upon LPS or CpG stimulation expression was elevated 12- or 9-fold, respectively. Expression of CTLA-4 on B cells has been previously described (Quandt et al., 2007, Pioli et al., 2000, Kuiper et al., 1995, Xerri et al., 1997) although with conflicting results. Quandt and colleagues (2007) demonstrated that ~20% of B cells from stimulated total splenocytes showed intracellular CTLA-4 expression. In contrast, studies by Pioli *et al* (2000) demonstrated that CTLA-4 expression was T cell dependent and expression by freshly isolated B cells from mouse splenocytes was negligible. In the same study, however, the same B cells, when stimulated with LPS and IL-4, expressed CTLA-4 at levels comparable to that described for T cells (~80%) (Pioli et al., 2000). The expression of CTLA-4 on the B cell was transient and maximal after 48-72 hours of stimulation, similar to the expression of CTLA-4 by T cells (Quandt et al., 2007, Pioli et al., 2000, Kuiper et al., 1995). Thus, although CTLA-4 expression by B cells has been reported, its functional role is yet to be clarified.

The majority of studies on CTLA-4 focus on its role as a regulator of T cells, where together with CD28, CTLA-4 functions to regulate T cell immune responses. Both CTLA-4 and CD28 form homodimers and bind to the B7 family members CD80 and CD86, which are expressed on the surface of antigen presenting cells (APCs) including B cells (Greenwald et al., 2005, Chambers et al., 2001). In concert with peptide-MHC recognition by the T cell receptor (TCR), in most circumstances T cells require ligation of CD28 in order to become completely activated, mice deficient in CD28 showing reduced T cell proliferation in response to peptide antigen (Shahinian et al., 1993). In contrast, CTLA-4 competes with CD28 for ligand binding, and as a result dampens the T cell immune response. This process is essential for the prevention of autoimmune diseases (Chambers et al., 2001), mice deficient in CTLA-4 showing an elevated frequency of T cells expressing activation markers, lymphoproliferative disorders and autoimmune diseases (Tivol et al., 1995, Waterhouse et al., 1995).

The mechanism by which CTLA-4 negatively regulates T cell immune responses is surrounded by controversy. Studies have demonstrated that CTLA-4 can capture its B7 ligands from opposing cells by trans-endocytosis. The B7 molecules are subsequently degraded inside the CTLA-4 expressing cells, resulting in impaired costimulation by CD28 (Qureshi et al., 2011). Down regulation of CD80 and CD86 expression on APCs via trans-endocytosis has been demonstrated to be mediated by CTLA- 4 expressing effector T cells, Tregs, (Qureshi et al., 2011) and iTregs (Gu et al., 2012). Interestingly, the trans-endocytosis of B7 molecules by CTLA-4 has remarkable similarities to the process of membrane exchange between B cells, where antigen receptor transfer involves the concomitant transfer of plasma membranes. Using the membrane lipid dye, PKH26, Qureshi et al (2011) demonstrated that transfer of CD80 and CD86 also involved transfer of membrane lipid. Moreover, the process operates in an antigen-dependent manner, where antigen stimulation of T cells promotes the removal and degradation of CD80 and CD86 by CTLA-4 (Gu et al., 2012, Qureshi et al., 2011). Although the process of membrane exchange between B cells is not entirely antigen dependent, the process requires that the B cells be activated, and antigen-specific activation does significantly enhance transfer. It should be noted, however, that unlike transfer between B cells in which transferred proteins are detected at the cell surface, CTLA-4 captures and degrades its ligands inside the CTLA-4 expressing cell. Nevertheless, we postulated that CTLA-4 on the surface of B cells could potentially interact with B7 ligands on neighbouring B cells and mediate exchange of membranes and proteins between B cells. However, initial studies using a CTLA-4 mAb that blocks B7 ligand recognition had no effect on membrane transfer between activated B cells (Figure 4.10b and c), suggesting that CTLA-4 does not play a major role in membrane exchange.

4.4.4 Synaptotagmin-like protein 3 (Slp3)

There are five synaptotagmin-like proteins (Slps) that have been described in the literature (Fukuda and Mikoshiba, 2001, Kuroda et al., 2002b, Fukuda et al., 2001). Synaptotagmin-like proteins are defined by a conserved synaptotagmin-like homology domain (SHD) at the N terminus, which binds to Rab27, which is involved in exocytosis (described below). At their C termini they contain two tandem C2-type Ig-like domains that are separated by a short linker. These C2 domains are the main functional module of Slp molecules (Fukuda, 2002). Multiple C2-domains, as discussed above, are involved in phospholipid binding and are commonly implicated in membrane fusion events (Martens and McMahon, 2011). In the current study, expression of one of these Slp molecules, namely synaptotagmin-like protein 3 or Slp3, was enhanced in LPS stimulated B cells in comparison to CpG stimulated and unstimulated B cells. We speculate that it may be involved in the mechanism of membrane transfer between B cells.

Synaptotagmin-like protein 3 (Slp3) is a 610 amino acid peripheral membrane protein that associates with the cytoplasmic side of the plasma membrane in a calcium dependent manner. The C2 domain is responsible for the interaction between Slp3 and the phospholipid membrane. Interestingly, a polybasic sequence in the C2 structure is crucial for the phospholipid binding activity of the C2 domain (Fukuda, 2002), indicating a CPP motif may mediate this interaction. Although the C2 domains are located on the cytoplasmic side of the plasma membrane, we speculate that in activated B cells, Slp3 binds to the cytoplasmic side of the plasma membrane, inducing curvature of the membrane, which facilitates fusion via lowering the high-energy barrier of the apposing membranes.

Slps have been documented to be involved in regulated exocytosis through binding of Rab GTPase effector molecules in a variety of different cell types (van Breevoort et al., 2014, Hampson et al., 2013, Galvez-Santisteban et al., 2012). Rab27 is a specialised Rab, well known to regulate the efficiency and specificity of exocytosis in hematopoietic cells, including neutrophils, cytotoxic T cells, NK cells and mast cells. Processes may include multiple steps of the secretory process such as tethering, docking, priming and fusion. The mechanisms involved are specific to the cell type and effector molecules involved. The SHD of Slp3 specifically binds Rab27a, and has been shown to be an essential effector of the lytic granule exocytic machinery in cytotoxic T lymphocytes (CTLs) (Kuroda et al., 2002a, Kurowska et al., 2012). Studies have demonstrated that this interaction, in concert with kinesin-1, is required for the final movement of lytic granules in cytotoxic T cells at the immunological synapse for exocytosis (Kurowska et al., 2012). Although Slp3 expression is induced in B cells under specific stimulation conditions, the relevance of its expression remains unknown. Rab27 is highly expressed in the spleen (Barral et al., 2002) and its interaction with Slp3 in B cells may play a role in membrane transfer between neighbouring B cells. Analysis of such processes would be greatly assisted by the availability of Slp3-specific mAbs.

4.4.5 T cell immunoreceptor with Ig and ITIM domains (TIGIT)

T cell immunoreceptor with Ig and ITIM domains, or TIGIT, is a cell surface protein consisting of an immunoglobulin variable domain (IgV), a transmembrane domain, and two immunoreceptor tyrosine-based inhibitory motifs (ITIM). To date, studies have described TIGITs expression on NK cells and regulatory, memory and activated T cells (Yu et al., 2009, Boles et al., 2009, Stanietsky et al., 2009). The current study demonstrated that expression of TIGIT is not restricted to these cell subsets. Microarray analysis showed that expression of the gene encoding TIGIT was at least 4-fold more highly expressed in LPS stimulated B cells in comparison to unstimulated B cells and CpG stimulated B cells. Consistent with literature reports on T cells (Joller et al., 2011, Yu et al., 2009), the expression of TIGIT protein on the B cell surface was induced by cell activation, with LPS stimulated B cells displaying significantly more protein on their cell surface than unstimulated B cells.

TIGIT is a relatively newly described protein identified in 2009 by several independent groups (Boles et al., 2009, Yu et al., 2009, Stanietsky et al., 2009). As such, the protein was alternatively designated TIGIT, Washington University Cell Adhesion Molecule (WUCAM) or Vstm3, and several different functions were proposed. Boles *et al* (2009) demonstrated that TIGIT expression is induced by activation and suggested that it mediates the adhesion of T follicular helper cells to follicular dendritic cells. Stanietsky *et al* (2009) demonstrated that TIGIT inhibits NK cell cytotoxicity directly through its ITIM, and several years later noted that this inhibitory effect is a result of TIGITs interaction with the poliovirus receptor (PVR, CD155) (Stanietsky et al., 2013). Yu *et al* (2009) also suggested that this cell surface protein exerts immunosuppressive effects, this time on effector T cells via binding PVR on dendritic cells and inducing the production of interleukin 10. Levin et al (2011) described TIGIT as a member of the CD28 family, and again, identified PVR in addition to CD112 as TIGIT ligands. The authors suggest that TIGIT functions as an inhibitory receptor on T cells, and these effects are through the prevention of CD226 costimulation (Levin et al., 2011), as earlier studies had demonstrated that PVR and CD112 are ligands for CD226 (DNAM-1), an activating receptor found on NK and cytotoxic T cells (Shibuya et al., 1996).

TIGIT binds to PVR with a higher affinity than CD226 (Levin et al., 2011, Stanietsky et al., 2013). Thus the TIGIT-CD226-PVR-CD112 network is highly reminiscent of other costimulatory/inhibitory pathways such as the CTLA-4-CD28-CD80-CD86 pathway. As discussed previously, CTLA-4 mediated inhibition of T cell activation is the result of the CD28 activator being ‘outcompeted' for binding by increasing amounts of inhibitory CTLA-4 which displays a higher affinity towards the receptors CD80 and CD86. Correspondingly, Stanietsky *et al* (2013) demonstrated that TIGIT-mediated inhibition is dominant over the signals delivered by the CD226-PVR/CD112 interaction and, as such, leads to the inhibition of NK cell cytotoxicity.

Previous studies have suggested that TIGIT inhibits T cell responses through production of IL-10. Yu *et al* (2009) demonstrated that engagement of TIGIT with PVR on dendritic cells induced phosphorylation of PVR and Erk, and led to enhanced production of IL-10 and decreased production of the pro-inflammatory cytokine IL-12 (Yu et al., 2009). They suggest that TIGIT exerts its immunosuppressive effects by binding to PVR and modulating cytokine production by dendritic cells, however, these findings remain to be confirmed. Thus, the mechanism of how TIGIT exerts its inhibitory effects remains unclear. The resemblance with the CTLA-4 network also suggests that TIGIT may inhibit T cell responses in the same way that CTLA-4 does, by trans-endocytosis of its ligands, PVR and CD112. As discussed previously, the mechanism of trans-endocytosis shares many similarities with membrane transfer.

TIGIT–PVR binding is reliant upon a distinct lock-and-key motif that is highly conserved across PVR family members (Stengel et al., 2012). The extracellular domains of PVR family members (nectins, and nectin-like molecules) form ligand-dependant homo- or heterodimers, either between molecules located on the same cell surface, or neighbouring cell surfaces, respectively (Stengel et al., 2012, Aricescu and Jones, 2007, Dong et al., 2006). Interestingly, TIGIT-PVR binding forms a heterotetrameric structure with a core TIGIT/TIGIT interface, distinct from the TIGIT/PVR interface, that can exist in preformed dimers at the cell surface (Stengel et al., 2012). Stengel et al (2012) demonstrated that disruption of TIGIT homodimers results in reduced cell clustering, impaired cell adhesion and limited TIGIT-induced PVR phosphorylation. This indicates the importance of TIGIT clustering on the cell surface in facilitating adhesion of adjacent immune cells.

The experiments with mAbs specific for TIGIT and PVR reported in this thesis demonstrated that expression of both molecules is dramatically upregulated by LPS-activated B cells. This is a surprising situation as TIGIT and its ligand, PVR, are normally expressed on different cell types, but does resemble the situation with CTLA-4 where the molecule is expressed simultaneously with its B7 ligands on activated B cells (see Section 4.4.3). Furthermore, adding an anti-TIGIT mAb enhanced membrane transfer between neighbouring B cells and adding the anti-PVR and anti-TIGIT mAbs in combination had a cumulative effect on membrane transfer.. It is possible that the addition of these mAbs may result in the formation of clusters on the surface of B cells between these antibodies and their target antigens. Currently, there are no commercially available TIGIT or PVR-specific mAbs that block the TIGIT-PVR interaction, thus it could be postulated that the mAbs used in this study created densely packed areas of available binding sites for TIGIT and PVR, respectively, on neighbouring cell surfaces. In support of this hypothesis, studies by Lui et al (2013) demonstrated that TIGIT is recruited to the immunological synapse, thus upon stimulation and addition of these antibodies we are enhancing clustering of cell surface proteins at the immunological synapse. This implies the presence of lipid rafts and, as described previously, these could be vital components of membrane transfer between B cells. Thus TIGIT could facilitate the process of membrane exchange between B cells through the formation of lipid rafts, and the adhesion of adjacent B cells via PVR recognition.

4.4.6 Conclusions

Previous studies have reported that crosslinking of the BCR strongly enhances membrane transfer between B cells (Poupot and Fournie, 2003, Quah et al., 2008). Poupot and Fournie (2003) demonstrated a similar but lower enhancement of membrane transfer was achievable with an anti-CD19 mAb, CD19 being associated with the BCR complex, but this did not occur with antibodies to CD20, CD22 or CD40, with similar findings being reported by Quah et. al. (Quah et al., 2008). In concurrence with this, results presented in this thesis demonstrated that upon crosslinking of the BCR with specific antigen (HEL) membrane transfer was dramatically enhanced between activated B cells, and to a lesser extent, naïve B cells. Furthermore, the data presented in this Chapter indicates that antibodies to ALCAM, TIGIT and PVR alone, and in combination, were similarly capable of enhancing transfer between B cells. This model suggests that the crosslinking of specific receptors creates a patching effect, similar to a lipid raft, in which there are areas of localised membrane destabilisation and, consequently, more accessible areas for membrane fusion. These processes are likely to be complementary for the transfer of membranes and cell surface proteins between B cells.

Due to a lack of available antibodies and other evidence, the contribution of the identified candidate genes (i.e., ALCAM, AMIGO2, CTLA-4, Slp3 and TIGIT) to membrane exchange between B cells remains unclear. Although addition of anti-ALCAM, anti-TIGIT and anti-PVR mAbs results in enhanced transfer likely through amplifying the coalescence of molecules into micro-domains, membrane transfer in the absence of these antibodies still occurs. It could be speculated that under certain activation conditions the expression of candidate genes is upregulated, resulting in the increased expression of proteins encoded by these genes at the B cell surface. It could be that one of these proteins, or perhaps several, bring about membrane transfer through mediating adhesion and membrane fusion between neighbouring B cells, this effect being enhanced by crosslinking mAbs. Further studies using RNA interference (RNAi) to specifically silence targeted mRNAs could ascertain their potential role in mediating transfer. Additionally, where available, mice with these particular genes knocked out could provide valuable information regarding the roles of the candidate proteins in membrane transfer.

Chapter 5

Investigation into whether TCR sharing between CTLs can be harnessed for adoptive immunotherapy of tumours

5.1 Abstract

Previous studies in my supervisor's laboratory have demonstrated that, similar to B cells, antigen specific $CD8^+$ T cells share their T cell receptors (TCR) with neighbouring $CD8^+$ T cells of an unrelated specificity. In this Chapter an adoptive T cell immunotherapy model was used to investigate whether TCR sharing can be harnessed in an effort to control tumour growth. The model involved utilising the OVA expressing EG7 (EG7-OVA) cell line to establish tumours in mice, which can be eradicated using OVA-specific TCR transgenic OT-I CTLs. Previous reports have shown that OT-I CTLs necessitate the use of the protein perforin to eliminate EG7 cells. As such, it was hypothesised that (a) perforin deficient, OVA-specific OT-I CTLs, and non-specific B6.SJL.TCRP14 CTLs when transferred alone will be incapable of tumour regression and (b) when these cells are adoptively transferred together, and TCR transfer occurs, the resultant B6.SJL.TCRP14 cells with OVA-specific TCR (from the OT-I *Prf1-/-* cells) have the capacity to recognize and destroy the OVA-expressing EG7 cells and lead to the regression of established EG7 tumours. However, in contrast with previous findings, this Chapter shows that perforin deficient OVA-specific, OT-I CTL, but not non-specific B6.SJL.TCRP14 CTLs, are as efficient as wild type OT-I CTL at clearing established EG7-OVA tumours. This indicates that although control of tumour growth is antigen specific, the mechanism used by CTLs in this model to control tumour growth does not involve perforin, with *in vitro* studies suggesting that the Fas/FasL pathway may be involved. Furthermore, results reported in this Chapter indicate that *in vivo* extraordinarily small numbers of CTLs within tumours can induce tumour regression. This suggests that *in vivo* many other mechanisms work in concert to control EG7-OVA tumour growth, NK cells being the most obvious, and it is likely that when

one host effector mechanism is silenced, other host effector mechanisms will compensate in its absence. In addition, variations in results reported in various laboratories may be related to genetic drift in the EG7-OVA cell line.

5.2 Introduction

Previously it has been demonstrated that antigen specific CD8$^+$ T cells can share their T cell receptors (TCR) with neighbouring CD8$^+$ T cells of an unrelated specificity and as a consequence result in proliferation-independent expansion of virus-specific T cells (Chaudhri et al., 2009). A study by Chaudhri *et al* (2009) demonstrated that ectromelia virus (ECTV)-specific CD8$^+$ T cells deficient in the lytic protein perforin (*Prf1-/-*) are unable to clear virus from ECTV infected mice. Furthermore, adoptive transfer of influenza A virus (IAV)-specific CD8$^+$ T cells into ECTV infected recipients were also ineffective at reducing virus titres. In contrast, ECTV infected mice receiving a mixture of *Prf1-/-* ECTV-specific CD8$^+$ T cells and IAV-specific CD8$^+$ T cells were capable of reducing viral titres to similar levels as wild type ECTV-specific CD8$^+$ T cells. Subsequently, Chaudhri *et al (*2009) demonstrated using flow cytometry cell sorting that the IAV-specific CD8$^+$ T cells had gained the ability to effectively kill ECTV-infected target cells, indicating that TCR sharing has the potential to expand the number of pathogen-specific CD8$^+$ T cells.

Based on the current understanding of antigen receptor sharing, and the results obtained by Chaudhri *et al* (2009), it should be possible to harness this phenomenon to enhance antigen-specific CD8$^+$ T cell responses in the adoptive immunotherapy of established tumours. It is well established that CD8$^+$ T cells play a critical role in immunity against cancer. The presence of CD8$^+$ T cells in a tumour is associated with a good prognosis, however, a critical concentration of antigen-specific T cells is required in order to successfully control and eradicate tumour cells (Budhu et al, 2010). Often, the curability of a cancer is dependent on the capability to deliver and maintain a sufficient intra-tumoral concentration of antigen-specific T cells/ml of tumour for a sufficient time period to kill 100% of the tumour cells (Dudley and Rosenberg, 2003). This has prompted the development of approaches to genetically engineer tumour antigen-specific T cells to target tumours.

In this study, the thymoma cell line EL4 expressing OVA (EG7-OVA) was used to investigate the role of antigen receptor sharing between CD8$^+$ T cells in an adoptive immunotherapy T cell transfer model. The EG7-OVA tumour model has been extensively studied in adoptive immunotherapy assays in mice (Huang and Xiang, 2004, Hollenbaugh et al., 2004, Dobrzanski et al., 2004, Helmich and Dutton, 2001, Morales-Kastresana et al., 2013). These studies demonstrate that adoptive transfer of *in vitro* activated CD8$^+$ T cells from OVA-specific TCR transgenic mice (OT-I) results in significant cytotoxicity for EG7 tumour cells and consequently a reduction in EG7-OVA tumour growth.

To establish the influence of antigen receptor sharing in the control of tumour growth the current study utilised the finding that in the absence of the cytolytic protein, perforin, CD8$^+$ T cells are less effective at bringing about tumour rejection than their wild type counterparts (Huang and Xiang, 2004, Morales-Kastresana et al., 2013). Perforin is a cytolytic protein found in the granules of cytotoxic T cells and NK cells. Upon recognition of a target cell the T cell degranulates, and the perforin released inserts itself into the target cells plasma membrane. Here it punctures a hole in the target cell membrane and accompanied by granzymes it causes the target cells to lyse (Squier and John Cohen, 1994). Thus, although perforin-lacking OT-I CD8$^+$ T cells (OT-I *Prf1-/-*) will be able to recognise EG7-OVA tumour cells, the lack of perforin will diminish the T cell’s killing capacity.

In addition to perforin-lacking OVA-specific CD8$^+$ T cells, a vital component of the adoptive immunotherapy model is the presence of effector T cells that are unable to recognise OVA. The current model uses B6.SJL.TCRP14 mice, which have TCR transgenic CD8^{+} T cells specific for the lymphocytic choriomeningitis virus (LMCV) peptide gp33. It is anticipated that OT-I *Prf1-/-* CTLs and B6.SJL.TCRP14 CTLs transferred alone will be unable to control tumour growth. However, if TCR sharing occurs the co-transfer of these two CTL populations will result in B6.SJL.TCRP14 CTLs gaining the OVA-specific TCR. As a consequence, the B6.SJL.TCRP14 CTLs bearing donor TCRs will be able to recognise and eliminate EG7-OVA tumour cells. If this is the case, this model could be used to formally demonstrate that TCR sharing can be exploited to enhance the CTL response against a tumour.

5.3 Results

5.3.1 Establishing the optimum adoptive immunotherapy model for analysis of tumour regression.

Previously, C57BL/6 mice have been commonly used in EG7-OVA models of adoptive immunotherapy (Helmich and Dutton, 2001, Dobrzanski et al., 1999, Huang et al., 2005). However, in the current studies the adoptive immunotherapy model took some time to establish with the predominant problem being rejection of EG7-OVA subcutaneous tumours in the right flank of recipient C57BL/6 mice, presumably due to genetic drift of the cell type from the host mice. To overcome this problem *Rag1-/-* mice, which lack mature T and B cells, were used as the host mice for subsequent experiments (Mombaerts et al., 1992). Recipient *Rag1-/-* mice proficiently grew EG7-OVA subcutaneous tumours (described in detail below), and further assisted the experiments as the lack of mature T cells in the *Rag1-/-* mice ensured no interference from recipient T cells in the T cell transfer assay.

In addition, the variation in the size and growth rate of EG7-OVA tumours was initially a problem and is a common issue in tumour studies (personal communication, Dr Joe Altin and Dr Lucy Coupland). This was overcome by adopting the following measures (i) the EG7-OVA tumour cell suspension was brought to room temperature prior to injection, (ii) the EG7-OVA tumour cell preparation was gently but thoroughly mixed immediately prior to being drawn into a syringe, (iii) the volume drawn into the syringe was adequate for one mouse, not several, ensuring each mouse received the same volume, and a new syringe used each time and (iv) post injection at the subcutaneous site, the needle was removed and the site was NOT pressed or rubbed. This resulted in dramatically increased uniformity in size of subcutaneous tumours in recipient mice.

Previous studies have indicated that subcutaneous injection of $1x10^6$ EG7-OVA cells into the flank of mice provides growth kinetics suitable for functional assays, with tumours reaching ~5-7 mm in diameter at 10-12 days post-inoculation (Huang and Xiang, 2004, Huang et al., 2005). Thus, in initial studies five *Rag1-/-* mice received subcutaneous injections of $1x10^6$ EG7-OVA tumour cells in their right flanks. Tumour growth was monitored and tumour size was recorded by multiplying the measured lengths of two perpendicular axes every 2 days (Figure 5.1). Tumours became apparent ~8 days post inoculation of tumour cells, and achieved a size of ~25 mm^2 (approximately 5 mm diameter) by day 10 (Figure 5.1). Mice were sacrificed when tumours reached a size of 250 mm^2 (Figure 5.1).

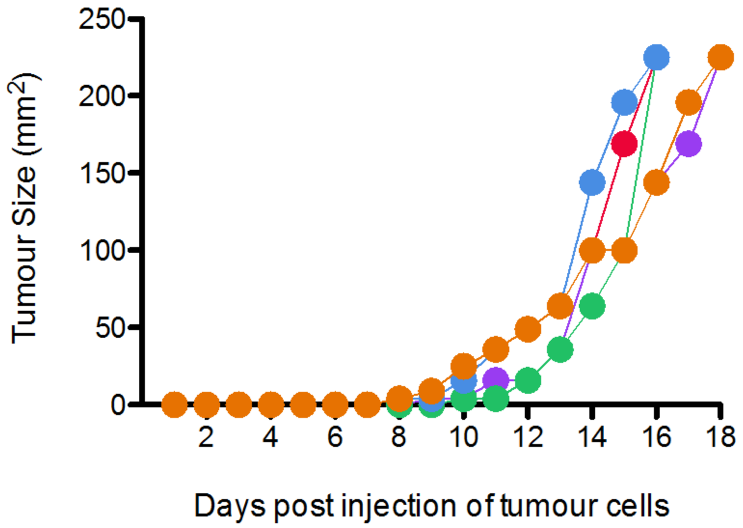

Figure 5.1 Tumour growth of EG7-OVA cells after subcutaneous injection into *Rag1-/-* mice. *Rag1-/-* mice (n=5) were injected subcutaneously in the right flank with 1x10^6 EG7-OVA cells. Tumour growth was monitored and tumour size measured every 2 days on two perpendicular axes using vernier callipers. Tumour size was calculated by multiplying the lengths of the two measured axis (mm^2). Data presented for 5 individual recipient *Rag1-/-* mice.

At a subcutaneous tumour size of ~25 mm^2 previous studies have indicated that EG7-OVA tumour regression is achievable with intravenous injection of activated OT-I $CD8^+$ T cells from TCR transgenic mice expressing an OVA-peptide specific TCR (Dobrzanski et al., 1999, Huang et al., 2002). To establish this adoptive transfer system, CTL effector populations were generated from OVA-specific wild type OT-I mice by culture with SIINFEKL-pulsed C57BL/6 splenocytes, LPS and IL-2 for 4 days and then were i.v. injected ($5x10^6$/mouse) into *Rag1-/-* mice carrying 10 day established tumours of ~25 mm^2 in size. Tumour rejection started 2-4 days after adoptive transfer of activated OT-I CTLs (Figure 5.2), and growth remained suppressed until day-18, upon which time the mice were sacrificed (Figure 5.2). In the absence of the adoptive transfer of activated OT-I CTLs, the tumours grew progressively until the mice were sacrificed at a tumour size of 250 mm^2 (Figure 5.2).

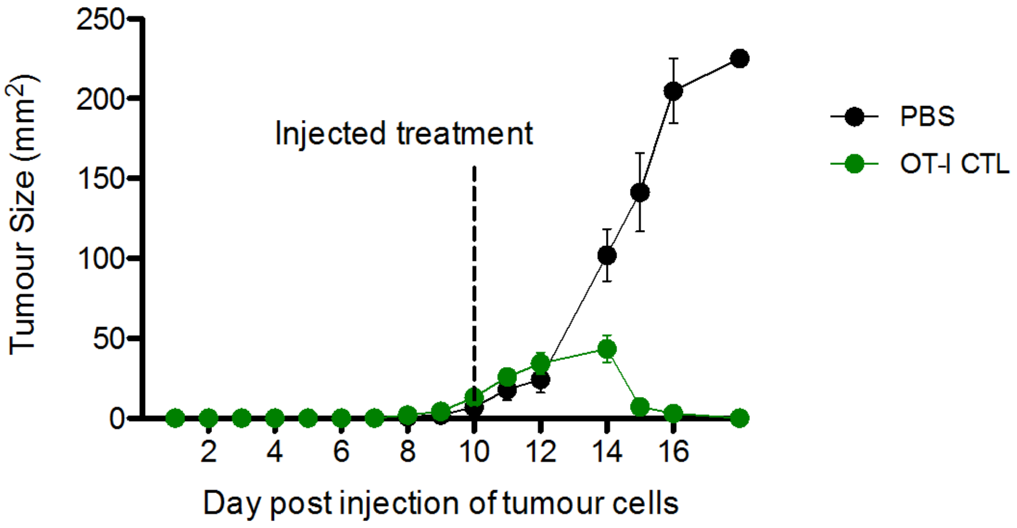

Figure 5.2 Growth of EG7-OVA tumours in untreated and OT-I CTL treated mice. EG7-OVA subcutaneous tumours were established as described in Figure 5.1. Activated OT-I CTLs were prepared by stimulation of naïve OT-I splenocytes *in vitro* for 4 days with SIINFEKL-pulsed C57BL/6 splenocytes, LPS, and IL-2. Ten-day tumour-bearing *Rag1-/-* mice were injected i.v. with $5x10^6$ activated OT-I CTL (green) or PBS (black). Tumour growth was monitored and measured every 2 days as described in Figure 5.1. Data expressed as mean ± SEM (n=5). Data are representative of 3 independent experiments.

5.3.2 Effect of antigen-specific TCR transfer between CD8+ T cells on tumour growth

Previously Chaudhri *et al* (2009) demonstrated that during a viral infection, antigen-specific effector CD8$^+$ T cells have the ability to share their TCR with neighbouring effector CD8$^+$ T cells of an irrelevant specificity, thereby rapidly expanding the pool of virus-specific effector T cells. This study showed that transfer of the TCR was via membrane exchange and, importantly, TCR recipient T cells were capable of reducing viral titres to similar levels as TCR donor T cells (Chaudhri et al., 2009). Based on these results and our current understanding of antigen receptor sharing it should be possible to harness this phenomenon and increase the efficacy of adoptive immunotherapy.

Adoptive transfer experiments used in this study follow a similar design to that used by Chaudhri *et al* (2009). OVA-specific OT-I CTLs were prepared by stimulation of naïve OT-I splenocytes *in vitro* for 4 days with SIINFEKL-pulsed C57BL/6 splenocytes, LPS, and IL-2. *In vitro* activated OVA-specific OT-I CTL ($5x10^6$ CTL/recipient) that are perforin deficient (OT-I *Prf1-/-*), were adoptively transferred into EG7-OVA tumour bearing mice (subcutaneous tumours ~5 mm in diameter), either alone or in conjunction with $5x10^6$ activated CTLs of an unrelated specificity, namely P14 TCR transgenic CTLs specific for the lymphocytic choriomeningitis virus (LCMV) peptide gp33 (B6.SJL.TCRP14 CTL)(Pircher et al., 1989). LCMV-specific B6.SJL.P14 CTLs were prepared in a similar manner to OT-I CTLs, being stimulated *in vitro* for 4 days with C57BL/6 splenocytes that were pulsed with gp33 (C9M) peptide, LPS and IL-2. As previously shown, $5x10^6$ wild type OT-I T cells alone results in EG7-OVA tumour regression (Figure 5.2). However, studies by Huang et al (2005) indicate that the perforin-mediated pathway plays a major role in the OT-I CTL killing of

EG7-OVA. Thus, we anticipated that OT-I *Prf1-/-* and B6.SJL.TCRP14 CTL transferred alone would be unable to result in the control of tumour growth, however, if TCR sharing occurs, the co-transfer of these two CTL populations would lead to tumour regression.

As expected, wild type B6.SJL.TCRP14 CTLs were ineffective at controlling tumour growth in tumour-bearing mice, resulting in progressive growth similar to untreated tumour-bearing mice (Figure 5.3). Surprisingly, however, mice receiving OT-I *Prf1-/-* CTLs either alone or in conjunction with B6.SJL.TCRP14 CTL were equally effective at controlling tumour growth and within 5 days a reduction in tumour volume (Figure 5.3) was observed. Approximately 10 days post CTL treatment tumour volumes had regressed to undetectable levels and remained so until day 25, upon which time the mice were sacrificed (Figure 5.3). These results suggest that OT-I *Prf1-/-* CTLs control tumour growth alone, in contrast to previous reports that have used perforin deficient CTLs in *in vitro* models and shown reduced tumour clearance (Huang and Xiang, 2004, Hollenbaugh et al., 2004, Morales-Kastresana et al., 2013).

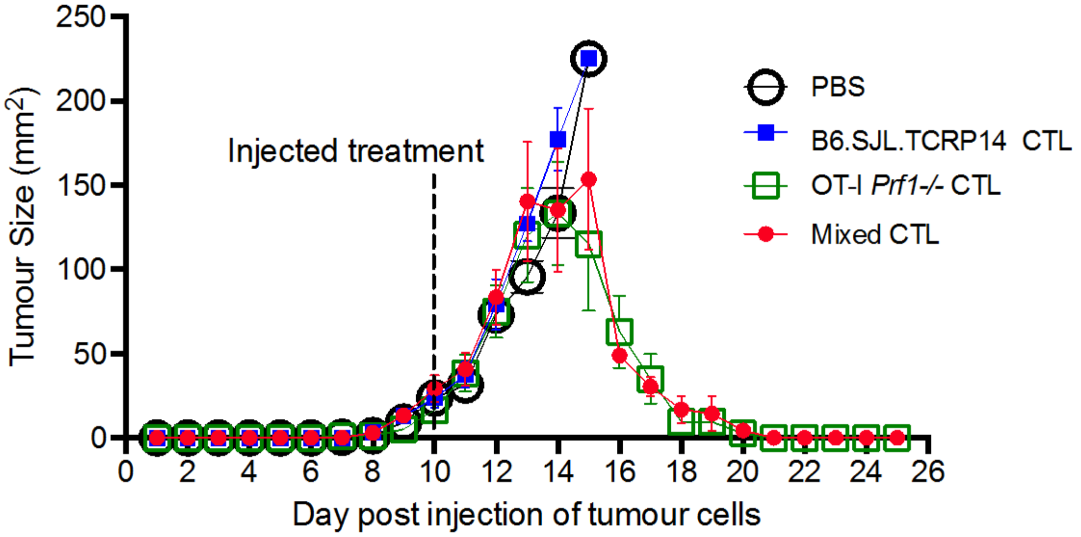

Figure 5.3 Impact of TCR transfer on EG7-OVA tumour growth. EG7-OVA subcutaneous tumours were established as described in Figure 5.1. OT-I and B6.SJL.TCRP14 CTL were prepared by stimulation of naïve splenocytes *in vitro* for 4 days with LPS, IL-2 and C57BL/6 splenocytes pulsed with SIINFEKL and gp33 peptides, respectively. *Rag1-/-* mice bearing 10-day EG7-OVA tumours were given i.v. injections of 5x10^6 OT-I *Prf1-/-* CTLs (green), 5x10^6 B6.SJL.TCRP14 CTLs (blue), mixture of 5x10^6 OT-I *Prf1-/-* CTLs and 5x10^6 B6.SJL.TCRP14 CTLs (red), or PBS (black). Tumour growth was monitored and measured every 2 days as described in Figure 5.1. Data expressed as mean ± SEM (n=5).

5.3.3 Leukocyte infiltrates in EG7-OVA tumours in untreated and OVA-specific OT-I CTL treated mice

Figure 5.3 shows that CTL effectors from perforin deficient mice have similar efficacy to CTL effectors from wild type mice in bringing about reduction in tumour volume. In addition, the results indicate that the killing mechanism is antigen specific, as the non-OVA specific B6.SJL.TCRP14 CTLs were incapable of controlling tumour growth of established EG7-OVA tumours (Figure 5.2) but OVA-specific wild type OT-I (Figure 5.2) and OT-I *Prf1-/-* (Figure 5.3) CTLs efficiently induced regression of established tumours. Previously it has been suggested that *in vitro* generated CTLs do not kill the tumour target cells by direct contact-mediated lysis, but merely serve as the trigger to a host-mediated killing mechanism (Hollenbaugh et al., 2004). This may suggest that the CTLs deliver an antigen specific signal to tumours rendering the tumours vulnerable to attack by host-mediated processes. Potential host killing mechanisms could involve recruitment of NK cells, neutrophils or macrophages (Hollenbaugh et al., 2004, James et al., 2013, Fridlender and Albelda, 2012, Komohara et al., 2009), remembering that *Rag1-/-* recipient mice were being used, hence host T and B lymphocytes were not involved. To assess if antigen-specific CTL treatment in tumour-bearing mice resulted in the recruitment of host effector mechanisms EG7-OVA tumours from untreated and OT-I CTL treated mice were excised 4 days post CTL treatment for analysis of potential effector cells present at the tumour site. Histological examination of H&E stained tumour tissues (at day 14) showed that control tumour-bearing mice (i.e., mice that did not receive adoptive immunotherapy) had dense tumour tissue, with little evidence of necrosis and no infiltration of immune cells (Figure 5.4a and c). In contrast, tumour-bearing mice treated with wild type OT-I CTL displayed significantly smaller tumour volumes, with large areas of necrosis evident from increased pink staining with the eosin dye (Figure 5.4b and d).

Flow cytometric analysis was used to investigate the presence of host infiltrating leukocytes that may potentially assist donor CTLs in controlling tumour growth. Tumour tissues were excised from day-15 established tumours in *Rag1-/-* mice that had been treated with either PBS or OT-I CTLs. Forward scatter and side scatter were used to discriminate viable cells from dead cells and cell debris. In addition, Hoechst 33258, a nucleic acid stain that emits fluorescence when bound to dsDNA, was used to identify and remove remaining dead cells from the cell population (data not shown). Leukocytes were then distinguished using a suite of antibodies to common antigens. In PBS treated tumour-bearing mice there is one dominant population of infiltrating leukocytes (39.1%) present, it being CD8^{low}, NK1.1^{low}, CD11b^{med} and F4/80^{med} (Figure 5.4e and g), with a minor population of CD11b^{hi} leukocytes also being detected. In contrast, OT-I CTL treated tumour-bearing mice show a massive influx of tumour infiltrating leukocytes. There were also CD8^{+} cells present (8.89%), indicating the presence of adoptively transferred OT-I CTLs. Cells expressing NK1.1^{+} were detected, indicative of NK cells, at levels equivalent to that of CD8^{+} cells found in the tumours (Figure 5.4f). Cells expressing neither CD8 nor NK1.1 were separated into a further four significant populations of myeloid cells being delineated based on F4/80 and CD11b expression (Figure 5.4h). Previous studies in mice (Narni-Mancinelli et al., 2011, Taylor et al., 2003) defined different myeloid populations based on CD11b and F4/80 expression. CD11b^{high}, F4/80^{low} cells were defined as neutrophils (Narni-Mancinelli et al., 2011), CD11b^{high}, F4/80^{med} and CD11b^{high}, F4/80^{high} cells as eosinophils and monocytes (Taylor et al., 2003), and CD11b^{med}, F4/80$^{med\text{-}high}$ cells as infiltrating macrophages (Narni-Mancinelli et al., 2011) (Figure 5.4h). The population of $CD11b^{med}$, $F4/80^{med\text{-}high}$ cells present in the untreated mice (Figure 5.4g) is equivalent in size to that seen in the OT-I CTL treated mice (Figure 5.4h). However, it is clearly evident that this population has increased its expression of both CD11b and F4/80 in the OT-I CTL treated mice, this change being commonly seen in inflammatory sites (Stables et al., 2011).

Figure 5.4 Substantial numbers of infiltrating leukocytes are evident within tumours during acute OT-I CTL mediated rejection. EG7-OVA subcutaneous tumours were established in the right flank of *Rag1-/-* mice as described in Figure 5.1. OT-I CTL were activated as described in Figure 5.2. Ten day EG7-OVA tumour-bearing recipients were injected with PBS (a, c, e and g) or $5x10^6$ OT-I CTLs (b, d, f and h). Paraffin embedded tumour sections from excised day-15 established EG7-OVA tumours were stained with hematoxylin and eosin (H&E) and examined by light microscopy (a-d). Excised tumours were processed into single cell suspensions and stained with anti-CD8, anti-NK1.1, anti-F4/80 and anti-CD11b mAbs (e-h) and analysed by flow cytometry. Percentage of cells in each gated area is indicated in panels e-h. Data are representative of at least 3 experiments.

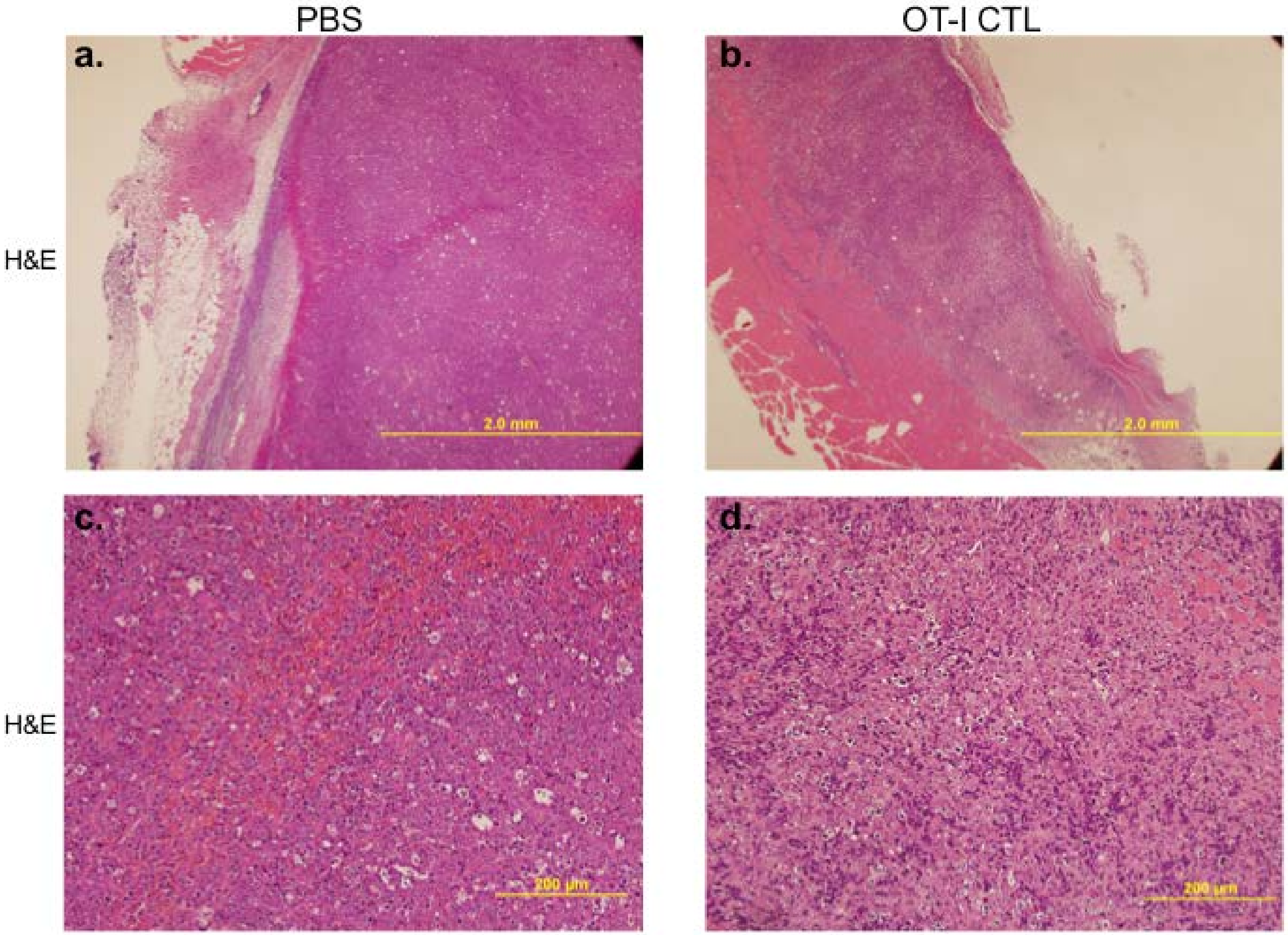
PBS
OT-I CTL
H&E
H&E
a.
b.
c.
d.
2.0 mm
2.0 mm
200 µm
200 µm

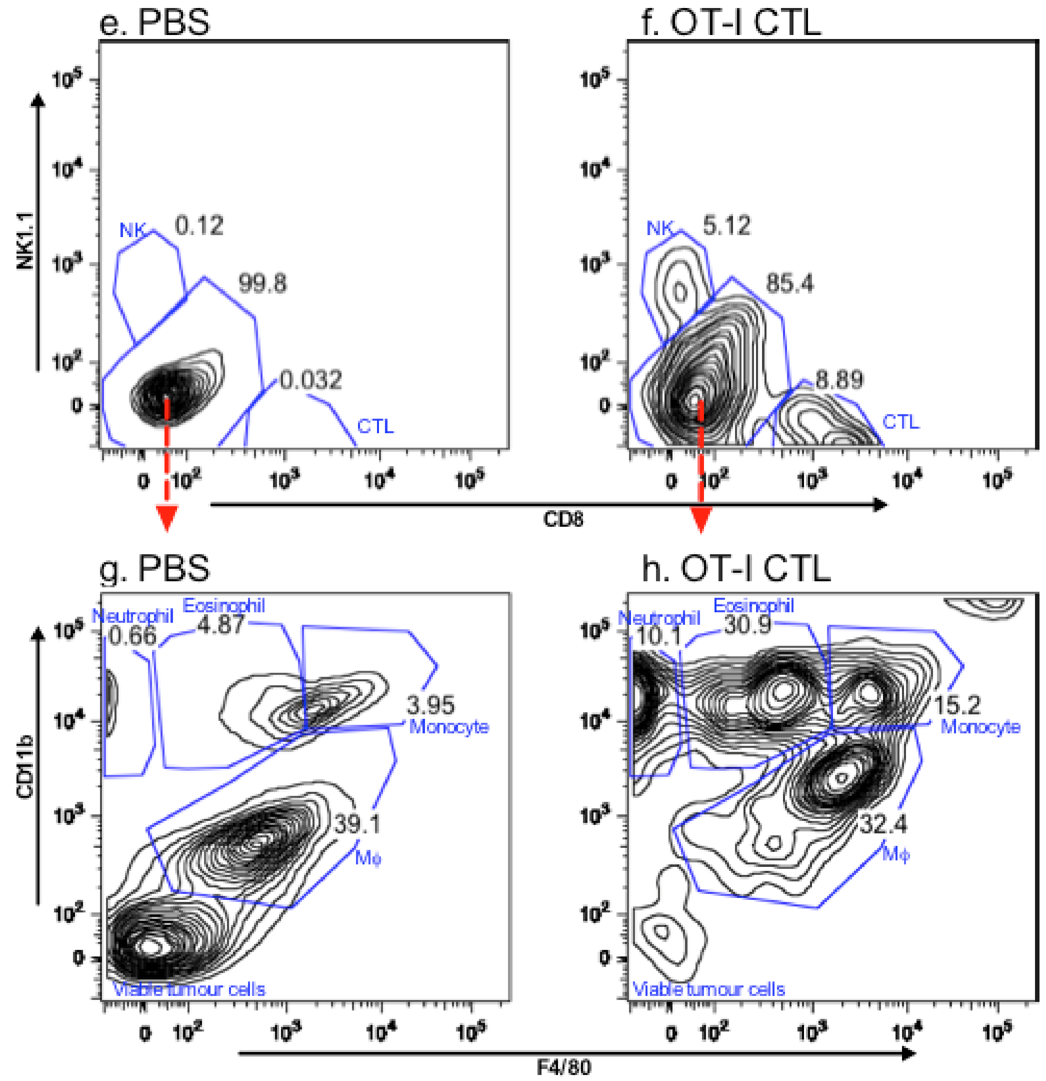
e. PBS
f. OT-I CTL
NK1.1
NK
0.12
99.8
0.032
CTL
NK
5.12
85.4
8.89
CTL
CD8
g. PBS
h. OT-I CTL
CD11b
Neutrophil
0.66
Eosinophil
4.87
3.95
Monocyte
39.1
Mφ
Viable tumour cells
Neutrophil
10.1
Eosinophil
30.9
15.2
Monocyte
32.4
Mφ
Viable tumour cells
F4/80
0
10²
10³
10⁴
10⁵

5.3.4 Effect of OVA-specific OT-II CD4+ T cells and OT-I CTL-derived IFNγ on EG7-OVA tumour growth

It is clearly evident that the injection of OT-I CTLs into tumour-bearing mice induces a large infiltration of leukocytes at the tumour site (Figure 5.4). It is well known that the tumour microenvironment contains a multitude of cell types that can produce a variety of cytokines, with many of these being important in anti-tumour immunity (Hollenbaugh and Dutton, 2006, Helmich and Dutton, 2001, Blohm et al., 2006). Interferon-γ (IFNγ) is a cytokine commonly produced by CTLs following antigen-specific activation (Schoenborn and Wilson, 2007). Previous studies have implicated its involvement in anti-tumour immunity (Bohm et al., 1998, Hollenbaugh and Dutton, 2006) by facilitating apoptosis of tumour cells (Dobrzanski et al., 2001), regulating angiogenesis (Qin et al., 2003) and in the recruitment and activation of macrophages (Schultz, 1987) and NK cells (Wendel et al., 2008). Furthermore, studies have demonstrated that $CD4^+$ T cells can reject tumours in the absence of $CD8^+$ T cells (Hung et al., 1998). It has been suggested that $CD4^+$ T cells eliminate tumour cells through the recruitment and activation of host leukocytes as effector cells, and this may be through the secretion of IFNγ (Hung et al., 1998). To determine if $CD4^+$ T cells and/or CTL-derived IFNγ play a role in the EG7 transfer tumour model appropriate transgenic and knock out mice were used, namely TCR transgenic mice that generate $CD4^+$ T cells that recognise OVA (OT-II), and OT-I TCR transgenic mice that lack the expression of IFNγ (OT-I IFNγ-/-).

As in earlier experiments, *Rag1-/-* mice were injected subcutaneously with $1x10^6$ EG7-OVA tumour cells on day 0 and then PBS or $5x10^6$ effector T cells injected i.v. on day 10 with the tumour growth curves for each group being shown in Figure 5.5. In the untreated control (PBS) the tumours continued to grow and the mice were sacrificed at day 18 (Figure 5.5, black circles). $CD4^+$ T cells (OT-II) that are specific for $OVA_{323-339}$ were activated by culture with $OVA_{323-339}$-pulsed C57BL/6 splenocytes, LPS, IL-2 and $OVA_{323-339}$ peptide for 4 days. These activated OT-II $CD4^+$ T cells, when injected alone were incapable of clearing the tumour with tumour growth following the same pattern as untreated mice (Figure 5.5, blue circles). This suggests that although OT-I CTL appear to be controlling tumour growth via the recruitment of host effector cells, OT-II $CD4^+$ T cells are not similarly capable of achieving this, and thus it seems that the presence of CTLs is important. This result is not surprising as most tumour cells, including EG7-OVA, do not express MHC-II and therefore cannot be directly recognised by $CD4^+$ T cells (Moore et al., 1988). Furthermore, injection of wild type OT-I CTLs or IFNγ deficient CTLs readily led to tumour regression (Figure 5.5, green circles and red circles) suggesting that there is no involvement of donor CTL-derived IFNγ in the control of tumour growth in the EG7 tumour model. Also, leukocyte infiltrates were similar in tumours from mice treated with either OT-I or IFNγ deficient OT-I CTL (data not shown). Thus it can be concluded that $CD8^+$ CTL can use cytokines other than IFNγ to recruit host cells to the tumour site.

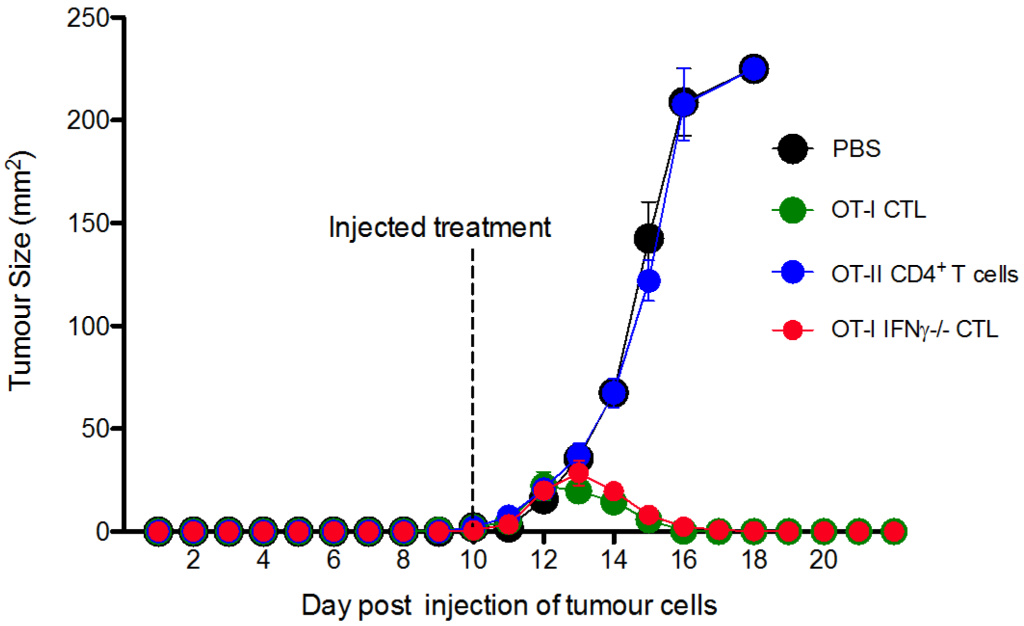

Figure 5.5 CD4$^+$ T cells and CTL-derived IFNγ are not important for EG7-OVA rejection by adoptively transferred OT-I CTLs. EG7-OVA subcutaneous tumours were established in the right flank of *Rag1-/-* mice as described in Figure 5.1. OT-I CTL were activated as described in Figure 5.2. OT-II CD4$^+$ T cells were activated by culture with OVA$_{323-339}$ peptide-pulsed C57BL/6 splenocytes, LPS, IL-2 and the OVA$_{323-339}$ peptide for 4 days. Ten-day tumour-bearing *Rag1-/-* mice were injected i.v. with 5x10^6 wild type OT-I CTLs (green), 5x10^6 activated OT-II CD4 T cells (blue), 5x10^6 OT-I IFNγ-/- CTLs (red) or PBS (black). Tumour growth was monitored and measured every 2 days as described in Figure 5.1. Data expressed as mean ± SEM (n=5).

5.3.5 The efficiency of OVA-specific OT-I CTLs in achieving regression of EG7-OVA tumours in Rag1-/- mice in the absence of NK cells

Natural killer (NK) cells are known to be potent anti-tumour effector cells (Villegas et al., 2002, Ishigami et al., 2000, Coca et al., 1997, Habu et al., 1981). Activation of NK cells is regulated by the expression of MHC-I (James et al., 2013), which is present on virtually all healthy cells and is the ligand for NK cell inhibitory receptors (Purdy and Campbell, 2009). The ligation of NK cell inhibitory receptors and MHC-I results in the suppression of NK cell activation. Many tumours and infected cells downregulate MHC-I as a mechanism to avoid recognition by CTLs, however, this downregulation also leaves them vulnerable to NK cell-mediated attack (James et al., 2013). Upon recognition of a tumour cell, NK cells become activated and subsequently release cytolytic perforin and granzymes, resulting in destruction of the tumour target. In addition to direct cytolytic killing mechanisms, NK cells are also a potent supply of cytokines and chemokines, which are released upon activation to promote differentiation, activation and recruitment of other immune cells (Stojanovic and Cerwenka, 2011, Stojanovic et al., 2013).

In addition to the well-known anti-tumorigenic capabilities of NK cells, it is also known that mice that lack Rag1 accumulate NK cells differently to their wild type counterparts. A study by Andrews and Smyth (2010) demonstrated that spleen and bone marrow NK cell subsets are absent in the neonatal *Rag1-/-* mouse. In addition, there is an over representation of a precursor NK cell subset, normally found in the liver but present in the bone marrow of Rag1 deficient mice. This suggests that in the absence of Rag1, liver NK cell precursors may seed into the other organs to compensate for the absence of bone-marrow derived NK cells, thus generating an independent pool of NK cells with specific characteristics that may differ from those in wild type mice (Andrews and Smyth, 2010). Altogether, these findings indicate that analysis of the role of NK cells in the EG7 adoptive immunotherapy model is worth investigating.

Asialo-GM1 is a glycolipid present on both NK cells and a subset of monocyte/macrophages in the mouse spleen. The anti-asialo-GM1 polyclonal antibody (pAb) recognises this glycolipid specifically and has been previously shown to effectively deplete NK cells. Single administrations of 500 μg of an anti-asialo-GM1 pAb results in a significant reduction in NK cells in mouse spleen for up to ten days from the day following administration (Saijo et al., 1984). Studies by Dr Lucy Coupland, in my supervisor's laboratory, demonstrated that NK cells are depleted from mouse spleen as early as 1 hour post i.v. administration of 50 μl of a rabbit polyclonal anti-asialo GM1 antiserum (#986-10001, Wako Pure Chemical Industries, Osaka, Japan) mixed with 100 μl of 0.9% saline (personal communication, Dr Lucy Coupland). Thus, to examine the role of NK cells in the OT-I CTL dependent elimination of EG7-OVA tumours from RAG1-/- mice, a well characterised anti-asialo-GM1 pAb was employed. Ten-day EG7-OVA tumour bearing *Rag1-/-* mice were injected i.v. with an anti-asialo-GM1 pAb 24 hours prior to injection of 1x10^6 wild type or perforin deficient (*Prf1-/-*) OT-I CTLs.

In accordance with the results shown previously (Figure 5.1, 5.2, 5.3 and 5.5), in the absence of OT-I CTLs, the tumours continued to grow until a point where the mice were sacrificed (day 18)(Figure 5.6a, black circle). In the presence of OT-I CTLs, both wild type and perforin deficient, the tumours rapidly regressed (Figure 5.6a, green circles and blue circles). In mice that received the anti-asialo-GM1 pAb in addition to OT-I or OT-I *Prf1-/-* CTLs, the tumours similarly regressed, albeit at a significantly slower rate (Figure 5.6a, red circles and orange circles). In accordance with other studies (Hollenbaugh et al., 2004), it was noted that tumour growth continued for 2-4 days following adoptive CTL treatment, presumably while CTL and other effector cells migrated to the tumour site. This is then followed by a rapid reduction in tumour size, to a point where the tumour becomes undetectable by visual inspection. However, in anti-asialo-GM1 pAb treated mice, tumour growth continued like controls for 4-5 days before showing signs of tumour regression (Figure 5.6a, red circles and orange circles). Regression of tumours in these mice however, occurred at a similarly rapid rate to NK cell replete mice to a point of tumours being undetectable (Figure 5.6a, red circles and orange circles).

To ascertain if this lag effect in tumour regression correlated with the efficiency NK cell depletion the splenocytes of anti-asialo-GM1 pAb treated mice and untreated mice were examined 4 days after treatment. Flow cytometric analysis of splenocytes (Figure 5.6b) revealed a substantially decreased number of NK cells in anti-asialo-GM1 pAb treated *Rag1-/-* mice receiving OT-I CTL compared with OT-I CTL treated mice that did not receive the anti-asialo-GM1 pAb. In addition, the number of NK cells present in tumours from anti-asialo-GM1 pAb/OT-I CTL treated mice was approximately the same as the number of NK cells in tumours from mice that had received no treatment (PBS) (Figure 5.6c). This was approximately 10-fold less NK cells than OT-I CTL treated mice that had not received the NK cell-depleting antibody (Figure 5.6c).

Altogether, these results suggest that NK cells may play a significant role in controlling tumour growth in this adoptive immunotherapy model. However, in the absence of NK cells eradication of tumours is still evident, albeit slower, suggesting that CTLs employ additional mechanisms for mediating tumour regression.

Figure 5.6 Host NK cells may assist in EG7-OVA rejection by adoptively transferred OT-I CTLs. EG7-OVA subcutaneous tumours were established in the right flank of *Rag1-/-* mice as described in Figure 5.1. OT-I and OT-I *Prf1-/-* CTLs were activated as described in Figure 5.2 and 5.3. Ten-day tumour-bearing *Rag1-/-* mice were injected i.v. with 50 μl of the NK cell depleting anti-asialo-GM1 (anti-asialo) pAb or saline. One day (24 hr) later the same mice were injected i.v. with $5x10^6$ wild type OT-I CTLs, $5x10^6$ OT-I *Prf1-/-* CTLs or PBS. (a) Tumour growth was monitored and measured every 2 days as described in Figure 5.1. Data expressed as mean ± SEM (n=4-7). * $p< 0.05$. The p values refer to days 14, 15 and 16, and are comparisons of EG7-OVA tumour bearing mice treated with OT-I CTL with or without the anti-asialo pAb, or mice treated with OT-I *Prf1-/-* CTL with or without the anti-asialo pAb. Comparisons between the mice that received the anti-asialo pAb treatment and the mice that did not receive the anti-asialo pAb treatment were statistically significant with a maximum $p = 0.0389$. Data are representative of one of two experiments. Four days (day 14) post treatment spleens (b) and tumours (c) were removed from mice (n=3) untreated or treated with wild type OT-I CTLs with or without the anti-asialo pAb. Cells were extracted, stained with a mAb specific for NK1.1 and analysed using flow cytometry. (b) Gate represents viable NK cells present in splenocyte preparations as detected using Hoechst forward scatter (ssc-a) and antibodies specific for NK1.1. Percentage of splenocytes in NK1.1 gate is indicated. (c) A comparison of number of NK cells present in subcutaneous EG7-OVA tumours from different treatment groups. Data are representative of cells pooled from 3 mice.

a.

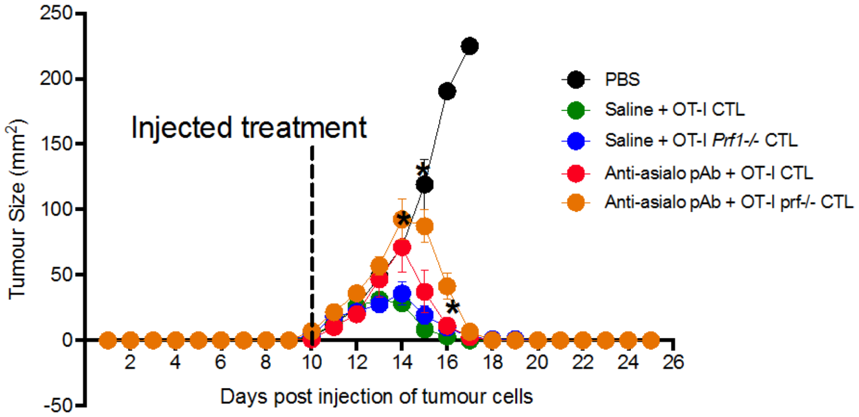

b. Splenocytes

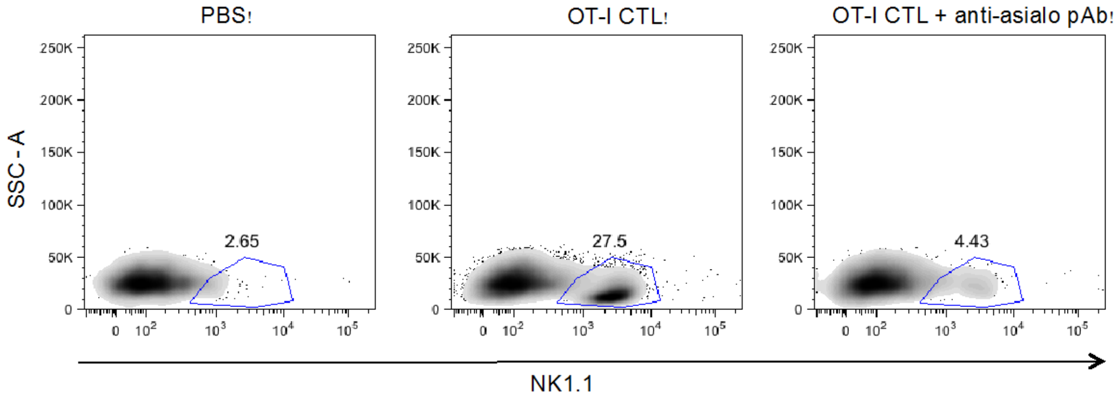

C. Tumour

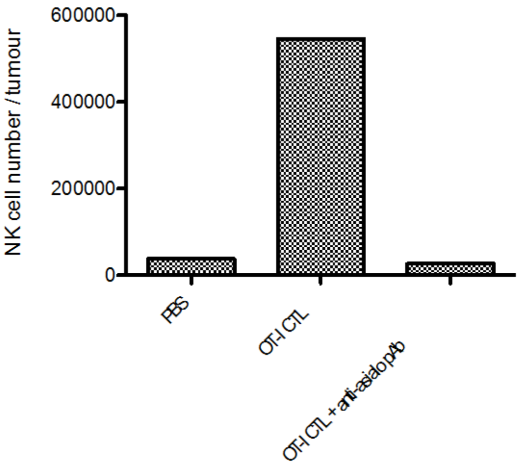

5.3.6 The efficiency of OVA-specific OT-I CTLs in achieving regression of EG7-OVA tumours in Rag1-/- mice in the absence of neutrophils

The exact role of neutrophils in tumour progression is controversial and their pro-tumour and anti-tumour effects have been recently reviewed (Fridlender and Albelda, 2012). Neutrophils have been shown to elicit pro-tumorigenic responses including enhancement of angiogenesis and neovascularisation thereby triggering tumour progression (Tazzyman et al., 2009), secretion of high levels of basement membrane degrading enzymes thereby promoting tumour invasion and assisting tumour cell metastases (Welch et al., 1989, Sun and Yang, 2004), and inhibiting $CD8^+$ T cell effector functions (Hao et al., 2013). Despite this, there are also several studies that report anti-tumorigenic properties of neutrophils. They can directly kill tumour cells by releasing cytotoxic mediators such as free oxygen radicals (Zivkovic et al., 2007, Zivkovic et al., 2005, Colombo et al., 1996), by mediating Fas-ligand associated apoptosis (Chen et al., 2002) and through antibody-dependent cellular cytotoxicity (Kindzelskii and Petty, 1999, Clynes et al., 2000). Studies have also demonstrated neutrophils in immunostimulatory roles, in which they recruit and activate $CD8^+$ T cells by secreting certain T cell attracting chemokines and cytokines (Scapini et al., 2000). Furthermore, neutrophils can cross-present antigen *in vivo,* and antigen-pulsed neutrophils promoted the activation of $CD8^+$ T cells (Beauvillain et al., 2007). In addition, there have been many reports documenting that depletion of neutrophils not only inhibited their anti-tumour effects, but also resulted in enhanced tumour growth (Suttmann et al., 2006, Kousis et al., 2007).

To assess the involvement of neutrophils in the elimination of tumour cells in our adoptive immunotherapy model, *Rag1-/-* mice were depleted of neutrophils using monoclonal antibodies. The depletion was performed using a Ly6G-specific antibody (1A8), which selectively depletes neutrophils (Daley et al., 2008, Jaeger et al., 2012). The 1A8 antibody is highly efficient at depleting neutrophils within minutes of administration and it is believed that opsonisation by complement plays a key role in its ability to deplete neutrophils (Lee et al 2013). Antibody was injected 3 hours prior to adoptive CTL therapy (i.e. PBS or $5x10^6$ wild type or perforin deficient OT-I CTLs) and the progression of tumour growth was recorded (Figure 5.7a). As demonstrated previously, PBS had no effect on tumour growth, and the tumours continued to increase in size until the mice were sacrificed (Figure 5.7a, black circles and blue circles). In addition, OT-I CTLs again cleared the tumours to an undetectable level (Figure 5.7a, green circles). Injection of the 1A8 antibody had no effect on the ability of OT-I or OT-I *Prf1-/-* CTLs to induce tumour regression (Figure 5.7a, red circles and orange circles). The monoclonal antibody 7/4 (synonymous with Ly6B) labels immature and mature neutrophils and monocytes, but not macrophages, eosinophils or lymphocytes (Rehg et al., 2012, Hirsch and Gordon, 1983b, Hirsch and Gordon, 1983a) and thus was used to detect the presence of neutrophils following their depletion using the 1A8 antibody. Flow cytometric analysis of CD11b and 7/4 antibody labelling of splenocytes, and tumour tissue from treated mice confirmed the depletion of neutrophils from the spleen and tumours (Figure 5.7b, c and d). Collectively these data indicate that in the EG7 adoptive immunotherapy tumour model neutrophils do not appear to play a significant role.

Figure 5.7 The role of neutrophils in EG7-OVA rejection by adoptively transferred OT-I CTLs. EG7-OVA subcutaneous tumours were established in the right flank of *Rag1-/-* mice as described in Figure 5.1. OT-I and OT-I *Prf1-/-* CTLs were activated as described in Figure 5.2 and 5.3. Ten-day tumour-bearing *Rag1-/-* mice were injected i.p. with the neutrophil depleting anti-Ly6G monoclonal antibody 1A8 (1A8 mAb) or an isotype control (Cont. mAb). Three hours later the same mice were injected i.v. with 5x106 wild type OT-I CTLs, 5x106 OT-I *Prf1-/-* CTLs or PBS. (a) Tumour growth was monitored and measured every 2 days and expressed as mean tumour volume ± SEM (n=4-7). Data are representative of three independent experiments. Four days post treatment spleens and tumours were removed from mice (n=3). (b) Splenocytes were extracted, stained with mAbs and analysed using flow cytometry. Gates represent neutrophils present in different splenocyte populations (%) as detected using monoclonal antibodies specific for CD11b and Ly6B (7/4). (c and d) Bar graphs show total neutrophil numbers from spleens (c) and subcutaneous EG7-OVA tumours (d) from pooled cell populations (n=4) of 1A8 mAb treated and untreated mice.

a.

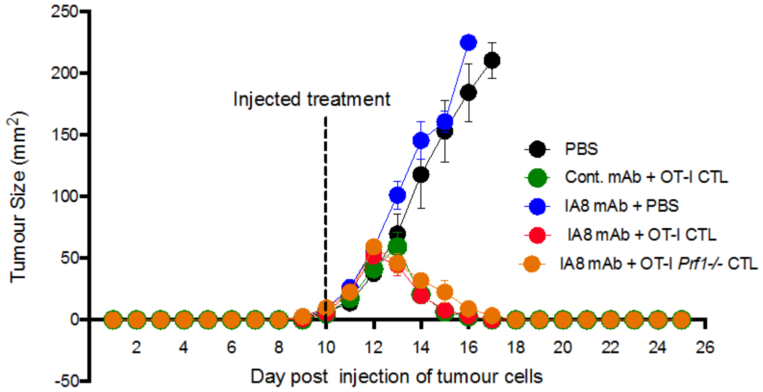

b. Splenocytes

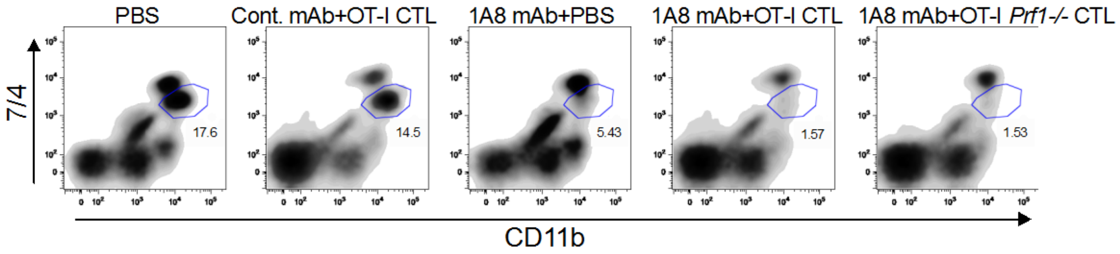

c. Spleen

d. Tumour

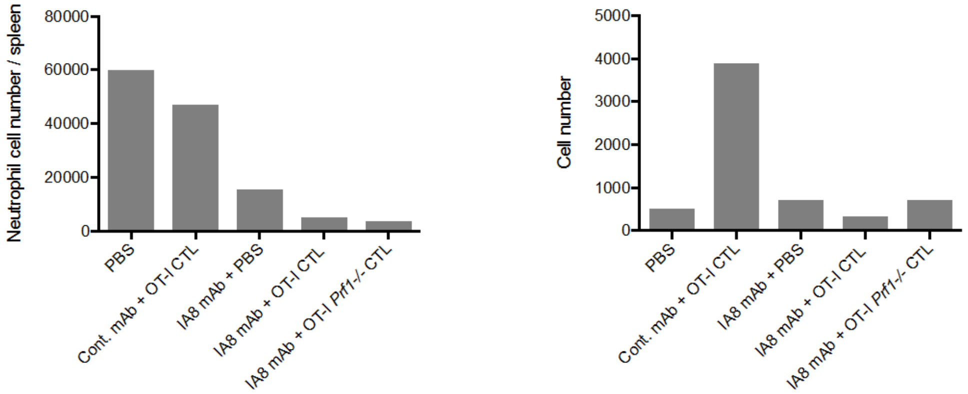

5.3.7 The efficiency of OVA-specific OT-I CTLs in achieving regression of EG7-OVA tumours in Rag1-/- mice in the absence of macrophages

Similar to neutrophils, macrophages have several pro- and anti-tumorigenic properties. They are often the most prominent infiltrating cell type in a solid tumour and are commonly referred to as tumour associated macrophages (TAM). Macrophages begin as immature monocytes, released from the bone marrow to circulate throughout the blood stream before settling in different tissues, such as spleen, liver or tumours, where they differentiate into mature macrophages (Gordon and Taylor, 2005). The microenvironment in which the monocyte finally resides dictates the functional programme that the mature macrophage will express. The two extremes of this range of functional states are the M1 and M2 phenotypes (Allavena et al., 2008). In tumours, when monocytes are exposed to IL-4 and IL-13 they develop into activated M2 macrophages (Allavena et al., 2008). These macrophages have poor antigen presenting capacity, and are involved in tumour progression by fostering tissue remodelling and invasion, angiogenesis, metastases and suppression of anti-tumour inflammatory responses (Siveen and Kuttan, 2009). Many observations indicate that the M2 phenotype is that which dominates in tumours and there is a considerable body of data linking the density of macrophages in a solid tumour to a poor prognosis (Rodriguez et al., 2013). In contrast, the classically activated M1 macrophages are induced by IFNγ either alone or in concert with microbial stimuli such as LPS, or cytokines such as TNFα and GM-CSF (Allavena et al., 2008). M1 macrophages are efficient immune effector cells with a high capacity to present antigens and produce IL-12 and IL-23. They produce high levels of cytotoxic effector molecules (e.g. nitric oxide and reactive oxygen intermediates) and pro-inflammatory cytokines (Allavena et al., 2008). Based on this, M1 macrophages are generally regarded as potent effectors and inducers in polarised Th1 responses, such as in the defence against tumour cells.

To investigate the function of TAM in EG7-OVA tumour regression, macrophage depletion was performed with dichloromethylene-bisphosphonate (clodronate) encapsulated liposomes (ClodLip). Clodronate encapsulated liposomes are ingested by macrophages via endocytosis. After fusion of the liposomes with lysosomes the lipid bilayer of the liposomes is disrupted thereby releasing clodronate within the cell. Cellular death occurs after enough clodronate accumulates in cells, although the exact mechanism of how clodronate accomplishes this is unknown (Rooijen and Sanders, 1994). *Rag1-/-* mice were injected i.v. with PBS (PBSLip) or Clodronate encapsulated liposomes (ClodLip) 24 hours prior to injection with either PBS, 5x10^6 OT-I or 5x10^6 OT-I *Prf1-/-* CTLs and tumour growth monitored (Figure 5.8a). Tumour growth in ClodLip treated mice was no different to that in control treated mice, with tumour regression occurring at approximately the same rate (Figure 5.8a). In Figure 5.8a it is evident that there is a slight lag in tumour regression in ClodLip and wild type OT-I CTL treated mice, however, this is not significant and the variation in tumour growth observed is evident in the error bars. Depletion of a subset of macrophages, splenic red pulp macrophages, was successful as seen by the lack of F4/80^+CD11b^- cells in the splenocyte population from ClodLip treated mice (Figure 5.8b)(Mitchell et al., 2010). Interestingly, also evident is a population of F4/80^+/CD11b^+ cells, indicative of monocytes and eosinophils, that increases substantially as the population of F4/80+/CD11b- diminishes (Figure 5.8b). This may indicate a population of monocytes that exhibit less avid

Figure 5.8 The role of macrophages in EG7-OVA rejection by adoptively transferred OT-I CTLs. EG7-OVA subcutaneous tumours were established in the right flank of *Rag1-/-* mice as described in Figure 5.1. OT-I and OT-I *Prf1-/-* CTLs were activated as described in Figure 5.2 and 5.3. Ten-day tumour-bearing *Rag1-/-* mice were injected i.v. with clodronate or PBS filled liposomes (Clod Lip and PBS Lip, respectively). One day later the same mice were injected i.v. with $5x10^6$ wild type OT-I CTLs, $5x10^6$ OT-I *Prf1-/-* CTLs or PBS. (a) Tumour growth was monitored and measured every 2 days and expressed as mean ± SEM tumour volume (n=4-7). Data are representative of two independent experiments. Four days post treatment spleens and tumours were removed from mice (n=3). ns = no significant difference between EG7-OVA tumour bearing mice treated with Clod Lip and OT-I CTL compared with other treatment groups (excluding PBS treated control) (b) Splenocytes were extracted, stained with mAbs and analysed using flow cytometry. Gates represent $CD11b^-/F4/80^+$ macrophages present in different splenocyte populations (%) as detected using antibodies specific for CD11b and F4/80. (c and d) Bar graphs show $CD11b^-/F4/80^+$ macrophage numbers from spleens (c) and subcutaneous EG7-OVA tumours (d) from Clod Lip treated and PBS Lip treated / untreated mice.

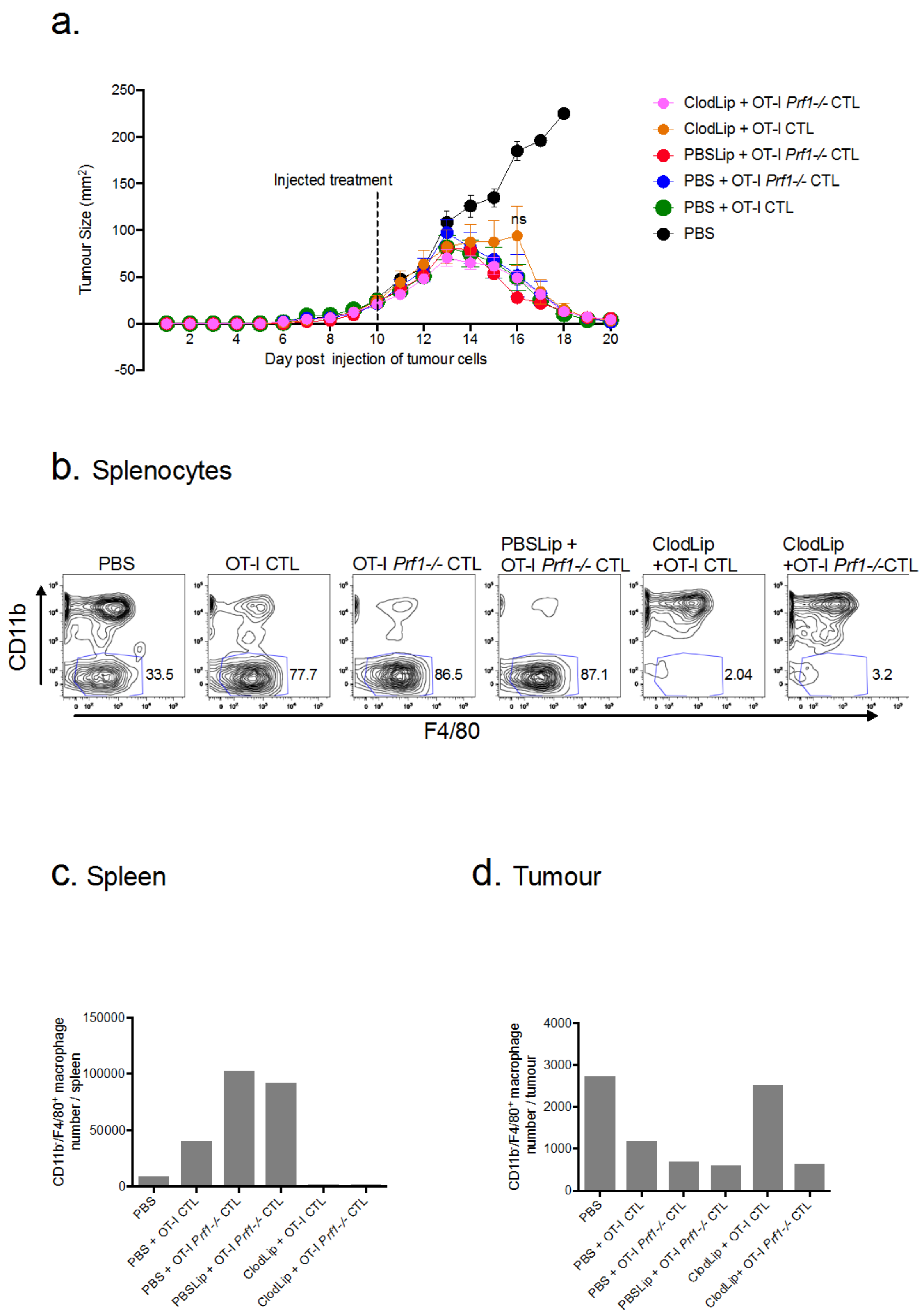
a.
Tumour Size (mm^2)
250
200
150
100
50
0
-50
Injected treatment
ns
2
4
6
8
10
12
14
16
18
20
Day post injection of tumour cells
ClodLip + OT-I *Prf1-/-* CTL
ClodLip + OT-I CTL
PBSLip + OT-I *Prf1-/-* CTL
PBS + OT-I *Prf1-/-* CTL
PBS + OT-I CTL
PBS
b. Splenocytes
PBS
OT-I CTL
OT-I *Prf1-/-* CTL
PBSLip + OT-I *Prf1-/-* CTL
ClodLip +OT-I CTL
ClodLip +OT-I *Prf1-/-*CTL
CD11b
F4/80
33.5
77.7
86.5
87.1
2.04
3.2
c. Spleen
CD11b$^-$/F4/80$^+$ macrophage number / spleen
150000
100000
50000
0
PBS
PBS + OT-I CTL
PBS + OT-I *Prf1-/-* CTL
PBSLip + OT-I *Prf1-/-* CTL
ClodLip + OT-I CTL
ClodLip + OT-I *Prf1-/-* CTL
d. Tumour
CD11b$^-$/F4/80$^+$ macrophage number / tumour
4000
3000
2000
1000
0
PBS
PBS + OT-I CTL
PBS + OT-I *Prf1-/-* CTL
PBSLip + OT-I *Prf1-/-* CTL
ClodLip + OT-I CTL
ClodLip+ OT-I *Prf1-/-* CTL

phagocytic behaviors, and suggest a mechanism by which other leukocytes compensate for the lack of macrophages present. Cell counts of F4/80$^+$CD11b$^-$ cells further confirmed their depletion in the spleen (Figure 5.8c), but this depletion was not evident in tumour tissues with ClodLip and wild type OT-I CTL treated mice having nearly the highest number of F4/80$^+$CD11b$^-$ cells present in the tumours (Figure 5.8c). Furthermore, the number of F4/80$^+$CD11b$^-$ cells in the ClodLip and OT-I *Prf1-/-* CTL treated mice was similar to that seen in mice treated with PBSLip and OT-I *Prf1-/-* CTL (Figure 5.8c). This indicated that the clodronate encapsulated liposomes, although depleting macrophages in the spleen, failed to do so in the tumours. This could suggest that the route of administration may not be the best method for depletion of macrophages in solid tumours. In addition, studies have demonstrated that i.p. injection of clodronate liposomes is also less effective at depleting macrophages from tumours in comparison to the depletion observed in peripheral blood and the peritoneal cavity (Grugan et al., 2012). It may be that clodronate liposomes do not infiltrate the tumour microenvironment, thus not eliminating phagocytic cells that already reside in the tumour. Thus, it cannot be excluded that macrophages may be involved in the CD8-dependent regression of EG7-OVA tumours. To address this at another level, an *in vitro* CTL killing assay was designed.

5.3.8 Cytolytic activity of OVA-specific wild type and perforin deficient OT-I CTLs in vitro

There was concern that the strategies used to deplete infiltrating cells in solid tumours, particularly in the case for macrophages, were not efficient enough.

In an effort to distinguish the cell types responsible for the elimination of established EG7-OVA tumours in *Rag1-/-* mice we designed an *in vitro*

CFSE/DiI-based cytotoxicity assay. It was anticipated that upon establishment of an *in vitro* cytotoxicity assay we can add specific cell types, such as NK cells, macrophages and neutrophils, extracted from *Rag1-/-* mice and compare the killing to CTLs alone.

Figure 5.9 demonstrates the design of the CFSE/DiI -based cytotoxicity assay using three targets, SIINFEKL-pulsed EL4, unpulsed EL4, and EG7-OVA. Labelling of the target cell populations with CFSE and the fluorescent, membrane intercalating dye DiI not only allows discrimination between different target cell populations but also allows the discrimination between CFSE/DiI-labelled target cells and the effector cells. EG7-OVA and unpulsed EL4 target cells were labelled with differing concentrations of CFSE (5000 nM and 250 nM, respectively). All three targets (SIINFEKL-pulsed EL4, unpulsed EL4, and EG7-OVA) were then combined in equal numbers and labelled with DiI to discriminate the target cells from the effector T cells. Dot plots are shown of the discriminated target populations (Figure 5.9). CFSE^{++}, DiI^{++} denotes EG7-OVA target cells, CFSE^{+}, DiI^{++} denotes unpulsed EL4 targets, and CFSE^{-}, DiI^{+} denotes SIINFEKL-pulsed EL4 (Figure 5.9). It should be noted that the cells labelled with CFSE (namely EG7-OVA and unpulsed EL4) appear to exhibit a higher DiI fluorescence due to the overlapping FITC and PE channels used for CFSE and DiI, respectively. Effector T cells were distinguished as CFSE^{-}, DiI^{-}, CD8^{+} (if using CTLs) population (data not shown). Calculation of the ratio between the number of viable target cells and a fixed number of fluorescent beads allowed quantification of cytotoxicity.

To determine the effectiveness of OT-I and OT-I *Prf1-/-* CTLs *in vitro*, EG7-OVA (target) cells and EL4 (control) cells were stained with differing concentrations of CFSE (5000 nM and 250 nM, respectively). *In vitro* activated OT-I wild type and OT-I *Prf1-/-* CTLs were generated as for the *in vivo* experiments (Section 6.3.2), and with the OT-I *Prf1-/-* CTLs their deficiency in perforin confirmed using PCR (data not shown). Equal numbers of target cells and control cells were incubated together with graded numbers of CTLs and the ratio of the numbers of the two CFSE-labelled cells determined by flow cytometry after 24 hours incubation. The percentage lysis of target cells was then calculated using the formula 1 minus the ratio of target to control in the presence of effectors over the ratio of target to control in the absence of effectors, i.e.

$$\text{specific killing} = \left(1 - \frac{(\text{targets primed/targets primed control})}{(\text{targets unprimed/ targets unprimed control})}\right) \text{x}100.$$

Surprisingly, OT-I CTLs that are deficient in perforin are equally as effective in lysing EG7-OVA targets as their wild type counterparts, at all effector to target ratios examined (Figure 5.10). A ratio of 1 OT-I *Prf1-/-* CTL effector to 1 EG7-OVA target achieved close to 100% tumour cell lysis. This result is in contrast to those results obtained by Dobrzanski *et al* (2004) where at a ratio of 100 OT-I *Prf1-/-* CTL effectors to 1 EG7-OVA target, tumour cell lysis was still less than 10%. Another study demonstrated that a ratio of 100 OT-I *Prf1-/-* CTLs to 1 SIINFEKL–pulsed EL4 target cell was required to achieve ~25% tumour cell lysis, and this was 100 times less effective that the tumour cell lysis observed with wild-type OT-I CTL effectors (Hollenbaugh et al., 2004). The discrepancy with these results suggest variation between EG7-OVA cell lines, between EG7-OVA and EL4 cell lines, or between OT-I *Prf1-/-* CTLs. Polymerase chain reaction (PCR) assessment of OT-I *Prf1-/-* CTLs, ensured that the cells were in fact perforin deficient (data not shown), thus there is speculation that variation exists between cell lines.

Experiments conducted in the current study were based on previous studies (Huang and Xiang, 2004, Hollenbaugh et al., 2004, Morales-Kastresana et al., 2013) that reported inefficient killing of tumour cells by CTLs in the absence of perforin *in vitro.* However, the current *in vitro* assay demonstrated that perforin deficient OT-I CTLs are equally able to lyse target tumour cells as their wild type counterparts, demonstrating a possibility of variation between EG7-OVA cell lines, and between EG7-OVA and EL4 cell lines. In the absence of EG7-OVA cell lines from different laboratories, experiments were designed to investigate if variation exists between EG7-OVA and EL4 cell lines. In a similar *in vitro* CTL killing assay as described above, SIINFEKL pulsed-EL4 target cells and control EL4 cells without peptide were labelled with two different concentrations of CFSE, and equal numbers of each were incubated together with graded numbers of wild type and perforin deficient OT-I CTLs. Similar to Hollenbaugh *et al* (2004), 100 times more perforin deficient OT-I CTLs were required to achieve the same amount of lysis of tumour cells as seen with wild type OT-I CTLs (Figure 5.11). Although this could be explained by lower expression of OVA peptide on the cell surface of EL4 cells in comparison to EG7-OVA cells, it is also possible that there is significant variation in the two cell types, perhaps as a result of genetic drift.

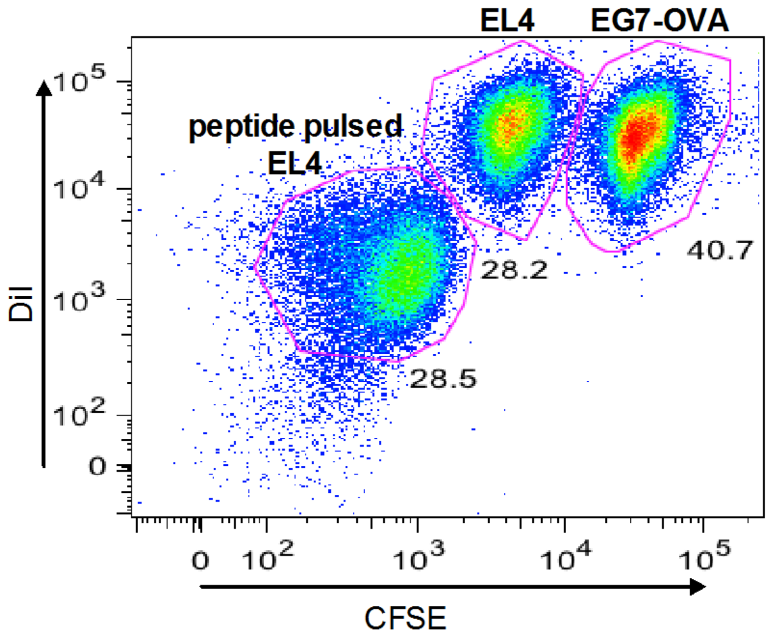

Figure 5.9 The design of the CFSE-based cytotoxicity assay with three targets, EL4, peptide-pulsed EL4, and EG7-OVA tumour cell lines. EG7-OVA, and unpulsed EL4 target cells were labelled with 5000 nM and 250 nM CFSE, respectively, and the SIINFEKL-pulsed EL4 not labelled with CFSE. All three targets (SIINFEKL-pulsed EL4, unpulsed EL4, and EG7-OVA) were then combined in equal numbers, labelled with the lipophilic membrane intercalating fluorescent dye DiI and analysed using flow cytometry. Dot plots of different target cell populations are shown with the percentage of each target population in the mixture indicated.

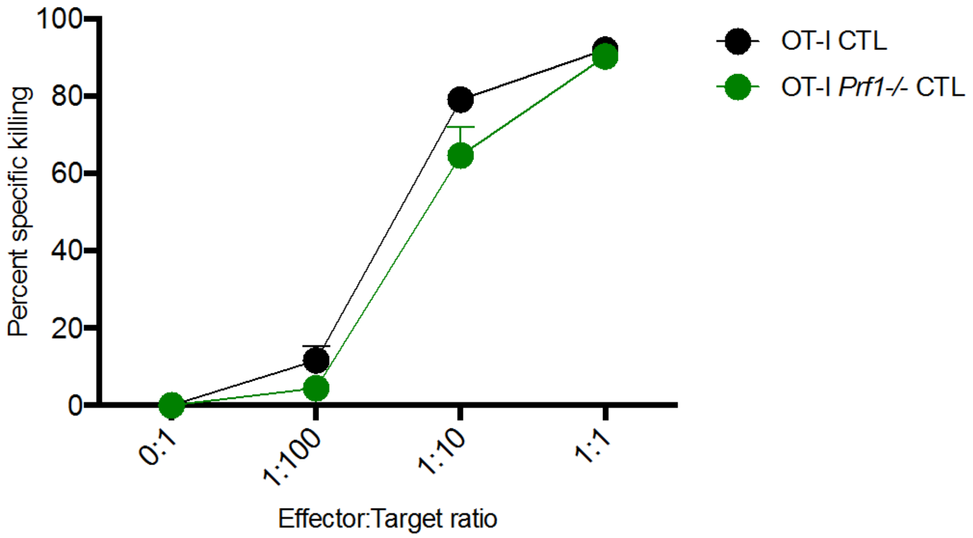

Figure 5.10 EG7-OVA cell lysis by OT-I and OT-I prf-/- CTLs *in vitro*. EG7-OVA targets were labelled with 5000 nM CFSE. OT-I and OT-I *Prf1-/-* CTLs, generated as described in Figure 5.2 and 5.3, were incubated in various effector: target ratios and cultured for 24 hours. The numbers of surviving target and control cells were determined by flow cytometry and the percentage of target cell lysis was calculated as described in the Materials and Methods. Data presented as mean % killing ± SEM (n=3).

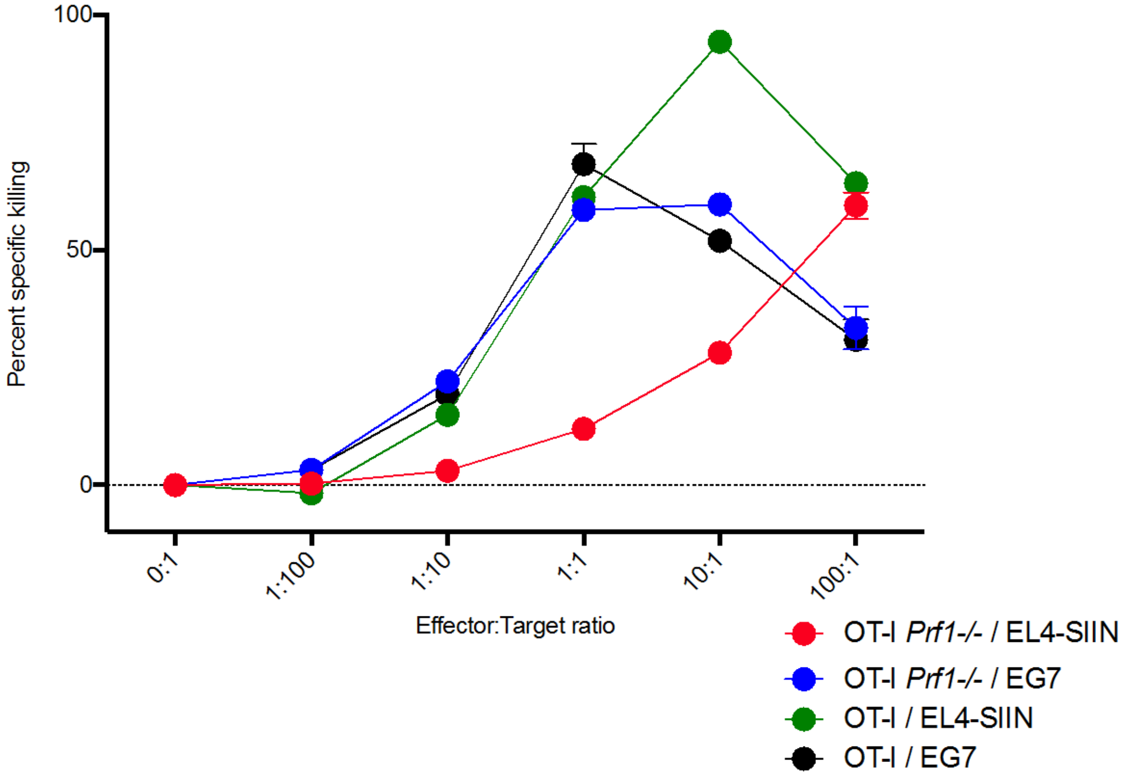

Figure 5.11 SIINFEKL-pulsed EL4 cell lysis by OT-I and OT-I prf-/- CTLs. SIINFEKL peptide-pulsed EL4 targets (EL4-SIIN) and EL4 control (without peptide) cells labelled with 5000 nM and 250 nM CFSE, respectively, were mixed with EG7-OVA target cells in equal numbers and labelled with DiI (5 μM). Target and control cells were incubated together with 4 day activated OT-I and OT-I *Prf1-/-* CTLs, generated as described in Figure 5.2 and 5.3, at various effector:target ratios and cultured for 24 hours. The numbers of surviving target and control cells were determined by flow cytometry and the percentage of target cell lysis was calculated as described in the Materials and Methods. Data presented as mean % killing ± SEM (n=3).

5.3.9 Role of Fas/FasL pathway in the cytolytic activities of OVA-specific wild type and perforin deficient OT-I CTLs in vitro

Based on the data presented in Figure 5.10 it is clearly evident that both perforin deficient OT-I CTLs and wild type OT-I CTLs are equally effective at lysing EG7-OVA tumour cells. As mentioned previously, there are several studies that have demonstrated that perforin deficiency results in less effective killing *in vitro* (Hollenbaugh et al., 2004, Dobrzanski et al., 2004, Morales-Kastresana et al., 2013) and *in vivo* (Huang and Xiang, 2004) of EG7-OVA tumours. A study by Huang and Xiang (2004) showed that inhibition of the perforin pathway resulted in ~90% inhibition of CTL activity. In the same study, a distinct cytolytic pathway used by CTLs to kill target cells, namely the Fas/FasL pathway, was also inhibited. Inhibition of the Fas/FasL pathway resulted in ~10% inhibition of CTL activity. EG7-OVA cells do express FasL and are, therefore, potentially sensitive to OT-I CTL Fas mediated killing. Furthermore, the *in vitro* study described in Figure 5.10 demonstrates that OT-I *Prf1-/-* CTLs are capable of directly killing tumour cells and that it is unlikely that other cells are involved, suggesting that there is a more intrinsic process involved. Thus, it was speculated that OT-I CTLs in this model may be using the Fas/FasL pathway for cytolytic killing of EG7-OVA target cells.

To test the possibility of Fas/FasL killing in our model, we employed a neutralising anti-FasL monoclonal antibody (mAb). Equal numbers of CFSE labelled EG7-OVA target cells and CFSE labelled EL4 control cells were mixed and pre-incubated with or without the neutralising anti-FasL mAb. Graded numbers of OT-I CTLs were added, and the ratio of the target and control cells determined as described above. Figure 5.12 shows that, in agreement with previous results described in this thesis, OT-I CTLs efficiently kill EG7-OVA tumour cells. However, in the presence of neutralising anti-FasL mAb, specific lysis of EG7-OVA cells was substantially compromised, with a maximum lysis capacity of 25% (Figure 5.12). This suggests that OT-I CTLs, and potentially OT-I *Prf1-/-* CTLs, are killing target cells predominantly via the Fas/FasL pathway *in vitro,* and possibly by the same mechanism *in vivo*.

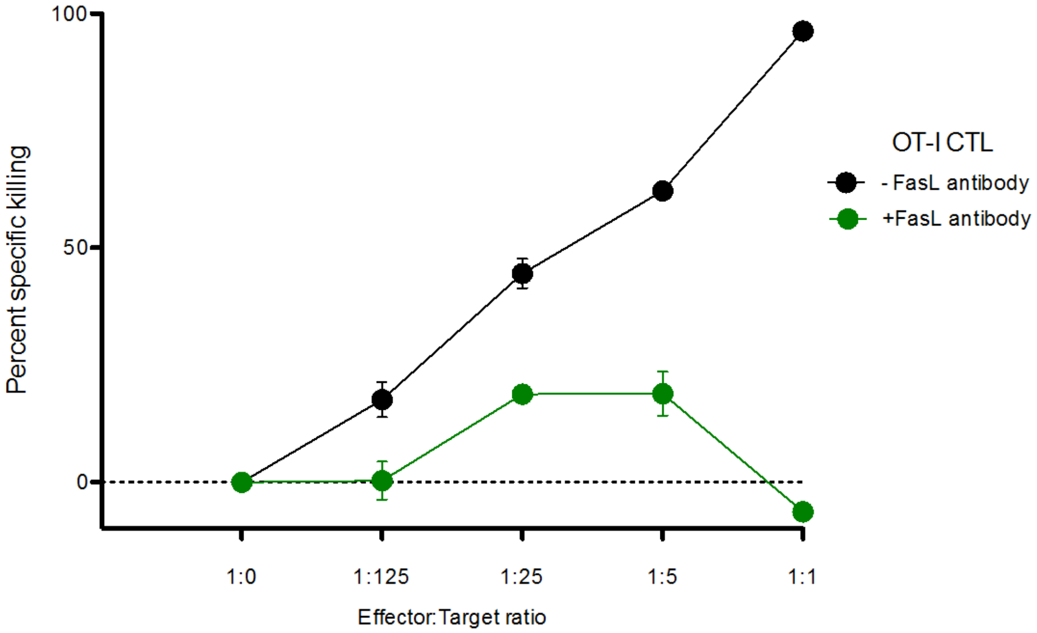

Figure 5.12 EG7-OVA cell lysis by OT-I CTL in the presence of a FasL blocking antibody. EG7-OVA targets and EL4 control cells were labelled with 5000 nM and 250 nM CFSE, respectively, and pre-incubated with or without a blocking anti-FasL mAb (10 µg/ml). Equal numbers of target and control cells were incubated together with 4 day OT-I CTLs, generated as described in Figure 5.2, at various effector:target ratios and cultured for 24 hours. The numbers of surviving target and control cells were determined by flow cytometry and the percentage of target cell lysis was calculated as described in the Materials and Methods. Data presented as mean % killing ± SEM (n=3).

5.4 Discussion

It has been previously demonstrated that CTLs are capable of transferring their T cell receptors (TCR) to neighbouring CTLs of an unrelated specificity, and as such, result in the rapid expansion of virus specific T cells. Chaudhri *et al* (2009) showed that TCR transfer can rapidly expand the number of antigen-specific CTL and rescue mice from a lethal viral infection. The transfer of TCRs was via membrane exchange, and the recipient T cells then became capable of recognising the virus-infected targets and eliminating them. The study presented here examined whether TCR sharing between CTLs could be harnessed for adoptive immunotherapy of tumours.

Based on studies by Huang and Xiang (2004) an *in vivo* adoptive immunotherapy model was established in which OVA expressing EL4 tumour cells (EG7-OVA) and OVA-specific CTLs derived from OT-I mice were used. In this model CTLs which recognise the tumour antigen OVA (OT-I) were injected into tumour-bearing *Rag1-/-* mice and monitored *in vivo* for tumour growth. Similar to results obtained by Huang and Xiang (2004), the OT-I CTLs in the current study efficiently eliminated the EG7-OVA tumours.

Several studies have demonstrated that the predominant pathway used by OT-I CTLs killing OVA-expressing target cells is perforin-mediated cytotoxicity (Dobrzanski et al., 2004, Hollenbaugh et al., 2004). Dobrzanski *et al* (2004) demonstrated that CTLs derived from perforin deficient OT-I mice showed markedly lower levels of EG7-OVA tumour cell lysis at all effector to target ratios assessed. Huang and Xiang (2004) demonstrated that treatment using CMA (used to inhibit perforin mediated cytotoxicity) and emetin (used to inhibit Fas/FasL mediated cytotoxicity) inhibited 95% and 10% of total CTL cytotoxicity, respectively, indicating OT-I CTLs predominantly use the perforin-mediated pathway for cytotoxic killing of EG7-OVA tumour cells. Furthermore, a long-term (48 hour) *in vitro* assay using SIINFEKL (peptide epitope of OVA) peptide-pulsed EL4 targets demonstrated that tumour killing was 99% dependent on perforin-mediated lysis (Hollenbaugh et al., 2004). Using these studies as a foundation to test the hypothesis that receptor sharing between CTLs can assist in the adoptive immunotherapy of tumours, activated perforin deficient OT-I CTLs (OT-I *Prf1-/-*) and lymphocytic choriomeningitis virus (LMCV)-specific CTLs (B6.SJL.TCRP14) were injected either alone or together into EG7-OVA tumour bearing Rag1 -/- mice. As expected the B6.SJL.TCRP14 CTLs alone were unable to recognise EG7-OVA expressing tumour cells and thus did not lead to tumour regression. However, in contrast to previous reports, it was found that perforin deficient CTLs displayed significant anti-tumour activity, resulting in EG7-OVA tumour regression similar to that observed with wild type OT-I CTLs both *in vivo and in vitro*. Interestingly, when the killing capacity of OT-I *Prf1-/-*CTLs for EL4 cells that had been peptide-pulsed with SIINFEKL, a peptide epitope of OVA, was investigated it was found that 100 times more effector T cells were required to achieve the same amount of killing as wild type OT-I CTLs, in concordance with the results obtained by Hollenbaugh *et al* (2004). Although this could be due to lower expression of OVA peptide on the surface of the SIINFEKL-pulsed EL4 cells, it appears likely that there exists intrinsic differences between the EL4 cells and the OVA expressing EL4 cells, EG7-OVA. These differences are likely due to genotypic and phenotypic drift during long-term culture, a relatively common phenomenon with cell lines (Osborne et al., 1987, Hiorns et al., 2004).

A closer evaluation of the literature reveals that variation exists not only between the EL4 and EG7-OVA cell lines, but also between different EG7-OVA tumour cells lines. Several independent EG7-OVA cell lines are identifiable. In the studies by Daylot-Herman *et al* (2000), naïve OT-I CTLs did not inhibit EG7-OVA tumour growth and were not stimulated to proliferate in the lymphoid organs of EG7-OVA tumour bearing mice. However, if the OT-I CTLs were pre-activated tumour growth was efficiently controlled (Dalyot-Herman et al., 2000). In contrast, Shrikant and Mescher (1999) used an EG7-OVA cell line that was able to stimulate Ag-specific immune responses by naïve OT-I CTLs. They demonstrated that OT-I CTLs migrate to the site of tumour growth and undergo clonal expansion (Shrikant and Mescher, 1999). In these studies, the donor T cells controlled tumour growth, but this effect was only transient and the OT-I T cells subsequently failed to reject the EG7-OVA tumour unless the hosts were treated with IL-2 or anti-CTLA-4 therapy (Shrikant and Mescher, 1999, Shrikant et al., 1999). Tumours produced by the EG7-OVA cell line in studies by Hollenbaugh and Dutton (2006) stimulated naïve OT-I T cells to divide, but failed to be controlled by 10^7 naïve OT-I T cells injected into tumour bearing mice. However, *in vitro* activated OT-I CTLs were capable of controlling EG7-OVA tumour growth using a mechanism independent of contact-mediated lysis, as OT-I CTLs deficient in perforin or Fas, or doubly deficient, were therapeutically comparable to wild-type OT-I CTLs at reducing tumour burden (Hollenbaugh and Dutton, 2006). The control of tumours arising from the EG7-OVA cell line used by Hollenbaugh and Dutton (2006) was diminished when OT-I CTLs were deficient in IFNγ, indicating recruitment of host effectors. Collectively, these findings demonstrate that *in vitro* activated OT-I T cells can eliminate EG7-OVA tumours, however the mechanism employed by these cells is dependent on many factors including the EG7-OVA cell line used in the laboratory. This raises concerns that comparisons of published data using cultures of cell lines with the same name may not be reliable or appropriate.

The EG7-OVA cell line used in the experiments in this thesis expresses Fas (CD95) *in vitro* (data not shown), however, other studies have reported that FasL-deficient OT-I CTLs were as effective as wild type OT-I CTLs at clearing EG7-OVA tumours (Hollenbaugh and Dutton, 2006, Huang and Xiang, 2004). Nevertheless, we investigated whether, in our hands, in the absence of perforin CTL effectors may eliminate EG7-OVA tumours via Fas/FasL mediated lysis. Indeed, our data demonstrate that, *in vitro*, the killing of EG7-OVA cells by OT-I CTL is compromised in the presence of a neutralising anti-FasL antibody, indicating that *in vitro* OT-I CTLs may be utilising the Fas/FasL pathway to mediate tumour cell lysis. However, based on other considerations discussed below it is unlikely that Fas/FasL on OT-I CTLs plays a role *in vivo* in EG7-OVA tumour clearance.

Based on an approximate calculation of the effector OT-I CTL to target cell ratio *in vivo* Hollenbaugh *et al* (2004) suggested that it would be unlikely that direct-contact mediated lysis would be capable of achieving EG7-OVA tumour regression as seen in the experiments described in this thesis. They make the assumption that during the 7-day period between injection of 1x10^6 EG7-OVA tumour cells and injection of effector CTLs, the tumour cell numbers will have doubled approximately 5 times. Thus, by the time CTLs arrive at the site of the tumour, there will be in the order of 10^8 tumour cells present. Rapid and complete reduction in tumour volume can be seen after i.v. injection of 5x10^6 CTLs, however, it is unlikely that more than 2% of the injected T cells actually enter the tumour, roughly equalling 1 effector T cell to every 1000 tumour cell targets. Hollenbaugh *et al* (2004) suggest that it is unlikely that such a low ratio of CTL to target cells could bring about such a rapid regression of solid tumours >10 mm in diameter without triggering the recruitment and activation of a host immune response. In support of this concept, the data presented in this thesis demonstrate minimal, if any, killing of EG7-OVA cells at a ratio of 1 effector T cell to 100 tumour target cells *in vitro*, suggesting involvement of host effector mechanisms *in vivo*.

So how do perforin deficient OT-I CTLs bring about tumour regression in an antigen-specific manner? Many studies have suggested that direct contact mediated lysis is not involved in tumour reduction, and instead CTLs rely on the recruitment of host effector cells (Hollenbaugh and Dutton, 2006, Komohara et al., 2009, Suttmann et al., 2006). Hollenbaugh and Dutton (2006) demonstrated that compromising IFNγ production by OT-I CTLs decreases their ability to eliminate solid tumours, and infer that CTL effectors migrate to the tumour site and induce the secretion of a number of chemokines and cytokines that in turn recruit host cells that can attack the tumour. In this same study, they suggested that the host cells responsible are NO producing macrophages and neutrophils. In the study by Komohara et al (2009) the growth of EL4 tumours was significantly delayed in scavenger receptor-A (SR-A) deficient mice, a receptor expressed by macrophages, and that increased levels of NO and IFNγ may have induced this suppression of tumour growth, inferring a role for macrophages. In a related earlier study, Maekawa *et al* (1988) demonstrated an anti-tumour effect of IFNγ against EL4 cells *in vivo,* and suggested that this was due to IFNγ-activated effector cells such as NK cells and macrophages (Maekawa et al., 1988). It was proposed that T cells might kill tumour cells indirectly via an IFNγ induced recruitment of host effector cells, such as macrophages. However, results reported in this thesis showed that OT-I CTLs deficient in IFNγ are equally capable of controlling EG7-OVA tumour growth as their wild type counterparts. This contrasts with previous findings, discussed above, in which IFNγ production by CTLs enhanced tumour elimination (Maekawa et al., 1988, Komohara et al., 2009, Hollenbaugh and Dutton, 2006), although our results do not exclude the possibility of host cell recruitment via other mechanisms. CTLs can secrete various chemokines and cytokines that could efficiently recruit host leukocytes to tumours. Indeed, it was evident from our studies that increased numbers of NK cells, macrophages and neutrophils appeared in the tumours of mice that had received OT-I CTL in comparison with tumour-bearing mice that received PBS alone. Thus, to determine whether or not anti-tumour host cells are involved in assisting donor CTLs in controlling and eradicating tumours, *Rag1-/-* mice were depleted of NK cells, neutrophils or macrophages. Although tumour regression was significantly delayed in NK cell depleted hosts compared with controls, in neither case was there any reduction in the end effect, being complete tumour regression. Based on these data it appears that NK cells do play a role in assisting the CTLs to achieve tumour regression, but in the absence of NK cells it is likely that the CTLs recruit alternate host effector cells. In contrast, depletion of neutrophils and macrophages had no effect on OT-I CTL mediated tumour regression. However, there was a lack of confidence that the strategy used to deplete *Rag1-/-* mice of macrophages worked as efficiently as was originally expected, as the flow cytometric analysis of the tumour infiltrate in macrophage depleted mice revealed large numbers of F4/80^{+}CD11b^{-} macrophages still in the tumours. It is likely that when one host cell type is disabled, the CTLs recruit other host effector mechanisms to compensate. Mouse models in which these effector cells are knocked out either individually or in combination would enable a more complete investigation into their roles in tumour regression, although such studies were beyond the time limits of this PhD thesis.

One possibility is that the OT-I CTLs may impart antigen specificity to neighbouring host effector cells through antigen receptor sharing, thereby harnessing the effectors with the ability to recognise antigen-expressing tumour cells and eliminate them. Macrophages have been shown to function as effector cells in an IL-12 induced, T cell-dependent eradication of established MCA207 tumours through a contact-dependent mechanism (Tsung et al., 2002). Furthermore, macrophages are capable of capturing membrane components from lymphocytes, the membrane transfer not being a result of phagocytosis (Daubeuf et al., 2010b). Macrophages have also been shown to acquire B cell-derived membrane and/or intracellular components, including Ag, thereby assisting the B cell in increasing the frequency of antigen presenting cells (Harvey et al., 2008). In addition, other haematopoietic cells also capture membrane fragments. Interactions between neutrophils and antigen-opsonised Raji cells leads to the capture of membrane fragments by the neutrophils and neutrophil-mediated antibody-dependent tumour cell lysis (Horner et al., 2007). Many studies have also documented the bi-directional transfer of membrane fragments during cytolytic and non-cytolytic cell-cell interactions (Vanherberghen et al., 2004, Roda-Navarro et al., 2006, Carlin et al., 2001). Thus, it is suggested that in the current study host effector cells are acquiring antigen specificity from OT-I CTLs and assisting in controlling tumour growth.

In conclusion, findings from this study indicate that drawing comparisons and conclusions between studies using the same named cell lines should be approached with caution. In addition, it appears that there exists many mechanisms by which EG7-OVA tumour growth can be controlled by OT-I

CTLs. For our EG7-OVA cell line a mechanism of tumour eradication is suggested, involving host effector cells gaining antigen specificity, possibly through the membrane transfer of TCR from donor OT-I CTLs in combination with the Fas/FasL pathway, although further studies are required to validate these intriguing possibilities.

Chapter 6

Final Discussion

6.1 Introduction

Membrane transfer involves the transfer of plasma membrane and membrane associated proteins between neighbouring cells. This phenomenon has been widely described between cells of the immune system (Harshyne et al., 2001, Hudrisier et al., 2007, Cho et al., 2014, Aucher et al., 2008) and is experimentally easily identifiable. Although the transfer of membranes and associated proteins between cells is common, the molecular basis of this exchange remains elusive. Numerous mechanisms have been proposed including membrane bridges (Stinchcombe et al., 2001), nanotubes (Onfelt et al., 2004), membrane vesicles (Arnold and Mannie, 1999) and torn pieces of membrane (Hudrisier and Bongrand, 2002).

From the literature it appears that a ‘one size fits all’ mechanism of transfer is unlikely. Factors including the membrane topology, activation state, the surrounding environment and the type of both the recipient and donor cells involved are all likely to contribute to both the efficiency of transfer and exactly how it occurs. The results reported in this thesis provide insights into the molecular mechanisms involved in membrane transfer between B cells (and probably T cells) and touch on how this relatively newly recognised phenomenon could have applications in the clinic.

Specifically, the results in this thesis demonstrate many similarities between the direct translocation of cell penetrating peptides into B cells and the membrane transfer between B cells (Chapter 3). Exactly how CPPs directly translocate into cells is largely unknown, similar to the lack of knowledge regarding membrane transfer mechanisms, thus together these results may provide insights into the mechanism of both processes. From the results presented in Chapter 3 it could be suggested that a highly positively charged protein on the surface of the B cell could be the mediator of membrane transfer. Using notable differences in activation conditions to achieve membrane transfer between B cells (i.e., LPS versus CpG), several cell surface associated proteins containing CPP motifs were identified (Chapter 4) and proposed to play a role in mediating membrane transfer. Furthermore, when some of these proteins were incubated with specific mAbs the efficiency of membrane transfer between activated B cells significantly increased (Chapter 4, Section 4.3.7), suggesting that crosslinking of particular proteins on the B cell surface is favourable for membrane transfer. Chapter 5 of this thesis extended these findings to a potential clinical application of membrane transfer involving transfer between CTLs in an adoptive cancer immunotherapy model. Although the results obtained indicated that many immunological mechanisms can mediate tumour eradication and outlined the requirement for more stringent techniques in cell line authentication, it gave rise to intriguing hypotheses involving membrane transfer between CTL and other immune cells at the tumour site and their involvement in tumour cell elimination.

In this concluding Chapter the major implications of the research findings described in this thesis are discussed. In particular, the potential molecular basis of membrane transfer between B cells is proposed. Furthermore, the many physiological consequences of membrane transfer are discussed, it being suggested that membrane exchange between leukocytes is a common process affecting many aspects of an immune response as well as providing a potential mechanism that can be used therapeutically, notably in cancer immunotherapy. Finally, future research directions are briefly outlined.

6.2 Mechanisms of membrane transfer between B cells

Apart from B cells, membrane transfer has been demonstrated in a variety of other immune cell types including CTLs (Chaudhri et al., 2009), NK cells (Nakamura et al., 2013), dendritic cells (Harshyne et al., 2001) and macrophages (Pham et al., 2011), as well as with tumour cells (Rafii et al., 2008), with the process often being termed ‘trogocytosis’. Moreover, transfer of membranes is not only described *in vitro*, but also *in vivo* (Riond et al., 2007, Quah et al., 2008). Although it appears that the mechanism of membrane transfer is dependent on the particular cell type involved, a common feature of all is that initiation of membrane transfer requires direct cell contact and, thus, is likely to involve the engagement of cell surface receptors.

A unique feature of membrane transfer between B cells is that it occurs at 4ºC, indicating that the process involves an energy independent pathway. Additionally, it is evident that B cell membrane transfer is not a random event.as B cells require appropriate activation conditions in order to transfer membrane components, with minimal transfer being demonstrated between resting B cells or between B cells stimulated with CpG. Furthermore, the addition of BCR specific antigen enhanced membrane transfer between LPS activated B cells and bystander B cells by up to 50%.

Based on these considerations, the following sections will consider key molecular features of membrane transfer identified in this thesis.

6.2.1 Cell Penetrating Peptides (CPPs) as potential mediators of membrane transfer

CPPs are of interest due to their unique ability to rapidly translocate across plasma membranes made possible by their typically high cationic amino acid composition. In addition, CPPs are capable of achieving translocation at temperatures as low as 4ºC, a similarly important and unique feature of membrane transfer between B cells. Three key findings in this thesis suggest that the receptors involved in the initiation of membrane transfer events between B cells contain CPP motifs, and it is these motifs that facilitate the interaction between neighbouring cells.

Finding 1: Membrane transfer between B cells and the interaction of CPP with B cells is enhanced following B cell activation with LPS. The results presented in this thesis confirmed the earlier finding that activation enhanced membrane transfer between B cells, with LPS activated B cells exhibiting a 4-fold increase in the transfer of DiI labelled membranes when compared to naïve B cells. In the same manner, all three CPPs tested (TAT, penetratin and TP10) interacted with LPS activated B cells to a far greater extent than was evident with naïve B cells (Section 3.3.3.3).

Finding 2: Membrane transfer between B cells and the interaction of CPP with B cells follows the same kinetics in activated B cells.. Thus, the results presented in this thesis demonstrate that the period of incubation with LPS required for the enhancement of membrane exchange between B cells is very similar to that needed to enhance the interaction of B cells with CPPs, the key incubation period being approximately 8-24 hours (Section 3.3.3.5).

Finding 3: Membrane transfer between B cells and the interaction of CPPs with B cells occurs at both 4ºC and 37ºC. It was confirmed that B cells are efficient at transferring membranes to neighbouring B cells at both 4ºC and 37ºC (Section 3.3.2.2) indicating a mechanism that does not require high metabolic activity. Interestingly, results presented in this thesis have shown that CPPs are also capable of interacting with B cell membranes at 4ºC, demonstrating that they interact with and cross plasma membranes using an energy independent mechanism (Section 3.3.3.4).

Collectively these data suggest that both cellular activation and temperature are important and unique features of both membrane transfer between B cells and direct translocation of CPPs into B cells. There are limited studies examining the direct translocation of CPPs into primary lymphocytes, and it appears that there are none assessing the effect of lymphocyte activation on CPP uptake. Thus, for the first time, results in this thesis have demonstrated that B cells at both 4ºC and 37ºC efficiently take up CPPs and that cellular activation significantly enhances CPP translocation. It is reasonably well established that activated NK cells and T cells are more efficient than their resting counterparts at acquiring membranes and cell surface proteins (Tabiasco et al., 2002, Tatari-Calderone et al., 2002), however, the extent of activation and the reason for this difference remains unknown. In contrast, the effect of leukocyte activation on the kinetics of CPP uptake has not previously been studied and, in addition to the impact these findings may have on membrane transfer between B cells, they could also have important implications for CPP-based drug delivery systems, particularly those targeting the immune system.

Membrane transfer between B cells occurs rapidly, within minutes of activated B cells being incubated together (Tatari-Calderone et al., 2002, Tabiasco et al., 2002). It also occurs at 4ºC (Section 3.3.2.2) indicating that protein synthesis and signalling is not required and that the activated B cells already possess the essential machinery required for transfer. From results presented in this thesis, it could be hypothesised that following certain B cell activation conditions cell surface proteins containing a CPP motif are either upregulated or are induced to expose a CPP motif via a conformational change, the positively charged

CPPs providing a strong electrostatic interaction with negatively charged molecules on the surface of bystander B cells. Upon binding of a protein containing a CPP motif to its ligand on a neighbouring B cell there is a conformational change creating a disturbance in the lipid membrane and favourable conditions for membrane fusion and transfer. CPPs are capable of interacting with multiple cell surface molecules, including membrane lipids and membrane-associated proteoglycans (Nakase et al., 2008). It is often these interactions that facilitate clustering events, which enable the internalisation of CPPs (Kopatz et al., 2004, Ziegler and Seelig, 2011). From the results presented in this thesis, we suggest that the proteins on the B cell surface involved in mediating membrane transfer between B cells contain CPP motifs.

6.2.2 Cell surface protein involvement in transfer

The exact relationship between B cell activation and membrane transfer remains unclear, however, it appears likely that activation leads to upregulation of proteins involved in mediating transfer. The B cell mitogen CpG is capable of efficiently activating B cells, however, CpG activated B cells fail to exhibit membrane transfer at a level beyond that of naïve B cells. In comparison, B cells activated with LPS (Section 3.3.2.1) or CD40L (Quah et al., 2008) achieve significantly higher transfer. Additionally, when LPS-activated B cells are stimulated with BCR specific antigen membrane transfer is further enhanced (Section 4.3.8).

Using the notable difference in membrane transfer between LPS and CpG activated B cells, several proteins (CTLA-4, ALCAM, TIGIT, AMIGO2 and Slp3) were identified that could potentially be involved in membrane transfer (Chapter 4). These proteins were upregulated in B cells following activation with LPS but not CpG. The identified proteins also contain CPP motifs, are known to be associated with the plasma membrane, and are functionally involved in cellular communication or adhesion processes. Thus, it was expected that impeding the function of these proteins would result in inhibition of membrane transfer. Interestingly, treatment of activated B cells with ALCAM-specific or TIGIT-specific mAbs resulted in enhanced membrane transfer. Furthermore, incubating B cells with an antibody specific for the TIGIT ligand, PVR, in addition to an anti-TIGIT antibody had an additive effect, further enhancing membrane transfer beyond that observed in the presence of either antibody alone. Previous studies have demonstrated a similar enhancement of membrane transfer to T lymphocytes with the addition of certain antibodies (Hudrisier et al., 2007) and with crosslinking of the BCR (Quah et al., 2008). Similarly, results in this thesis demonstrate that activation of B cells with BCR specific antigen dramatically enhanced membrane transfer between neighbouring LPS-activated B cells (Section 4.3.8). Collectively these data suggest that crosslinking of certain cell surface receptors, either via specific antibodies or endogenous ligands, on the B cell surface enhances membrane transfer.

The binding of antigen to the BCR results in receptor crosslinking and its rapid translocation into highly organised micro-domains (Cheng et al., 2001, Cheng et al., 1999). BCR proximal signalling is accompanied by the dynamic depolymerisation of the actin cytoskeleton (Hao and August, 2005) and ultimately results in conformational changes that facilitate the aggregation of the highly organised micro-domains into much larger clusters (Depoil et al., 2008). This central cluster (commonly referred to as the central supramolecular activation cluster (cSMAC) and the B cell Immunological synapse) preferentially includes particular molecules such as CD19 (Depoil et al., 2008) and excludes others such as CD45 and CD22 (Batista et al., 2001). CD19 is essential in the response to membrane-bound, but not soluble, antigen. In response to membrane-bound antigen, CD19 has been shown to enhance micro-domain formation and accordingly the recruitment of further signalling molecules such as Syk, thereby enhancing B cell activation (Depoil et al., 2008). In addition, BCRs when co-ligated to the CD19/CD21 complex have a longer retention time in lipid rafts than BCRs that are only cross-linked to themselves (Cherukuri et al., 2001). Interestingly, a study investigating membrane transfer between Daudi cells, a human B lymphoblastoid cell line, demonstrated enhanced membrane transfer following BCR crosslinking using anti-IgM or anti-CD19 antibodies, however, no enhancement was seen with anti-CD20, anti-CD22 and anti-CD40 mAbs (Poupot and Fournie, 2003). Similarly, Quah *et al* (2008) demonstrated significant enhancement of membrane transfer between LPS-activated B cells following incubation with an anti-CD19 antibody, however, incubation with an anti-CD45R mAb showed no effect. These data suggest that crosslinking receptors that are recruited to, or induce the formation of BCR micro-domains, could facilitate membrane transfer.

Both TIGIT and ALCAM require a certain level of clustering at the cell surface to enable ligand binding (Stengel et al., 2012, van Kempen et al., 2001). The LPS-induced increase in expression of these molecules at the cell surface may allow the formation of densely packed available binding sites for neighbouring B cells, consistent with the requirement of appropriate activation conditions for membrane exchange to occur. In addition, T cell activation results in the recruitment of both ALCAM and TIGIT to the immunological synapse (Grakoui et al., 1999, Liu et al., 2013) and we propose that this similarly occurs under certain B cell activation conditions.

It should be noted that partitioning into micro-domains is intrinsic to the BCR, with crosslinking of the BCR inducing its translocation. This event is independent of BCR signalling and the actin cytoskeleton and, importantly, occurs at 4°C (Cheng et al., 2001). Furthermore, the co-localisation of the BCR with the CD19/21 complex that results in the prolonged residency of the BCR in micro-domains also occurs efficiently at both 4°C and 37°C (Cherukuri et al., 2001).

Previous studies have shown that transduction of CPPs coincides spatially and temporarily with clustering of the CPPs at the cell surface (Ziegler et al., 2005, Mayhew et al., 1973) (Kopatz et al., 2004). CPPs and glycosaminoglycans (GAGs) have multiple binding sites that are likely to interact electrostatically via their respective positive and negative charges, resulting in electrostatic crosslinking or clustering (Ziegler and Seelig, 2011). In fact, Ziegler and Seeling (2011) demonstrated that the transduction of CPPs through plasma membranes proceeds via GAG clustering events, with inhibition of clustering preventing CPP uptake. PEGylated CPPs were incapable of inducing clustering during GAG binding and this had a significant effect on their mechanism of uptake. In contrast, CPPs that were able to encourage GAG clustering rapidly translocated into cells and diffused through the cytoplasm (Ziegler and Seelig, 2011). These findings lend support to the idea that the crosslinking of specific proteins containing CPP motifs, such as ALCAM and TIGIT, could facilitate the aggregation of micro-domains and, in effect, be the enabling feature of membrane transfer.

6.2.3 Proposed mechanism of membrane transfer between B cells

The findings reported in this thesis suggest an active role for the formation of micro-domains, alternatively known as lipid rafts, in facilitating membrane transfer between B cells. As discussed above, the proposed model suggests that following appropriate activation conditions certain proteins containing CPP motifs, with a significant proportion of positively charged residues, are preferentially upregulated on the B cell surface. These proteins will be attracted to and crosslink with negatively charged ligands on neighbouring B cells subsequently leading to their rapid recruitment into micro-domains, thus facilitating greater membrane fusion between neighbouring cells. The cumulative effect of micro-domain formation and the interaction of CPPs with their ligands ultimately leads to a localised area of membrane destabilisation. This weakened membrane on the donor B cell surface results in a favourable environment for the transfer of cell surface proteins and membranes from donor to recipient B cells (see Figure 6.1).

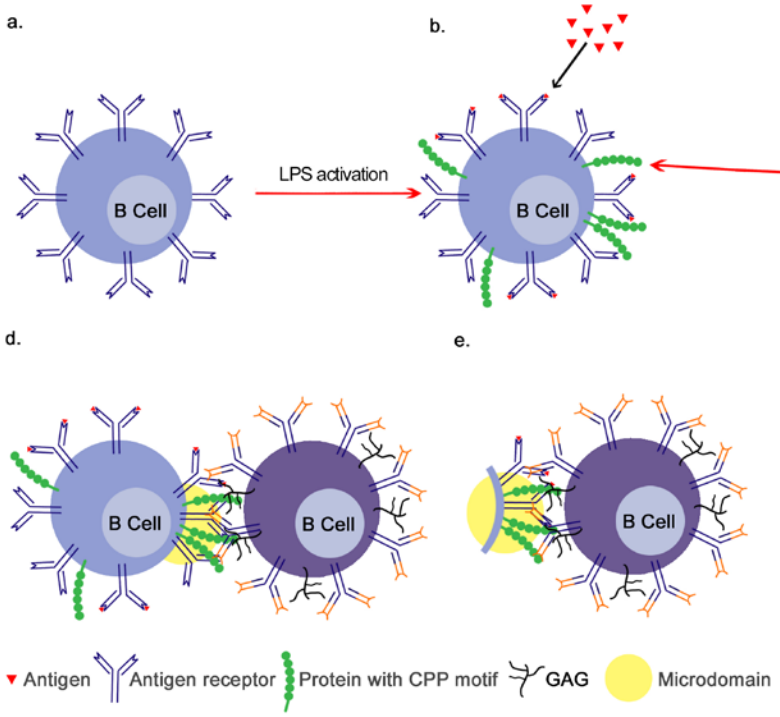
a.
b.
c.
LPS activation
B Cell
B Cell
B Cell
d.
e.
f.
B Cell
B Cell
B Cell
B Cell
▼ Antigen
Antigen receptor
Protein with CPP motif
GAG
Microdomain

Figure 6.1 Proposed mechanism of membrane transfer between B cells. Under certain activation conditions, such as following LPS activation (a), B cells preferentially upregulate particular cell surface proteins containing CPP motifs (b). These motifs subsequently interact with their ligands or negatively charged GAGs on the surface of neighbouring B cells, a process enhanced by the presence of BCR specific antigen (c). This binding induces the formation of a microdomain creating an area of membrane re-organisation and destabilisation that is anticipated to be favourable for membrane transfer (d). This destabilised membrane region is then physically uprooted (e) and incorporated in the cell surface of the recipient B cell (f).

6.3 Physiological relevance of membrane exchange

Although the findings presented in this thesis are based primarily on *in vitro* experiments, transfer of membrane and cell surface molecules has also been described *in vivo* (Riond et al., 2007, Ford McIntyre et al., 2008, Boross et al., 2012). The ability of the membrane patches acquired by recipient cells to integrate and behave as endogenous molecules has been demonstrated in many circumstances (Quah et al., 2008, Schneiders et al., 2014, Hwang et al., 2000), although the physiological roles that the acquired molecules may have in immune responses are still debated. From an immunological perspective, it appears that transfer may be involved in immune regulation.

An important feature of the immune response is its ability to rapidly respond to invading pathogens. Following activation via antigenic stimulation, B cells process and present antigen in association with MHC class II molecules to CD4+ T cells (Batista and Harwood, 2009). B cells are capable of responding to antigen through a variety of mechanisms depending on the nature and size of the antigen and the cellular context in which the exposure occurs (Batista and Harwood, 2009), thus providing effective protection to the host. Results reported in this thesis and by others (Quah et al., 2008, Batista et al., 2001) have demonstrated that activated B cells are capable of transferring antigen-specific BCRs to neighbouring B cells of an irrelevant specificity via direct membrane donation. Recipient B cells that acquire antigen-specific BCR demonstrate a dramatically enhanced ability to capture and present specific antigen to CD4+ T cells, evident by the upregulation of CD69 and proliferation of the T cells (Quah et al., 2008) and the production of IL-2 by the T cells (Batista et al., 2001). BCR transfer was also evident *in vivo* with up to approximately 60% of endogenous B cells acquiring antigen-specific BCR from adoptively transferred Tg B cells following activation with specific antigen and in the presence of CD4$^+$ T cell help, representing a considerable boost in the number of B cells able to present specific antigen to T cells (Quah et al., 2008).

Although the studies reported in this thesis suggest the importance of membrane transfer in the positive regulation of immune responses, other studies indicate that intercellular transfer of membranes and cell surface molecules may also downregulate immune responses. Numerous studies have implicated membrane transfer as a mechanism to prevent immune hyper-responsiveness (Nakamura et al., 2013, Cox et al., 2007) and to limit clonal expansion (Tsang et al., 2003). Huang *et al* (1999) showed that peptide-MHC class I complexes transferred to CTLs from DCs rendered the antigen presenting CTLs susceptible to antigen-specific lysis by neighbouring CTLs (fratricidal killing). However, incredibly high antigen concentrations are required to trigger fratricide, significantly higher amounts than that required for T cell activation (Huang et al., 1999, Hudrisier et al., 2001, Hudrisier et al., 2005). This may indicate a new mechanism of T cell exhaustion whereby during instances of high antigenic load, such as during viral infections, a high density of MHC-peptide complexes would be transferred to CTLs rendering them susceptible to fratricide. Similarly, presentation of acquired MHC molecules containing self-antigen during T-T cell interactions may also contribute to peripheral tolerance. For example, mouse CD4$^+$ T cells that have acquired peptide-MHC class II complexes from APCs present these to other CD4$^+$ T cells and, consequently, induce both apoptosis and hypo-responsiveness (Tsang et al., 2003).

Regulatory T cells (Tregs) are essential for maintaining peripheral tolerance. Tregs suppressive function is largely reliant on the expression of CTLA-4, which is upregulated following T cell activation (Pentcheva-Hoang et al., 2004). CTLA-

4 competes with co-stimulatory molecule CD28 for two ligands, CD80 and CD86, expressed on the surface of APCs. CD28 is constitutively expressed on T cells and upon binding to its ligand concomitantly with TCR and MHC/peptide complex binding, enhances T cell proliferation and cytokine production, in addition to preventing T-cell anergy induced by CTLA-4 binding (Acuto and Michel, 2003). CTLA-4 induced inhibition of T cell activation is less well understood, but upon binding to its receptors impedes IL-2 production and cell cycle progression (Egen and Allison, 2002). Recently, membrane transfer has been proposed as another mechanism by which Tregs can maintain tolerance (Qureshi et al., 2011, Gu et al., 2012). Following co-culture with DCs, induced Tregs (iTregs) acquire CD86, and to a lesser extent CD80, from DCs and express these molecules in small localised areas on their cell surface. This acquisition is independent of CTLA-4 and CD28 and occurs in parallel with a substantial downregulation of CD80/86 on DCs. Furthermore, CD86 recipient iTregs show a significantly enhanced suppressive capacity in comparison to iTregs that do not acquire CD86 (Gu et al., 2012). Similarly, Qureshi et al (2011) demonstrated that both effector T cells and Tregs can downregulate CD80 and CD86 expression on APCs by a process they termed CTLA-4-mediated trans-endocytosis. However, the process described was slightly different to traditional membrane transfer. Although cell contact and T cell activation were still requirements, following acquisition the ligands were degraded inside CTLA-4$^+$ cells, and not detected at the cell surface. Since the level of expression of cell surface CD80/86 on DCs dictates the ability of DCs to activate T cells, these data suggest that depletion of CD80/86 on DCs by membrane transfer is a mechanism that iTregs utilise to regulate immune responses.

6.4 Clinical implications: the adoptive immunotherapy of tumours

Transfer of plasma membranes and cell surface molecules between cells is common and has the potential to alter the course of an immune response; thus it is essential to consider its application in therapeutic situations.

Membrane transfer provides a unique opportunity to facilitate the enhancement of an immune response, with the obvious clinical application being adoptive cancer immunotherapy. Tumour-infiltrating CTLs play a significant role in antitumour responses and immunotherapies based on adoptive transfer of these cells are often the best treatment option available, particularly for patients with melanoma (Restifo et al., 2012, Rosenberg et al., 2011). The current study investigated the possibility of OVA-specific OT-I *Prf1-/-* CTLs donating their TCRs to bystander P14 CTLs to result in the eradication of EG7-OVA tumours *in vivo.* However, the OT-I *Prf1-/-* CTLs, despite the lack of perforin, displayed significant cytolytic activity against the EG7-OVA tumour. Confirmation of OT-I *Prf1-/-* CTL cytolytic killing activity was further confirmed *in vitro,* however the number of CTLs required for efficient tumour cell killing was calculated to be at least 1 effector CTL to every 10 tumour cells that was ~100-fold higher than the ratio between CTL and tumour cells that could be achieved in established tumours *in vivo* (see below). Based on calculations by Hollenbaugh *et al* (2004), using the same tumour model used in this thesis, 1x10^6 injected EG7-OVA tumour cells would result in tumours containing approximately 10^8 EG7-OVA tumour cells at the time of CTL administration. Furthermore, whilst the CTLs demonstrated efficient activity *in vitro*, it is unlikely that more than 2% of the injected OT-I CTLs would reach the tumours due to non-specific entrapment of the CTL in various organs (Ratner et al., 2005, Hollenbaugh et al., 2004). This suggests that the effector to target ratio at the site of the tumour will be roughly equivalent to 1 OT-I CTL to 1000 EG7-OVA cells. However, although *in vitro* studies indicate that EG7-OVA tumour control is unachievable at such low effector to target ratios, the *in vivo* results demonstrated very efficient elimination of established EG7-OVA tumours by the administered CTLs.

Many studies suggest a role for host cells in bringing about tumour cell elimination. Following injection, CTL effectors migrate to the tumour site and release a variety of chemokines and cytokines that attract and activate host leukocytes that subsequently attack the tumour cells. A range of leukocytes, cytokines and chemokines have been reported to be crucial in facilitating tumour rejection including IFNγ (Hollenbaugh and Dutton, 2006), macrophages and correspondingly NO (Komohara et al., 2009), NK cells (Wendel et al., 2008), neutrophils (Cairns et al., 2001) and CD4$^+$ T cells (Hung et al., 1998). Certainly, excepting CD4$^+$ T cells, other leukocytes were present in abundant numbers in excised solid EG7-OVA tumours in this study, however, elimination of each individual cell type had no effect on tumour elimination. It is plausible that in the event of one effector mechanism being disabled the body utilises another to compensate, suggesting that a combination of mechanisms exist and contribute to tumour eradication. Future studies using mouse models whereby different combinations of leukocytes are knocked out may provide a more complete view of the CTL-induced regression of EG7-OVA tumours.

Results reported in this thesis indicate, however, that CTL-induced tumour elimination is dependent on recognition of specific antigen by effector CTLs, as P14 CTLs or OT-II CD4$^+$ T cells alone were incapable of eliciting an anti-tumour response. As discussed previously, CTLs can acquire tumour antigens from tumour cells via membrane transfer (Uzana et al., 2015). In fact, a recently described assay to identify tumour-reactive T cells is dependent on their ability to acquire molecular components of tumour cells (Eisenberg et al., 2013). This might allow for the enrichment of tumour antigen-specific T cells for adoptive immunotherapy. Following interaction with tumour cells, the tumour antigen acquiring CTLs are endowed with antigen presenting capabilities and thus could potentially activate neighbouring tumour-specific CTLs. Studies have demonstrated that APC-CTLs become an antigen presenting entity that can trigger both intra- and inter-clonal CTL activation in an antigen specific manner (Uzana et al., 2015). Furthermore, Uzana *et al* (2015) demonstrated that CTLs that had acquired tumour membrane fragments were not only capable of activating neighbouring CTLs, but are also able to further transfer membrane fragments to these cells. Although the adoptive immunotherapy model used in the current thesis involves the use of *Rag1-/-* mice, which contain no mature T or B cells, in the absence of bystander T cells APC-CTLs could alternatively transfer these membrane patches to other immune cell subsets, thereby imparting the recipient cells, via acquired TCRs, with an antigen-specific mechanism to further enhance an anti-tumour immune response. Furthermore, it has been demonstrated that membranes that have previously been acquired are preferentially transferred again to other cells, suggesting that acquired membranes are not randomly distributed at the cell surface but rather localised in an organised manner (Alegre et al., 2010). Serial membrane transfers, where immune cells acquire membranes and then transfer them again, have been described previously (Alegre et al., 2010) and could be an important mechanism to spread tumour antigen specificity to recipient lymphoid and myeloid cells. Such a concept is highly provocative but deserves future study.

6.5 Future research

In order to better understand membrane transfer between B cells and T cells it is crucial that future work unequivocally identifies key molecules involved in this process. Without such information it will be very difficult to quantify the importance of membrane transfer and BCR/TCR acquisition by bystander cells in adaptive immune responses.

In this thesis, a comparative expression analysis of the transcriptomes of LPS stimulated B cells, CpG stimulated B cells and unstimulated B cells identified several candidate genes that contain CPP motifs and may play a role in membrane transfer, including TIGIT, ALCAM, Slp3, AMIGO2 and CTLA-4. It was hypothesised that where blocking antibodies were available and added to co-culture there would be an observable decrease in the amount of membrane transfer between B cells. Currently there are only known and available blocking antibodies to CTLA-4, and addition of the anti-CTLA-4 blocking antibody had no effect on membrane transfer. Antibodies to ALCAM and TIGIT are described, but are not necessarily blocking antibodies. Further studies are required to determine the role that these proteins may have in mediating membrane transfer between B cells. In the absence of specific blocking antibodies, RNAi could be used as a means to silence these genes and thus prevent the expression of these proteins on the surface of B cells. Alternatively, mice with these particular genes knocked out could be utilised and membrane transfer assessed in the absence of these proteins.

In contrast to an anti-CTLA-4 blocking mAb having no effect on membrane transfer between B cells, the presence of mAbs specific for ALCAM and TIGIT, and for the TIGIT ligand, PVR, resulted in membrane transfer between B cells being significantly enhanced. Furthermore, when these mAbs were combined an additive effect on the level of membrane transfer was observed. The triggering of membrane transfer by the engagement of a specific set of cell surface receptors has been described before (Hudrisier et al., 2007, Poupot and Fournie, 2003, Quah et al., 2008). Furthermore, Hudrisier *et al* (2007) showed that mAbs specific for the BCR, MHC class II and to MHC class I triggered enhanced membrane transfer, with mAbs specific for a number of other cell surface molecules having no effect. Similarly, Poupot and Fournie (2003) observed enhanced membrane transfer between B cells in the presence of anti-IgM and anti-CD19 antibodies (CD19 being associated with the BCR complex), a combination of these mAbs acting additively, whilst antibodies to CD20, CD22 and CD40 showed no such effect. Understanding why some cell surface molecules, when exposed to mAbs enhance transfer and others do not could help define the molecular basis of membrane transfer between B cells.

Although still to be clarified, the addition of ALCAM, TIGIT and PVR specific antibodies to co-cultures of B6.CD45.1 and MD4 B cells appeared to, surprisingly, affect membrane transfer primarily in one direction, with acquisition of MD4 membranes by B6.CD45.1 B cells being significantly enhanced. In contrast, membrane transfer in the opposite direction (i.e., B6.CD45.1 B cells acting as the donor cells) was usually similar to background levels of transfer unless the different antibodies were combined. It should be noted that the two B cell populations used in these experiments are somewhat different. The MD4 B cells that exhibited enhanced membrane transfer are BCR transgenic, expressing a BCR-specific for HEL. In contrast, the B6.CD45.1 B cells are polyclonal B cells on a normal C57BL/6 background but carrying a different CD45 allotype to allow identification in co-cultures. This suggests that the nature of the BCR may have some effect on the enhanced membrane transfer observed, HEL being a highly basic protein that may result in the MD4 BCR recognising basic CPP motifs exposed on antibody treated bystander B cells. Whatever the explanation of this unexpected effect, bidirectional enhancement of membrane exchange is restored when the B cells are exposed to multiple mAbs that enhance membrane transfer unidirectionally when used alone.

Of course, the direction of membrane transfer (whether a cell is likely to donate or accept membrane fragments) is often bidirectional, as observed in this thesis between LPS stimulated B cells (Section 4.3.7.1). However, it is also commonly unidirectional in other systems, particularly in the process of trogocytosis, with the parameters that govern the direction of membrane transfer unknown. For example, following opsonisation with mAbs directed against certain surface molecules both B and T cells can function as recipient cells and acquire membrane molecules when they interacted with FcγR expressing P815 cells (Hudrisier et al., 2007). In contrast, binding of the anti-CD20 antibody rituximab (RTX) to CD20 on B cells can lead to macrophage acquisition of RTX-CD20 complexes from B cells concomitantly with membrane fragments thus, in this case, B cells function as the membrane donor cells (Pham et al., 2011). Based on these findings, Daubeuf *et al* (2010) proposed that mAbs trigger membrane transfer and suggested it was the identity of the FcγR-expressing cell that drives the directionality of the transfer. However, results reported in this thesis demonstrate that opsonising antibodies are not required for membrane transfer as LPS stimulated B cells efficiently transferred membranes in the absence of antibody. However, antibodies to certain cell surface antigens did enhance membrane exchange between LPS-activated B cells, particularly in one direction. It would be interesting to investigate the factors that determine the directionality of transfer between B cells as this may give us further clues regarding the molecular basis of membrane exchange.

6.6 Conclusions

The molecular mechanisms that are involved in membrane transfer between B cells remain elusive, however, this study has identified a number of vital factors required for transfer to occur efficiently and unique concepts that could provide further insights into the process. For instance, results presented in Chapter 3 demonstrated that membrane transfer between B cells is influenced by the activation state of B cells, with activated B cells exchanging membrane molecules to a far greater extent than their naïve counterparts. Additionally, B cells are capable of exchanging membranes with neighbouring B cells at both 4ºC and 37ºC indicating an energy independent mechanism of transfer. Interestingly, it was found that CPPs are similarly able to achieve translocation into B cells under the same conditions that favour membrane exchange, therefore suggesting that the cell surface receptors involved in the initiation of membrane transfer contain CPP motifs that facilitate interaction between neighbouring B cells.

Results described in Chapter 4 demonstrated that crosslinking of the BCR with specific antigen dramatically enhanced membrane transfer between activated B cells and to a lesser extent between naïve B cells. It was also demonstrated that the nature of the B cell stimulus (i.e., LPS or CpG) controls whether or not membrane transfer will occur, this difference being exploited to identify five molecules that could be involved in membrane transfer, with antibodies to three of these molecules, namely ALCAM, TIGIT and PVR, alone and in concert, enhancing transfer between B cells.

From these results and the available literature a mechanism for membrane transfer can be proposed that involves the formation of micro-domains, alternatively known as patches or lipid rafts, that facilitate the exchange of membranes between B cells.

Finally, in Chapter 5 attempts were made to harness membrane transfer between CTLs in adoptive CTL immunotherapy of cancer. Although the study was inconclusive for a range of technical reasons, it was found that CTLs mediate tumour clearance by a number of mechanisms, one possibility being via TCR transfer to bystander leukocytes recruited into tumours.

Thus, overall this thesis provides important clues as to the molecular basis of membrane transfer between lymphocytes, particularly B cells, and insights into when such transfer may occur.

References

ACUTO, O. & MICHEL, F. 2003. CD28-mediated co-stimulation: a quantitative support for TCR signalling. *Nat Rev Immunol,* 3**,** 939-51.

AFFYMETRIX, I. 2007. GeneChip® Gene 1.0 ST Array System for Human, Mouse and Rat, A simple and affordable solution for advanced gene-level expression profiling. *Affymetrix Data Sheet (*http://media.affymetrix.com/support/technical/datasheets/gene_1_0_st_datasheet.pdf*)*.

AHMED, K. A., MUNEGOWDA, M. A., XIE, Y. & XIANG, J. 2008. Intercellular trogocytosis plays an important role in modulation of immune responses. *Cellular & molecular immunology,* 5**,** 261-9.

AHMED, K. A. & XIANG, J. 2011. Mechanisms of cellular communication through intercellular protein transfer. *Journal of Cellular and Molecular Medicine,* 15**,** 1458-1473.

ALEGRE, E., HOWANGYIN, K. Y., FAVIER, B., BAUDHUIN, J., LESPORT, E., DAOUYA, M., GONZALEZ, A., CAROSELLA, E. D. & LEMAOULT, J. 2010. Membrane redistributions through multi-intercellular exchanges and serial trogocytosis. *Cell Res,* 20**,** 1239-51.

ALLAVENA, P., SICA, A., SOLINAS, G., PORTA, C. & MANTOVANI, A. 2008. The inflammatory micro-environment in tumor progression: the role of tumor-associated macrophages. *Crit Rev Oncol Hematol,* 66**,** 1-9.

ANDREWS, D. M. & SMYTH, M. J. 2010. A potential role for RAG-1 in NK cell development revealed by analysis of NK cells during ontogeny. *Immunol Cell Biol,* 88**,** 107-16.

ARICESCU, A. R. & JONES, E. Y. 2007. Immunoglobulin superfamily cell adhesion molecules: zippers and signals. *Curr Opin Cell Biol,* 19**,** 543-50.

ARNOLD, P. Y. & MANNIE, M. D. 1999. Vesicles bearing MHC class II molecules mediate transfer of antigen from antigen-presenting cells to CD4+ T cells. *Eur J Immunol,* 29**,** 1363-73.

AUCHER, A., MAGDELEINE, E., JOLY, E. & HUDRISIER, D. 2008. Capture of plasma membrane fragments from target cells by trogocytosis requires signaling in T cells but not in B cells. *Blood,* 111**,** 5621-5628.

AVALOS, A. M., BILATE, A. M., WITTE, M. D., TAI, A. K., HE, J., FRUSHICHEVA, M. P., THILL, P. D., MEYER-WENTRUP, F., THEILE, C. S., CHAKRABORTY, A. K., ZHUANG, X. & PLOEGH, H. L. 2014. Monovalent engagement of the BCR activates ovalbumin-specific transnuclear B cells. *J Exp Med,* 211**,** 365-79.

BARNDEN, M. J., ALLISON, J., HEATH, W. R. & CARBONE, F. R. 1998. Defective TCR expression in transgenic mice constructed using cDNA-based [agr]- and [bgr]-chain genes under the control of heterologous regulatory elements. *Immunol Cell Biol,* 76**,** 34-40.

BARRAL, D. C., RAMALHO, J. S., ANDERS, R., HUME, A. N., KNAPTON, H. J., TOLMACHOVA, T., COLLINSON, L. M., GOULDING, D., AUTHI, K. S. & SEABRA, M. C. 2002. Functional redundancy of Rab27 proteins and the pathogenesis of Griscelli syndrome. *J Clin Invest,* 110**,** 247-57.

BATISTA, F. D. & HARWOOD, N. E. 2009. The who, how and where of antigen presentation to B cells. *Nat Rev Immunol,* 9**,** 15-27.

BATISTA, F. D., IBER, D. & NEUBERGER, M. S. 2001. B cells acquire antigen from target cells after synapse formation. *Nature,* 411**,** 489-94.

BEAUVILLAIN, C., DELNESTE, Y., SCOTET, M., PERES, A., GASCAN, H., GUERMONPREZ, P., BARNABA, V. & JEANNIN, P. 2007. Neutrophils efficiently cross-prime naive T cells in vivo. *Blood,* 110**,** 2965-73.

BECHARA, C. & SAGAN, S. 2013. Cell-penetrating peptides: 20 years later, where do we stand? *FEBS Letters,* 587**,** 1693-1702.

BELLA, J., HINDLE, K. L., MCEWAN, P. A. & LOVELL, S. C. 2008. The leucine-rich repeat structure. *Cellular and Molecular Life Sciences,* 65**,** 2307-2333.

BERTRAND, F. E., ECKFELDT, C. E., FINK, J. R., LYSHOLM, A. S., PRIBYL, J. A., SHAH, N. & LEBIEN, T. W. 2000. Microenvironmental influences on human B-cell development. *Immunol Rev,* 175**,** 175-86.

BEVAN, M. J. 2006. Cross-priming. *Nat Immunol,* 7**,** 363-5.

BIGLER, J., RAND, H. A., KERKOF, K., TIMOUR, M. & RUSSELL, C. B. 2013. Cross-Study Homogeneity of Psoriasis Gene Expression in Skin across a Large Expression Range. *PLoS ONE,* 8**,** e52242.

BLOHM, U., POTTHOFF, D., VAN DER KOGEL, A. J. & PIRCHER, H. 2006. Solid tumors "melt" from the inside after successful CD8 T cell attack. *Eur J Immunol,* 36**,** 468-77.

BOHM, W., THOMA, S., LEITHAUSER, F., MOLLER, P., SCHIRMBECK, R. & REIMANN, J. 1998. T cell-mediated, IFN-gamma-facilitated rejection of murine B16 melanomas. *J Immunol,* 161**,** 897-908.

BOLES, K. S., VERMI, W., FACCHETTI, F., FUCHS, A., WILSON, T. J., DIACOVO, T. G., CELLA, M. & COLONNA, M. 2009. A novel molecular interaction for the adhesion of follicular CD4 T cells to follicular DC. *Eur J Immunol,* 39**,** 695-703.

BONA, C., ROBINEAUX, R., ANTEUNIS, A., HEUCLIN, C. & ASTESANO, A. 1973. Transfer of antigen from macrophages to lymphocytes: II. Immunological significance of the transfer of lipopolysaccharide. *Immunology,* 24**,** 831-840.

BONACCORSI, I., MORANDI, B., ANTSIFEROVA, O., COSTA, G., OLIVERI, D., CONTE, R., PEZZINO, G., VERMIGLIO, G., ANASTASI, G. P., NAVARRA, G., MUNZ, C., DI CARLO, E., MINGARI, M. C. & FERLAZZO, G. 2014. Membrane transfer from tumor cells overcomes deficient phagocytic ability of plasmacytoid dendritic cells for the acquisition and presentation of tumor antigens. *J Immunol,* 192**,** 824-32.

BOROSS, P., JANSEN, J. H., PASTULA, A., VAN DER POEL, C. E. & LEUSEN, J. H. 2012. Both activating and inhibitory Fc gamma receptors mediate rituximab-induced trogocytosis of CD20 in mice. *Immunol Lett,* 143**,** 44-52.

BOWEN, M. A., BAJORATH, J., SIADAK, A. W., MODRELL, B., MALACKO, A. R., MARQUARDT, H., NADLER, S. G. & ARUFFO, A. 1996. The amino-terminal immunoglobulin-like domain of activated leukocyte cell adhesion molecule binds specifically to the membrane-proximal scavenger receptor cysteine-rich domain of CD6 with a 1:1 stoichiometry. *J Biol Chem,* 271**,** 17390-6.

BOWEN, M. A., PATEL, D. D., LI, X., MODRELL, B., MALACKO, A. R., WANG, W. C., MARQUARDT, H., NEUBAUER, M., PESANDO, J. M. & FRANCKE, U. 1995. Cloning, mapping, and characterization of activated leukocyte-cell adhesion molecule (ALCAM), a CD6 ligand. *The Journal of Experimental Medicine,* 181**,** 2213-2220.

BREZINSCHEK, R. I., OPPENHEIMER-MARKS, N. & LIPSKY, P. E. 1999. Activated T Cells Acquire Endothelial Cell Surface Determinants During Transendothelial Migration. *The Journal of Immunology,* 162**,** 1677-1684.

BROWN, D. A. & LONDON, E. 1998. FUNCTIONS OF LIPID RAFTS IN BIOLOGICAL MEMBRANES. *Annual Review of Cell and Developmental Biology,* 14**,** 111-136.

BROWN, R., KABANI, K., FAVALORO, J., YANG, S., HO, P. J., GIBSON, J., FROMM, P., SUEN, H., WOODLAND, N., NASSIF, N., HART, D. & JOSHUA, D. 2012. CD86+ or HLA-G+ can be transferred via trogocytosis from myeloma cells to T cells and are associated with poor prognosis. *Blood,* 120**,** 2055-63.

BURNET, F. M. 1957. A modification of Jerne's theory of antibody production using the concept of clonal selection. *Aust. J. Sci.,* 20**,** 67-69.

CAIRNS, C. M., GORDON, J. R., LI, F., BACA-ESTRADA, M. E., MOYANA, T. & XIANG, J. 2001. Lymphotactin expression by engineered myeloma cells drives tumor regression: mediation by CD4+ and CD8+ T cells and neutrophils expressing XCR1 receptor. *J Immunol,* 167**,** 57-65.

CARLIN, L. M., ELEME, K., MCCANN, F. E. & DAVIS, D. M. 2001. Intercellular transfer and supramolecular organization of human leukocyte antigen C at inhibitory natural killer cell immune synapses. *J Exp Med,* 194**,** 1507-17.

CARRASCO, Y. R., FLEIRE, S. J., CAMERON, T., DUSTIN, M. L. & BATISTA, F. D. 2004. LFA-1/ICAM-1 interaction lowers the threshold of B cell activation by facilitating B cell adhesion and synapse formation. *Immunity,* 20**,** 589-99.

CAUMARTIN, J., FAVIER, B., DAOUYA, M., GUILLARD, C., MOREAU, P., CAROSELLA, E. D. & LEMAOULT, J. 2007. Trogocytosis-based generation of suppressive NK cells. *EMBO J,* 26**,** 1423-33.

CEMERSKI, S., DAS, J., GIURISATO, E., MARKIEWICZ, M. A., ALLEN, P. M., CHAKRABORTY, A. K. & SHAW, A. S. 2008. The balance between T cell receptor signaling and degradation at the center of the immunological synapse is determined by antigen quality. *Immunity,* 29**,** 414-22.

CHAMBERS, C. A., KUHNS, M. S., EGEN, J. G. & ALLISON, J. P. 2001. CTLA-4-MEDIATED INHIBITION IN REGULATION OF T CELL RESPONSES: Mechanisms and Manipulation in Tumor Immunotherapy. *Annual Review of Immunology,* 19**,** 565-594.

CHAPMAN, E. R. 2008. How does synaptotagmin trigger neurotransmitter release? *Annu Rev Biochem,* 77**,** 615-41.

CHAUDHRI, G., QUAH, B. J., WANG, Y., TAN, A. H., ZHOU, J., KARUPIAH, G. & PARISH, C. R. 2009. T cell receptor sharing by cytotoxic T lymphocytes facilitates efficient virus control. *Proc Natl Acad Sci U S A*.

CHEN, Y. L., WANG, J. Y., CHEN, S. H. & YANG, B. C. 2002. Granulocytes mediates the Fas-L-associated apoptosis during lung metastasis of melanoma that determines the metastatic behaviour. *Br J Cancer,* 87**,** 359-65.

CHENG, P. C., BROWN, B. K., SONG, W. & PIERCE, S. K. 2001. Translocation of the B cell antigen receptor into lipid rafts reveals a novel step in signaling. *J Immunol,* 166**,** 3693-701.

CHENG, P. C., DYKSTRA, M. L., MITCHELL, R. N. & PIERCE, S. K. 1999. A Role for Lipid Rafts in B Cell Antigen Receptor Signaling and Antigen Targeting. *The Journal of Experimental Medicine,* 190**,** 1549-1560.

CHERUKURI, A., CHENG, P. C., SOHN, H. W. & PIERCE, S. K. 2001. The CD19/CD21 complex functions to prolong B cell antigen receptor signaling from lipid rafts. *Immunity,* 14**,** 169-79.

CHO, F. N., CHANG, T. H., SHU, C. W., KO, M. C., LIAO, S. K., WU, K. H., YU, M. S., LIN, S. J., HONG, Y. C., CHEN, C. H., HUNG, C. H. & CHANG, Y. H. 2014. Enhanced cytotoxicity of natural killer cells following the acquisition of chimeric antigen receptors through trogocytosis. *PLoS One,* 9**,** e109352.

CHRISTIAENS, B., GROOTEN, J., REUSENS, M., JOLIOT, A., GOETHALS, M., VANDEKERCKHOVE, J., PROCHIANTZ, A. & ROSSENEU, M. 2004. Membrane interaction and cellular internalization of penetratin peptides. *European Journal of Biochemistry,* 271**,** 1187-1197.

CLYNES, R. A., TOWERS, T. L., PRESTA, L. G. & RAVETCH, J. V. 2000. Inhibitory Fc receptors modulate in vivo cytotoxicity against tumor targets. *Nat Med,* 6**,** 443-6.

COCA, S., PEREZ-PIQUERAS, J., MARTINEZ, D., COLMENAREJO, A., SAEZ, M. A., VALLEJO, C., MARTOS, J. A. & MORENO, M. 1997. The prognostic significance of intratumoral natural killer cells in patients with colorectal carcinoma. *Cancer,* 79**,** 2320-8.

COLOMBO, M. P., LOMBARDI, L., MELANI, C., PARENZA, M., BARONI, C., RUCO, L. & STOPPACCIARO, A. 1996. Hypoxic tumor cell death and modulation of endothelial adhesion molecules in the regression of granulocyte colony-stimulating factor-transduced tumors. *Am J Pathol,* 148**,** 473-83.

CONE, R. E., SPRENT, J. & MARCHALONIS, J. J. 1972. Antigen-Binding Specificity of Isolated Cell-Surface Immunoglobulin from Thymus Cells Activated to Histocompatibility Antigens. *Proceedings of the National Academy of Sciences,* 69**,** 2556-2560.

COX, J. H., MCMICHAEL, A. J., SCREATON, G. R. & XU, X. N. 2007. CTLs target Th cells that acquire bystander MHC class I-peptide complex from APCs. *J Immunol,* 179**,** 830-6.

DALEY, J. M., THOMAY, A. A., CONNOLLY, M. D., REICHNER, J. S. & ALBINA, J. E. 2008. Use of Ly6G-specific monoclonal antibody to deplete neutrophils in mice. *J Leukoc Biol,* 83**,** 64-70.

DALYOT-HERMAN, N., BATHE, O. F. & MALEK, T. R. 2000. Reversal of CD8+ T Cell Ignorance and Induction of Anti-Tumor Immunity by Peptide-Pulsed APC. *The Journal of Immunology,* 165**,** 6731-6737.

DAUBEUF, S., AUCHER, A., BORDIER, C., SALLES, A., SERRE, L., GAIBELET, G. R., FAYE, J.-C., FAVRE, G., JOLY, E. & HUDRISIER, D. 2010a. Preferential Transfer of Certain Plasma Membrane Proteins onto T and B Cells by Trogocytosis. *PLoS ONE,* 5**,** e8716.

DAUBEUF, S., LINDORFER, M. A., TAYLOR, R. P., JOLY, E. & HUDRISIER, D. 2010b. The direction of plasma membrane exchange between lymphocytes and accessory cells by trogocytosis is influenced by the nature of the accessory cell. *J Immunol,* 184**,** 1897-908.

DAVIS, D. M. 2007. Intercellular transfer of cell-surface proteins is common and can affect many stages of an immune response. *Nat Rev Immunol,* 7**,** 238-243.

DAVIS, D. M. & SOWINSKI, S. 2008. Membrane nanotubes: dynamic long-distance connections between animal cells. *Nat Rev Mol Cell Biol,* 9**,** 431-6.

DELGADO, P., CUBELOS, B., CALLEJA, E., MARTINEZ-MARTIN, N., CIPRES, A., MERIDA, I., BELLAS, C., BUSTELO, X. R. & ALARCON, B. 2009. Essential function for the GTPase TC21 in homeostatic antigen receptor signaling. *Nat Immunol,* 10**,** 880-8.

DEN HAAN, J. M., ARENS, R. & VAN ZELM, M. C. 2014. The activation of the adaptive immune system: cross-talk between antigen-presenting cells, T cells and B cells. *Immunol Lett,* 162**,** 103-12.

DEPOIL, D., FLEIRE, S., TREANOR, B. L., WEBER, M., HARWOOD, N. E., MARCHBANK, K. L., TYBULEWICZ, V. L. & BATISTA, F. D. 2008. CD19 is essential for B cell activation by promoting B cell receptor-antigen microcluster formation in response to membrane-bound ligand. *Nat Immunol,* 9**,** 63-72.

DEPOIL, D., WEBER, M., TREANOR, B., FLEIRE, S. J., CARRASCO, Y. R., HARWOOD, N. E. & BATISTA, F. D. 2009. Early events of B cell activation by antigen. *Sci Signal,* 2**,** pt1.

DERISI, J., VAN DEN HAZEL, B., MARC, P., BALZI, E., BROWN, P., JACQ, C. & GOFFEAU, A. 2000. Genome microarray analysis of transcriptional activation in multidrug resistance yeast mutants. *FEBS Letters,* 470**,** 156-160.

DEROSSI, D., CHASSAING, G. & PROCHIANTZ, A. 1998. Trojan peptides: the penetratin system for intracellular delivery. *Trends in cell biology,* 8**,** 84-87.

DEROSSI, D., JOLIOT, A. H., CHASSAING, G. & PROCHIANTZ, A. 1994. The third helix of the Antennapedia homeodomain translocates through biological membranes. *Journal of Biological Chemistry,* 269**,** 10444-50.

DESHAYES, S. B., DECAFFMEYER, M., BRASSEUR, R. & THOMAS, A. 2008. Structural polymorphism of two CPP: An important parameter of activity. *Biochimica et Biophysica Acta (BBA) - Biomembranes,* 1778**,** 1197-1205.

DOBRZANSKI, M. J., REOME, J. B. & DUTTON, R. W. 1999. Therapeutic Effects of Tumor-Reactive Type 1 and Type 2 CD8+ T Cell Subpopulations in Established Pulmonary Metastases. *The Journal of Immunology,* 162**,** 6671-6680.

DOBRZANSKI, M. J., REOME, J. B. & DUTTON, R. W. 2001. Immunopotentiating role of IFN-gamma in early and late stages of type 1 CD8 effector cell-mediated tumor rejection. *Clin Immunol,* 98**,** 70-84.

DOBRZANSKI, M. J., REOME, J. B., HOLLENBAUGH, J. A., HYLIND, J. C. & DUTTON, R. W. 2004. Effector Cell-Derived Lymphotoxin {alpha} and Fas Ligand, but not Perforin, Promote Tc1 and Tc2 Effector Cell-Mediated Tumor Therapy in Established Pulmonary Metastases. *Cancer Res,* 64**,** 406-414.

DOLAN, B. P., GIBBS, K. D., JR. & OSTRAND-ROSENBERG, S. 2006a. Dendritic cells cross-dressed with peptide MHC class I complexes prime CD8+ T cells. *J Immunol,* 177**,** 6018-24.

DOLAN, B. P., GIBBS, K. D., JR. & OSTRAND-ROSENBERG, S. 2006b. Tumor-specific CD4+ T cells are activated by "cross-dressed" dendritic cells presenting peptide-MHC class II complexes acquired from cell-based cancer vaccines. *J Immunol,* 176**,** 1447-55.

DONG, X., XU, F., GONG, Y., GAO, J., LIN, P., CHEN, T., PENG, Y., QIANG, B., YUAN, J., PENG, X. & RAO, Z. 2006. Crystal structure of the V domain of human Nectin-like molecule-1/Syncam3/Tsll1/Igsf4b, a neural tissue-specific immunoglobulin-like cell-cell adhesion molecule. *J Biol Chem,* 281**,** 10610-7.

DOW, G. 2003. Effect of sample size and P-value filtering techniques on the detection of transcriptional changes induced in rat neuroblastoma (NG108) cells by mefloquine. *Malaria Journal,* 2**,** 4.

DUDLEY, M. E. & ROSENBERG, S. A. 2003. Adoptive-cell-transfer therapy for the treatment of patients with cancer. *Nat Rev Cancer,* 3**,** 666-75.

DUFFY, K. R. & HODGKIN, P. D. 2012. Intracellular competition for fates in the immune system. *Trends Cell Biol,* 22**,** 457-64.

DUSTIN, M. L. & DEPOIL, D. 2011. New insights into the T cell synapse from single molecule techniques. *Nat Rev Immunol,* 11**,** 672-84.

DYKSTRA, M., CHERUKURI, A., SOHN, H. W., TZENG, S.-J. & PIERCE, S. K. 2003. LOCATION IS EVERYTHING: Lipid Rafts and Immune Cell Signaling*. *Annual Review of Immunology,* 21**,** 457-481.

EGEN, J. G. & ALLISON, J. P. 2002. Cytotoxic T lymphocyte antigen-4 accumulation in the immunological synapse is regulated by TCR signal strength. *Immunity,* 16**,** 23-35.

EISENBERG, G., UZANA, R., PATO, A., FRANKENBURG, S., MERIMS, S., YEFENOF, E., FERRONE, S., PERETZ, T., MACHLENKIN, A. & LOTEM, M. 2013. Imprinting of lymphocytes with melanoma antigens acquired by trogocytosis facilitates identification of tumor-reactive T cells. *J Immunol,* 190**,** 5856-65.

FIALA, G. J., KASCHEK, D., BLUMENTHAL, B., RETH, M., TIMMER, J. & SCHAMEL, W. W. 2013. Pre-clustering of the B cell antigen receptor demonstrated by mathematically extended electron microscopy. *Front Immunol,* 4**,** 427.

FISCHER, P. M., ZHELEV, N. Z., WANG, S., MELVILLE, J. E., FÅHRAEUS, R. & LANE, D. P. 2000. Structure–activity relationship of truncated and substituted analogues of the intracellular delivery vector Penetratin. *The Journal of Peptide Research,* 55**,** 163-172.

FISCHER, R., WAIZENEGGER, T., KÖHLER, K. & BROCK, R. 2002. A quantitative validation of fluorophore-labelled cell-permeable peptide conjugates: fluorophore and cargo dependence of import. *Biochimica et Biophysica Acta (BBA) - Biomembranes,* 1564**,** 365-374.

FORD MCINTYRE, M. S., YOUNG, K. J., GAO, J., JOE, B. & ZHANG, L. 2008. Cutting edge: in vivo trogocytosis as a mechanism of double negative regulatory T cell-mediated antigen-specific suppression. *J Immunol,* 181**,** 2271-5.

FRANKEL, A. D. & PABO, C. O. 1988. Cellular uptake of the tat protein from human immunodeficiency virus. *Cell,* 55**,** 1189-1193.

FRAUWIRTH, K. A. & THOMPSON, C. B. 2002. Activation and inhibition of lymphocytes by costimulation. *The Journal of Clinical Investigation,* 109**,** 295-299.

FRETZ, M. M., PENNING, N. A., AL-TAEI, S., FUTAKI, S., TAKEUCHI, T., NAKASE, I., STORM, G. & JONES, A. T. 2007. Temperature-, concentration- and cholesterol-dependent translocation of L- and D-octa-arginine across the plasma and nuclear membrane of CD34+ leukaemia cells. *Biochem J,* 403**,** 335-342.

FRIDLENDER, Z. G. & ALBELDA, S. M. 2012. Tumor Associated Neutrophils: Friend or Foe? *Carcinogenesis*.

FUKUDA, M. 2002. The C2A domain of synaptotagmin-like protein 3 (Slp3) is an atypical calcium-dependent phospholipid-binding machine: comparison with the C2A domain of synaptotagmin I. *Biochem J,* 366**,** 681-7.

FUKUDA, M. & MIKOSHIBA, K. 2001. Synaptotagmin-like Protein 1-3: A Novel Family of C-Terminal-Type Tandem C2 Proteins. *Biochemical and Biophysical Research Communications,* 281**,** 1226-1233.

FUKUDA, M., SAEGUSA, C. & MIKOSHIBA, K. 2001. Novel splicing isoforms of synaptotagmin-like proteins 2 and 3: identification of the Slp homology domain. *Biochem Biophys Res Commun,* 283**,** 513-9.

GALVEZ-SANTISTEBAN, M., RODRIGUEZ-FRATICELLI, A. E., BRYANT, D. M., VERGARAJAUREGUI, S., YASUDA, T., BANON-RODRIGUEZ, I., BERNASCONE, I., DATTA, A., SPIVAK, N., YOUNG, K., SLIM, C. L., BRAKEMAN, P. R., FUKUDA, M., MOSTOV, K. E. & MARTIN-BELMONTE, F. 2012. Synaptotagmin-like proteins control the formation of a single apical membrane domain in epithelial cells. *Nat Cell Biol,* 14**,** 838-49.

GAME, D. S., ROGERS, N. J. & LECHLER, R. I. 2005. Acquisition of HLA-DR and costimulatory molecules by T cells from allogeneic antigen presenting cells. *Am J Transplant,* 5**,** 1614-25.

GAUS, K., CHKLOVSKAIA, E., FAZEKAS DE ST. GROTH, B., JESSUP, W. & HARDER, T. 2005. Condensation of the plasma membrane at the site of T lymphocyte activation. *The Journal of Cell Biology,* 171**,** 121-131.

GERDES, H. H. & CARVALHO, R. N. 2008. Intercellular transfer mediated by tunneling nanotubes. *Curr Opin Cell Biol,* 20**,** 470-5.

GILLETTE, J. M., LAROCHELLE, A., DUNBAR, C. E. & LIPPINCOTT-SCHWARTZ, J. 2009. Intercellular transfer to signalling endosomes regulates an ex vivo bone marrow niche. *Nat Cell Biol,* 11**,** 303-311.

GOODNOW, C. C., CROSBIE, J., ADELSTEIN, S., LAVOIE, T. B., SMITH-GILL, S. J., BRINK, R. A., PRITCHARD-BRISCOE, H., WOTHERSPOON, J. S., LOBLAY, R. H., RAPHAEL, K., TRENT, R. J. & BASTEN, A. 1988. Altered immunoglobulin expression and functional silencing of self-reactive B lymphocytes in transgenic mice

. *Nature,* 334**,** 7.

GORDON, S. & TAYLOR, P. R. 2005. Monocyte and macrophage heterogeneity. *Nat Rev Immunol,* 5**,** 953-64.

GRAKOUI, A., BROMLEY, S. K., SUMEN, C., DAVIS, M. M., SHAW, A. S., ALLEN, P. M. & DUSTIN, M. L. 1999. The immunological synapse: a molecular machine controlling T cell activation. *Science,* 285**,** 221-7.

GREENWALD, R. J., FREEMAN, G. J. & SHARPE, A. H. 2005. THE B7 FAMILY REVISITED. *Annual Review of Immunology,* 23**,** 515-548.

GROFFEN, A. J., MARTENS, S., DIEZ ARAZOLA, R., CORNELISSE, L. N., LOZOVAYA, N., DE JONG, A. P., GORIOUNOVA, N. A., HABETS, R. L., TAKAI, Y., BORST, J. G., BROSE, N., MCMAHON, H. T. & VERHAGE, M. 2010. Doc2b is a high-affinity Ca2+ sensor for spontaneous neurotransmitter release. *Science,* 327**,** 1614-8.

GRUGAN, K. D., MCCABE, F. L., KINDER, M., GREENPLATE, A. R., HARMAN, B. C., EKERT, J. E., VAN ROOIJEN, N., ANDERSON, G. M., NEMETH, J. A., STROHL, W. R., JORDAN, R. E. & BREZSKI, R. J. 2012. Tumor-associated macrophages promote invasion while retaining Fc-dependent anti-tumor function. *J Immunol,* 189**,** 5457-66.

GU, P., GAO, J. F., D'SOUZA, C. A., KOWALCZYK, A., CHOU, K. Y. & ZHANG, L. 2012. Trogocytosis of CD80 and CD86 by induced regulatory T cells. *Cell Mol Immunol,* 9**,** 136-46.

GUPTA, N. & DEFRANCO, A. L. 2007. Lipid rafts and B cell signaling. *Seminars in Cell & Developmental Biology,* 18**,** 616-626.

HABU, S., FUKUI, H., SHIMAMURA, K., KASAI, M., NAGAI, Y., OKUMURA, K. & TAMAOKI, N. 1981. In vivo effects of anti-asialo GM1. I. Reduction of NK activity and enhancement of transplanted tumor growth in nude mice. *J Immunol,* 127**,** 34-8.

HALIN, C., MORA, J. R., SUMEN, C. & VON ANDRIAN, U. H. 2005. In vivo imaging of lymphocyte trafficking. *Annu Rev Cell Dev Biol,* 21**,** 581-603.

HAMPSON, A., O'CONNOR, A. & SMOLENSKI, A. 2013. Synaptotagmin-like protein 4 and Rab8 interact and increase dense granule release in platelets. *J Thromb Haemost,* 11**,** 161-8.

HAO, S., ANDERSEN, M. & YU, H. 2013. Detection of immune suppressive neutrophils in peripheral blood samples of cancer patients. *Am J Blood Res,* 3**,** 239-45.

HAO, S. & AUGUST, A. 2005. Actin Depolymerization Transduces the Strength of B-Cell Receptor Stimulation. *Molecular Biology of the Cell,* 16**,** 2275-2284.

HARSHYNE, L. A., WATKINS, S. C., GAMBOTTO, A. & BARRATT-BOYES, S. M. 2001. Dendritic cells acquire antigens from live cells for cross-presentation to CTL. *J Immunol,* 166**,** 3717-23.

HARVEY, B. P., QUAN, T. E., RUDENGA, B. J., ROMAN, R. M., CRAFT, J. & MAMULA, M. J. 2008. Editing Antigen Presentation: Antigen Transfer between Human B Lymphocytes and Macrophages Mediated by Class A Scavenger Receptors. *The Journal of Immunology,* 181**,** 4043-4051.

HARWOOD, N. E. & BATISTA, F. D. 2011. The cytoskeleton coordinates the early events of B-cell activation. *Cold Spring Harb Perspect Biol,* 3.

HASSAN, N. J., BARCLAY, A. N. & BROWN, M. H. 2004. Frontline: Optimal T cell activation requires the engagement of CD6 and CD166. *European Journal of Immunology,* 34**,** 930-940.

HAWKINS, E. D., MARKHAM, J. F., MCGUINNESS, L. P. & HODGKIN, P. D. 2009. A single-cell pedigree analysis of alternative stochastic lymphocyte fates. *Proceedings of the National Academy of Sciences,* 106**,** 13457-13462.

HE, T., TANG, C., LIU, Y., YE, Z., WU, X., WEI, Y., MOYANA, T. & XIANG, J. 2007. Bidirectional membrane molecule transfer between dendritic and T cells. *Biochem Biophys Res Commun,* 359**,** 202-8.

HELMICH, B. K. & DUTTON, R. W. 2001. The Role of Adoptively Transferred CD8 T Cells and Host Cells in the Control of the Growth of the EG7 Thymoma: Factors That Determine the Relative

Effectiveness and Homing Properties of Tc1 and Tc2 Effectors. *The Journal of Immunology,* 166**,** 6500-6508.

HERCE, H. D., GARCIA, A. E., LITT, J., KANE, R. S., MARTIN, P., ENRIQUE, N., REBOLLEDO, A. & MILESI, V. 2009. Arginine-Rich Peptides Destabilize the Plasma Membrane, Consistent with a Pore Formation Translocation Mechanism of Cell-Penetrating Peptides. *Biophysical Journal,* 97**,** 1917-1925.

HERRERA, O. B., GOLSHAYAN, D., TIBBOTT, R., SALCIDO OCHOA, F., JAMES, M. J., MARELLI-BERG, F. M. & LECHLER, R. I. 2004. A novel pathway of alloantigen presentation by dendritic cells. *J Immunol,* 173**,** 4828-37.

HERRICK, D. Z., STERBLING, S., RASCH, K. A., HINDERLITER, A. & CAFISO, D. S. 2006. Position of synaptotagmin I at the membrane interface: cooperative interactions of tandem C2 domains. *Biochemistry,* 45**,** 9668-74.

HIORNS, L. R., BRADSHAW, T. D., SKELTON, L. A., YU, Q., KELLAND, L. R. & LEYLAND-JONES, B. 2004. Variation in RNA expression and genomic DNA content acquired during cell culture. *Br J Cancer,* 90**,** 476-82.

HIRSCH, S. & GORDON, S. 1983a. Polymorphic expression of a neutrophil differentiation antigen revealed by monoclonal antibody 7/4. *Immunogenetics,* 18**,** 229-39.

HIRSCH, S. & GORDON, S. 1983b. Surface antigens as markers of mouse macrophage differentiation. *Int Rev Exp Pathol,* 25**,** 51-75.

HIVROZ, C. & SAITAKIS, M. 2016. Biophysical Aspects of T Lymphocyte Activation at the Immune Synapse. *Front Immunol,* 7**,** 46.

HOGQUIST, K. A., JAMESON, S. C., HEATH, W. R., HOWARD, J. L., BEVAN, M. J. & CARBONE, F. R. 1994. T cell receptor antagonist peptides induce positive selection. *Cell,* 76**,** 17-27.

HOGUE, I. B., GROVER, J. R., SOHEILIAN, F., NAGASHIMA, K. & ONO, A. 2011. Gag Induces the Coalescence of Clustered Lipid Rafts and Tetraspanin-Enriched Microdomains at HIV-1 Assembly Sites on the Plasma Membrane. *Journal of Virology,* 85**,** 9749-9766.

HOLLENBAUGH, J. A. & DUTTON, R. W. 2006. IFN-gamma regulates donor CD8 T cell expansion, migration, and leads to apoptosis of cells of a solid tumor. *J Immunol,* 177**,** 3004-11.

HOLLENBAUGH, J. A., REOME, J., DOBRZANSKI, M. & DUTTON, R. W. 2004. The Rate of the CD8-Dependent Initial Reduction in Tumor Volume Is Not Limited by Contact-Dependent Perforin, Fas Ligand, or TNF-Mediated Cytolysis. *The Journal of Immunology,* 173**,** 1738-1743.

HORNER, H., FRANK, C., DECHANT, C., REPP, R., GLENNIE, M., HERRMANN, M. & STOCKMEYER, B. 2007. Intimate Cell

Conjugate Formation and Exchange of Membrane Lipids Precede Apoptosis Induction in Target Cells during Antibody-Dependent, Granulocyte-Mediated Cytotoxicity. *The Journal of Immunology,* 179**,** 337-345.

HUANG, H., BI, X. G., YUAN, J. Y., XU, S. L., GUO, X. L. & XIANG, J. 2005. Combined CD4+ Th1 effect and lymphotactin transgene expression enhance CD8+ Tc1 tumor localization and therapy. *Gene Ther,* 12**,** 999-1010.

HUANG, H., LI, F., GORDON, J. R. & XIANG, J. 2002. Synergistic enhancement of antitumor immunity with adoptively transferred tumor-specific CD4+ and CD8+ T cells and intratumoral lymphotactin transgene expression. *Cancer Res,* 62**,** 2043-51.

HUANG, H. & XIANG, J. 2004. Synergistic effect of lymphotactin and interferon gamma-inducible protein-10 transgene expression in T-cell localization and adoptive T-cell therapy of tumors. *International Journal of Cancer,* 109**,** 817-825.

HUANG, J. F., YANG, Y., SEPULVEDA, H., SHI, W., HWANG, I., PETERSON, P. A., JACKSON, M. R., SPRENT, J. & CAI, Z. 1999. TCR-Mediated internalization of peptide-MHC complexes acquired by T cells. *Science,* 286**,** 952-4.

HUDRISIER, D., AUCHER, A., PUAUX, A.-L., BORDIER, C. & JOLY, E. 2007. Capture of Target Cell Membrane Components via Trogocytosis Is Triggered by a Selected Set of Surface Molecules on T or B Cells. *The Journal of Immunology,* 178**,** 3637-3647.

HUDRISIER, D. & BONGRAND, P. 2002. Intercellular transfer of antigen-presenting cell determinants onto T cells: molecular mechanisms and biological significance. *FASEB J,* 16**,** 477-86.

HUDRISIER, D. & JOLY, E. 2002. Plasma membrane nibbling: all lymphocytes do it, but why? *ELSO Gaz.,* 9**,** 1-5.

HUDRISIER, D., RIOND, J., GARIDOU, L., DUTHOIT, C. & JOLY, E. 2005. T cell activation correlates with an increasedproportion of antigen among the materials acquiredfrom target cells. *European Journal of Immunology,* 35**,** 2284-2294.

HUDRISIER, D., RIOND, J., MAZARGUIL, H., GAIRIN, J. E. & JOLY, E. 2001. Cutting Edge: CTLs Rapidly Capture Membrane Fragments from Target Cells in a TCR Signaling-Dependent Manner. *The Journal of Immunology,* 166**,** 3645-3649.

HUDSON, L. & SPRENT, J. 1976. Specific adsorption of IgM antibody onto H-2-activated mouse T lymphocytes. *The Journal of Experimental Medicine,* 143**,** 444-449.

HUDSON, L., SPRENT, J., MILLER, J. F. A. P. & PLAYFAIR, J. H. L. 1974. B cell-derived immunoglobulin on activated mouse T lymphocytes. *Nature,* 251**,** 60-62.

HUNG, K., HAYASHI, R., LAFOND-WALKER, A., LOWENSTEIN, C., PARDOLL, D. & LEVITSKY, H. 1998. The central role of CD4(+) T cells in the antitumor immune response. *J Exp Med,* 188**,** 2357-68.

HWANG, I., HUANG, J. F., KISHIMOTO, H., BRUNMARK, A., PETERSON, P. A., JACKSON, M. R., SURH, C. D., CAI, Z. & SPRENT, J. 2000. T cells can use either T cell receptor or CD28 receptors to absorb and internalize cell surface molecules derived from antigen-presenting cells. *J Exp Med,* 191**,** 1137-48.

IDEKER, T., THORSSON, V., SIEGEL, A. F. & HOOD, L. E. 2000. Testing for Differentially-Expressed Genes by Maximum-Likelihood Analysis of Microarray Data. *Journal of Computational Biology,* 7**,** 805-817.

ISHIGAMI, S., NATSUGOE, S., TOKUDA, K., NAKAJO, A., CHE, X., IWASHIGE, H., ARIDOME, K., HOKITA, S. & AIKOU, T. 2000. Prognostic value of intratumoral natural killer cells in gastric carcinoma. *Cancer,* 88**,** 577-83.

ISLAM, M., GOR, J., PERKINS, S. J., ISHIKAWA, Y., BACHINGER, H. P. & HOHENESTER, E. 2013. The concave face of decorin mediates reversible dimerization and collagen binding. *J Biol Chem,* 288**,** 35526-33.

IYER, V. R., EISEN, M. B., ROSS, D. T., SCHULER, G., MOORE, T., LEE, J. C. F., TRENT, J. M., STAUDT, L. M., HUDSON, J., BOGUSKI, M. S., LASHKARI, D., SHALON, D., BOTSTEIN, D. & BROWN, P. O. 1999. The Transcriptional Program in the Response of Human Fibroblasts to Serum. *Science,* 283**,** 83-87.

JAEGER, B. N., DONADIEU, J., COGNET, C., BERNAT, C., ORDONEZ-RUEDA, D., BARLOGIS, V., MAHLAOUI, N., FENIS, A., NARNI-MANCINELLI, E., BEAUPAIN, B., BELLANNE-CHANTELOT, C., BAJENOFF, M., MALISSEN, B., MALISSEN, M., VIVIER, E. & UGOLINI, S. 2012. Neutrophil depletion impairs natural killer cell maturation, function, and homeostasis. *J Exp Med,* 209**,** 565-80.

JAMES, A. M., COHEN, A. D. & CAMPBELL, K. S. 2013. Combination immune therapies to enhance anti-tumor responses by NK cells. *Frontiers in Immunology,* 4.

JIAO, C.-Y., DELAROCHE, D., BURLINA, F., ALVES, I. D., CHASSAING, G. R. & SAGAN, S. 2009. Translocation and Endocytosis for Cell-penetrating Peptide Internalization. *Journal of Biological Chemistry,* 284**,** 33957-33965.

JOLLER, N., HAFLER, J. P., BRYNEDAL, B., KASSAM, N., SPOERL, S., LEVIN, S. D., SHARPE, A. H. & KUCHROO, V. K. 2011. Cutting edge: TIGIT has T cell-intrinsic inhibitory functions. *J Immunol,* 186**,** 1338-42.

JOLY, E. & HUDRISIER, D. 2003. What is trogocytosis and what is its purpose? *Nat Immunol,* 4**,** 815.

KAJANDER, T., KUJA-PANULA, J., RAUVALA, H. & GOLDMAN, A. 2011. Crystal Structure and Role of Glycans and Dimerization in Folding of Neuronal Leucine-Rich Repeat Protein AMIGO-1. *Journal of Molecular Biology,* 413**,** 1001-1015.

KAWAMOTO, S., TAKASU, M., MIYAKAWA, T., MORIKAWA, R., ODA, T., FUTAKI, S. & NAGAO, H. 2011. Inverted micelle formation of cell-penetrating peptide studied by coarse-grained simulation: Importance of attractive force between cell-penetrating peptides and lipid head group. *The Journal of Chemical Physics,* 134**,** -.

KIM, Y.-M., PAN, J. Y.-J., KORBEL, G. A., PEPERZAK, V., BOES, M. & PLOEGH, H. L. 2006. Monovalent ligation of the B cell receptor induces receptor activation but fails to promote antigen presentation. *Proceedings of the National Academy of Sciences of the United States of America,* 103**,** 3327-3332.

KINDZELSKII, A. L. & PETTY, H. R. 1999. Early membrane rupture events during neutrophil-mediated antibody-dependent tumor cell cytolysis. *J Immunol,* 162**,** 3188-92.

KO, J. 2012. The leucine-rich repeat superfamily of synaptic adhesion molecules: LRRTMs and Slitrks. *Molecules and Cells,* 34**,** 335-340.

KOBE, B. & KAJAVA, A. V. 2001. The leucine-rich repeat as a protein recognition motif. *Current Opinion in Structural Biology,* 11**,** 725-732.

KOMOHARA, Y., TAKEMURA, K., LEI, X. F., SAKASHITA, N., HARADA, M., SUZUKI, H., KODAMA, T. & TAKEYA, M. 2009. Delayed growth of EL4 lymphoma in SR-A-deficient mice is due to upregulation of nitric oxide and interferon-γ production by tumor-associated macrophages. *Cancer Science,* 100**,** 2160-2166.

KOPATZ, I., REMY, J. S. & BEHR, J. P. 2004. A model for non-viral gene delivery: through syndecan adhesion molecules and powered by actin. *J Gene Med,* 6**,** 769-76.

KOUSIS, P. C., HENDERSON, B. W., MAIER, P. G. & GOLLNICK, S. O. 2007. Photodynamic therapy enhancement of antitumor immunity is regulated by neutrophils. *Cancer Res,* 67**,** 10501-10.

KRAMER, S. D. & WUNDERLI-ALLENSPACH, H. 2003. No entry for TAT(44,Äì57) into liposomes and intact MDCK cells: novel approach to study membrane permeation of cell-penetrating peptides. *Biochimica et Biophysica Acta (BBA) - Biomembranes,* 1609**,** 161-169.

KUIPER, H. M., BROUWER, M., LINSLEY, P. S. & VAN LIER, R. A. 1995. Activated T cells can induce high levels of CTLA-4 expression on B cells. *The Journal of Immunology,* 155**,** 1776-83.

KUJA-PANULA, J., KIILTOM√§KI, M., YAMASHIRO, T., ROUHIAINEN, A. & RAUVALA, H. 2003. AMIGO, a transmembrane protein implicated in axon tract development, defines a novel protein family with leucine-rich repeats. *The Journal of Cell Biology,* 160**,** 963-973.

KUKURBA, K. R. & MONTGOMERY, S. B. 2015. RNA Sequencing and Analysis. *Cold Spring Harb Protoc.***,** 951-969.

KUMARI, S., CURADO, S., MAYYA, V. & DUSTIN, M. L. 2014. T cell antigen receptor activation and actin cytoskeleton remodeling. *Biochim Biophys Acta,* 1838**,** 546-56.

KUOKKANEN, E., SUSTAR, V. & MATTILA, P. K. 2015. Molecular control of B cell activation and immunological synapse formation. *Traffic,* 16**,** 311-26.

KURODA, T. S., FUKUDA, M., ARIGA, H. & MIKOSHIBA, K. 2002a. The Slp Homology Domain of Synaptotagmin-like Proteins 1,Äì4 and Slac2 Functions as a Novel Rab27A Binding Domain. *Journal of Biological Chemistry,* 277**,** 9212-9218.

KURODA, T. S., FUKUDA, M., ARIGA, H. & MIKOSHIBA, K. 2002b. Synaptotagmin-like protein 5: a novel Rab27A effector with C-terminal tandem C2 domains. *Biochem Biophys Res Commun,* 293**,** 899-906.

KUROWSKA, M., GOUDIN, N., NEHME, N. T., COURT, M., GARIN, J. R. M., FISCHER, A., DE SAINT BASILE, G. V. & M√©NASCH√©, G. L. 2012. Terminal transport of lytic granules to the immune synapse is mediated by the kinesin-1/Slp3/Rab27a complex. *Blood,* 119**,** 3879-3889.

LAMAZIERE, A., MANITI, O., WOLF, C., LAMBERT, O., CHASSAING, G., TRUGNAN, G. & AYALA-SANMARTIN, J. 2010. Lipid domain separation, bilayer thickening and pearling induced by the cell penetrating peptide penetratin. *Biochimica et Biophysica Acta (BBA) - Biomembranes,* 1798**,** 2223-2230.

LATTIG-TUNNEMANN, G., PRINZ, M., HOFFMANN, D., BEHLKE, J., PALM-APERGI, C., MORANO, I., HERCE, H. D. & CARDOSO, M. C. 2011. Backbone rigidity and static presentation of guanidinium groups increases cellular uptake of arginine-rich cell-penetrating peptides. *Nat Commun,* 2**,** 453.

LEMAOULT, J., CAUMARTIN, J., DAOUYA, M., FAVIER, B., LE ROND, S., GONZALEZ, A. & CAROSELLA, E. D. 2007. Immune regulation by pretenders: cell-to-cell transfers of HLA-G make effector T cells act as regulatory cells. *Blood,* 109**,** 2040-8.

LETOHA, T., GAÁL, S., SOMLAI, C., CZAJLIK, A., PERCZEL, A. & PENKE, B. 2003. Membrane translocation of penetratin and its derivatives in different cell lines. *Journal of Molecular Recognition,* 16**,** 272-279.

LEVIN, S. D., TAFT, D. W., BRANDT, C. S., BUCHER, C., HOWARD, E. D., CHADWICK, E. M., JOHNSTON, J., HAMMOND, A., BONTADELLI, K., ARDOUREL, D., HEBB, L., WOLF, A., BUKOWSKI, T. R., RIXON, M. W., KUIJPER, J. L., OSTRANDER, C. D., WEST, J. W., BILSBOROUGH, J., FOX, B., GAO, Z., XU, W., RAMSDELL, F., BLAZAR, B. R. & LEWIS, K. E. 2011. Vstm3 is a member of the CD28 family and an important modulator of T-cell function. *Eur J Immunol,* 41**,** 902-15.

LI, N., YANG, H., LU, L., DUAN, C., ZHAO, C. & ZHAO, H. 2008. Comparison of the labeling efficiency of BrdU, DiI and FISH labeling techniques in bone marrow stromal cells. *Brain Research,* 1215**,** 11-19.

LIU, S., ZHANG, H., LI, M., HU, D., LI, C., GE, B., JIN, B. & FAN, Z. 2013. Recruitment of Grb2 and SHIP1 by the ITT-like motif of TIGIT suppresses granule polarization and cytotoxicity of NK cells. *Cell Death Differ,* 20**,** 456-64.

LIU, W., MECKEL, T., TOLAR, P., SOHN, H. W. & PIERCE, S. K. 2010. Intrinsic properties of immunoglobulin IgG1 isotype-switched B cell receptors promote microclustering and the initiation of signaling. *Immunity,* 32**,** 778-89.

LLINAS, L., LAZARO, A., DE SALORT, J., MATESANZ-ISABEL, J., SINTES, J. & ENGEL, P. 2011. Expression profiles of novel cell surface molecules on B-cell subsets and plasma cells as analyzed by flow cytometry. *Immunol Lett,* 134**,** 113-21.

LOPEZ-COBO, S., ROMERA-CARDENAS, G., GARCIA-CUESTA, E. M., REYBURN, H. T. & VALES-GOMEZ, M. 2015. Transfer of the human NKG2D ligands UL16 binding proteins (ULBP) 1-3 is related to lytic granule release and leads to ligand retransfer and killing of ULBP-recipient natural killer cells. *Immunology*.

MADANI, F., LINDBERG, S., LANGEL, #220, LO, FUTAKI, S., GR, #228 & SLUND, A. 2011. Mechanisms of Cellular Uptake of Cell-Penetrating Peptides. *Journal of Biophysics,* 2011.

MAEKAWA, R., KITAGAWA, T., HOJO, K., WADA, T. & SATO, K. 1988. Distinct antitumor mechanisms of recombinant murine interferon-gamma against two murine tumor models. *J Interferon Res,* 8**,** 227-39.

MAGZOUB, M., ERIKSSON, L. E. G. R. & GR√ §SLUND, A. 2002. Conformational states of the cell-penetrating peptide penetratin when interacting with phospholipid vesicles: effects of surface charge and peptide concentration. *Biochimica et Biophysica Acta (BBA) - Biomembranes,* 1563**,** 53-63.

MAGZOUB, M., ERIKSSON, L. E. G. R. & GR√ §SLUND, A. 2003. Comparison of the interaction, positioning, structure induction and membrane perturbation of cell-penetrating peptides and non-translocating variants with phospholipid vesicles. *Biophysical Chemistry,* 103**,** 271-288.

MAKI, G., HAYES, G. M., NAJI, A., TYLER, T., CAROSELLA, E. D., ROUAS-FREISS, N. & GREGORY, S. A. 2008. NK resistance of tumor cells from multiple myeloma and chronic lymphocytic leukemia patients: implication of HLA-G. *Leukemia,* 22**,** 998-1006.

MALISSEN, B., GREGOIRE, C., MALISSEN, M. & RONCAGALLI, R. 2014. Integrative biology of T cell activation. *Nat Immunol,* 15**,** 790-7.

MARTENS, S., KOZLOV, M. M. & MCMAHON, H. T. 2007. How synaptotagmin promotes membrane fusion. *Science,* 316**,** 1205-8.

MARTENS, S. & MCMAHON, H. T. 2011. C2 domains and membrane fusion. *Curr Top Membr,* 68**,** 141-59.

MARTINEZ-MARTIN, N., FERNANDEZ-ARENAS, E., CEMERSKI, S., DELGADO, P., TURNER, M., HEUSER, J., IRVINE, D. J., HUANG, B., BUSTELO, X. R., SHAW, A. & ALARCON, B. 2011. T cell receptor internalization from the immunological synapse is mediated by TC21 and RhoG GTPase-dependent phagocytosis. *Immunity,* 35**,** 208-22.

MASON, D. Y., JONES, M. & GOODNOW, C. C. 1992. Development and follicular localization of tolerant B lymphocytes in lysozyme/anti-lysozyme IgM/IgD transgenic mice. *International Immunology,* 4**,** 163-175.

MAYHEW, E., HARLOS, J. P. & JULIANO, R. L. 1973. The effect of polycations on cell membrane stability and transport processes. *J Membr Biol,* 14**,** 213-28.

MCCANN, F. E., EISSMANN, P., ONFELT, B., LEUNG, R. & DAVIS, D. M. 2007. The activating NKG2D ligand MHC class I-related chain A transfers from target cells to NK cells in a manner that allows functional consequences. *J Immunol,* 178**,** 3418-26.

MCMAHON, H. T., KOZLOV, M. M. & MARTENS, S. 2010. Membrane Curvature in Synaptic Vesicle Fusion and Beyond. *Cell,* 140**,** 601-605.

MEDZHITOV, R. 2007. Recognition of microorganisms and activation of the immune response. *Nature,* 449**,** 819-26.

MERKENSCHLAGER, M. 1996. Tracing interactions of thymocytes with individual stromal cell partners. *European Journal of Immunology,* 26**,** 892-896.

MI, H., MURUGANUJAN, A. & THOMAS, P. D. 2013. PANTHER in 2013: modeling the evolution of gene function, and other gene attributes, in the context of phylogenetic trees. *Nucleic Acids Res,* 41**,** D377-86.

MITCHELL, A. J., PRADEL, L. C., CHASSON, L., VAN ROOIJEN, N., GRAU, G. E., HUNT, N. H. & CHIMINI, G. 2010. Technical

Advance: Autofluorescence as a tool for myeloid cell analysis. *Journal of Leukocyte Biology,* 88**,** 597-603.

MITTELBRUNN, M., GUTIERREZ-VAZQUEZ, C., VILLARROYA-BELTRI, C., GONZALEZ, S., SANCHEZ-CABO, F., GONZALEZ, M. A., BERNAD, A. & SANCHEZ-MADRID, F. 2011. Unidirectional transfer of microRNA-loaded exosomes from T cells to antigen-presenting cells. *Nat Commun,* 2**,** 282.

MOMBAERTS, P., IACOMINI, J., JOHNSON, R. S., HERRUP, K., TONEGAWA, S. & PAPAIOANNOU, V. E. 1992. RAG-1-deficient mice have no mature B and T lymphocytes. *Cell,* 68**,** 869-877.

MOORE, M. W., CARBONE, F. R. & BEVAN, M. J. 1988. Introduction of soluble protein into the class I pathway of antigen processing and presentation. *Cell,* 54**,** 777-785.

MORALES-KASTRESANA, A., CATALAN, E., HERVAS-STUBBS, S., PALAZON, A., AZPILIKUETA, A., BOLANOS, E., ANEL, A., PARDO, J. & MELERO, I. 2013. Essential complicity of perforin-granzyme and FAS-L mechanisms to achieve tumor rejection following treatment with anti-CD137 mAb. *Journal for ImmunoTherapy of Cancer,* 1**,** 3.

MORELLI, A. E., LARREGINA, A. T., SHUFESKY, W. J., SULLIVAN, M. L., STOLZ, D. B., PAPWORTH, G. D., ZAHORCHAK, A. F., LOGAR, A. J., WANG, Z., WATKINS, S. C., FALO, L. D., JR. & THOMSON, A. W. 2004. Endocytosis, intracellular sorting, and processing of exosomes by dendritic cells. *Blood,* 104**,** 3257-66.

MOREY, J., RYAN, J. & DOLAH, F. 2006. Microarray validation: factors influencing correlation between oligonucleotide microarrays and real-time PCR. *Biological Procedures Online,* 8**,** 175-193.

MUKHERJEE, S., ZHU, J., ZIKHERMAN, J., PARAMESWARAN, R., KADLECEK, T. A., WANG, Q., AU-YEUNG, B., PLOEGH, H., KURIYAN, J., DAS, J. & WEISS, A. 2013. Monovalent and multivalent ligation of the B cell receptor exhibit differential dependence upon Syk and Src family kinases. *Sci Signal,* 6**,** ra1.

MULLER, R., MISUND, K., HOLIEN, T., BACHKE, S., GILLJAM, K. M., VATSVEEN, T. K., RO, T. B., BELLACCHIO, E., SUNDAN, A. & OTTERLEI, M. 2013. Targeting Proliferating Cell Nuclear Antigen and Its Protein Interactions Induces Apoptosis in Multiple Myeloma Cells. *PLoS ONE,* 8**,** e70430.

NAKAMURA, K., NAKAYAMA, M., KAWANO, M., ISHII, T., HARIGAE, H. & OGASAWARA, K. 2013. NK-cell fratricide: Dynamic crosstalk between NK and cancer cells. *Oncoimmunology,* 2**,** e26529.

NAKASE, I., TAKEUCHI, T., TANAKA, G. & FUTAKI, S. 2008. Methodological and cellular aspects that govern the internalization mechanisms of arginine-rich cell-penetrating peptides. *Advanced Drug Delivery Reviews,* 60**,** 598-607.

NARNI-MANCINELLI, E., SOUDJA, S. M. H., CROZAT, K., DALOD, M., GOUNON, P., GEISSMANN, F. & LAUVAU, G. 2011. Inflammatory Monocytes and Neutrophils Are Licensed to Kill during Memory Responses <italic>In Vivo</italic>. *PLoS Pathog,* 7**,** e1002457.

NELISSEN, J. M., PETERS, I. M., DE GROOTH, B. G., VAN KOOYK, Y. & FIGDOR, C. G. 2000. Dynamic regulation of activated leukocyte cell adhesion molecule-mediated homotypic cell adhesion through the actin cytoskeleton. *Mol Biol Cell,* 11**,** 2057-68.

NISHIDA, N., XIE, C., SHIMAOKA, M., CHENG, Y., WALZ, T. & SPRINGER, T. A. 2006. Activation of leukocyte beta2 integrins by conversion from bent to extended conformations. *Immunity,* 25**,** 583-94.

NOLTE-'T HOEN, E. N., BUSCHOW, S. I., ANDERTON, S. M., STOORVOGEL, W. & WAUBEN, M. H. 2009. Activated T cells recruit exosomes secreted by dendritic cells via LFA-1. *Blood,* 113**,** 1977-81.

OGASAWARA, K., HAMERMAN, J. A., HSIN, H., CHIKUMA, S., BOUR-JORDAN, H., CHEN, T., PERTEL, T., CARNAUD, C., BLUESTONE, J. A. & LANIER, L. L. 2003. Impairment of NK cell function by NKG2D modulation in NOD mice. *Immunity,* 18**,** 41-51.

ONFELT, B., NEDVETZKI, S., YANAGI, K. & DAVIS, D. M. 2004. Cutting edge: Membrane nanotubes connect immune cells. *J Immunol,* 173**,** 1511-3.

ONO, T., SEKINO-SUZUKI, N., KIKKAWA, Y., YONEKAWA, H. & KAWASHIMA, S. 2003. Alivin 1, a Novel Neuronal Activity-Dependent Gene, Inhibits Apoptosis and Promotes Survival of Cerebellar Granule Neurons. *The Journal of Neuroscience,* 23**,** 5887-5896.

OSBORNE, C. K., HOBBS, K. & TRENT, J. M. 1987. Biological differences among MCF-7 human breast cancer cell lines from different laboratories. *Breast Cancer Res Treat,* 9**,** 111-21.

OSBORNE, D. G. & WETZEL, S. A. 2012. Trogocytosis results in sustained intracellular signaling in CD4(+) T cells. *J Immunol,* 189**,** 4728-39.

OVERTON, W. R. 1988. Modified histogram subtraction technique for analysis of flow cytometry data. *Cytometry,* 9**,** 619-26.

PENG, S. L. 2005. Signaling in B cells via Toll-like receptors. *Curr Opin Immunol,* 17**,** 230-6.

PENTCHEVA-HOANG, T., EGEN, J. G., WOJNOONSKI, K. & ALLISON, J. P. 2004. B7-1 and B7-2 selectively recruit CTLA-4 and CD28 to the immunological synapse. *Immunity,* 21**,** 401-13.

PERSSON, D., THOR√©N, P. E. G., HERNER, M., LINCOLN, P. & NORD√©N, B. 2002. Application of a Novel Analysis To Measure the Binding of the Membrane-Translocating Peptide Penetratin to Negatively Charged Liposomes,Ä†. *Biochemistry,* 42**,** 421-429.

PHAM, T., MERO, P. & BOOTH, J. W. 2011. Dynamics of macrophage trogocytosis of rituximab-coated B cells. *PLoS One,* 6**,** e14498.

PIERCE, S. K. 2002. Lipid rafts and B-cell activation. *Nat Rev Immunol,* 2**,** 96-105.

PIOLI, C., GATTA, L., UBALDI, V. & DORIA, G. 2000. Inhibition of IgG1 and IgE Production by Stimulation of the B Cell CTLA-4 Receptor. *The Journal of Immunology,* 165**,** 5530-5536.

PIRCHER, H., BURKI, K., LANG, R., HENGARTNER, H. & ZINKERNAGEL, R. M. 1989. Tolerance induction in double specific T-cell receptor transgenic mice varies with antigen. *Nature,* 342**,** 559-61.

POUPOT, M. & FOURNIE, J. J. 2003. Spontaneous membrane transfer through homotypic synapses between lymphoma cells. *J Immunol,* 171**,** 2517-23.

PRINTEN, J. A., WOODARD, S. L., HERMAN, J. R., ROESS, D. A. & BARISAS, B. G. 1993. Membrane changes in lipopolysaccharide-stimulated murine B lymphocytes associated with cell activation. *Biochimica et Biophysica Acta (BBA) - Biomembranes,* 1148**,** 91-96.

PURDY, A. K. & CAMPBELL, K. S. 2009. SHP-2 Expression Negatively Regulates NK Cell Function. *The Journal of Immunology,* 183**,** 7234-7243.

QIN, Z., SCHWARTZKOPFF, J., PRADERA, F., KAMMERTOENS, T., SELIGER, B., PIRCHER, H. & BLANKENSTEIN, T. 2003. A critical requirement of interferon gamma-mediated angiostasis for tumor rejection by CD8+ T cells. *Cancer Res,* 63**,** 4095-100.

QUAH, B. J., BARLOW, V. P., MCPHUN, V., MATTHAEI, K. I., HULETT, M. D. & PARISH, C. R. 2008. Bystander B cells rapidly acquire antigen receptors from activated B cells by membrane transfer. *Proc Natl Acad Sci U S A,* 105**,** 4259-64.

QUANDT, D., HOFF, H., RUDOLPH, M., FILLATREAU, S. & BRUNNER-WEINZIERL, M. C. 2007. A New Role of CTLA-4 on B Cells in Thymus-Dependent Immune Responses In Vivo. *The Journal of Immunology,* 179**,** 7316-7324.

QURESHI, O. S., ZHENG, Y., NAKAMURA, K., ATTRIDGE, K., MANZOTTI, C., SCHMIDT, E. M., BAKER, J., JEFFERY, L. E., KAUR, S., BRIGGS, Z., HOU, T. Z., FUTTER, C. E., ANDERSON, G., WALKER, L. S. & SANSOM, D. M. 2011. Trans-endocytosis of CD80 and CD86: a molecular basis for the cell-extrinsic function of CTLA-4. *Science,* 332**,** 600-3.

RAFII, A., MIRSHAHI, P., POUPOT, M., FAUSSAT, A. M., SIMON, A., DUCROS, E., MERY, E., COUDERC, B., LIS, R., CAPDET, J., BERGALET, J., QUERLEU, D., DAGONNET, F., FOURNIE, J. J., MARIE, J. P., PUJADE-LAURAINE, E., FAVRE, G., SORIA, J. & MIRSHAHI, M. 2008. Oncologic trogocytosis of an original stromal cells induces chemoresistance of ovarian tumours. *PLoS One,* 3**,** e3894.

RAINY, N., CHETRIT, D., ROUGER, V., VERNITSKY, H., RECHAVI, O., MARGUET, D., GOLDSTEIN, I., EHRLICH, M. & KLOOG, Y. 2013. H-Ras transfers from B to T cells via tunneling nanotubes. *Cell Death Dis,* 4**,** e726.

RATNER, S., WEI, W. Z., OLIVER, J. & OLIVER, J. 2005. Enhancement of T cell localization in mammary tumors through transient inhibition of T cell myosin function. *Cell Immunol,* 233**,** 1-10.

RECHAVI, O., GOLDSTEIN, I. & KLOOG, Y. 2009. Intercellular exchange of proteins: the immune cell habit of sharing. *FEBS Lett,* 583**,** 1792-9.

RECHAVI, O., GOLDSTEIN, I., VERNITSKY, H., ROTBLAT, B. & KLOOG, Y. 2007. Intercellular transfer of oncogenic H-Ras at the immunological synapse. *PLoS One,* 2**,** e1204.

REHG, J. E., BUSH, D. & WARD, J. M. 2012. The utility of immunohistochemistry for the identification of hematopoietic and lymphoid cells in normal tissues and interpretation of proliferative and inflammatory lesions of mice and rats. *Toxicol Pathol,* 40**,** 345-74.

RESTIFO, N. P., DUDLEY, M. E. & ROSENBERG, S. A. 2012. Adoptive immunotherapy for cancer: harnessing the T cell response. *Nat Rev Immunol,* 12**,** 269-81.

RICHARD, K., PIERCE, S. K. & SONG, W. 2008. The Agonists of TLR4 and 9 Are Sufficient to Activate Memory B Cells to Differentiate into Plasma Cells In Vitro but Not In Vivo. *The Journal of Immunology,* 181**,** 1746-1752.

RIOND, J., ELHMOUZI, J., HUDRISIER, D. & GAIRIN, J. E. 2007. Capture of membrane components via trogocytosis occurs in vivo during both dendritic cells and target cells encounter by CD8(+) T cells. *Scand J Immunol,* 66**,** 441-50.

RIZO, J. & SUDHOF, T. C. 1998. C2-domains, structure and function of a universal Ca2+-binding domain. *J Biol Chem,* 273**,** 15879-82.

ROCHA-PERUGINI, V., SANCHEZ-MADRID, F. & MARTINEZ DEL HOYO, G. 2015. Function and Dynamics of Tetraspanins during Antigen Recognition and Immunological Synapse Formation. *Front Immunol,* 6**,** 653.

RODA-NAVARRO, P., VALES-GOMEZ, M., CHISHOLM, S. E. & REYBURN, H. T. 2006. Transfer of NKG2D and MICB at the cytotoxic NK cell immune synapse correlates with a reduction in NK cell cytotoxic function. *Proc Natl Acad Sci U S A,* 103**,** 11258-63.

RODRIGUES, M., DE LA TORRE, B. G., ANDREU, D. & SANTOS, N. C. 2013. Kinetic uptake profiles of cell penetrating peptides in lymphocytes and monocytes. *Biochimica et Biophysica Acta (BBA) - General Subjects,* 1830**,** 4554-4563.

RODRIGUEZ, D., SILVERA, R., CARRIO, R., NADJI, M., CASO, R., RODRIGUEZ, G., IRAGAVARAPU-CHARYULU, V. & TORROELLA-KOURI, M. 2013. Tumor microenvironment profoundly modifies functional status of macrophages: peritoneal and tumor-associated macrophages are two very different subpopulations. *Cell Immunol,* 283**,** 51-60.

ROOIJEN, N. V. & SANDERS, A. 1994. Liposome mediated depletion of macrophages: mechanism of action, preparation of liposomes and applications. *Journal of Immunological Methods,* 174**,** 83-93.

ROSENBERG, S. A., YANG, J. C., SHERRY, R. M., KAMMULA, U. S., HUGHES, M. S., PHAN, G. Q., CITRIN, D. E., RESTIFO, N. P., ROBBINS, P. F., WUNDERLICH, J. R., MORTON, K. E., LAURENCOT, C. M., STEINBERG, S. M., WHITE, D. E. & DUDLEY, M. E. 2011. Durable complete responses in heavily pretreated patients with metastatic melanoma using T-cell transfer immunotherapy. *Clin Cancer Res,* 17**,** 4550-7.

ROTHBARD, J. B., JESSOP, T. C. & WENDER, P. A. 2005. Adaptive translocation: the role of hydrogen bonding and membrane potential in the uptake of guanidinium-rich transporters into cells. *Advanced Drug Delivery Reviews,* 57**,** 495-504.

RUSSO, V., ZHOU, D., SARTIRANA, C., ROVERE, P., VILLA, A., ROSSINI, S., TRAVERSARI, C. & BORDIGNON, C. 2000. Acquisition of intact allogeneic human leukocyte antigen molecules by human dendritic cells. *Blood,* 95**,** 3473-7.

SÄÄLIK, P., NIINEP, A., PAE, J., HANSEN, M., LUBENETS, D., LANGEL, Ü. & POOGA, M. 2011. Penetration without cells: Membrane translocation of cell-penetrating peptides in the model giant plasma membrane vesicles. *Journal of Controlled Release,* 153**,** 117-125.

SAAR, K. L., LINDGREN, M., HANSEN, M., EIR√≠KSD√≥TTIR, E. A., JIANG, Y., ROSENTHAL-AIZMAN, K., SASSIAN, M. & LANGEL, Ú. 2005. Cell-penetrating peptides: A comparative membrane toxicity study. *Analytical Biochemistry,* 345**,** 55-65.

SABZEVARI, H., KANTOR, J., JAIGIRDAR, A., TAGAYA, Y., NARAMURA, M., HODGE, J., BERNON, J. & SCHLOM, J. 2001. Acquisition of CD80 (B7-1) by T cells. *J Immunol,* 166**,** 2505-13.

SAIJO, N., OZAKI, A., BEPPU, Y., TAKAHASHI, K., FUJITA, J., SASAKI, Y., NOMORI, H., KIMATA, M., SHIMIZU, E. & HOSHI, A. 1984.

Analysis of metastatic spread and growth of tumor cells in mice with depressed natural killer activity by anti-asialo GM1 antibody or anticancer agents. *J Cancer Res Clin Oncol,* 107**,** 157-63.

SASAKI, Y., MINAMIZAWA, M., AMBO, A., SUGAWARA, S., OGAWA, Y. & NITTA, K. 2008. Cell-penetrating peptide-conjugated XIAP-inhibitory cyclic hexapeptides enter into Jurkat cells and inhibit cell proliferation. *FEBS Journal,* 275**,** 6011-6021.

SCAPINI, P., LAPINET-VERA, J. A., GASPERINI, S., CALZETTI, F., BAZZONI, F. & CASSATELLA, M. A. 2000. The neutrophil as a cellular source of chemokines. *Immunol Rev,* 177**,** 195-203.

SCHAMEL, W. W. & RETH, M. 2000. Monomeric and oligomeric complexes of the B cell antigen receptor. *Immunity,* 13**,** 5-14.

SCHMIDT, N., MISHRA, A., LAI, G. H. & WONG, G. C. L. 2010. Arginine-rich cell-penetrating peptides. *FEBS Letters,* 584**,** 1806-1813.

SCHNEIDERS, F. L., PRODOHL, J., RUBEN, J. M., O'TOOLE, T., SCHEPER, R. J., BONNEVILLE, M., SCOTET, E., VERHEUL, H. M., DE GRUIJL, T. D. & VAN DER VLIET, H. J. 2014. CD1d-restricted antigen presentation by Vgamma9Vdelta2-T cells requires trogocytosis. *Cancer Immunol Res,* 2**,** 732-40.

SCHOENBORN, J. R. & WILSON, C. B. 2007. Regulation of interferon-gamma during innate and adaptive immune responses. *Adv Immunol,* 96**,** 41-101.

SCHROEDER, A., MUELLER, O., STOCKER, S., SALOWSKY, R., LEIBER, M., GASSMANN, M., LIGHTFOOT, S., MENZEL, W., GRANZOW, M. & RAGG, T. 2006. The RIN: an RNA integrity number for assigning integrity values to RNA measurements. *BMC Molecular Biology,* 7**,** 3.

SCHULTZ, R. M. 1987. Interleukin 1 and interferon-gamma: cytokines that provide reciprocal regulation of macrophage and T cell function. *Toxicol Pathol,* 15**,** 333-7.

SHAHINIAN, A., PFEFFER, K., LEE, K. P., KUNDIG, T. M., KISHIHARA, K., WAKEHAM, A., KAWAI, K., OHASHI, P. S., THOMPSON, C. B. & MAK, T. W. 1993. DiferentialT CellCostimulatory Requirements in CD28-DeficientMice. *Science,* 261**,** 609-612.

SHEN, F. W., SAGA, Y., LITMAN, G., FREEMAN, G., TUNG, J. S., CANTOR, H. & BOYSE, E. A. 1985. Cloning of Ly-5 cDNA. *Proc Natl Acad Sci U S A,* 82**,** 7360-3.

SHIBUYA, A., CAMPBELL, D., HANNUM, C., YSSEL, H., FRANZ-BACON, K., MCCLANAHAN, T., KITAMURA, T., NICHOLL, J., SUTHERLAND, G. R., LANIER, L. L. & PHILLIPS, J. H. 1996. DNAM-1, a novel adhesion molecule involved in the cytolytic function of T lymphocytes. *Immunity,* 4**,** 573-81.

SHRIKANT, P., KHORUTS, A. & MESCHER, M. F. 1999. CTLA-4 Blockade Reverses CD8+ T Cell Tolerance to Tumor by a CD4+ T Cell– and IL-2-Dependent Mechanism. *Immunity,* 11**,** 483-493.

SHRIKANT, P. & MESCHER, M. F. 1999. Control of syngeneic tumor growth by activation of CD8+ T cells: efficacy is limited by migration away from the site and induction of nonresponsiveness. *J Immunol,* 162**,** 2858-66.

SIVEEN, K. S. & KUTTAN, G. 2009. Role of macrophages in tumour progression. *Immunol Lett,* 123**,** 97-102.

SMITH-GARVIN, J. E., KORETZKY, G. A. & JORDAN, M. S. 2009. T cell activation. *Annu Rev Immunol,* 27**,** 591-619.

SMYTH, L. A., HARKER, N., TURNBULL, W., EL-DOUEIK, H., KLAVINSKIS, L., KIOUSSIS, D., LOMBARDI, G. & LECHLER, R. 2008. The relative efficiency of acquisition of MHC:peptide complexes and cross-presentation depends on dendritic cell type. *J Immunol,* 181**,** 3212-20.

SOOMETS, U., LINDGREN, M., GALLET, X., H√§LLBRINK, M., ELMQUIST, A., BALASPIRI, L., ZORKO, M., POOGA, M., BRASSEUR, R. & LANGEL, Ú. 2000. Deletion analogues of transportan. *Biochimica et Biophysica Acta (BBA) - Biomembranes,* 1467**,** 165-176.

SOT, B., BEHRMANN, E., RAUNSER, S. & WITTINGHOFER, A. 2013. Ras GTPase activating (RasGAP) activity of the dual specificity GAP protein Rasal requires colocalization and C2 domain binding to lipid membranes. *Proc Natl Acad Sci U S A,* 110**,** 111-6.

SOWINSKI, S., JOLLY, C., BERNINGHAUSEN, O., PURBHOO, M. A., CHAUVEAU, A., KOHLER, K., ODDOS, S., EISSMANN, P., BRODSKY, F. M., HOPKINS, C., ONFELT, B., SATTENTAU, Q. & DAVIS, D. M. 2008. Membrane nanotubes physically connect T cells over long distances presenting a novel route for HIV-1 transmission. *Nat Cell Biol,* 10**,** 211-9.

SPRENT, J. 2005. Swapping molecules during cell-cell interactions. *Sci STKE,* 2005**,** pe8.

SQUIER, M. K. T. & JOHN COHEN, J. 1994. Cell-mediated cytotoxic mechanisms. *Current Opinion in Immunology,* 6**,** 447-452.

ST. LAURENT, G., SHTOKALO, D., TACKETT, M. R., YANG, Z., VYATKIN, Y., MILOS, P. M., SEILHEIMER, B., MCCAFFREY, T. A. & KAPRANOV, P. 2013. On the importance of small changes in RNA expression. *Methods,* 63**,** 18-24.

STABLES, M. J., SHAH, S., CAMON, E. B., LOVERING, R. C., NEWSON, J., BYSTROM, J., FARROW, S. & GILROY, D. W. 2011. Transcriptomic analyses of murine resolution-phase macrophages. *Blood,* 118**,** e192-e208.

STANIETSKY, N., ROVIS, T. L., GLASNER, A., SEIDEL, E., TSUKERMAN, P., YAMIN, R., ENK, J., JONJIC, S. & MANDELBOIM, O. 2013. Mouse TIGIT inhibits NK-cell cytotoxicity upon interaction with PVR. *Eur J Immunol,* 43**,** 2138-50.

STANIETSKY, N., SIMIC, H., ARAPOVIC, J., TOPORIK, A., LEVY, O., NOVIK, A., LEVINE, Z., BEIMAN, M., DASSA, L., ACHDOUT, H., STERN-GINOSSAR, N., TSUKERMAN, P., JONJIC, S. & MANDELBOIM, O. 2009. The interaction of TIGIT with PVR and PVRL2 inhibits human NK cell cytotoxicity. *Proc Natl Acad Sci U S A,* 106**,** 17858-63.

STENGEL, K. F., HARDEN-BOWLES, K., YU, X., ROUGE, L., YIN, J., COMPS-AGRAR, L. T., WIESMANN, C., BAZAN, J. F., EATON, D. L. & GROGAN, J. L. 2012. Structure of TIGIT immunoreceptor bound to poliovirus receptor reveals a cell,Äìcell adhesion and signaling mechanism that requires cis-trans receptor clustering. *Proceedings of the National Academy of Sciences,* 109**,** 5399-5404.

STINCHCOMBE, J. C., BOSSI, G., BOOTH, S. & GRIFFITHS, G. M. 2001. The immunological synapse of CTL contains a secretory domain and membrane bridges. *Immunity,* 15**,** 751-61.

STOJANOVIC, A. & CERWENKA, A. 2011. Natural Killer Cells and Solid Tumors. *Journal of Innate Immunity,* 3**,** 355-364.

STOJANOVIC, A., CORREIA, M. & CERWENKA, A. 2013. Shaping of NK Cell Responses by the Tumor Microenvironment. *Cancer Microenvironment,* 6**,** 135-146.

SUN, Z. & YANG, P. 2004. Role of imbalance between neutrophil elastase and alpha 1-antitrypsin in cancer development and progression. *Lancet Oncol,* 5**,** 182-90.

SUTTMANN, H., RIEMENSBERGER, J., BENTIEN, G., SCHMALTZ, D., STOCKLE, M., JOCHAM, D., BOHLE, A. & BRANDAU, S. 2006. Neutrophil granulocytes are required for effective Bacillus Calmette-Guerin immunotherapy of bladder cancer and orchestrate local immune responses. *Cancer Res,* 66**,** 8250-7.

SWART, G. W. M. 2002. Activated leukocyte cell adhesion molecule (CD166/ALCAM): Developmental and mechanistic aspects of cell clustering and cell migration. *European Journal of Cell Biology,* 81**,** 313-321.

TABIASCO, J., ESPINOSA, E., HUDRISIER, D., JOLY, E., FOURNIE, J. J. & VERCELLONE, A. 2002. Active trans-synaptic capture of membrane fragments by natural killer cells. *Eur J Immunol,* 32**,** 1502-8.

TAKEDA, K., KAISHO, T. & AKIRA, S. 2003. Toll-like receptors. *Annu Rev Immunol,* 21**,** 335-76.

TATARI-CALDERONE, Z., SEMNANI, R. T., NUTMAN, T. B., SCHLOM, J. & SABZEVARI, H. 2002. Acquisition of CD80 by human T cells at early stages of activation: functional involvement of CD80 acquisition in T cell to T cell interaction. *J Immunol,* 169**,** 6162-9.

TAYLOR, P. R., BROWN, G. D., GELDHOF, A. B., MARTINEZ-POMARES, L. & GORDON, S. 2003. Pattern recognition receptors and differentiation antigens define murine myeloid cell heterogeneity ex vivo. *European Journal of Immunology,* 33**,** 2090-2097.

TAZZYMAN, S., LEWIS, C. E. & MURDOCH, C. 2009. Neutrophils: key mediators of tumour angiogenesis. *Int J Exp Pathol,* 90**,** 222-31.

TER-AVETISYAN, G., T√°NNEMANN, G., NOWAK, D., NITSCHKE, M., HERRMANN, A., DRAB, M. & CARDOSO, M. C. 2009. Cell Entry of Arginine-rich Peptides Is Independent of Endocytosis. *Journal of Biological Chemistry,* 284**,** 3370-3378.

THERY, C., DUBAN, L., SEGURA, E., VERON, P., LANTZ, O. & AMIGORENA, S. 2002. Indirect activation of naive CD4+ T cells by dendritic cell-derived exosomes. *Nat Immunol,* 3**,** 1156-62.

THERY, C., OSTROWSKI, M. & SEGURA, E. 2009. Membrane vesicles as conveyors of immune responses. *Nat Rev Immunol,* 9**,** 581-93.

TIVOL, E. A., BORRIELLO, F., SCHWEITZER, A. N., LYNCH, W. P., BLUESTONE, J. A. & SHARPE, A. H. 1995. Loss of CTLA-4 leads to massive lymphoproliferation and fatal multiorgan tissue destruction, revealing a critical negative regulatory role of CTLA-4. *Immunity,* 3**,** 541-547.

TOLAR, P. & PIERCE, S. K. 2010. A conformation-induced oligomerization model for B cell receptor microclustering and signaling. *Curr Top Microbiol Immunol,* 340**,** 155-69.

TSANG, J. Y., CHAI, J. G. & LECHLER, R. 2003. Antigen presentation by mouse CD4+ T cells involving acquired MHC class II:peptide complexes: another mechanism to limit clonal expansion? *Blood,* 101**,** 2704-10.

TSUNG, K., DOLAN, J. P., TSUNG, Y. L. & NORTON, J. A. 2002. Macrophages as effector cells in interleukin 12-induced T cell-dependent tumor rejection. *Cancer Res,* 62**,** 5069-75.

UEDA, H., MORPHEW, M. K., MCINTOSH, J. R. & DAVIS, M. M. 2011. CD4(+) T-cell synapses involve multiple distinct stages. *Proceedings of the National Academy of Sciences of the United States of America,* 108**,** 17099-17104.

UMESHAPPA, C. S., HUANG, H., XIE, Y., WEI, Y., MULLIGAN, S. J., DENG, Y. & XIANG, J. 2009. CD4+ Th-APC with Acquired Peptide/MHC Class I and II Complexes Stimulate Type 1 Helper CD4+ and Central Memory CD8+ T Cell Responses. *The Journal of Immunology,* 182**,** 193-206.

UZANA, R., EISENBERG, G., MERIMS, S., FRANKENBURG, S., PATO, A., YEFENOF, E., ENGELSTEIN, R., PERETZ, T., MACHLENKIN, A. & LOTEM, M. 2015. Human T cell crosstalk is induced by tumor membrane transfer. *PLoS One,* 10**,** e0118244.

VAN BREEVOORT, D., SNIJDERS, A. P., HELLEN, N., WECKHUYSEN, S., VAN HOOREN, K. W., EIKENBOOM, J., VALENTIJN, K., FERNANDEZ-BORJA, M., CEULEMANS, B., DE JONGHE, P., VOORBERG, J., HANNAH, M., CARTER, T. & BIERINGS, R. 2014. STXBP1 promotes Weibel-Palade body exocytosis through its interaction with the Rab27A effector Slp4-a. *Blood,* 123**,** 3185-94.

VAN KEMPEN, L. O. C. L. T., NELISSEN, J. M. D. T., DEGEN, W. G. J., TORENSMA, R., WEIDLE, U. H., BLOEMERS, H. P. J., FIGDOR, C. G. & SWART, G. W. M. 2001. Molecular Basis for the Homophilic Activated Leukocyte Cell Adhesion Molecule (ALCAM)-ALCAM Interaction. *Journal of Biological Chemistry,* 276**,** 25783-25790.

VAN NIEL, G., PORTO-CARREIRO, I., SIMOES, S. & RAPOSO, G. S. 2006. Exosomes: A Common Pathway for a Specialized Function. *Journal of Biochemistry,* 140**,** 13-21.

VANHERBERGHEN, B., ANDERSSON, K., CARLIN, L. M., NOLTE-'T HOEN, E. N., WILLIAMS, G. S., HOGLUND, P. & DAVIS, D. M. 2004. Human and murine inhibitory natural killer cell receptors transfer from natural killer cells to target cells. *Proc Natl Acad Sci U S A,* 101**,** 16873-8.

VERDURMEN, W. P. R., WALLBRECHER, R., SCHMIDT, S., EILANDER, J., BOVEE-GEURTS, P., FANGHÄNEL, S., BÜRCK, J., WADHWANI, P., ULRICH, A. S. & BROCK, R. 2013. Cell surface clustering of heparan sulfate proteoglycans by amphipathic cell-penetrating peptides does not contribute to uptake. *Journal of Controlled Release,* 170**,** 83-91.

VILLEGAS, F. R., COCA, S., VILLARRUBIA, V. G., JIMÉNEZ, R., CHILLÓN, M. A. J., JAREÑO, J., ZUIL, M. & CALLOL, L. 2002. Prognostic significance of tumor infiltrating natural killer cells subset CD57 in patients with squamous cell lung cancer. *Lung Cancer,* 35**,** 23-28.

VIVES, E., BRODIN, P. & LEBLEU, B. 1997. A Truncated HIV-1 Tat Protein Basic Domain Rapidly Translocates through the Plasma Membrane and Accumulates in the Cell Nucleus. *Journal of Biological Chemistry,* 272**,** 16010-16017.

VOGEL, C. & MARCOTTE, E. M. 2012. Insights into the regulation of protein abundance from proteomic and transcriptomic analyses. *Nat Rev Genet,* 13**,** 227-32.

VOS, Q., LEES, A., WU, Z. Q., SNAPPER, C. M. & MOND, J. J. 2000. B-cell activation by T-cell-independent type 2 antigens as an integral part of the humoral immune response to pathogenic microorganisms. *Immunol Rev,* 176**,** 154-70.

WAKIM, L. M. & BEVAN, M. J. 2011. Cross-dressed dendritic cells drive memory CD8+ T-cell activation after viral infection. *Nature,* 471**,** 629-32.

WALKER, L. S. & SANSOM, D. M. 2011. The emerging role of CTLA4 as a cell-extrinsic regulator of T cell responses. *Nat Rev Immunol,* 11**,** 852-63.

WATERHOUSE, P., PENNINGER, J. M., TIMMS, E., WAKEHAM, A., SHAHINIAN, A., LEE, K. P., THOMPSON, C. B., GRIESSER, H. & MAK, T. W. 1995. Lymphoproliferative Disorders with Early Lethality in Mice Deficient in Ctla-4. *Science,* 270**,** 985-988.

WATKINS, S. C. & SALTER, R. D. 2005. Functional connectivity between immune cells mediated by tunneling nanotubules. *Immunity,* 23**,** 309-18.

WEIDLE, U. H., EGGLE, D., KLOSTERMANN, S. & SWART, G. W. M. 2010. ALCAM/CD166: Cancer-related Issues. *Cancer Genomics - Proteomics,* 7**,** 231-243.

WELCH, D. R., SCHISSEL, D. J., HOWREY, R. P. & AEED, P. A. 1989. Tumor-elicited polymorphonuclear cells, in contrast to "normal" circulating polymorphonuclear cells, stimulate invasive and metastatic potentials of rat mammary adenocarcinoma cells. *Proc Natl Acad Sci U S A,* 86**,** 5859-63.

WENDEL, M., GALANI, I. E., SURI-PAYER, E. & CERWENKA, A. 2008. Natural Killer Cell Accumulation in Tumors Is Dependent on IFN-γ and CXCR3 Ligands. *Cancer Research,* 68**,** 8437-8445.

WETZEL, S. A., MCKEITHAN, T. W. & PARKER, D. C. 2005. Peptide-specific intercellular transfer of MHC class II to CD4+ T cells directly from the immunological synapse upon cellular dissociation. *J Immunol,* 174**,** 80-9.

WOLFERS, J., LOZIER, A., RAPOSO, G., REGNAULT, A., THERY, C., MASURIER, C., FLAMENT, C., POUZIEUX, S., FAURE, F., TURSZ, T., ANGEVIN, E., AMIGORENA, S. & ZITVOGEL, L. 2001. Tumor-derived exosomes are a source of shared tumor rejection antigens for CTL cross-priming. *Nat Med,* 7**,** 297-303.

WURMBACH, E., YUEN, T. & SEALFON, S. C. 2003. Focused microarray analysis. *Methods,* 31**,** 306-16.

XERRI, L., DEVILARD, E., HASSOUN, J., OLIVE, D. & BIRG, F. 1997. In vivo expression of the CTLA4 inhibitory receptor in malignant and reactive cells from Human lymphomas. *The Journal of Pathology,* 183**,** 182-187.

XIANG, J., HUANG, H. & LIU, Y. 2005. A New Dynamic Model of CD8+ T Effector Cell Responses via CD4+ T Helper-Antigen-Presenting Cells. *The Journal of Immunology,* 174**,** 7497-7505.

YANDEK, L. E., POKORNY, A., FLOREN, A., KNOELKE, K., LANGEL, U. & ALMEIDA, P. F. F. 2007. Mechanism of the Cell-Penetrating Peptide Transportan 10 Permeation of Lipid Bilayers. *Biophysical Journal,* 92**,** 2434-2444.

YANG, J. & RETH, M. 2010. The dissociation activation model of B cell antigen receptor triggering. *FEBS Lett,* 584**,** 4872-7.

YU, X., HARDEN, K., GONZALEZ, L. C., FRANCESCO, M., CHIANG, E., IRVING, B., TOM, I., IVELJA, S., REFINO, C. J., CLARK, H., EATON, D. & GROGAN, J. L. 2009. The surface protein TIGIT suppresses T cell activation by promoting the generation of mature immunoregulatory dendritic cells. *Nat Immunol,* 10**,** 48-57.

YUSEFF, M. I., PIEROBON, P., REVERSAT, A. & LENNON-DUMENIL, A. M. 2013. How B cells capture, process and present antigens: a crucial role for cell polarity. *Nat Rev Immunol,* 13**,** 475-86.

ZHOU, J., TAGAYA, Y., TOLOUEI-SEMNANI, R., SCHLOM, J. & SABZEVARI, H. 2005. Physiological relevance of antigen presentasome (APS), an acquired MHC/costimulatory complex, in the sustained activation of CD4+ T cells in the absence of APCs. *Blood,* 105**,** 3238-46.

ZIEGLER, A. 2008. Thermodynamic studies and binding mechanisms of cell-penetrating peptides with lipids and glycosaminoglycans. *Advanced Drug Delivery Reviews,* 60**,** 580-597.

ZIEGLER, A., NERVI, P., DURRENBERGER, M. & SEELIG, J. 2005. The cationic cell-penetrating peptide CPP(TAT) derived from the HIV-1 protein TAT is rapidly transported into living fibroblasts: optical, biophysical, and metabolic evidence. *Biochemistry,* 44**,** 138-48.

ZIEGLER, A. & SEELIG, J. 2004. Interaction of the Protein Transduction Domain of HIV-1 TAT with Heparan Sulfate: Binding Mechanism and Thermodynamic Parameters. *Biophysical Journal,* 86**,** 254-263.

ZIEGLER, A. & SEELIG, J. 2011. Contributions of Glycosaminoglycan Binding and Clustering to the Biological Uptake of the Nonamphipathic Cell-Penetrating Peptide WR9. *Biochemistry,* 50**,** 4650-4664.

ZIMMERMAN, A. W., JOOSTEN, B., TORENSMA, R., PARNES, J. R., VAN LEEUWEN, F. N. & FIGDOR, C. G. 2006. Long-term engagement of CD6 and ALCAM is essential for T-cell proliferation induced by dendritic cells. *Blood,* 107**,** 3212-3220.

ZIVKOVIC, M., POLJAK-BLAZI, M., EGGER, G., SUNJIC, S. B., SCHAUR, R. J. & ZARKOVIC, N. 2005. Oxidative burst and anticancer activities of rat neutrophils. *Biofactors,* 24**,** 305-12.

ZIVKOVIC, M., POLJAK-BLAZI, M., ZARKOVIC, K., MIHALJEVIC, D., SCHAUR, R. J. & ZARKOVIC, N. 2007. Oxidative burst of neutrophils against melanoma B16-F10. *Cancer Lett,* 246**,** 100-8.

ZOMER, A., VENDRIG, T., HOPMANS, E. S., VAN EIJNDHOVEN, M., MIDDELDORP, J. M. & PEGTEL, D. M. 2010. Exosomes: Fit to deliver small RNA. *Commun Integr Biol,* 3**,** 447-50.